Development of A Multi-Axial Transtibial Powered Prosthesis Driven by EMG Signals

A thesis submitted to
The University of Manchester
for the degree of
Doctor of Philosophy
in the Faculty of
Science and Engineering

2018

Unéné N. Gregory

School of Mechanical, Aerospace & Civil Engineering

Table of Contents

Word Count: 44653

List of Figures

List of Tables

Chapter 5

Chapter 6

Appendixes

List of Abbreviations and Acronyms

ESR	Energy storage and release
CoM	Centre of Mass
DoF	Degree of Freedom
MVC	Maximum voluntary contraction
GRF	Ground reaction force
EMG	Electromyography
TA	Tibialis Anterior
MGas	Medial Gastrocnemius
LGas	Lateral Gastrocnemius
LDA	Linear Discriminant Analysis
ROM	Range of Motion
LG	Level-ground
UT	Uneven Terrain
FEA	Finite element analysis
ES condition	Electrode shift condition

I. Abstract

Human locomotion extends beyond walking at self-selected speeds. It encompasses running, walking over varied terrain, being able to move laterally and other such non-cyclic behaviour, all while being able to maintain one's stability. The loss of a limb necessitates adaptation. In the case of lower limb amputation, and depending on the level of amputation, it could mean having to re-learn how to walk.

The objective of this research was to develop a control strategy that was primarily driven by user acquired real-time electromyography (EMG) signals, and to test said control strategy on a developed transtibial powered prosthesis prototype. The development of the control strategy was based on analysing how able-bodied individuals maintained their dynamic stability during ambulation, particularly as they walked over fixed, uneven terrain. This was done by conducting a gait experiment with six able-bodied participants who performed walking trials on both level ground and a fixed, uneven terrain.

The observed gait adaptations implemented by the participants included increased ground reaction force (GRF) variation, particularly along the frontal plane (foot eversion and inversion). These were coupled with aligned co-activation of the participant's lower limb antagonist muscle pairs. These findings highlighted the importance of the human ankle being able to move along multiple planes and how this movement, along with synchronised activation of the lower limb muscles, facilitated the maintenance of dynamic stability.

In the pursuit of developing a volitionally controlled transtibial powered prostheses, various control approaches were tested. The EMG data acquired during the gait experiment formed the basis for the explored controllers. The control approach that yielded the best accuracy when tested using both offline and real-time EMG data was then implemented as the final control strategy to be tested on a prosthesis prototype. Validating the developed control strategy meant testing its functionality with real-life application. To this end, a multi-axial transtibial powered prostheses prototype was developed. The prototype was designed in such a way that it could mimic able-bodied gait both in form, i.e. range of motion (ROM), and in function, i.e. output torque during the gait cycle. The chosen control strategy was implemented on the prototype and tested in real-time with able-bodied participants walking over level ground and on the same fixed, uneven terrain used for the gait experiment.

The control strategy was able to generalise to new participants, there was only a ±10% decrease in accuracy using new data compared to using the training data. Testing the prototype, and by extension the control strategy, led to range of motion (ROM) and torque output results that were similar to able-bodied ankle ROM and torque output. The peak torque was observed around push-off (powered plantarflexion) which demonstrated the prototype's ability to supply energy at appropriate stages of the gait cycle. The findings indicated that the developed control strategy could enable traversal over level-ground and fixed, uneven terrain based solely on real-time user EMG data. It was also found that the control strategy could facilitate movements that, unlike human walking, were not cyclic in nature. Therefore, the aim of this research project was achieved.

Keywords: Control strategy, transtibial powered prostheses, electromyography (EMG), intent prediction, volitional control.

II. Declaration

I declare that no portion of the work referred to in the thesis has been submitted in support of an application for another degree or qualification of this or any other university or other institute of learning

III. Copyright Statement

The author of this thesis (including any appendices and/or schedules to this thesis) owns certain copyright or related rights in it (the "Copyright") and s/he has given The University of Manchester certain rights to use such Copyright, including for administrative purposes.

Copies of this thesis, either in full or in extracts and whether in hard or electronic copy, may be made **only** in accordance with the Copyright, Designs and Patents Act 1988 (as amended) and regulations issued under it or, where appropriate, in accordance with licensing agreements which the University has from time to time. This page must form part of any such copies made.

The ownership of certain Copyright, patents, designs, trademarks and other intellectual property (the "Intellectual Property") and any reproductions of copyright works in the thesis, for example graphs and tables ("Reproductions"), which may be described in this thesis, may not be owned by the author and may be owned by third parties. Such Intellectual Property and Reproductions cannot and must not be made available for use without the prior written permission of the owner(s) of the relevant Intellectual Property and/or Reproductions.

Further information on the conditions under which disclosure, publication and commercialisation of this thesis, the Copyright and any Intellectual Property and/or Reproductions described in it may take place is available in the University IP Policy (see http://documents.manchester.ac.uk/DocuInfo.aspx?DocID=24420), in any relevant Thesis restriction declarations deposited in the University Library, The University Library's regulations (see http://www.library.manchester.ac.uk/about/regulations/) and in The University's policy on Presentation of Theses.

IV. Acknowledgements

V. The Author

Miss Unéné Gregory graduated with a degree in Mechatronics engineering from Tshwane University of Technology (TUT) in Pretoria, South Africa. She went on to receive two Master's degrees, a MTech in Electrical Engineering from TUT and a MSc in Electronic Engineering, with a specialisation in control systems, from ESIEE in France.

Her master's degree research was on developing a system that could assist individuals with paraplegia transition between sitting and standing, and to support them whilst in a standing position. The research resulted in a patent being filed with TUT in 2013.

Miss Gregory presented her doctoral research at the Defence Medical Rehabilitation Centre Headley (DMRC Headley Court) in Surrey, England and submitted a short video presenting her research at the 2017 University of Manchester Postgraduate Summer Research Showcase, for which she won second prize.

Chapter 1
Introduction

1.1 The Importance of Mobility

We often take mobility, and the freedom it affords us, for granted. Activities such as walking around, participating in sports or being outdoors become a norm. This is, until we are stripped of said mobility or are reminded of its importance. Walking is one of the most fundamental of human actions, usually learnt from infancy and adapted throughout our lives. It facilitates our interaction with our environment. It is also an unconscious motion for able bodied individuals which, some believe, is facilitated at a reflex/motor control level rather than being actioned on a conscious level during normal walking conditions [1, 2].

The urban environment most humans inhabit is made up of uneven and varying terrain. This kind of terrain is more dominant in other inhabited places compared to more level ground terrain (i.e. tarred roads, pavements, etc). Traversing uneven terrain is unconsciously achieved by able bodied individuals due to their inherent ability of maintaining dynamic stability by altering gait parameters. These parameters include lowering one's centre of mass (COM), widening step width or employing muscle co-activation [3-5]. This ability to alter gait parameters as and when required allows able bodied individuals to perform a plethora of lower limb motions. Within this study, dynamic stability refers to individuals being able to remain in an upright position and continuing to propel themselves forward along the direction of movement, while performing functional tasks that enlist the activation of antagonist muscle pairs.

For individuals with lower limb amputations, the capability of performing a large variety of locomotion related tasks becomes a challenge due to the limitations introduced by their amputation(s). There is usually a correlation between the degree of mobility individuals retain/regain and their level/degree of amputation. With the increase in life expectancy and the rise of vascular related diseases, lower limb amputation is also expected to increase. This is also highlighted by the increase in funding made available for prosthesis related research, particularly in developed countries such as the UK [6, 7].

1.2 The Emergence of Lower Limb Powered Prostheses

Throughout the ages, prostheses, in all their variations, have been used to restore functionality to individuals who have undergone amputation. Variations of lower limb prostheses have been in existence for centuries. These have been fashioned from an assortment of materials including wood and leather, metal, plastic and even carbon fibre in recent years [8]. This is illustrated in figure 1.1.

Figure 1.1: Representative evolution of lower limb prostheses (©2000 George Steinmetz)

There exists a variety of lower limb prostheses depending on the level of amputation and the activity for which the prosthesis is required. There are five main classes of lower limb prostheses, namely partial feet, symes, transtibial, transfemoral and transpelvic prostheses. These are used following partial foot amputation, ankle disarticulation, below knee (BK) amputation, above knee (AK) amputation and following a hemipelvectomy, respectively [9].

The trend throughout history has been a higher incidence of lower extremity amputation compared to upper extremity amputation [10, 11]. However, contrary to this trend, more research and commercial work has been carried out on upper limb prostheses. These devices can now enable some extent of volitional control. Within this research, volitional control refers to a prosthesis user being able to control their powered device in a manner similar to how they would have controlled their now amputated limb. This includes users controlling their prosthesis using muscles in their residual limb. Fortunately, extensive research has been conducted in relation to human biomechanics and movement, the foundation upon which all prostheses are fundamentally based.

Research focusing on the use of myoelectric signals, in relation to powered prostheses, dates back to as early as the 1950's. Myoelectric signals are biological electrical impulses that cause muscle fibres to contract. However, said research was largely focused on upper extremity prostheses, as it continues to do so to this day and age. In his 1972 doctoral thesis, Flowers [12] stated that even with the (then) sudden emergence of research being conducted in the use of myoelectric signals within prostheses and orthoses, there had only been one lower limb prosthesis developed which made use of user acquired electromyography (EMG) signals to facilitate control. EMG research with regards to lower limb prostheses had mainly focused on above-knee prostheses.

In his 1981 paper, Mann [13] suggested that the lack of research being conducted with regards to EMG controlled lower limb prostheses was due to the ability of simple solutions, such as the SACH (solid ankle cushion heel) foot, to adequately replace the amputated biological limb and to allow users to regain mobility. Even though passive prostheses were, and still are, able to facilitate mobility for users, Mann did not take into consideration the mobility limitations such prostheses possess and the need for increased research within lower limb prostheses in order to enable these prostheses to be true replacements of their biological counterparts, as was the endeavour for upper extremity prostheses. In a study conducted by Demet et al [10], they found health related quality of life (HQRL) to be better for individuals with upper extremity amputation compared to those with lower extremity amputation.

As another reason for the lack of research in lower limb powered prostheses, Mann [13] also cited the challenges of providing, in a portable manner, the amount of energy required to perform certain locomotion tasks that would make these powered prostheses viable. Even though technological strides have been made in the past two decades in relation to smaller actuation systems and electronics, limited progress has been made with regards to developing control strategies for lower limb powered prostheses that are able to facilitate prostheses control in a manner that is synonymous to a biological limb. Adequate and compact power supply remains a challenge for developing more biologically similar lower limb powered prostheses. This is with regards to both the required output power to be supplied by a possible device and its physical dimensions.

The stance taken by Mann, with regards to the development of EMG driven lower limb powered prostheses, seems to have echoed the views of most scholars of the time as there has been a lack of research within this area until recent years. Research with regards to EMG driven lower limb powered prostheses still lags behind the work being conducted towards EMG driven upper extremity prostheses. However, this has also presented the opportunity to study what has worked, and not worked, when it comes to the control of EMG driven powered prostheses.

1.3 The Development of Transtibial Powered Prostheses

A characteristic of human walking not mimicked by passive transtibial (below knee) prostheses is the supply of net positive work, particularly at the push-off phase of gait. This supplied energy enables more efficient body propulsion and for the foot to lift off from the ground with greater ease, thus eliminating over flexion of the knee and hip joints as the foot clears the ground in preparation for the next step.

The evolution of lower limb prostheses has led to the development of devices that not only allow users to achieve a gait that is more similar to that of able bodied individuals, but devices that also aim to achieve a physical appearance, control and weight that is analogous to that of the amputated limb. One of the most significant developments with respect to lower limb prostheses has been the addition of actuation (power) to these devices [14-16].

Lower limb powered prostheses enable users to achieve gait that is similar to that of able-bodied individuals by supplying net positive work, particularly during push off (powered plantarflexion). This leads to a minimisation of the metabolic cost to the user during ambulation. Research suggests that powered prostheses also reduce the loading on the joints of the intact leg, for individuals with unilateral amputations [17, 18], which also minimises the incidence of secondary ailments such as osteoarthritis in the joints. This is attributed to users being able to relearn how to redistribute their body weight equally between both limbs, particularly during stance phase.

Another equally important factor in enabling users to emulate healthy biological gait is the implemented control strategy. The control strategy can be thought of as the central nervous system of a powered prosthesis. It utilises supplied inputs to drive appropriate system output, thus facilitating mobility.

Regardless of how well the physical prosthesis has been designed, the controller implemented on said device can essentially 'make or break' it. This is usually due to the controller being largely responsible for the manner in which the prosthesis operates.

Current commercially available lower limb prostheses do not actively enable users to traverse varied terrain [5]. Within this thesis, uneven terrain is terrain that displaces a person's centre of mass (CoM) outside their base of support (BoS) when being traversed. Such a terrain is one that necessitates ankle joint movement along the frontal (medial-lateral) plane. This limitation of lower limb prostheses leads to users facing difficulties when trying to maintain dynamic stability while walking over uneven terrain. These difficulties manifest themselves in the users' muscle activation patterns and in their gait patterns, e.g. spending more time on their intact limb for unilateral amputees.

The EMG data from such situations usually exhibits high levels of muscle co-contractions within the antagonist muscle pairs [19, 20]. Muscle co-contraction is a tactic usually unconsciously implemented by individuals to ensure that the interface between their residual limb and the prosthesis is maintained. This results in a shortened stance phase on the prosthesis side.

The motivation for this study was the control limitation exhibited by a majority of transtibial powered prostheses, which preclude adaptive control over uneven terrain and thus limit users' ability to volitionally control their prosthesis.

1.4 Research Aim, Objectives and Novel Contributions

The overarching aim of this research was to develop an EMG driven control strategy that could enable a transtibial powered prosthesis to traverse a fixed, uneven terrain. This extended to developing a powered prototype that could move along more than a single degree of freedom.

Research objectives were defined to achieve the overarching aim; these included:

1. Understanding able bodied human walking, over both level ground and uneven terrain, and determining the gait and muscle activation strategies implemented during said motions;
2. Developing a control strategy that could facilitate the observed able-bodied gait strategies on a transtibial powered prosthesis prototype;

19

3. Developing a transtibial prosthesis prototype that could physically achieve similar motion to that observed during the gait experiment; and

4. Testing the functionality of the developed control solution, using the developed prototype, to ascertain the level of agreement between its output motion and that of the able-bodied ankle-foot system.

The research questions included:

1. Can limited real-time EMG data be used as the sole control signal for a transtibial powered prosthesis?

2. Will the control strategy allow users to adapt to changing walking surfaces?

3. How well will the control strategy be able to adapt to new users? (i.e. how generalised will it be?)

4. Does the physical structure of the prosthesis significantly affect the functioning of an implemented control strategy?

The novel contributions of this research included:

1. Demonstrating that a generic approach, with a machine learning algorithm, yielded the best prediction accuracy when using a combined data set.

2. Facilitating powered control of two degrees of freedom (DoF) solely using EMG data from the lower leg muscles.

3. Facilitating volitional control on a transtibial powered prosthesis prototype using limited EMG data, only data from three lower leg muscles.

1.5 Thesis Overview

The succeeding chapter presents research that has been conducted within the field of lower limb prostheses to date, with a focus on powered prostheses and the control strategies implemented on these devices. The literature presented formed the basis of understanding of what is 'state of the art' research within this field and provided a basis from which to begin with the knowledge of best practice, as is relevant to this field.

Lower limb powered prostheses owe their development to continuing research being conducted within the field of human biomechanics. There has been limited gait research conducted with regards to humans walking over fixed, uneven terrain, compared to walking over level ground, ramp traversal or running. Inherently, research with regards to individuals with lower limb amputations traversing fixed, uneven terrain is even more limited.

Even though lower limb powered prostheses have enabled users to perform a wider range of locomotive activities with more ease, compared to passive prostheses. Unlike their biological counterparts, these prostheses are not designed to adaptively react to a changing walk surface.

An understanding of human biomechanics was required to develop a device that could facilitate gait that was comparable to able bodied human walking. The starting point of this research was gaining an understanding of how able-bodied human gait occurs as individuals walk over fixed, uneven terrain compared to level-ground. Chapters 3 presents the methodology used to conduct a gait experiment with able-bodied participants and the results acquired from said experiment. The overarching objective being the development of a control strategy that could facilitate gait over more varied terrain meant that a device that could physically realise such motion was required. As such, the development of a prototype which could move in a manner similar to that of a biological ankle-foot system, and upon which the performance of the developed control strategy was tested, is presented in chapter 4.

The endeavour of this research was to allow users more control over their prostheses. As such, user acquired EMG data was explored as a control alternative to currently implemented control approaches. The tendency to date has been to implement EMG signals as part of a sensor fusion approach. These signals are part of the inputs to high-level controllers, along with other data measured from prosthesis mounted sensors. This is as opposed to using real-time user acquired EMG signals to directly affect the output dynamics of a prosthesis.

Prostheses are meant to be functional extensions of the users. As such, the approach taken in this research, when developing the control strategy, was the pursuit of a way to facilitate prosthesis prototype output that was similar to that of able-bodied gait, based solely on real-time user acquired EMG data. The developed control strategy is presented in chapter 5. The various iterations and variations of prospective controllers, and their suitability to facilitate the desired output motion, are discussed within said chapter.

Testing the control strategy on a device that was similar to what it could be implemented on, were it a commercial product, was of importance. This meant that the performance of the entire system, and the achievable output, could be compared to that of the able-bodied human ankle-foot system. The methodology used to test and validate the developed system, both the control strategy and the developed prototype, is presented in chapter 6 along with the results from the validation experiment.

Chapter 7 brings a conclusion to this thesis and the work carried out during this research. The implications of the work presented are highlighted once again in this chapter, drawing a link between each of the research objectives, providing answers to the questions raised and summarising the overall contribution of this work. Future work is also presented in said chapter, along with possible applications from the research findings.

Chapter 2
Literature Review

Most developments in the field of lower limb powered prostheses occurred in the past two decades. However, these devices have been around for the last half a century. These prostheses have enabled users to achieve greater mobility, compared to their predecessors. Transtibial powered prostheses have enabled users to achieve a level-ground walking gait that is similar to that of able-bodied individuals. They have also been able to minimise user's energy expenditure (metabolic cost) when walking at self-selected, normal speeds [16].

The aim of this research was to develop a control strategy that could enable prostheses users to walk over fixed, uneven terrain. Further to this, was to empower the control strategy to facilitate some level of volitional control over a transtibial powered prosthesis prototype. EMG data is of significance when probing how movement is facilitated by the human body. This is because EMG data gives an indication of the motion, torque and power produced (or that will be produced within the next <100ms [21, 22]) by a muscle when performing certain tasks. The precursor of muscle activation, before actual limb movement, can be exploited to facilitate prosthesis control that is more volitionally focused. This was the approach used for this research.

Sutherland and Perry are credited with most of the research done in relation to the integration of clinical EMG and EMG digitisation with regards to observational gait analysis [23-25]. Perry was one of the first scholars to clearly demarcate the gait sub-phases, particularly as they relate to muscle activation. The basis of all assistive technology stems from the principles of human biomechanics. This includes devices such as prostheses, exoskeletons and orthoses. As such, an understanding of able-bodied gait formed part of the foundation of this research.

This chapter primarily serves as an introduction to the more recent control strategies that have been implemented on lower limb powered prostheses. These strategies will be presented and discussed. The purpose of which is elucidating some of the reasons behind the developmental path taken in developing the control strategy presented in this thesis.

2.1 Biomechanics of Human Walking

Human beings are plantigrades, meaning that the foot makes full contact with the ground during healthy ambulation. One of the characteristics of human walking is always having one foot on the ground at any given time, thus supporting one's body weight. There are also instances of double support where both feet support a certain portion of the full body weight.

Human running differs from human walking in that there are instances where neither foot is on the ground. Human running is defined as human walking with the absence of double support. Instead, there are instances of double swing (sometimes referred to as 'double float') [26].

An increase in walking speed results in a decrease of the stance phase, and thus a decrease in double support. This subsequently results in an increase of the swing phase. Human ambulation is complex. When simplifying it, it is best described in relation to a gait cycle which begins at heel strike of one foot and ends at heel strike of the same foot.

The human gait cycle is divided into two phases, the stance and the swing phase. The stance phase is the weight-bearing phase and the swing phase is the non-weight-bearing phase. Both phases also consist of sub-phases. During human walking, the stance phase accounts for approximately 60% of the gait cycle while the swing phase accounts for the remaining 40%. This is shown in figure 2.1.
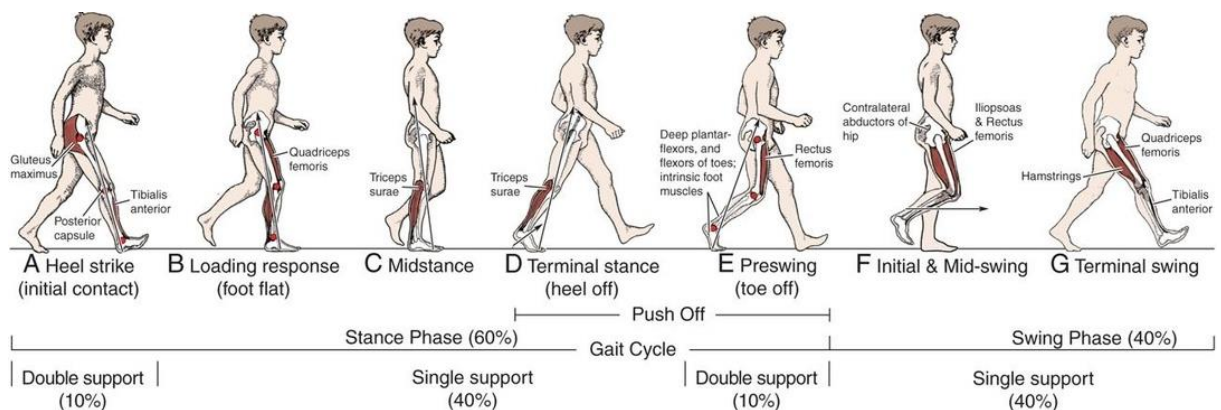
Figure 2.1: Human walking gait cycle (Copyright © 2011 Wolters Kluwer Health | Lippincott Williams & Wilkins)

Stance phase is made up of five sub-phases, namely heel strike, foot flat (foot loading), mid-stance, heel-off (terminal stance) and push-off (toe-off/pre-swing).

These sub-phases can be described as follows:

1. Heel strike – the heel of the foot makes initial contact with the ground and facilitates shock absorption. This is done by distributing the reaction forces from the impact through the lower leg bones and muscles. The leading leg also begins to bear some portion of the body weight, beginning double support.

2. Foot flat – the foot makes full contact with the ground. The leading leg begins bearing a larger portion of the body weight, more body weight than the trailing leg.

3. Mid-stance – the leading leg bears the full body weight (single support). The upper body and centre of mass (COM) transition from behind the leading leg to just in front of it.

4. Heel-off – the heel lifts off the ground. The body weight shifts to the ball of the foot. This motion is preparation for the body's forward propulsion.

5. Push-off – the leading leg bears less body weight as the trailing leg transitions forward towards heel strike. The weight on the leading leg shifts to the toes for push-off. The foot uses the ground reaction forces in response to its applied (muscle) force to flex the knee and hip joints. This propels the body forward and transitions the leading leg into the swing phase of the gait cycle.

The swing phase accounts for the remaining 40% of the human walking gait cycle. It consists of initial swing, mid-swing and terminal swing sub-phases, which can be described as follows:

1. Initial swing – the foot on the leading leg loses all contact with the ground. The leading leg knee and hip joints begin flexing in order to bring the leg forward.

2. Mid-swing – the leg is brought forward, and the knee extends in preparation for the next step ensuring the foot and toes clear the ground.

3. Terminal swing – the leg remains extended. The foot is dorsiflexed in preparation for the next step and to facilitate shock absorption upon heel strike.

Instances of double leg support occur between 0%-10% and 50%-60% of the gait cycle, illustrated in figure 2.1. This occurs as weight is transferred from one leg to the other. Instances of double support are observed when one foot experiences heel contact and the other foot is at heel-off (push off).

Average dorsiflexion and plantarflexion angles during human walking have been recorded to be ±10° and ±17° respectively, with respect to foot flat [27, 28]. The range of motion (ROM) of lower extremity joints is an important metric used in the study of human gait. The ROM data is usually coupled with ground reaction force (GRF) data. Joint moments and power are also used, along with the ROM and GRF data, in diagnosing gait problems.

The GRF data during able-bodied normal walking is shown in figure 2.2. The vertical reaction force is characterised by two peaks (fig. 2.2 A). The first peak occurs following heel-strike as the foot transitions to foot flat. The second peak occurs as the foot begins to push into the ground in preparation for push-off. The two peaks of the GRF along the anterior-posterior (AP) direction also occur following heel-strike and before push-off (fig. 2.2 B). The first peak occurs in the posterior direction as the foot slides forward slightly following heel-strike. It is the deceleration force (reaction) performed by the foot following the heel-strike, as part of shock absorption. The second peak along the AP direction occurs as the foot slides slightly backward during push-off, as the body is propelled forward. This reaction force is observed in the anterior direction as the foot slides posteriorly.

The final GRF is along the medial-lateral plane (fig. 2.2 C). This reaction force is the smallest of all three directions and remains relatively stable during level-ground able-bodied walking. The initial reaction force along the lateral direction occurs following heel-strike. It is in response to the foot moving medially following initial contact. The reaction force remains in the medial direction for most of the stance phase as the foot rolls laterally during this time. The first peak in the medial direction aligns with the first peak in the vertical GRF. The second, and usually largest, peak in the medial direction occurs around heel-off. This is during preparation for push-off. At this time, the foot begins to roll inwards which manifests as a lateral reaction force.
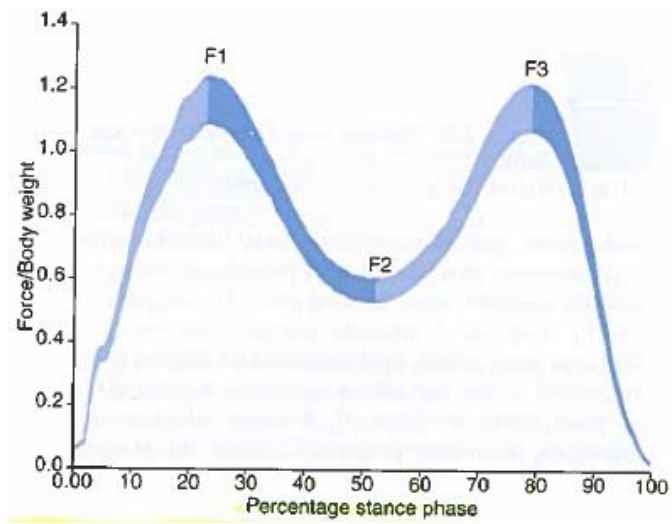
A) Vertical component of GRF
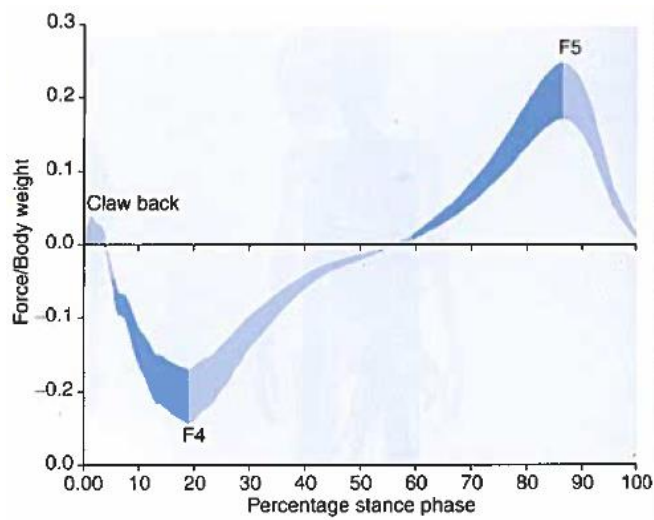
B) Anterior-posterior component of the GRF
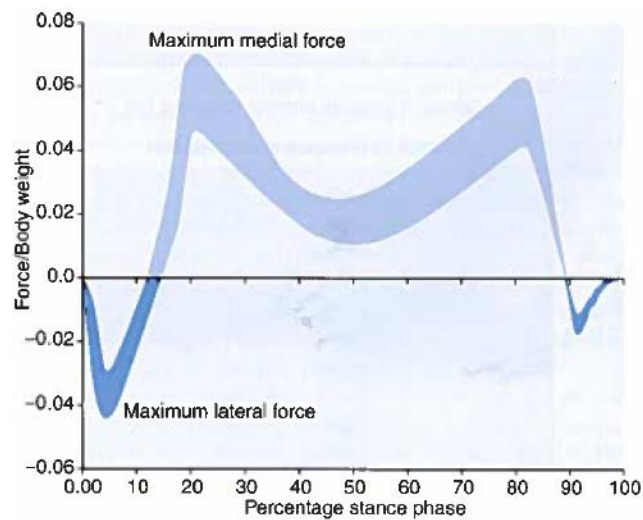
C) Medial-lateral component of the GRF

Figure 2.2: Able-bodied GRFs during normal walking [29]

Able-bodied ankle joint ROM is also shown in figure 2.3. The dorsiflexion angle increases throughout early stance phase and reaches its maximum around late mid-stance to heel-off. This is at approximately 40-50% of the gait cycle during able-bodied walking. Peak dorsiflexion is roughly aligned with the trough (F2 in fig. 2.2 A) of the vertical GRF. The foot transitions from dorsiflexion to plantarflexion as it begins to lift off the ground. This transition occurs more rapidly compared to the transition of the dorsiflexion angle. Peak plantarflexion occurs from heel-off and throughout push-off, as the body is being propelled forward. This is at approximately 60% of the gait cycle during able-bodied walking.

The ankle ROM along the frontal plane, particularly during able-bodied level ground walking, is akin to describing the foot roll angle. The foot is rotated slightly laterally (eversion) following heel strike. The foot remains more everted throughout stance phase. This portion of the gait cycle defines the foot roll angle. The foot then inverts during push-off as the body is propelled forward.

a) Sagittal plane   b) Frontal plane
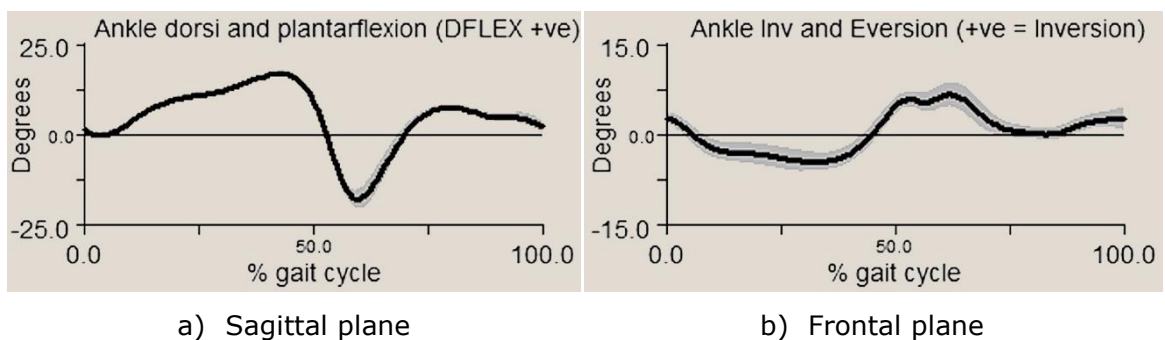
Figure 2.3: Ankle joint ROM during able-bodied normal walking [30].

Human ambulation is a dynamic and rather unstable action. It involves the solicitation of power from the muscles to provide skeletal motion and contribution from the tendons to facilitate balance and stability. The muscles in the thigh are also large contributors to walking [31]. These muscles are mostly used during the swing phase of the gait cycle whereas the muscles in the lower leg are mostly used during the stance phase of the gait cycle [32].

The muscle largely responsible for dorsiflexion is the tibialis anterior muscle. It is assisted by the peroneus tertius muscle. The gastrocnemius and soleus muscles are largely responsible for plantarflexion. They are assisted by the peroneus longus muscle. The tibialis anterior muscle is also responsible for foot inversion, while the peroneus longus, brevis and tertius muscles are mostly responsible for foot

eversion. Inversion and eversion of the foot is necessary for maintaining stability and balance on laterally inclined surfaces (inclined along the frontal plane) [27].

The complexity and limited understanding of human ambulation make mimicking human ambulation rather challenging. Particularly when wanting to understand the behaviour of the ankle-foot system as it functions under different terrain conditions. This challenge has to be overcome when designing and developing lower limb powered prostheses.

2.1.1 Muscle modelling

Muscle models have been developed to improve understanding on the functionality of muscles and to investigate the functioning of movements. One of the most fundamental muscle models is one developed by Hill [33]. This muscle model is phenomenological in nature. This means it can be thought of as a black box, reproducing known relationships between the input and output. A fundamental alternative to the Hill model is the cross-bridge theory of muscle contraction proposed by Huxley [34]. This theory explained how chemical energy was converted to mechanical work. It did so by explaining the rate of work during muscle shortening and the rate of energy (heat and work) liberation.

Nonetheless, the Hill-based muscle model is the most used particularly for movement simulation [35]. Hill-based muscle models usually consist of three components, as shown in figure 2.4. The relationship between muscle force and velocity is one of the most fundamental of muscle properties. Another fundamental relationship is that between muscle force and length. The muscle force and velocity are a function of the muscle (contractile element) length.

Hill was the first to measure and propose the hyperbolic relationship between muscle force and velocity during concentric contractions. This relationship is described by equation 2.1.

$$(F + a)(v + b) = b(F_o + a) \qquad \text{... (eq. 2.1)}$$

where:

F is the force (tension) in the muscle

a is the coefficient of shortening heat

v is the velocity of contraction

$$b = a \times {v_o}/{F_o}$$

F_o is the muscle's maximum isometric force

v_o is the maximum velocity, when F=0
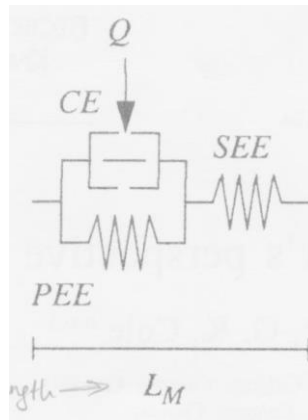
Figure 2.4: Hill muscle model consisting of the contractile element (CE), series elastic element (SEE) and parallel elastic element (PEE). Q indicates the muscle's level of activation and Lm is the muscle length [36].

Muscle models have also been used in the field of prostheses [37]. Their use has also extended to being used to inform the design of the actuation systems in lower limb powered prostheses [38]. This has led to these devices being able to produce output torque that is comparable to that of able-bodied individuals during level-ground walking [16, 39, 40]. They also minimise the foot-ground interaction at heel-strike and store and release passive energy through incorporated elastic elements [16, 39, 40]. These elastic elements are synonymous to the passive elastic element (PEE) in Hill-based muscle models (fig. 2.4). However, these prostheses remain incapable of producing the torque output required to facilitate locomotive tasks that require high-torque output [41]. This means they are still not as energy efficient as biological muscles.

2.2 Lower Limb Prostheses: The Evolution

Lower limb prostheses have evolved from basic peg legs [8] to devices that aim to achieve a physical appearance, control and weight that is similar to that of the amputated limb. Thus, current lower limb prostheses endeavour to go beyond simply allowing users to achieve mobility that is similar to that of able-bodied individuals. With regards to their design and functionality, lower limb prostheses can be grouped into three main categories. These are namely conventional feet, energy storage and return (ESR) devices and 'bionic'/powered feet.

However, from a control perspective, lower limb prostheses can be grouped into two categories. The first category is passive prostheses. The functionality of these prostheses relies solely on their construction. This includes the loading and unloading of passive elements (i.e. a mechanical spring) to assist with plantarflexion (push-off) during gait.

The second category is microprocessor-controlled prostheses. The functionality thereof is facilitated by a microprocessor. Some microprocessor-controlled prostheses *do not* add any net positive work (output energy) during gait; these are mechanically passive. Other such devices others *do* add net positive work during gait, assisting a user to attain a more biologically accurate gait. These are mechanically active or powered devices. Examples of these devices are presented in figure 2.5.
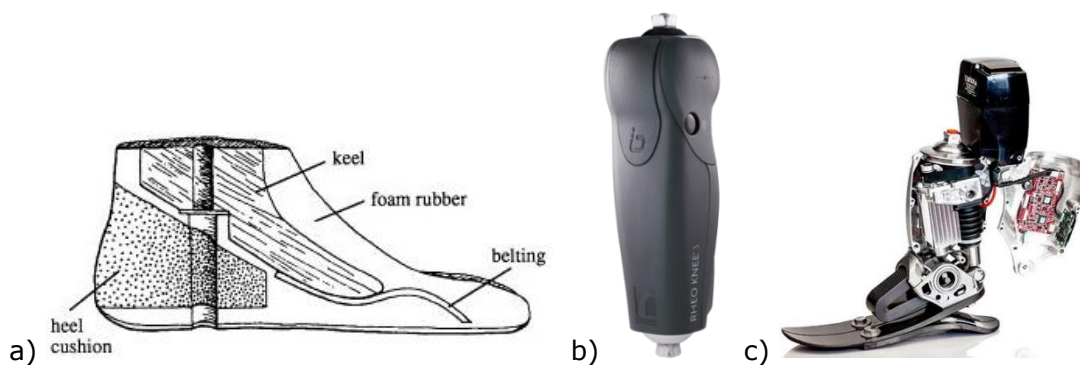
Figure 2.5: Example of the evolution of lower limb prostheses a) Representation of the SACH (solid ankle cushioned heel) ESR foot, b) the Rheo knee (Össur, Reykjavik, Iceland), a microcontrolled artificial knee and c) BiOM's microcontrolled powered ankle-foot

Microcontroller controlled artificial joints were developed to better mimic the behaviour of biological ankle and knee joints. Microcontrollers were initially fitted to passive ESR lower limb prostheses to control the output torque and movement of the artificial joints. This led to a decrease in the amount of effort required from the user during gait and alleviating the metabolic cost to the user [16].

Examples of such joints include the 3R80 knee (Ottobock, Duderstadt, Germany), the Proprio foot (Össur, Reykjavik, Iceland) and the Raize foot (Hosmer, Fillauer, California, USA). These prostheses have sensors that relay information such as joint angle and foot contact back to the microprocessor. In turn, the microprocessor alters the output behaviour of the prostheses to better mimic biological gait, such as extending the period of dorsiflexion. This type of prosthesis has enabled users to perform a number of different locomotion tasks which were previously more

physically taxing when using passive prostheses. An example of such a task is stair ascent and descent.

The main shortfall of passive prostheses, even those that are microprocessor controlled, is their inability to supply the user with positive energy during gait. Passive prostheses do not provide users with sufficient output energy during push-off. This additional energy is required to enable users to propel themselves forward in the most energy efficient manner. Positive work is present during healthy biological gait and is predominantly facilitated by the plantarflexor muscles, namely the gastrocnemius and soleus.

Lower limb powered prostheses preceded ESR prostheses and were developed to better mimic the ability of the biological limb to supply output energy. Powered prostheses are usually fitted with microcontroller-controlled joints. These prostheses have been proven to reduce the metabolic cost to a user during ambulation [16]. Examples of powered prosthesis include the SPARKy3 [39] and a powered ankle-foot prosthesis by the biomechatronics group of MIT[42].

Due to the design, composition and the functional needs required from powered prostheses, their control is more complicated than that of microcontrolled passive prostheses. Powered prostheses make use of sensors fitted on the prosthesis to relay information of the prosthesis' state and the user's current gait phase back to its microcontroller. Control strategies implemented on powered prostheses commonly use the information relayed back to the controller to facilitate the most appropriate output behaviour based on the sensed locomotion mode. The purpose of which is to approximate and respond to user intent. Thus, these prostheses make it easier for users to perform a larger variety of locomotion modes as compared to passive ESR prostheses [16].

Seminal work in the field of lower limb powered prostheses includes research conducted by Horn [43]. Horn used EMG signals from a participant's residual limb to control the locking mechanism of a prosthetic knee. Researchers from MIT later developed an above-knee powered prosthesis which had an artificial knee joint that was electrohydraulically powered [12, 44, 45]. This is shown in figure 2.6. Dyck et al [10, 46] also developed an electrohydraulical powered transfemoral prosthesis which had a knee joint that could be locked and unlocked by a participant activating a particular thigh muscle.
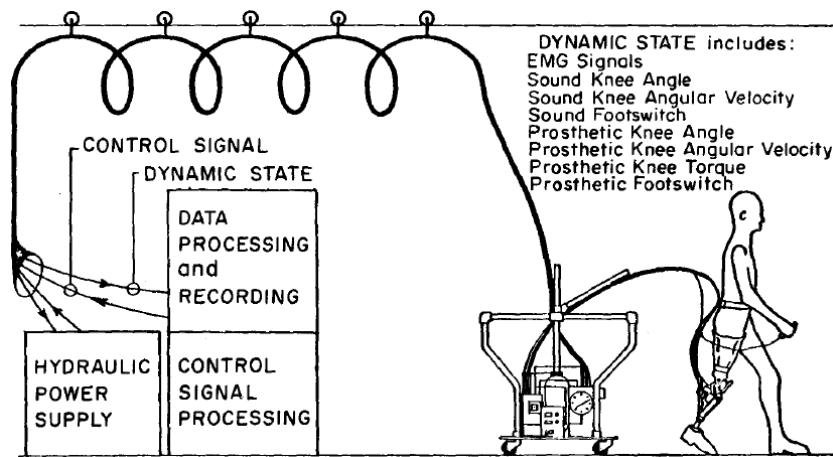
Figure 2.6: MIT electrohydraulically powered knee with human interactive prosthesis simulator [45]

Most of the research pertaining to lower limb powered prostheses has focused on transfemoral prostheses, as demonstrated by the aforementioned work. This remains the status quo. Further research still has to be conducted with regards to addressing the following challenges: 1) user instability, 2) the metabolic cost when performing a greater variety of locomotion tasks, 3) the limitation of the type of terrain users can traverse and 4) facilitation of volitional control over lower limb powered prostheses, particularly transtibial prostheses.

This review focuses on the various control strategies that have been implemented on lower extremity powered prostheses, predominantly within the last ten years. Within this thesis, these are deemed to be state-of-the-art powered prostheses. A brief review and summary of some of the state-of-the-art powered prostheses is presented in Appendix A. These are commercially available prostheses. Further details regarding the evolution of transtibial prostheses are presented in chapter 4.

The main emphasis was of this literature review was the feasibility of using user acquired EMG (electromyography) signals to facilitate control of lower limb powered prostheses. This was due to the research objective being to facilitate some level of volitional control over a multi-axial transtibial powered prosthesis.

Rather than being an exhaustive review of all research conducted in relation to lower limb prostheses, this review discusses what the author believes to be the most representative research conducted within the field of lower limb powered prostheses. This is specifically with regards to the control of these devices.

2.3 Electromyography (EMG) Signals

Myoelectric signals have been used for several years, largely within the medical field for the purpose of diagnosis and rehabilitation [47, 48]. EMG signals are electrical signals arising from the activation of skeletal muscles, measured using electrodes. These signals give an indication of the degree to which the muscles being observed are contracted. Muscles contract in response to nerve impulses which cause individual muscle fibres to twitch. The combined twitching of the individual muscle fibres leads to muscle contractions. EMG signals are measured as potentials (in Volts). They range from 50µV to 20-30mV [29]. The proportionality of the measured EMG signal to the level of muscle activation depends on the type of muscle contraction.

Two types of electrodes are commonly used to measure EMG signals. These are surface and intramuscular electrodes. Surface electrodes measure EMG signals from the skin above the muscle of interest. As such, care must be taken to ensure that muscle cross-talk is minimised. Intramuscular electrodes are needles inserted into the muscle itself. These electrodes are more robust in terms of minimising issues such as cross-talk. However, this method is more invasive compared to surface electrodes. Another disadvantage of intramuscular electrodes is that several electrodes are sometimes required to adequately measure signals from larger muscles.

EMG signals from various lower limb muscles are presented in figures 2.7 and 2.8. The differences between EMG signals measured using surface and intramuscular electrodes are shown in figure 2.7. It is observable that even though there are slight differences in EMG signals from the different electrodes, the signals still highly correlate. Emphasis is drawn to the differences in activation times between the thigh and lower leg muscles. The change in EMG activation timing and magnitude, in response to walking speed is shown in figure 2.8. It can be observed that an increase in walking speed leads to an increase in the level of muscle activation.
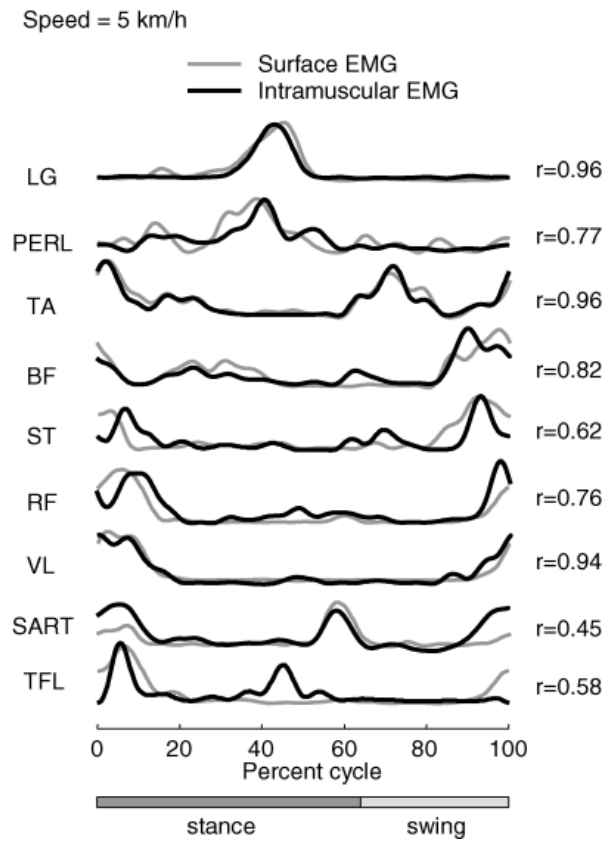
Figure 2.7: Intramuscular and surface EMG activity of 9 leg muscles recorded simultaneously in one subject stepping at 5 km h−1 on the treadmill. Correlation coefficients between intramuscular and surface EMG waveforms are shown on the right (r). [49]
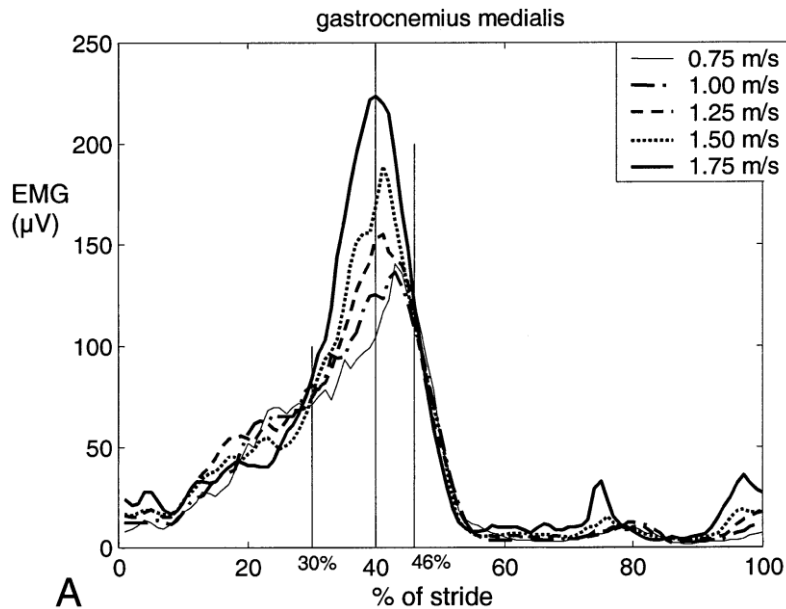
Figure 2.8: Averaged EMG profiles for GM muscle in walking at speeds of 0.75, 1.00, 1.25, 1.50, 1.75 ms−1 (from bottom to top) [50]

The use of EMG signals to control prostheses has been explored since around the mid 1950's [43, 51, 52]. Unlike for lower limb powered prostheses, myoelectric control of upper limb powered prostheses has been more extensively explored and these devices have been commercially available for decades [51]. As such, attempts have been made to use similar techniques implemented in EMG controlled upper limb powered prostheses on lower limb powered prostheses [53]. Lower limb prostheses have to support a user's entire body weight and safeguard user safety by ensuring that user stability is never comprised. This adds to the challenge of developing controllers for these devices.

Aspects such as the foot-ground interaction and differences in muscle activation make EMG control of lower limb powered prostheses challenging. The differences in muscle activations can stem from various sources such as myoplasty or muscle atrophy following amputation. The success of EMG control strategies implemented on upper limb powered prostheses can also be attributed to targeted muscle reinnervation that sometimes takes place before a prosthesis is made operational. Hargrove et al [54] successfully explored the use of targeted muscle reinnervation for the implementation of a lower limb powered prostheses.

The use of EMG signals in controlling lower limb powered prostheses can be divided into two categories. In the first category, EMG sensors form part of a sensor fusion data set (data fusion) which is used to reactively drive a prosthesis. Detection of the prosthetic's current locomotion mode is often part of this control approach [38, 55, 56]. In cases wherein the EMG data is used in some volitional manner, it comes from conscious activation of a specific muscle (or muscles). It is used to change some parameter of the prosthesis output behaviour, such as transitioning from level ground walking to traversing stairs [57]. As such, the implementation of EMG data can be seen as complimentary control to the main control strategy implemented.

The second category involves using EMG data as the key driver in altering prosthesis output behaviour [19, 53, 54]. This approach facilitates more volitional control over the prosthesis. This approach has mainly been implemented in transfemoral prostheses as opposed to transtibial prostheses. Presumably, this is due to there being larger muscles in the thigh compared to the shank, which makes reading EMG signals easier.

It is also because there is a reduced presence of motion artifact detectable at the thigh muscles as a result of foot-ground interaction during gait.

2.3.1 EMG Data as an Additional Input (Data Fusion)

With regards to powered prostheses, most research has focused on using EMG data as an input to a high-level controller. One such example was a study conducted by Au et al [58]. They compared a biomimetic control strategy to a neural network driven controller. They explored the controllers' ability to predict the desired ankle movement of a participant with a transtibial amputation. During the study, the desired ankle stiffness and position was communicated to the participant using a virtual model displayed on a screen.

Whilst in a seated position, the participant was asked to position their phantom ankle as displayed by the virtual model on a screen. EMG signals were recorded from the participant's tibialis anterior muscle during dorsiflexion and simultaneously from their gastrocnemius and soleus muscles during plantarflexion. Their biomimetic controller was a mathematical model based on the muscle model of the ankle-foot system. The participant acquired EMG data was used to train the biomimetic and neural network controllers to perform position control of an artificial ankle joint. Training of the controllers was done offline. They used an independent data set to test the performance of the developed controllers. Based on their results, both controllers could approximate the desired ankle trajectory. However, the output trajectory of the biomimetic controller was smoother than that of the neural network, which indicated the possible benefits of biologically inspired controllers in better mimicking human motion, if adequately formulated.

Au et al [57] tested the functionality of two finite state controllers with an EMG driven state transition during walking trials with a participant with bilateral transtibial amputation. One FSM (finite state machine) was used for level-ground walking and the other for stair descent. The prosthesis was equipped with sensors which provided the controllers with kinematic and kinetic data, along with ground reaction forces. They used EMG data acquired from the participant's residual limb to enable the participant to transition between the two finite state controllers. The EMG data was read in-socket during the trials. The system transitioned from the level-ground walking to the stair descent finite state controller when the user activated their gastrocnemii muscles to plantarflex during the swing phase.

The system transitioned back to the level-ground walking finite state controller when the user activated their tibialis anterior muscle. A neural network was used to classify the user's state transition intent based on the measured EMG data.

Transitioning between the two finite state controllers was successfully accomplished using the participant's EMG signals. Even though the participant had to consciously activate particular muscles to transition between the two locomotion modes, the control of the transtibial powered prosthesis was somewhat more natural as the muscles to be activated were those naturally used by able-bodied individuals during gait. With their study, Au et al [57] demonstrated that viable EMG signals can be read in-socket from the residual limb of an individual with a transtibial amputation and successfully used to facilitate control of a lower limb powered prosthesis. However, volitional control within each specified locomotion type (level ground or stair descent) was not possible as only the finite state controllers specified the output behaviour of the prosthesis based on the feedback from the extrinsic (prosthesis mounted) sensors.

Hargrove et al [54] developed an EMG driven transfemoral powered prosthesis. Their initial test was to ascertain the difference in accuracy when controlling a virtual powered prosthesis. They compared EMG signals from surgically reinnervated muscles to those from natively innervated muscles. This was done with a participant with a unilateral transfemoral amputation in a seated position. They found that classification accuracy was better for the surgically reinnervated muscles. Their second test was to determine how the addition of user acquired EMG signals affected the completion of various locomotion tasks.

The powered prosthesis was equipped with 13 sensors which were used to facilitate its control. These included an accelerometer, two magnetic encoders to measure ankle and knee joint positions, a uniaxial load cell and a load sensor. They implemented a dynamic Bayesian network to classify the data from the prosthesis mounted sensors and from the EMG signals, which were read in-socket. The classified data was used to interpret the participant's intent which was used to select a locomotion mode and to set the ankle and knee joint torques. Their results showed that classification accuracy increased with the inclusion of EMG data. The classification error for all locomotion modes was 12.9% when using the prosthesis mounted sensor data.

This error fell to 2.2% with the incorporation of EMG data from the natively innervated nerves and fell further to 1.8% with the incorporation of EMG data from the surgically reinnervated nerves. The highlight of the study was the participant being able to volitionally control both the ankle and the knee joints of the powered prosthesis while in a seated position. This was a non-weight bearing mode which allowed the participant to reposition their prosthetic leg without touching it.

2.3.2 EMG Data as the Primary Control Variable (Volitional Control)

Wang et al [42] developed a transtibial powered prosthesis that allowed its user to alter the degree of push-off during powered plantarflexion using their residual limb muscles. They used a FSM as a high-level controller to synchronise the gait cycle of the powered prosthesis. User acquired EMG data was used to alter the gain of the powered ankle joint during level-ground walking. This was done by making the controller's gain proportional to the measured EMG data, thus altering the prosthesis power output at push-off (powered plantarflexion). The EMG data was measured only from the lateral gastrocnemius muscle of the residual limb and was read from mid-stance to terminal stance. Their powered ankle allowed the user to achieve a gait similar to that of able-bodied individuals. However, the manner in which the FSM was implemented, and it being continuously active as the high-level controller, limited the volitional control of the prosthesis. Nonetheless, this study demonstrated that user acquired EMG data could be successfully used to alter control parameters of a powered prosthesis, even with limited manipulation of the raw EMG data.

Huang et al [53] developed a pneumatically powered ankle-foot prosthesis which allowed its user to volitionally control the device's plantarflexion. Proportional control was implemented to activate an artificial gastrocnemius muscle on the powered prosthesis based on user acquired EMG data. Their controller did not rely on gait phase detection and thus, facilitated more natural transitional control. EMG data was read from the participant's gastrocnemius muscle using electrodes placed at the residual limb-prosthesis socket interface. They proportionally scaled the output control signal according to the measured EMG data, which was used as an input signal to the pressure regulators of the device's plantarflexor pneumatic muscle. The pressure regulators of the device's dorsiflexor pneumatic muscle received a constant signal directly from the controller during walking. This meant that the participant could not control dorsiflexion of the powered prosthesis through muscle activation.

Their participant, who had a unilateral transtibial amputation, could generate a push-off ankle power of 7.28W/kg and achieve a sagittal plane ankle angle of 30°using the developed prosthesis, compared to the push-off ankle power of 3.35W/kg and ankle angle of 18° the participant achieved using their own prescribed prosthesis.

In their study, Huang et al [53] demonstrated the feasibility of successfully facilitating volitional control of a transtibial powered prosthesis using EMG data read from a participant's residual limb. Their results also demonstrated that prolonged use of the powered prosthesis allowed the participant to become more comfortable walking with the device. This was evident in their participant's muscle activation results which suggested that the participant was adjusting and adapting muscle activation, resulting in the participant's muscle activation over time becoming more similar to that of able-bodied individuals.

Dawley et al [19] used EMG data to drive a powered knee of a transfemoral prosthesis. A participant volitionally controlled the powered knee by activating the muscles in their residual limb in a manner synonymous to able-bodied individuals during level-ground walking. Their control strategy leveraged the characteristic behaviour of antagonist muscle pairs to facilitate motion. They focused on the antagonist muscle pairs in the thigh. This approach allowed the participant to activate their thigh muscles in a natural manner in order to drive the prosthesis, as opposed to training the participant to activate specific muscles in order to execute specific movements with the powered prosthesis.

The EMG data was read in-socket from the quadriceps and hamstrings muscles, which were responsible for flexion and extension of the participant's phantom knee. They used Principal Component Analysis (PCA) to define boundaries of an impedance range used when controlling the powered knee. The EMG data measured from the participant was used to alter the knee joint torque of the powered prosthesis. They developed a calibration algorithm to ensure that maximal EMG data could be measured from the participant with each donning of the prosthesis socket. Their calibration approach calculated the amount of antagonist muscle co-contraction on the participant's residual limb and compensated for it.

Their transfemoral powered prosthesis enabled the participant to better mimic biological gait and the participant's gait improved with longer use of the powered prosthesis. Performing calibration with each donning of the prosthesis made their controller more robust to slight electrode shift and to differences in muscle co-contraction levels.

2.4 Classification Algorithms

Recent control strategies implemented on powered prostheses use classification algorithms to ascertain the user's current locomotion mode or their level of muscle activation. This includes devices that use prosthesis mounted sensors. This is done to estimate the user's intended locomotion mode to facilitate appropriate corresponding prosthesis actuation/control action.

Classification algorithms are used to classify new data (inputs) into specified classes or categories using a criterion. When developing a classification criterion, algorithms are initially trained to map known input data to known, specified output groups or classes. Classification algorithms are a promising avenue to facilitate control of lower limb powered prostheses. However, their main drawback is the amount of data and time required to train them to accurately classify new data. The need for a prosthesis implemented algorithm to be capable of 'adapting' to new users further increases the amount of training data and time required. This is also the case when the data to be classified is EMG data. Lower limb powered prostheses that can be controlled via user muscle activation (EMG data) have the potential to facilitate natural gait that is volitionally controlled.

Factors that influence the generalisation of control strategies for EMG controlled lower limb powered prostheses include, but are not limited to, the level of amputation, the placement/relocation of muscles during the initial amputation operation, the manner in which an individual heals, whether or not repeat operations were performed following the initial amputation operation and changes in muscle volume. Numerous classification algorithms can and have been used on EMG data. Even though the computational requirements of classification algorithms remain relatively fixed and independent of their application, their performance and accuracy when implemented on EMG data for use in lower limb powered prostheses can be subject to several factors, namely:

1. The classification algorithm itself; the type and composition of the algorithm used, such as the number of hidden layers in Neural Networks.
2. The placement of EMG electrodes.
3. The features used for classification.
4. The number of EMG channels used.
5. The way data is computed and processed, e.g. analysis window size, windowing scheme, etc.
6. The training data used, including the number of EMG channels, the chosen features and the data size.

When classifying EMG data acquired from participants with transtibial amputations, LDA (linear discriminant analysis) was shown to be more accurate in the presence of electrode shift compared to using a SVM (support vector machine) [59]. However, for participants with transfemoral amputations, a SVM demonstrated better locomotion mode identification than LDA [56].

LDA also outperformed a NN (neural network) for participants with transfemoral amputations [55]. However, LDA was outperformed by a dynamic Bayesian network with regards to user intent recognition accuracy [60]. Fuzzy logic has also been implemented for user intent recognition using EMG data [61]. Its relative simplicity, ease of implementation and adaptation, makes it an appealing classification algorithm. However, fuzzy logic's generalisation to new data can be problematic at times due to its lack of robustness, usually because of inadequately defined membership functions. A Gaussian mixture model (GMM) was also used to determine user intent for a transfemoral powered prosthesis, resulting in good classification accuracy [62]. However, constructing an effective GMM based classifier can be a time-consuming process.

QDA (quadratic discriminant analysis) was used by Ha et al [63] in their study of an EMG controlled prosthetic knee during non-weight bearing activities. They opted for QDA instead of LDA because they wanted to classify user intent in the presence of muscle co-contraction. As QDA implements a quadratic decision boundary, as opposed to a linear decision boundary used by LDA, QDA is a comparably more robust classifier without it having a significant increase in its complexity. PCA (principal component analysis) has been used to reduce feature set dimensions and to identify the optimal features. These features are then used by a classification algorithm implemented for user intent recognition [64].

LDA has also been implemented to reduce feature set dimensionality [62]. PCA has proven useful in the presence of muscle co-contraction with regards to volitionally controlled lower limb powered prostheses, particularly for knee extension and flexion [19, 63].

Bayesian networks have seldom been used in powered prostheses. However, when used, they were mostly employed for the classification or filtering of EMG data from the upper limbs. Other instances wherein Bayesian networks were used in relation to prostheses was for the classification of EMG signals related to hand and wrist motions for controlling an upper limb powered prosthesis [65], predicting muscle activity with the future goal of stimulating muscles using FES (functional electrical stimulation) for prospective use in neuro-prosthetics [66] and, using a Bayesian filter, to derive control signals to be used in a powered prosthesis [67, 68]. The use of Bayesian networks to classify user intent has previously resulted in good accuracy. However, the availability of other less complex classifiers, able to recognise user intent based on EMG data with comparable accuracy, makes the use of Bayesian networks impractical for real-time use in lower limb powered prostheses.

Miller et al [59] used LDA and a SVM to classify seven locomotion modes for participants with unilateral transtibial amputations and for able-bodied participants. The seven locomotion modes to be classified included level-ground walking at three different speeds, namely self-selected, slow and fast. It also included stair ascent/ descent and ramp ascent/descent. EMG data was recorded from the tibialis anterior, medial gastrocnemius, vastus lateralis and biceps femoris muscles for both participant groups. Their results indicated that both classifiers were capable of classifying the participant's seven locomotion modes with reasonably good accuracy, as shown in table 2.1. However, in the presence of a simulated electrode shift condition along the medial gastrocnemius muscle, LDA outperformed the SVM.

Electrode shift, particularly along the medial gastrocnemius muscle, resulted in the largest reduction in classification accuracy for both classifiers. Miller et al [59] also found that the classification of the stair ascent/descent locomotion modes was the most resistant to electrode shift. This could be attributed to the uniqueness of muscle activity when performing stair ascent and stair descent motions.

Differentiating between the different level-ground walking speeds was the most challenging aspect as the muscle activation patterns and intensity amongst the three speeds were rather similar.

The LDA's performance and classification accuracy, especially in the presence of electrode shift, and its relatively low computational complexity makes it an appealing classifier for real world application in lower limb powered prostheses as compared to the SVM.

Table 2.1: Classification accuracy for participant group with unilateral transtibial amputations under optimal electrode positioning and electrode shift conditions (±SD) [59]

	LDA	SVM
Classification of Locomotion Modes Under Optimal Electrode Positioning	97.9% (±0.22)	97.9% (±1.39)
Classification of Locomotion Modes Under the MG-Shifted Electrode condition	82.1% (±17.8)	74.8% (±22.34)

Classification algorithms are powerful tools as they can ascertain user motion using a variety of inputs. The aim of this research was to develop a control strategy that can facilitate a level of volitional control over a transtibial powered prosthesis. As such, classification algorithms capable of determining the motion a user wants to implement were explored. The adequacy of classification algorithms, with relation to powered prostheses, comes down to various factors as presented in the preceding section.

2.4.1 Feature Types
Identifying features that will result in the best classification accuracy for user intent recognition, thus enabling a controller to best facilitate biological gait and natural locomotion mode transitions, is a challenge in developing an EMG driven controller for a lower limb powered prosthesis.

It has been suggested that the accuracy of classification algorithms implemented on EMG data is influenced more by the chosen feature set, the features chosen to ensure optimal class/motion separation, rather than the classification algorithm itself [69]. There are three types of features with regards to EMG data. These are time domain, frequency domain and time-frequency domain features [70].

Time domain features are in the same 'space'/domain as the raw data, meaning no mathematical transformation is required to compute them. This becomes advantageous when computing and implementing these features in real time. Examples include slope sign changes, variance and wavelet features [71]. This type of feature is best used to analyse EMG data that is periodical, such as data amplitude or patterns during cyclic movements.

Raw EMG data has to undergo mathematical transformation, usually implementing fast Fourier transform, to enable the computation of frequency domain features, which give an indication of the power spectrum density of the EMG signal. Examples include auto-regressive coefficients, frequency mean features and frequency ratio features [71]. These features are usually used in determining muscle fatigue and/or analysing EMG data from less cyclic and more dynamic movements, such as diagnosing movement disorders [72].

Time-frequency domain features aim to represent the EMG signal in both time and frequency domains, with the aim of having a more accurate and holistic representation of the signal. However, these features are the most computationally expensive. Examples of features within this domain include short time Fourier transform, wavelet transform and wavelet packet transform [71].

For all of the feature types, the objective becomes choosing features, or a combination thereof, that lead to the most optimal separation of data. This is particularly important when implementing a machine learning based control strategy.

2.4.2 Number of EMG Channels

The number of EMG channels used has also been shown to influence classification accuracy. Hargrove et al [64] demonstrated this factor in their study which investigated whether intramuscular EMG signals resulted in higher classification accuracy compared to surface EMG signals. The signals acquired using surface EMG electrodes had higher levels of crosstalk as compared to those acquired using the intramuscular EMG electrodes. They also investigated how the number of channels and channel subsets, particularly for surface EMG data, affected classification accuracy. They used two methods to select the most optimal channel subset. The first was a symmetrical method that symmetrically reduced the number of channel subsets. The second was an exhaustive method that investigated all possible channel subsets and determined the most optimal subset.

From their results, the optimal channel subset converged quicker to the maximum classification accuracy. Using the optimally chosen channel subset, using three channels resulted in a classification accuracy that was comparable to the initial number of channels used for the surface EMG, which was 16, as compared to 6 channels used for the intramuscular EMG [64]. The optimal three channel subset resulted in an average classification accuracy of 97% for the surface EMG data.

The results from Hargrove et al [64] also demonstrated a slight decrease in classification accuracy when the channel subset was increased past 8. This could have been due to a loss of useful data as the feature set to be used for classification was limited to only the first 40 principal components. Even though increasing the dimension of the feature set could potentially also increase the classification accuracy, this also increases the training time. It could also necessitate the use of a more complex data reduction algorithm to better acquire useful data for successful classification.

Findings from Young et al [60] suggested that there is a non-linear correlation between the reduction in classification error and the addition of EMG electrodes. In their study, Young et al [60] investigated the extent to which sensor fusion increased the classification error of an intent recognition algorithm. They also investigated which classification algorithms resulted in the best accuracy. Their study consisted of eight participants, six with transfemoral amputations and two with knee disarticulations. The participants donned a custom made transfemoral powered prosthesis for the experiment. The transfemoral powered prosthesis was equipped with sensors to determine the positions and velocities of the ankle and knee joints, an axial load cell, a six-axis inertial measurement unit (IMU) and EMG electrodes to measure data from nine lower leg muscles. The sensor data was used as input data to their classifier.

They found that the best classification accuracy was obtained when all the sensors were used. They also found that the second-best classification accuracy was obtained when the inertial and EMG data was used together, or when either the inertial or EMG data was used with any of the other data sets (sensor data). From their results, steady-state error was significantly reduced when two EMG electrodes were incorporated along with the prosthesis mounted sensors. These were placed on the biceps femoris and sartorius muscles, respectively. Little improvement was gained after the addition of four EMG electrodes.

For transitional error, three electrodes, placed on the biceps femoris, sartorius and adductor magnus muscles respectively, incorporated along with the prosthesis mounted sensors, resulted in a significant reduction in error. However, unlike for the steady-state case, the error continued to decrease with the sequential addition of the six remaining EMG electrodes.

2.4.3 Analyses Windows

Analysis window length and window size increment are other factors that have been shown to influence classification accuracy. This is mainly due to the non-stationary nature of EMG signals, particularly those from the lower limbs. The choice of analysis window length influences the 'quality' of the extracted features to be used by a classification algorithm.

Huang et al [55] conducted a preliminary study of identifying locomotion modes based on EMG data from muscles in the thigh, shank and foot of eight able-bodied participants and two participants with long transfemoral amputations. They found that analysis window lengths greater than 140ms produced the highest classification accuracies when used with window size increments of 30ms. This was with either time-domain (TD) features or autoregressive (AR) features. Autoregressive and time-domain features have been extensively used in studies aimed at classifying EMG data acquired from the lower limbs. This is because these types of features do not require signal transformation, meaning real-time control can be facilitated for a lower limb powered prosthesis with minimal delays from the controller [55, 59, 73].

Similar to the study by Huang et al [55], Young et al [60] used two analysis windows, one at toe-off and another at heel strike, to make classification decisions. They found that increasing the length of the analysis window from 50ms to 150ms during steady-state and even further, until 250ms, for transitions, improved the classification accuracy, but only up to a certain threshold for both steady-state and transitional errors. They also found that increasing the number of analysis windows decreased the classification accuracy for both the steady-state and the transitions. Their results supported the findings of other scholars that there is a non-linear correlation between increasing certain parameters, such as analysis window length, and decreasing classification errors for user intent recognition, with regards to lower limb powered prostheses [55].

The literature presented in this review suggests that even though there is a non-linear correlation between the reduction in classification error and the addition of EMG electrodes, this correlation is dependent on factors such as the muscles from which the EMG data is acquired, the selected features and the analysis window size.

2.4.4 Training Data (Sensor Fusion)

Powered prostheses are fundamentally robotic machines that work in unison with the user. Therefore, they have to facilitate movement when prompted to do so by the user. In order for these prostheses to facilitate appropriate movement, they have to be aware of the user's current locomotion mode and/or be attuned to the user's intended motion. Several approaches have been used to acquire relevant information to estimate the user's intended motion, with reference to their current locomotion mode. Various sensors have been used to keep track of users' locomotion modes. These include force sensitive resistors, placed on a shoe insole or under the prosthetic's sole, and inertial sensors mounted on the prosthesis. These types of sensors are also used to monitor changes in a user's environment, such as transitioning from level ground walking to traversing stairs.

However, as of late, user acquired EMG data has also been explored more extensively as a means of ascertaining a user's intended motion, also referred to as 'user intent'. User acquired EMG data has the potential to allow a system to pre-empt a user's motion based on certain muscle activations, as opposed to purely reacting to performed/perceived external actions, i.e. feedback from prosthesis mounted sensors. Other implemented approaches have also included measuring the change in capacitance from an instrumented band placed around a participant's thigh [74]. The disadvantage of such approaches is the need to instrument an 'unaffected' area, such as instrumenting the thigh area for transtibial amputees or placing sensors on the intact limb such that its motion can be mirrored by the affected limb.

One of the highest classification errors experienced during intent recognition, when either prosthesis mounted sensors or EMG data is used, occurs during ramp traversal [60]. Unlike when traversing stairs, similar muscles are activated to similar degrees during level-ground walking and ramp traversal, especially when the ramp incline is not significantly large (< 20°). To date, the classification error for ramp traversal has usually been lower when prosthesis mounted sensors were used as compared to when only EMG data was used. This is primarily because data acquired from prosthesis mounted sensors is less variable than EMG data [75].

Young et al [60] investigated a possible way of circumventing this problem by classifying ramp locomotion as level-ground walking for their implemented classifier. Their approach led to a reduction in classification error when prosthesis mounted sensors and EMG data were used individually. The reduction in classification error was even greater when both sensor types were used together. Their approach would be useful for ramps with small inclines (≤ 20°), though it could inhibit users from attaining biologically similar gait when traversing slopes with larger inclines as the powered prostheses would not make the required changes to the actuation and joint dynamics.

Other research [56, 76] supports the findings of Young et al [60] that the inclusion of other types of sensor data, in addition to user acquired EMG data, improves the overall accuracy of classification algorithms and thus the ability of a powered prosthesis to enable a user to achieve a more biologically similar gait. In their study, Huang et al [55] found that using EMG data solely from muscles in the shank and foot resulted in higher classification errors during locomotion mode detection as opposed to using EMG data from thigh muscles.

The study by Young et al [60], wherein sensor fusion data from 13 prosthesis mounted sensors was used to train a LDA classification algorithm to improve intent recognition accuracy, provides a good indication of how classification accuracy is dependent on the chosen training approach and data. From their study, the intent recognition accuracy using only the prosthesis mounted sensors was 84.5%, the accuracy increased to 93.9% with the inclusion of the transitional training data. Their findings support the hypothesis that incorporating different types of data improves the overall intent recognition accuracy [56] which leads to safer and more natural locomotion mode transitions, subsequently improving gait for the prosthesis user. Even though their approach of using transitional data to train their intent recognition classifier resulted in smoother transitions, it also resulted in higher steady-state errors. These steady-state errors were decision errors resulting from the classifier falsely specifying a transition when the user was actually walking in one of the five defined locomotion modes.

2.5 Output Control: Finite State Machines (FSMs)

Various control strategies are currently employed to facilitate the actuation of lower limb powered prostheses, with the objective of enabling gait that better mimics that of biological limbs. Control strategies employed often use algorithms which receive

inputs from external, prosthesis mounted sensors to trigger locomotion mode transitions. The output of these control strategies is usually either position (angle) or torque control. Though sometimes both control methods are facilitated at different levels on the same prosthesis.

Finite state machines are a type of control strategy wherein a specific event (an input) transitions the output from one state to another, thus resulting in a new output. There are a finite number of states and the system can only be in one state at any given time. Most powered prostheses make use of sensors, such as accelerometers or gyroscopes, to measure kinetic and kinematic data to provide feedback/inputs to high level controllers. In most lower limb powered prostheses, the information that is fed back to the controller(s) is used to facilitate transitions between locomotion modes, such as transitioning from level-ground walking to ramp traversal. FSMs are the most widely used control strategy for lower limb powered prostheses [40, 77-80]. A few new control strategies for lower limb powered prostheses also make use of EMG signals acquired from the user's residual limb, along with classification algorithms, to better predict the user's intended motion and to facilitate transitions between locomotion modes using FSMs [54, 55, 57].

When implemented on lower limb powered prostheses, FSMs are usually used to alter the output behaviour of the prosthesis based on either 1) the measured/sensed device state, such as the angles of the prosthetic joints or the foot contact, or 2) the output of higher level controllers, such as a classification outcome. In the first case, the FSM acts as a high-level controller or as the only control strategy implemented, using extrinsic (prosthesis mounted) sensors. In the second case, the FSM functions as a mid or low-level controller only specifying when or under what circumstances a specific output, as specified by a high-level controller, should be executed by the prosthesis.

2.5.1 Case 1: FSM as A High-Level Controller

An example of the first case of FSM usage was is a study by Sup et al [78]. They developed a control strategy for a knee and ankle powered prosthesis to allow a participant with a unilateral transfemoral amputation to better traverse upslopes (inclines/ramps). They used a finite state based approach along with sensors fitted on the prosthetic foot to control locomotion mode transitions. Using an accelerometer, they also implemented a threshold method to alter the angles of the powered ankle and knee joints in response to the changing terrain.

The output torque to be supplied by the device was with reference to that of healthy human gait. This meant the prosthesis would output a torque synonymous to that of an able-bodied individual for a particular gait phase.

The efficacy of their controller was tested by having a participant walk over level-ground, a 5° incline and a 10° incline using the developed powered prosthesis and also the participant's own daily-use prosthesis. The ankle and knee joint angles of the participant's passive prosthesis and those of the powered prosthesis were compared to those of able-bodied individuals walking over level-ground, an 8° incline and a 10° incline. The joint angles of the powered prosthesis were similar to those of able-bodied individuals even when the participant traversed the upslopes. The joint angles acquired when using the passive prosthesis were smaller than those acquired when using the powered prosthesis. This was due to the passive prosthesis not providing net positive work to the user during ambulation. Nor did it adapt its parameters, such as increasing ankle dorsiflexion, in response to the changing terrain.

2.5.2 Case 2: FSM as A Low-Level Controller

An example of the second case of FSM implementation is a study by Young et al [60]. They investigated whether training a classification algorithm using data acquired from prosthesis mounted sensors during smooth locomotion mode transitions could improve intent recognition accuracy. Six participants with transfemoral amputations took part in their study. Using a powered prosthesis, the participants completed a training circuit consisting of level-ground walking, stair ascent, stair descent, ramp ascent and ramp descent. Using software, smooth locomotion mode transitions were manually effected by an experimenter at heel contact or toe-off, preceding a change in the walking environment.

Data was recorded using 13 sensors mounted on the prosthesis. The sensor data recorded during transitions was used to train a LDA classifier. The same powered prosthesis used during the data acquisition phase was also used during the testing phase. A finite state machine with five states was implemented to facilitate transitions from one locomotion mode to another based on the classification outcome from the LDA.

2.5.3 Advantages and Disadvantages of FSMs

FSMs are a straight forward way of 'programming' powered prostheses to perform certain control actions at specific phases of the gait cycle and/or given certain feedback/inputs. By virtue of their design, FSMs are unable to facilitate control actions that are not pre-programmed, thereby usually limiting the user to certain pre-defined locomotion modes. Thus, they need to be 'programmed' for all likely prostheses output behaviours based on both the expected and unlikely, but still possible, input data scenarios. This could be a limiting factor in facilitating volitional control of lower limb powered prostheses.

Most lower limb powered prostheses use a FSM control strategy to ensure that state appropriate control is implemented [42, 57, 77-80]. This control strategy has proven effective in enabling users to achieve a biologically similar gait at normal, self-selected walking speeds. However, because prosthesis mounted sensors which measure the current state of the device are usually used as control inputs to drive the output behaviour of the prosthesis, users are unable to volitionally control their prostheses.

Within this research, user acquired EMG data has been explored as a possible control alternative to high-level FSM control, using only extrinsic sensors. This was in an endeavour to allow prospective users more control over their prostheses.

2.6 Challenges in Using EMG Data for Lower Limb Powered Prostheses

A study by Hargrove et al [54] highlighted the difficulty of developing an EMG controller to be implemented on a lower limb powered prosthesis. These difficulties are due to factors such as the feasibility of using surface electrodes for long periods of time, whilst also minimising motion artifact between the residual limb-socket interface. The majority of EMG usage with regards to lower limb powered prostheses has been in transfemoral prostheses. This could be attributed to it being easier to acquire EMG data from the thigh muscles, as compared to muscles in the shank, due to their size. Another factor could be that the knee joint is less susceptible to changes due to different kinds of shock loading, particularly at heel-strike, associated with foot-ground interaction compared to the ankle joint [81, 82]. The use of EMG data in transfemoral powered prostheses has largely focused on user intent recognition to alter the dynamics of the prosthetic knee joint.

One of the challenges associated with the use of EMG data to control protheses is the acquisition of said data. Silver-Thorn et al [83] investigated whether viable EMG data could be read in-socket from individuals with transtibial amputations. They also investigated whether said data could be used to control a transtibial powered prosthesis. They implemented a threshold method to determine when the muscles typically used for dorsiflexion and plantarflexion were respectively on or off. This was similar to that used in some commercially available upper limb powered prosthesis [84]. They read in-socket EMG data from three participants with transtibial amputations using low-profile surface electrodes. Their results indicated that individuals with transtibial amputations still maintained independent control of the residual muscles that were previously used to move the now amputated limb. However, the timing of said muscle activity was not always similar to that of able-bodied individuals. From the results presented by Silver-Thorn et al [83], one can deduce that the relocation of muscles in the residual limb following myoplasty has implications with regards to EMG crosstalk. In their study, this was most evident for one participant whose muscle pair, which is naturally posteriorly located, had been anteriorly relocated.

These results were similar to those reported by Huang and Ferris [85]. They also investigated whether muscle activation from individuals with transtibial amputations could be read between the residual limb-prosthesis socket interface. They used surface electrodes to measure EMG data from muscles in both the lower and upper leg. The EMG data was measured from participants with unilateral transtibial amputations (n=12) and able-bodied participants (n=12). Their results supported previous findings that surface EMG data could be read reliably from the residual muscles of individuals with transtibial amputations [83].

Most of the participants with transtibial amputation could volitionally activate their lower leg muscles as if performing dorsiflexion and plantarflexion with their phantom limb. During the walking trials, the lower leg EMG data from the participants with transtibial amputations differed from that of the able-bodied participants. However, the upper leg EMG data for both participant groups were similar. The participants with transtibial amputations generally had higher levels of muscle co-activation than the able-bodied participants, thus supporting the findings of Seyedali et al [20]. Huang and Ferris [85] suggested that this was due to a lack of visual feedback to the participants with transtibial amputations while performing said actions.

Their results also indicated the differences in muscle activation timings during ambulation and the degree of muscle co-activation present in the residual limbs of the participants with amputations, which differed to that of the able-bodied participants.

Seyedali et al [20] compared muscle co-contraction patterns of able-bodied individuals (n=5) and individuals with unilateral transtibial amputations (n=9). They used in-socket surface EMG electrodes for the participants with transtibial amputations. They compared the co-contraction patterns of the ankle antagonist muscle pair and the knee antagonist muscle pair in both limbs of both participant groups. Their results showed that co-contraction levels of the ankle muscles for the participants with transtibial amputations were larger in their residual limb, compared to their intact limb. The co-contractions levels were also larger than those of the able-bodied participants. For the knee antagonist muscle pair, their results showed that co-contraction levels in the residual limbs were the highest of all compared. Their results highlighted the difficulty of developing an EMG focused control strategy for transtibial prostheses. These difficulties lie in developing control strategies that can accurately decipher user intent from non-optimal muscle actuation.

Seyedali et al [20] indicated that the muscle co-contraction results for both the ankle and knee antagonist muscle pairs did not correlate with walking speed. The muscle co-contraction during stance phase of the residual limbs highlighted the lack of stability and shock absorption offered by passive prostheses. This resulted in the participants enlisting their knee muscles to improve stability at heel strike and throughout the stance phase. This highlighted the dependency between prosthesis function and muscle activation. Thus, indicating the importance of developing prostheses that foster muscle activation patterns that are more similar to that of able-bodied individuals.

The non-stationary behaviour of EMG data acquired from lower limb muscles poses another challenge to be overcome when using EMG data from individuals with lower limb amputations. This is in addition to challenges such as EMG crosstalk and high muscle co-activation levels. A controller for a powered prosthesis needs to be able to differentiate between EMG data read while a user is stationary and that measured when a user (un)consciously wants to execute a motion. The purpose of which is to not facilitate unintended movement.

The generalisation of a developed control solution is of importance. The approach usually taken for most research within this field is to focus on a specific area. This involves developing a solution based on data acquired from a small participant group and then validating the developed solution on the same participant group from which the data was obtained. This approach usually leads to favourable results and a probable solution for the participants from whom the training data was obtained. However, it usually also leads to poor generalisation of the developed solution to new data or circumstances. Examples of these are larger and more varied group of participants with differing residual limb physiologies.

Currently developed lower limb powered prostheses allow a user to achieve a more biological gait when performing certain 'pre-defined' locomotion tasks. These are tasks for which the controller was specifically designed to facilitate. However, a user has limited to no volitional control over the prosthesis. As such, the user is unable to recover from external perturbations. If the prosthesis is unable to identify sudden changes in circumstance, it is unable to facilitate the necessary motion in order to assist a user to recover from a perturbation. This is another factor to be addressed when developing lower limb powered prostheses.

Research has been conducted in the area of stumble and perturbation identification. The objective of which has been developing algorithms that can promptly identify changes in a user's environment or possible perturbations experienced by a user. Most algorithms targeted at recognising perturbations or stumbles experienced by a user do so by employing prosthesis mounted sensors or by 'scanning' the environment. Lawson et al [86] used accelerometers to determine whether a simulated perturbation resulted in the participant elevating or lowering their leg. They reported 100% accuracy in classifying the 'recovery' action as either elevating or lowering. Their study was only on able-bodied participants. On the other hand, co-contraction levels present in EMG signals have also been used as indicators of perturbations [87]. This approach could be easier to implement on an EMG controlled lower limb powered prosthesis, along with prosthesis mounted sensor data such as that from accelerometers.

Powered prostheses have the capability to assist users achieve a gait pattern that is biologically similar to that of able-bodied individuals. However, this is inhibited by the lack of volitional control in current commercially available lower limb prosthesis and the lack of somatosensory feedback to users. Both these factors limit a users' ability to perform a variety of locomotion tasks. With regards to the latter, a study conducted by Hoover et al [88] demonstrated the ambulation limitations introduced by the absence of somatosensory feedback to a user.

Hoover et al [88] developed a volitional control strategy specifically for stair ascent. They implemented their controller on a transfemoral prosthetic consisting of a powered knee joint and a passive ankle-foot prosthesis. The prosthesis was EMG driven during the stance phase of stair ascent. A nominal torque was specified during the swing phase to enable the participant to clear the steps and appropriately position their foot at the termination of swing phase. The user could override the specified torque or supplement it by activating their thigh muscles used for knee flexion. Their main reason for incorporating the nominal torque during swing phase was the lack of sensory feedback to the participant and reduced residual limb-socket interaction during swing phase. The absence of which made it difficult for the participant to perceive the orientation of the prosthetic limb in relation to the step to be cleared. This demonstrated the inherent limitations faced by users due to the lack of somatosensory feedback when using prostheses.

The implications of a participant not having somatosensory feedback were also noted in a study by Lawson et al [80]. A delay in knee extension on the prosthesis side was evident in the knee angle versus stride percentage trajectory of a participant with a unilateral transfemoral amputation. This was as participants performed stair ascent using a transfemoral powered prosthesis. The delay was attributed, in part, to "*the lack of proprioception on the amputee's affected side*" [80]. This necessitated the participant to confirm the placement of their prosthetic limb on the next step before shifting their body weight onto said limb. This resulted in an early and prolonged stance phase on their intact limb. The lack of somatosensory feedback has less of an impact on individuals with transtibial amputations. This is because they can compensate by flexing their knees further during locomotion tasks such as stair ascent. Nonetheless, it still affects their gait patterns and their capability to perform a variety of locomotion activities.

2.7 Conclusion

Powered prostheses are the next 'evolutionary' step for lower limb prostheses. However, their control is still largely extrinsic, meaning that a user is seldom capable of volitionally controlling the prosthesis without physically handling it. Various approaches can and have been used in developing control strategies for lower limb powered prostheses. This has been illustrated by the literature discussed in this chapter.

These include:

- o developing a controller based on a mathematical model of a biological limb,
- o using data from prosthesis mounted sensors to monitor gait phases and detect changes in the locomotion environment, to facilitate the most appropriate control action,
- o implementing classification algorithms on user acquired EMG data to facilitate control, and
- o even implementing a hybrid solution based on the other approaches mentioned.

However, each approach comes with its own limitations. Developed mathematical models are often simplistic approximations of the actual functionality of a biological system, this has some effect on the ability of such controllers to adequately mimic biological gait for a variety of locomotion modes. On the other hand, developing more in-depth mathematical models would also be time consuming and could lead to computational delays when implemented on physical systems due to their complexity.

Controllers that use prosthesis mounted sensor data, sometimes also incorporating EMG data as an input, have been more robust as they do not suffer from the non-stationary behaviour observed in EMG data. These controllers can often be applied in a straight forward manner, such as using FSMs. However, they 'drive' the prosthesis based on data received from the sensors. This could lead to growing errors if erroneous data was continuously fed back to the system. With this type of approach, a user has limited to no volitional control over their prosthesis, thus also limiting the number of locomotion activities that can be facilitated.

EMG driven powered prostheses have the potential of enabling a user to volitionally control their prosthesis. However, developing a controller that can adequately use the non-stationary signals, discern between noise and intended motion and be robust enough to withstand changes in the signal due to factors such as muscle fatigue is a challenge.

With regards to classification algorithms, LDA has been proven to be robust enough to classify user intent with reasonable accuracy while also possessing little computational complexity. Though in the presence of muscle co-contraction, QDA could be a more robust solution due to its quadratic decision boundary and relative computational simplicity, compared to other classifiers such as dynamic Bayesian networks. To further improve classification accuracy, PCA has been successfully implemented to reduce feature set dimensionality, which reduces computational time while also identifying the principal components to be used for classification.

The challenges associated with implementing user acquired EMG signals in lower limb powered prostheses are well documented and are yet to be effectively overcome, even though various tactics have been used to alleviate their effects. Nonetheless, research from other scholars within the field supports the notion of using participant acquired EMG data to successfully drive a lower limb powered prosthesis. The responsibility rests on a developed control strategy to overcome the known shortfalls of using user acquired EMG data and for it to achieve prosthesis output behaviour that would enable a user to realise biologically similar gait for a number of locomotion tasks, including those that are not cyclic in nature.

EMG driven control strategies that can enable a user to volitionally control the actuation of their prosthesis would be beneficial. Such control strategies could enable a user to perform a larger variety of locomotion tasks that are not cyclic in nature or particularly predictable.

Chapter 3
Gait Experiment: Methodology and Results

The primary purpose of a prosthesis is to replicate the functionality of the amputated limb, including its ability to maintain the body's stability when traversing uneven terrain. If one is to develop a true functional replacement of a biological limb, the mechanisms that govern and drive the biological limb have to be understood so that they can be replicated by a controller implemented on a powered prosthesis.

As such, the objective of the gait experiment was to ascertain the gait strategies employed by able-bodied individuals when walking over uneven terrain, such as those encountered within an urban environment. This was done by studying participants' ground reaction forces (GRFs) and muscle activation patterns (EMG); limb motion data was also recorded. The focus of the gait experiment was on the lower limbs. There was also some focus on the upper body as the participant's postural stability could be deduced using motion data of the upper body.

The data acquired from the gait experiments was used to develop a control strategy for a lower limb powered prosthesis that would be capable of enabling a user to traverse fixed uneven terrain. The experiment protocol for the gait experiment was approved by the University of Manchester Research Ethics Committee, UREC reference 16086. The approval letter is included in Appendix B. The fidelity of the recorded data and the thoroughness of the experiment protocol were ensured by first conducting a pilot study with one able-bodied male participant. The gait experiment succeeded the pilot study.

3.1 Experiment Methodology
3.1.1 Participants
Six able-bodied volunteers took part in the gait experiment. Only males participated in the gait experiment due to the need to instrument the torso. Participants were aged between 18 and 55. The upper age limit was chosen based on it being around the average age before which notable muscle weakening due to aging (a phenomenon known as Sarcopenia) occurs.

Participants had no musculoskeletal disease or limitations that would lead to their gait at self-selected speeds deviating from that of healthy able-bodied gait. Participants also had no conditions and/or illness, including a cold, flu, fever, sinus infection, etc. that would affect their balance or lead to their gait at self-selected speeds deviating from that reported for healthy able-bodied gait.

Participants walked barefoot during the gait experiment, such as in other similar human biomechanics studies [89, 90]. This was done to eliminate the possibility of their feet slipping or sliding in the shoes during the uneven walking trials. It was also to eliminate any differences in gait, however minor, that could be introduced by participants wearing different kinds of shoes during the experiment [91, 92].

3.1.2 Experiment Composition

The gait experiment took place in an indoor gait laboratory which had two 3D force plates that were placed flush with the ground. The force plates were level with the floor. A top view schematic of the gait laboratory is presented in figure 3.1. Participants walked at three self-selected speeds. These were normal, slow and fast. Participants began each walking trial from the same side of the laboratory. This facilitated repeatability of the experiment amongst different participants.
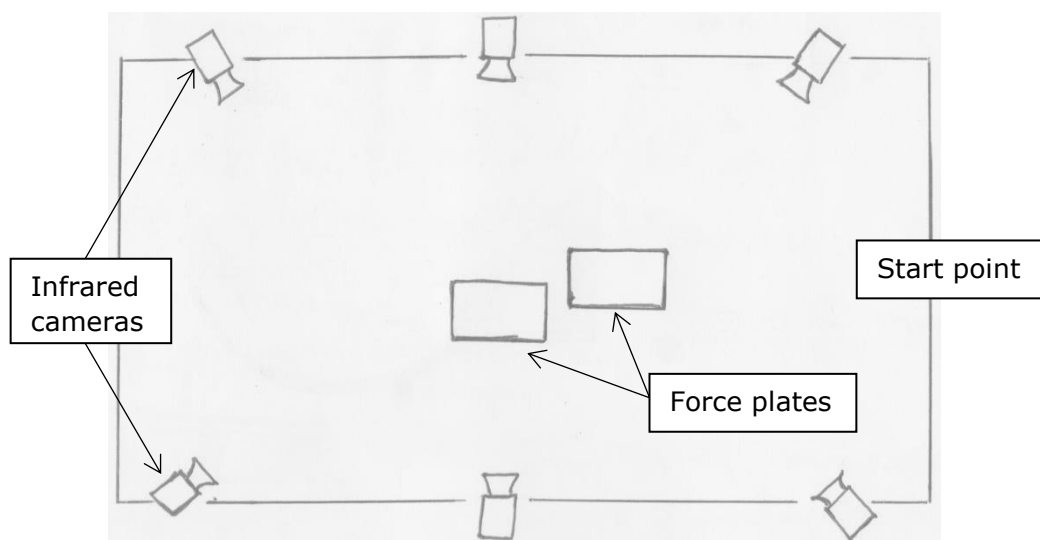
Figure 3.1: Top view schematic of gait laboratory

The participants walked over level-ground and over a custom made uneven terrain. 20 valid trials were captured for each walking speed. This was done for both the level-ground and uneven terrain trials. This resulted in a total of 120 valid gait trials being captured for each participant.

However, participants performed two walking trials for each change of speed and terrain. This was done to allow the participants to familiarise themselves with the change in speed or terrain. These two walking trials were done before beginning the 20 valid gait trials. The data for these practice trials was not captured.

During the level-ground gait trials, participants walked an average distance of 6m, from one end of the gait laboratory to the other. A trial was only deemed valid if participants stepped over both force plates in succession during the trial. This ensured kinetic and kinematic data for said trial could be computed from the force plate and motion capture data. All sensor data was recorded and synchronised for all gait trials.

Data synchronisation was done automatically using the motion capture system, Vicon. The two 3D force plates and the EMG system interfaced with the motion capture system by having them plugged into the Vicon computation box (desktop). Their connection to the motion capture system ensured that the two systems were simultaneously started with each motion capture trial. This ensured that readings from all three systems were automatically synchronised.

3.1.3 Materials and Sensors

  i.   A workspace computer to store the collected data.
 ii.   A Vicon (Oxford, England) T-series motion capture system with six infra-red cameras.
iii.   Two AMTI 3D force plates (Watertown, MA, USA).
 iv.   Wireless Delsys Trigno (Natick, MA, USA) surface EMG electrodes with 16 channels.
  v.   Delsys EMGWorks Analysis software.

3.1.4 Equipment Calibration and Participant Preparation

Muscle activation (EMG) data was recorded from participants' lower limbs to study how the muscles were activated throughout the gait trials. The ground reaction force (GRF) data was aligned with the EMG data so that the correlation between the participants' motion and their muscle activation during the gait experiment could be ascertained. Motion data was also captured so that variables such as the participants' joint forces and moments could be computed using inverse dynamics, with regards to rigid body dynamics, and the data from the force plates.

Vicon was the infrared camera system used to capture motion data. The system was calibrated using its proprietary software and a calibration wand with four reflective markers. Details of this procedure are available in the Vicon online documentation, under the section *Calibrate a Vicon system* [93]. This procedure was done to ensure accurate and robust motion capturing. The 3D position of the force plates in relation to the motion cameras was ascertained by the motion capture system. Motion data was captured at 200Hz and force plate data, GRF and moments, was captured at 1KHz. Calibration of the 3D force plates meant ensuring that the force directionality was correct. This included having the vertical GRF pointing upwards when visualised within the online 3D motion capture volume. The force plates were also re-zeroed when moving from level-ground walking to the uneven terrain.

Participants had both their lower limbs instrumented with EMG surface electrodes. Instrumenting both limbs allowed for muscle activation comparisons to be made. EMG electrodes were placed based on the SENIAM (Surface EMG for Non-Invasive Assessment of Muscles) recommendations [94-96], using palpation. The participants' skin upon which the electrodes would be placed was prepared. This was done prior to attaching the electrodes and involved removing any excess hair that could affect the quality of the recorded signal. The area was then cleaned using alcohol wipes. EMG surface electrodes were placed over the participants' lower limb muscles as shown in figure 3.2. These particular muscles were chosen due to them being largely responsible for actuating the ankle and knee joints, respectively. EMG data was captured at 2KHz. The accuracy of the electrode placement and the quality of the EMG data was verified in real-time prior to beginning the gait experiment. This was done using the Delsys EMGWorks Acquisition propriety software [97].

Maximum voluntary contractions (MVC) were recorded for each muscle group. Participants were asked to contract a muscle group to its maximum effort and to maintain that steady contraction for 3 seconds. The MVC procedure was similar to that reported in other human biomechanics research [98]. Three MVCs were recorded for each muscle group, with a 1 minute rest period between the contractions [98, 99]. Once the MVC had been recorded, reflective markers were then attached onto the participants.
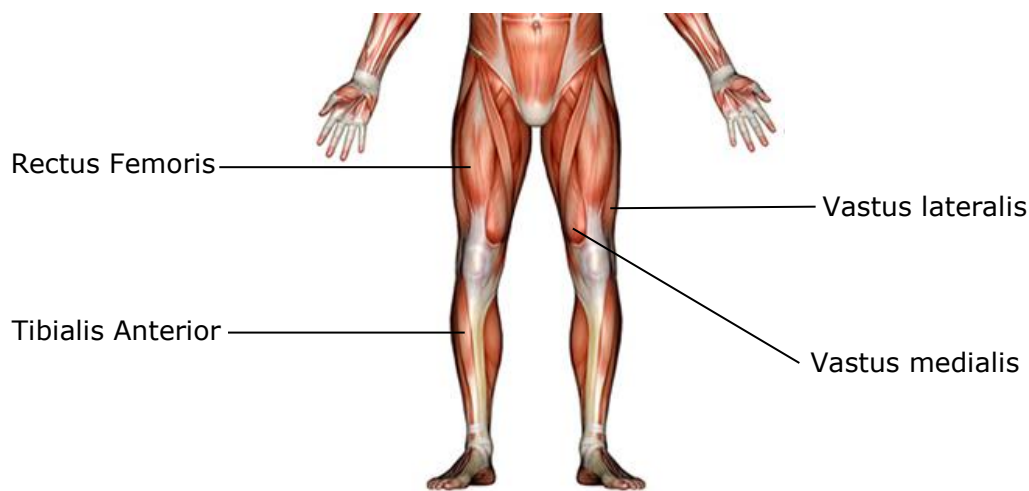
A) Anterior View of EMG Surface Electrode Placement
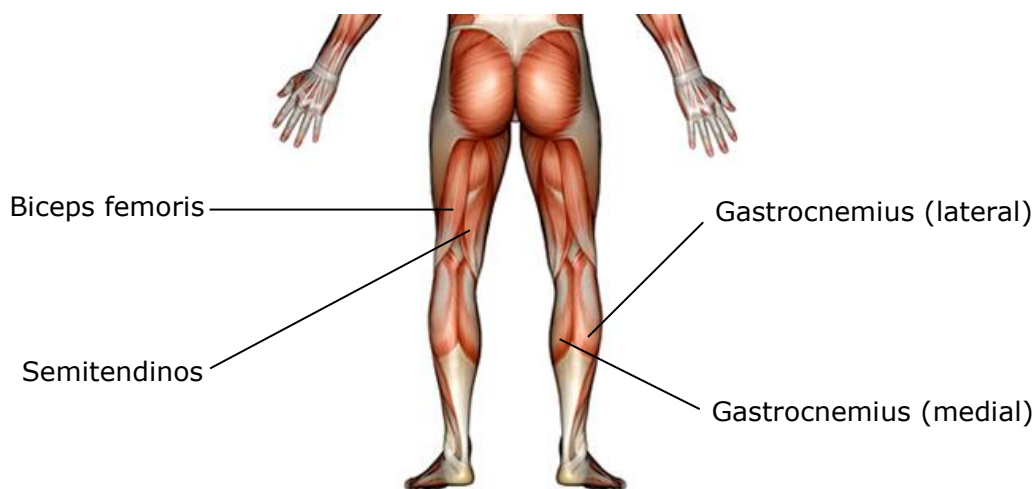
B) Posterior View of EMG Surface Electrode Placement

Figure 3.2: Muscles of interest for the gait experiment

Two calibration trials were performed for the motion capture system, a static trial and functional joint trial, also referred to as a dynamic trial. The calibration trials were based on the CAST (Calibrated Anatomical System Technique) technique [100].

The static trial was conducted to record anatomical landmark locations so that the 3D spatial description of the participants' body segments could be determined. The 3D spatial description could be used to determine the anthropometric data of the body segments in order to perform inverse dynamics calculations. During the static trial, participants stood in a T-Pose with their feet shoulder width apart and the positions of their anatomical markers were captured using the motion capture system.

The dynamic trial was conducted to determine the participants' hip joint centres which, unlike the other anatomical landmarks, cannot be determined through palpation alone. Participants continuously performed hip abduction/adduction, circumduction and extension/flexion for 30 seconds, at least three times. This procedure increased the likelihood of recording all the marker positions. The locations of the anatomical landmarks for each major body segment were based on [101] and are presented in table 3.1. Markers for the thighs, shanks and feet were placed on both sides of the body, left and right. Once calibration was complete, the gait trials were performed.

Table 3.1: Anatomical landmarks of each major body segment

Anatomical Landmark	Description	Property/Type
Torso		
IJUG	Jugular Notch of Sternum	bony
PXIP	Xiphoid Process	bony
C7SP	Spinous Process C7	bony
T8SP	Spinous Process T8	bony
Pelvis		
RASIS	Right Anterior Superior Iliac Spine	bony
LASIS	Left Anterior Superior Iliac Spine	bony
RPSIS	Right Posterior Superior Iliac Spine	bony
LPSIS	Left Posterior Superior Iliac Spine	bony
Femurs		
LEP	Lateral Epicondyle	bony
MEP	Medial Epicondyle	bony
HJCR	Hip Joint Centre	Virtual
Shanks		
TTB	Tibial Tuberosity	bony
HFB	Apex of Fibula Head	bony
MML	Medial Malleolus	bony
LML	Lateral Malleolus	bony
Feet		
CAR	Upper Ridge of the Calcaneus	bony
FMR	Dorsal Aspect of the First Metatarsal Head	bony
SMR	Dorsal Aspect of the Second Metatarsal Head	bony
VMR	Dorsal Aspect of the Fifth Metatarsal Head	bony

Technical markers, which were also reflective markers, were attached on each EMG electrode and at particular points on the participants' torso, pelvis and shank, respectively. These markers enabled the motion capture cameras to keep track of the participants' 3D motions. The locations of the technical markers are presented in table 3.2. Markers for the thighs, shanks and feet were placed on both sides of the body, left and right.

Table 3.2: Technical makers

Body Segment	Description
Torso	Manubrium – marker cluster of 4
Pelvis	Spinous process S2 (Sacrum 4) – marker cluster of 4
Thighs	Rectus femoris muscle – on EMG electrode
	Vastus medialis muscle – on EMG electrode
	Vastus lateralis muscle – on EMG electrode
	Biceps femoris muscle – on EMG electrode
	Semitendinosus muscle – on EMG electrode
Shanks	Tibialis anterior Muscle – on EMG electrode
	Lateral gastrocnemius muscle – on EMG electrode
	Medial gastrocnemius muscle – on EMG electrode
	Anterior mid-tibia
	Anterior tibia, 2/3 distance from the patella to the foot
	Posterior tibia, 2/3 distance from behind the patella to the upper ridge of the calcaneus
Feet	Upper ridge of the calcaneus
	Dorsal aspect of the first metatarsal head
	Dorsal aspect of the second metatarsal head
	Dorsal aspect of the fifth metatarsal head

The anatomical coordinate system for recording the 3D spatial marker coordinates was defined as shown in figure 3.3. The directions of the three Cartesian axes were mutually perpendicular. The y axis was defined as parallel to gravity, though it pointed upwards. The x axis defined the direction of progression and was along the anterior-posterior plane, pointing in the anterior direction. The z axis was defined as perpendicular to the sagittal plane, and thus also perpendicular to the x and y axes and pointed to the right. The local coordinate system was defined based on ISB recommendations and on [101] so that the angular orientations of the body segments could be computed.
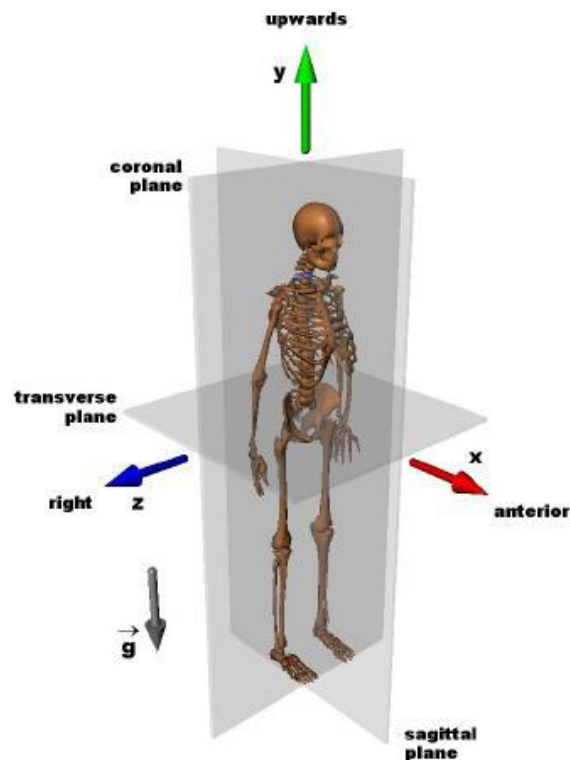
Figure 3.3: Anatomical coordinate system and planes

3.1.5 The Uneven Terrain

The uneven terrain used for the gait experiment was constructed to mimic fixed uneven walking surfaces commonly encountered within an urban environment, such as uneven paving. The layout of the uneven terrain was done in such a way that walking over the terrain necessitated participants to perform compensatory gait strategies. These would include muscle activation and gait manoeuvres that would ensure that they maintained their dynamic stability and retained their centre of mass (COM) within their base of support (BOS).

The uneven terrain consisted of six sloped steps fabricated from sheet metal, each 60cm long x 40cm wide in size. All the edges of the sloped steps were filleted. The slopes were covered with a thin layer of rubber to provide a safe, non-slip and comfortable walking surface. The slopes were fabricated in such a way that once placed on the ground, they remained secure and did not move or slide. They also remained rigid as participants walked over them at varying speeds. The uneven terrain was modular in design, so it could be taken apart and re-assembled as desired. The layout of the uneven terrain remained the same for all walking speeds and for all participants. This allowed for intra-participant and inter-participant gait and muscle activation comparison.

An inclination of 10° was shown to be the point where human gait begins to emulate that of ramp traversal [90]. Thus, a slope incline of 12°, along the respective sagittal or frontal planes, was chosen. The 12° slope incline ensured that the participants' COM would be displaced outside their BOS, whilst not having the slopes be a lot steeper than the gait altering threshold of 10°.

Participants were asked to walk as naturally as possible over the uneven terrain, ensuring that only one foot made contact with an uneven terrain slope during each step. Participants were also encouraged not to look down at the walking terrain unless they felt unstable or unsafe. This still resulted in participants demonstrating a comfortable and natural gait. The uneven terrain was, lengthwise and width-wise, aligned with the two triaxial force plates. The spacing between each slope ensured that participants remained unaware of where the force plates were located. An illustration of the uneven terrain is presented in figure 3.4.

Force plates
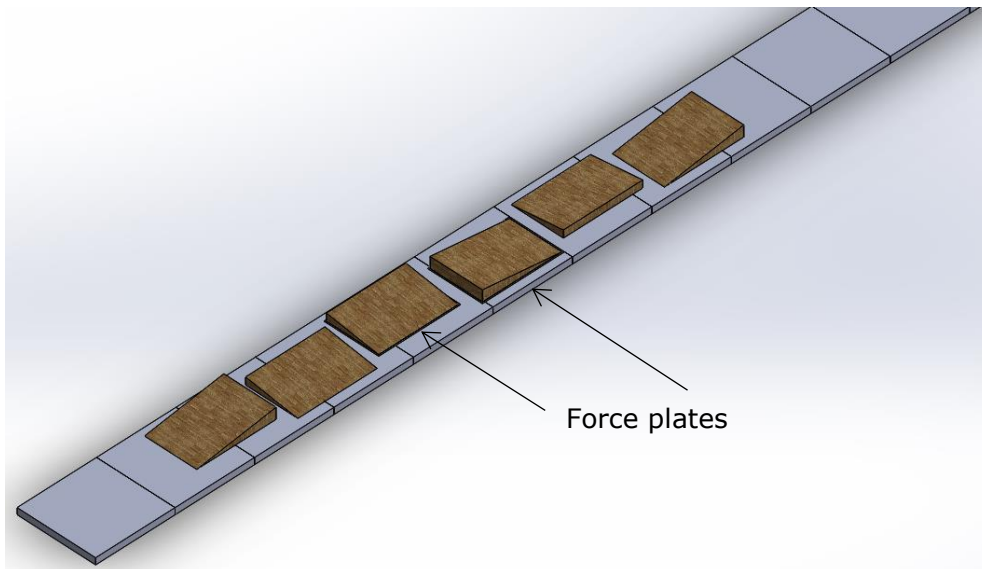
Figure 3.4: 3D Representation of the uneven terrain

3.2 Data Processing/Interpretation
3.2.1 Ground Reaction Force Data

The GRF data was processed in Matlab using a custom written code, which is detailed and included in Appendix J. The activation of a force plate constituted heel strike. However, this initial foot contact could have also been foot flat or contact with the forefoot when traversing a downward slope of the uneven terrain. The subsequent deactivation of the force plate constituted toe-off.

The GRF data was segmented using the successive activations and deactivations of the two force plates. Using said timings, and a knowledge of human biomechanics, the GRF data could be segmented to 100% of the gait cycle. Each participant's GRF data was amplitude normalised using their body weight (kg) such that the reaction force was measured in N/kg.

The GRF data was taken from all 20 valid trials for each participant. Each participant's data was averaged, creating a representative GRF profile from their data. This was done for each of the three walking speeds and for both terrains. As such, six intra-participant GRF profiles were created for each participant. The averaged individual participant data was then averaged, creating a representative GRF profile for the entire participant group. The group's GRF standard deviation was computed from this inter-participant data.

3.2.2 EMG Data

The measured EMG data was used to determine the activation pattern and magnitude of the respective muscles throughout the gait experiment [102]. Muscle co-activation of antagonist muscle pairs at certain points of the gait cycle was used to deduce stability maintenance strategies. The EMG data was taken from all 20 valid trials for each participant, for each speed. The measured EMG data had undergone bandpass filtering at 20-450 Hz using a Butterworth filter. This was carried out by the Delsys wireless electrodes and system. The specifications of the Delsys EMG system used are presented in Appendix C.

The EMG data was segmented according to the successive activation and deactivation of the force plates. This was the same procedure used to segment the GRF data. Thus, the EMG data was segmented to 100% of the gait cycle, synchronised with the GRF data. The EMG data was then amplitude normalised based on each participant's maximum (isometric) voluntary contraction (MVC) [99, 103]. The resulting EMG amplitude for each participant was with reference to their percentage of muscle activation (%), rather than being in volts (V). The data segmentation with regards to the gait cycle and the amplitude normalisation made intra- and inter-participant comparison possible.

The segmented and normalised EMG data was low-pass filtered using a 2nd order recursive Butterworth filter with a cut-off frequency of 20Hz. This was done to remove motion artifact [104]. The use of a recursive filter aided in preventing

temporal shifting of the data. The RMS (root mean square) was then computed for each muscle using a window length of 150ms and a window overlap of 50ms [55, 60]. This provided the mean power of the EMG signal and a rectified representation of the participants' muscle activation throughout the gait cycle [104].

Representative EMG profiles were computed for each muscle of interest, for each participant's data. This was done by averaging each participant's EMG data from all 20 of their valid trials, resulting in intra-participant EMG profiles. This was done for each walking speed and terrain type. Each participant's intra-participant data was then averaged with that of the other participants within the group. Thus, a representative inter-participant EMG profile was created for each muscle of interest. The standard deviation for the participant group's EMG data was computed from the inter-participant data. All the EMG data computations and analyses were done in Matlab using custom written code. This is detailed and included in Appendix J.

3.2.3 Motion Capture Data

The motion capture data was not processed as it was not required to develop the control strategy to be implemented on the transtibial powered prosthesis prototype. However, the motion capture data could later be processed and used for comparison against the gait of participants when testing the functionality of future versions of the developed system. This would be carried out by using the same experimental protocol presented above in future experiments, particularly with participants with unilateral transtibial amputations. The comparison between these motion capture data could be used a metric to judge the functionality of future versions of the developed transtibial powered prostheses prototype.

3.2.4 Statistical Analysis

Single standard deviations were computed from the inter-participant data and are included in the results. Statistical analysis was performed on the inter-participant GRF and EMG data. A two-tailed paired t-test was performed to investigate whether the type of terrain had a significant effect on the data. This was done for the GRF and EMG data, respectively. A one-way ANOVA was also performed to investigate whether the different walking speeds had a significant effect on the data. A confidence level of 95% was used ($\alpha = 0.05$).

3.3 Results

Figure 3.5 illustrates how the reflective markers and surface EMG electrodes were attached to participants. The level-ground and uneven terrain used for the experiment is shown in figure 3.6. The height and weight of the participant group were 1.7m ±0.08 and 74.2kg ±12.2, respectively. The height and weight of each participant is presented in table 3.3. The average walking speed of each participant per terrain type is given in table 3.4.

Figure 3.5: Participant preparation

Figure 3.6: Level-ground (left) and uneven terrain (right)

Table 3.3: Participant height and weight

Participant	1	2	3	4	5	6
Height	1,65	1,64	1.63	1,7	1,82	1,76
Weight	65	75	90	56	83	76

Table 3.4: Participant average walking speed (m/s)

Participant	Level-Ground			Uneven Terrain		
	Normal	Fast	Slow	Normal	Fast	Slow
1	0.81	1.03	0.67	0.83	0.99	0.62
2	1.04	1.23	0.77	0.89	1.02	0.63
3	1.05	1.43	0.63	1.05	1.28	0.67
4	1.11	1.45	0.89	0.89	1.13	0.70
5	0.91	1.20	0.83	0.97	1.28	0.74
6	1.06	1.24	0.86	1.12	1.33	0.78
Group Average	1.00 ±0.11	1.26 ±0.16	0.78 ±0.11	0.96 ±0.11	1.17 ±0.15	0.69 ±0.06

3.3.1 Ground Reaction Force (GRF) Data

The GRF data presented is for the entire participant group, for a single stride. It is only for stance phase (0-60% of the gait cycle) as there are no GRFs during swing phase. The GRF data for the level-ground and uneven terrain gait trials is presented in figures 3.7 and 3.8, respectively. Due to the positions of the force plates, GRF data for the entire length of the uneven terrain could not be segmented with absolute accuracy. This would have been data for each type of uneven terrain slope orientation. The data presented for the uneven terrain was acquired during right foot inversion.

3.3.1.1 Level-ground trials

The participant group GRF patterns for level-ground walking followed trends reported in other literature [29, 89] (fig. 3.7). The vertical reaction force increased with walking speed, indicating the need to decelerate the foot more rapidly after heel strike with increasing walking speed (indicated with an 'A' in fig. 3.7a). Increased walking speed also necessitated increased push-off force to propel the body forward quicker ('B' in fig. 3.7a).

The reaction force also increased along the anterior-posterior direction with increasing walking speed. Greater foot deceleration ('C' in fig. 3.7b) was required during the first half of stance phase following heel strike. Thus, the foot pushed/'slid' further forward with increasing walking speed. This manifested as a reaction force in the posterior direction. The increased force during push-off, with increased walking speed, resulted in the foot 'pushing' further backwards ('D' in fig. 3.7b). This manifested as an anterior reaction force.

The participant group demonstrated stable medial-lateral foot movement during normal and fast walking (fig. 3.7c). However, there was only minimal GRF during slow walking. During normal level-ground human walking, minimal force is observed along the medial-lateral direction [29, 89, 105]. Therefore, the reaction forces during normal and fast walking were as expected and similar to that in other research. The reduction in reaction force during slow walking indicated that minimal force was expanded along that direction and suggested that the participants achieved forward propulsion with the least risk to their stability.
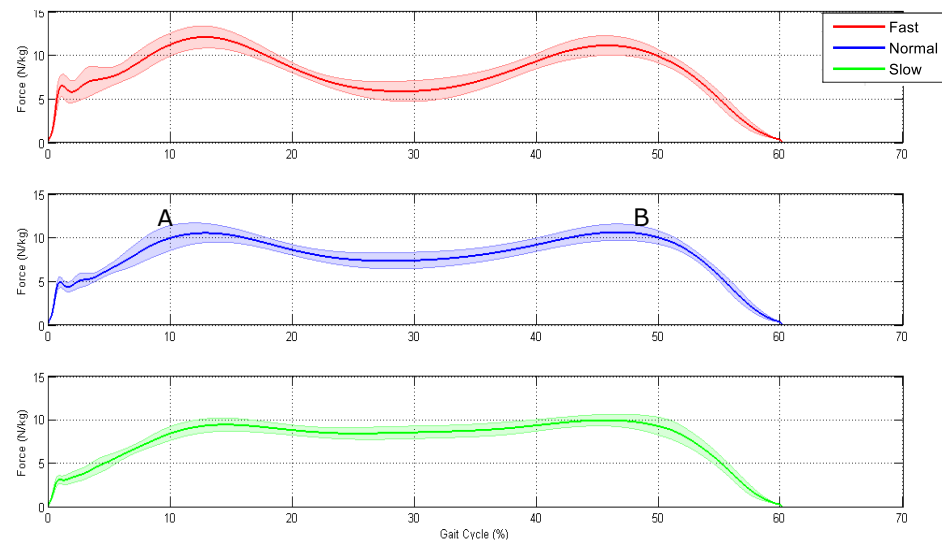
a) Vertical GRF
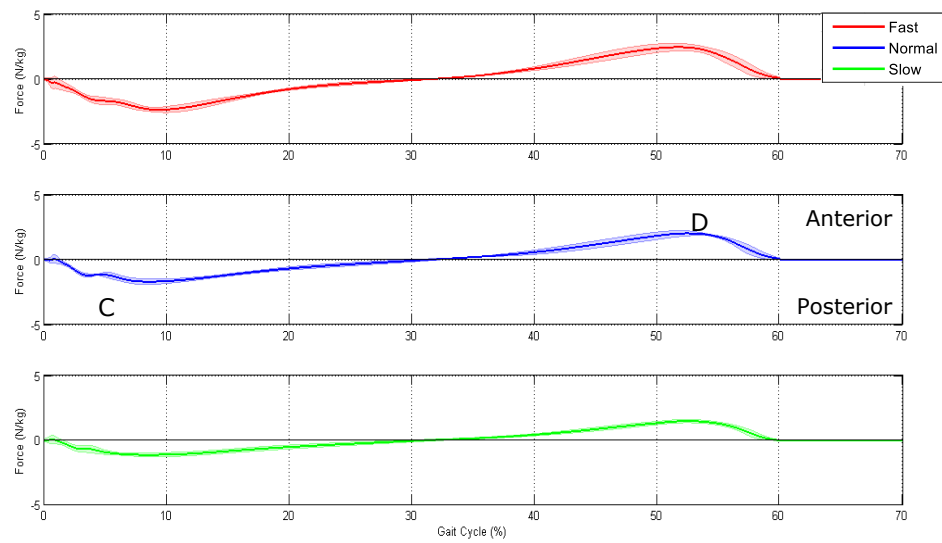
b) Anterior-posterior GRF
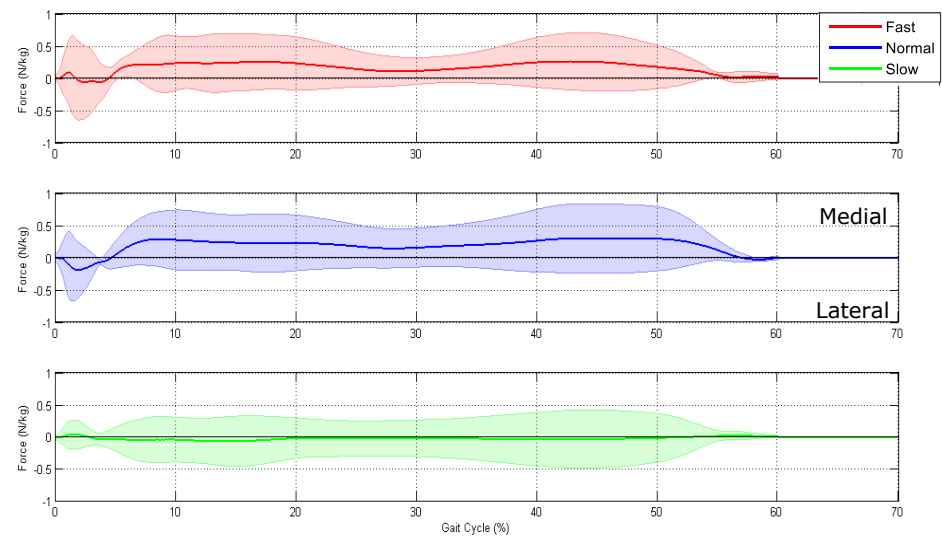
c) Medial-lateral GRF

Figure 3.7: Level-ground GRFs for participant group (N = 120 trials for each speed)

3.3.1.2 Uneven terrain trials

The GRF patterns for the uneven terrain trials were similar to that of the level-ground trials (fig. 3.8). The similarities included having two peaks along the vertical direction (fig. 3.8a). However, the variation of the GRF amplitudes, with respect to the three different walking speeds, was smaller compared to those of the level-ground trials. There was a 7.2% reduction in the group's overall walking speed during the uneven terrain trials, compared to the level-ground trials. Though this did not fully account for the reduction in GRF amplitude in response to changing walking speed [106]. The reduction in GRF amplitude along the vertical and anterior-posterior directions could be attributed to participants prioritising stability and centre of mass (CoM) control over the force required to achieve faster forward propulsion.

The vertical reaction force increased with walking speed. Though this increase was to a lesser degree compared to that of the level-ground trials. There was also a marginal increase in the reaction force along the anterior-posterior direction with increasing walking speed. Foot movement variation was also visibly present in the first half of the anterior-posterior reaction force (indicated with an 'E' in fig. 3.8b). This could be attributed to the instability introduced by walking on the uneven terrain and the participants' compensatory movements to maintain stability.

There was also large GRF variation for the uneven terrain trials along the medial-lateral direction. This occurred just after initial contact ('F' in fig. 3.8c). The variations gave an indication of the participants' foot motion when traversing the sloped step, indicating they strived to maintain their stability and CoM. These variations were most evident during fast walking. This was because greater joint and CoM stabilisation was required when generating higher forces to propel the body forward at a faster rate.

More variations were also present during slow walking. These were due to increased stabilisation being required with the slower transition of the participants' CoM. The amplitude of the medial-lateral GRF was also larger for the uneven terrain trials, compared to the level-ground trials. This supported the notion of the need for increased foot and CoM stabilisation along said direction.
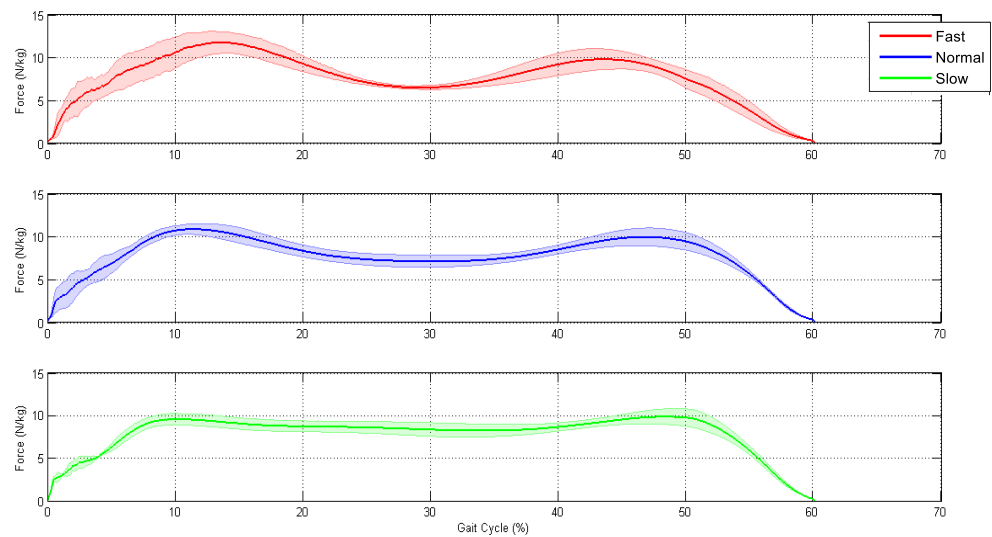
a) Vertical GRF
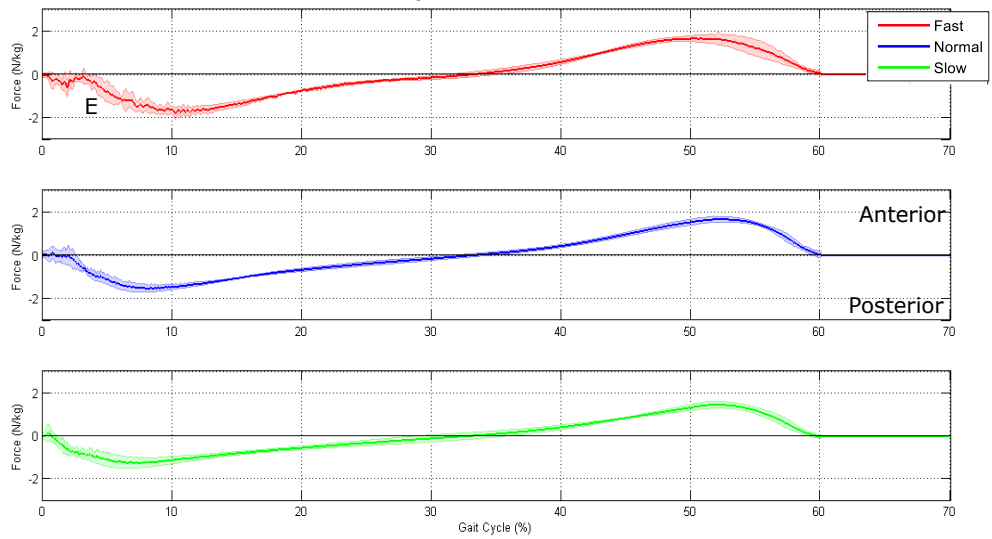
b) Anterior-posterior GRF
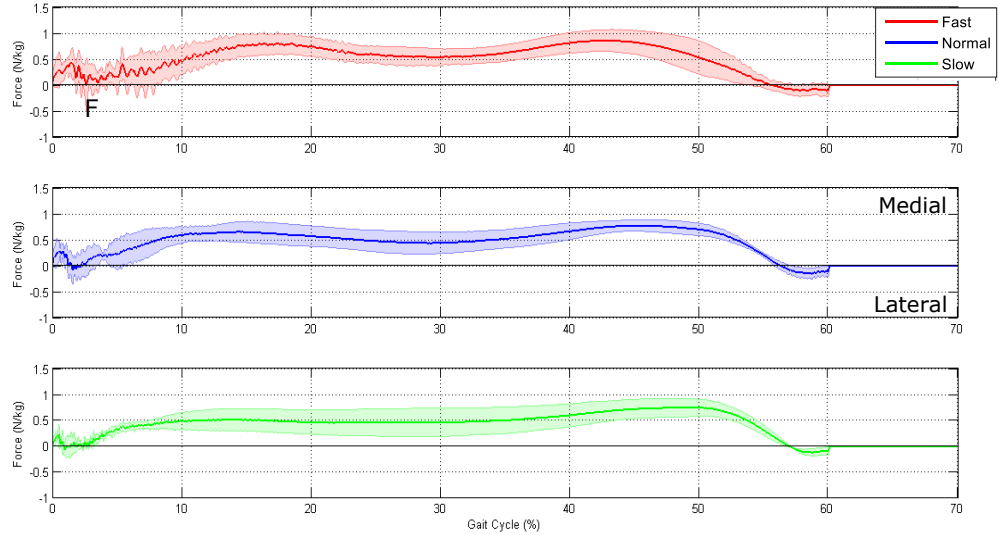
c) Medial-lateral GRF

Figure 3.8: Uneven terrain GRFs for participant group (N = 120 trials for each speed)

3.3.2 Electromyography (EMG) Data

The inter-participant (group) EMG data is presented in figures 3.9-3.16, for both terrain types. The results presented are muscle activations for the right leg. This was for right foot inversion for the uneven terrain trials. The EMG amplitudes are with reference to the participants' maximum MVC.

3.3.2.1 Lower leg EMG

The tibialis anterior muscle (TA) (fig. 3.9) was active largely just after heel-strike and around heel-off during stance phase of level-ground walking. This was between 0-10% of the gait phase and also around 50-±65% of the gait phase. TA activation during level-ground walking increased with walking speed, as expected, due to faster limb transitions.

The first peak which occurred following heel-strike decreased in response to decreasing walking speed. This was similar to TA activation in other research [49]. The second peak, which occurred at push-off (±60% gait phase), was also slightly earlier to TA activation presented in other studies [96, 106, 107]. This occurred particularly for level-ground walking. This could have been due to early muscle activation from one or two participants, which then altered the group EMG data.
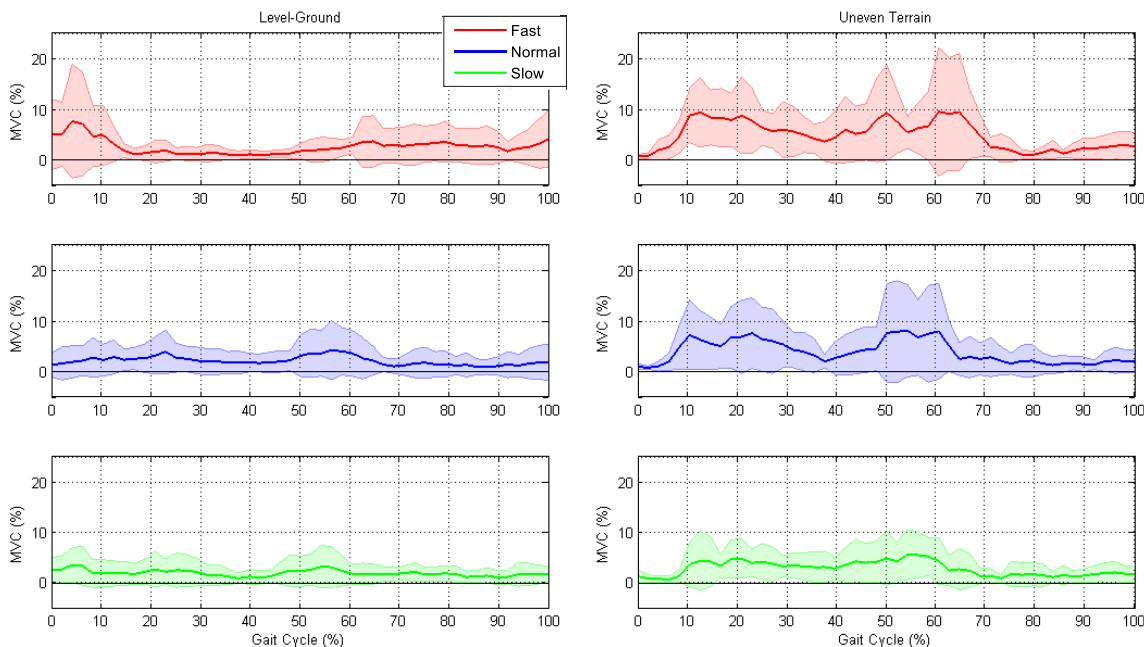
Figure 3.9: Participant group TA EMG data (N = 120 trials for each speed, per terrain)

TA remained more active throughout the stance phase during the uneven terrain trials. This was attributed to the need for medial-lateral stabilisation [105]. Peak TA activation occurred in the second half of the gait cycle and was higher compared to that of the level-ground trials. This was attributed to the participants first ensuring that their foot made proper contact with the sloped step prior to fully loading the foot. The largest TA activation occurred between heel-off (±40% gait cycle) and toe-off (±60% gait cycle). This was due to the requirement for increased foot clearance when traversing the uneven terrain. Though surprisingly, the muscle almost "switched off" from around mid-swing to the next heel strike.

The lack of TA activation from push-off correlated to maximum gastrocnemii activation during that gait phase for the uneven terrain trials. This indicated the adaptations participants made to their gait to ensure stability when walking over the uneven terrain. These adaptations were similar to those made to muscle activations in response to a disturbance [108]. The prolonged activation of TA during stance phase indicated the complimentary actions performed by the lower limb muscles to ensure ankle joint stability.

During the level-ground trials, the gastrocnemii muscles (i.e. medial gastrocnemius (MGas) (fig. 3.10) and lateral gastrocnemius (LGas) (fig. 3.11)) were active predominantly during stance phase. Maximum activation occurred around heel-off for the LG trials, which was similar to other research [106, 107]. The gastrocnemii peak activations occurred around push-off initiation (±40-60% gait cycle), enabling forward propulsion. Increased muscle activation occurred with increasing walking speed and was attributed to the need for increased push-off force. Due to the extensor muscles being predominantly active during stance phase, the prolonged activation of MGas and LGas, along with the decrease in their activation levels, was expected for slow walking [106].

The EMG pattern for MGas was more similar to that of the soleus muscle reported by Winter and Yack [96], rather than MGas patterns presented in other literature [106, 107]. This meant that maximum MGas activation occurred just before toe-off. This could have been due to either the EMG electrodes being placed closer to the soleus muscle or to the soleus muscle doing more work than MGas.

The latter explanation was favoured due to the presence of distinct MGas muscle activation around mid-stance (±30-40% gait cycle), particularly during slow and fast walking. However, the cause of the notable gastrocnemii activation peaks around terminal stance was unknown and not presented or reported in similar research [106, 107].
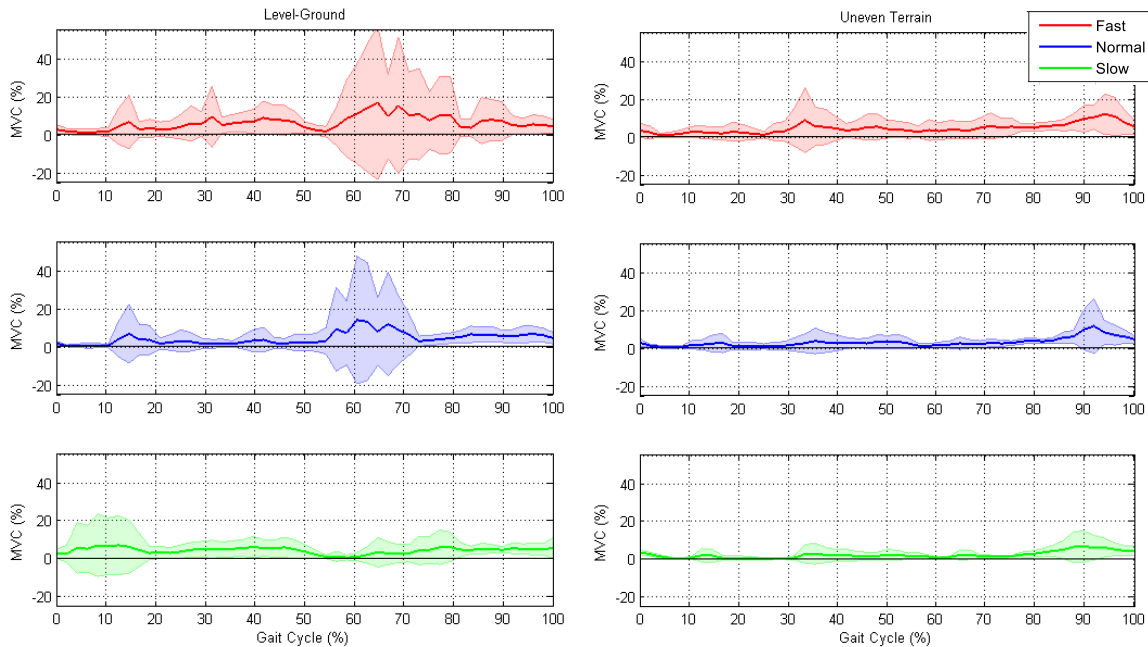
Figure 3.10: Participant group MGas EMG data (N = 120 trials for each speed, per terrain)
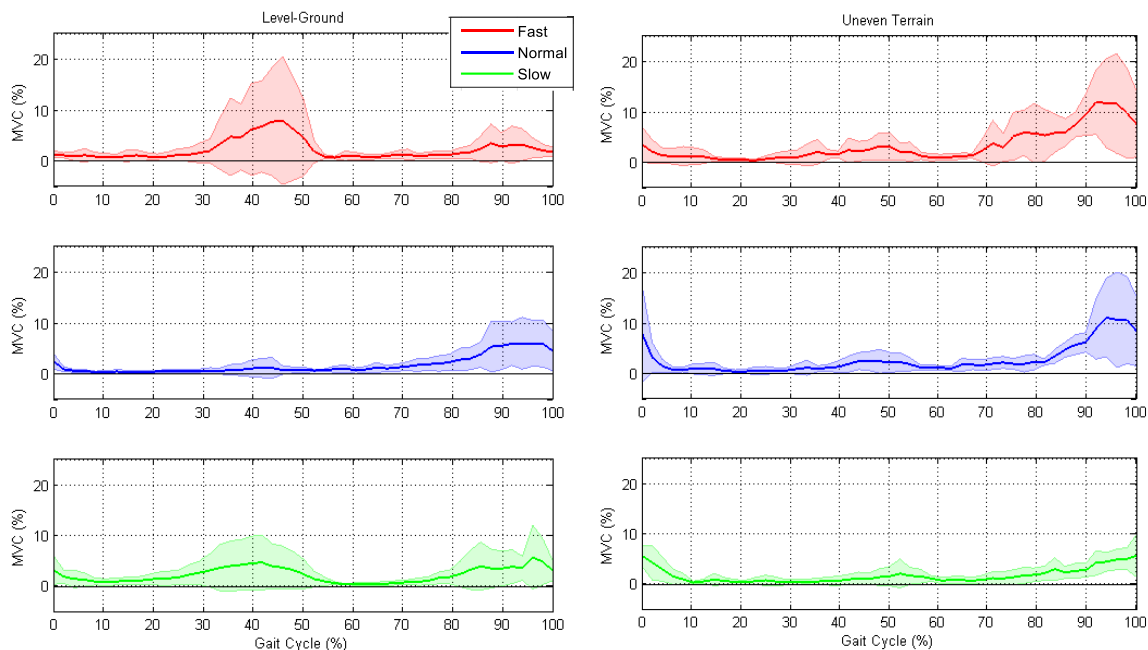
Figure 3.11: Participant group LGas EMG data (N = 120 trials for each speed, per terrain)

The gastrocnemii activation during the uneven terrain trials was dissimilar in pattern to that of the level-ground trials. This was with the exception of the large activations during late swing. Though similar to the level-ground trials, activation levels increased in response to increasing walking speed. The large activations during terminal swing (<±80% gait cycle) were dissimilar to findings presented in other research [4]. These were attributed to participants extending and preparing their foot for initial contact on the next elevated uneven terrain. This was supported by the delayed activation of TA during the uneven terrain trials.

The TA and gastrocnemii muscle activations suggested that participants wanted to establish adequate foot contact and joint stabilisation prior to loading their lead foot. Higher muscle activation was present in MGas as the EMG data was from participants performing foot inversion. The prolonged activation of MGas indicated the work done by the muscle, along with TA, to ensure joint and CoM stability [105].

3.3.2.2 Upper leg EMG

The activation patterns for the quadriceps muscles are presented in figures 3.12-3.14, respectively. This is EMG data for the rectus femoris (RF), vastus medialis (VM) and vastus lateralis (VL) muscles. Level-ground EMG patterns of the quadriceps muscles during fast and slow walking were similar those presented in other studies [96, 106, 107]. The dissimilarity of the quadriceps activation during normal walking was the presence of a reduced activation around foot flat and terminal swing.

The quadriceps' peak activations during fast and slow walking were from around initial foot contact to early mid-stance (±0-30% gait cycle). They were also during the latter part of push-off (±60% gait cycle). The peak activations for RF (fig. 3.12) were similar to that reported in [96, 106, 107]. Though similar activations were not reported for VM (fig. 3.13) and VL (fig. 3.14) [107]. VM and VL demonstrated distinct, though marginal, activation during the latter part of push-off [106]. These muscles' activations, with relation to the gait cycle, were congruent to this muscle group being responsible for flexion.

The uneven terrain activation patterns were dissimilar to comparable research [4]. The first peak, which was present in the quadriceps muscles during level-ground walking, was absent. This difference in EMG activation was attributed to the change

in terrain type. It was also attributed to the difference in the type of uneven terrain implemented in this research compared to that in [4].

In this study, greater foot clearance was required when traversing the uneven terrain. This necessitated greater knee flexion during push-off, which was observed in the uneven terrain EMG activations of the quadriceps. The similarities in activation for all three quadriceps muscles suggested that the primary objective for participants was to stabilise their knee joint when traversing the uneven terrain. This was supported by the increased VL activation, compared to its level-ground activation. Again, an increase in muscle activation was observed with increasing walking speed.
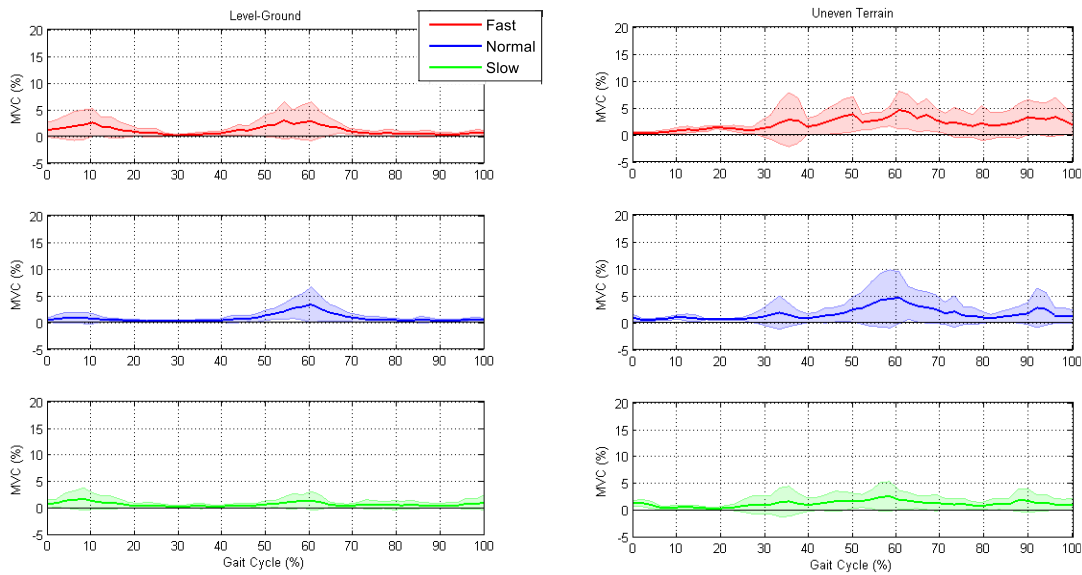
Figure 3.12: Participant group RF EMG data (N = 120 trials for each speed, per terrain)
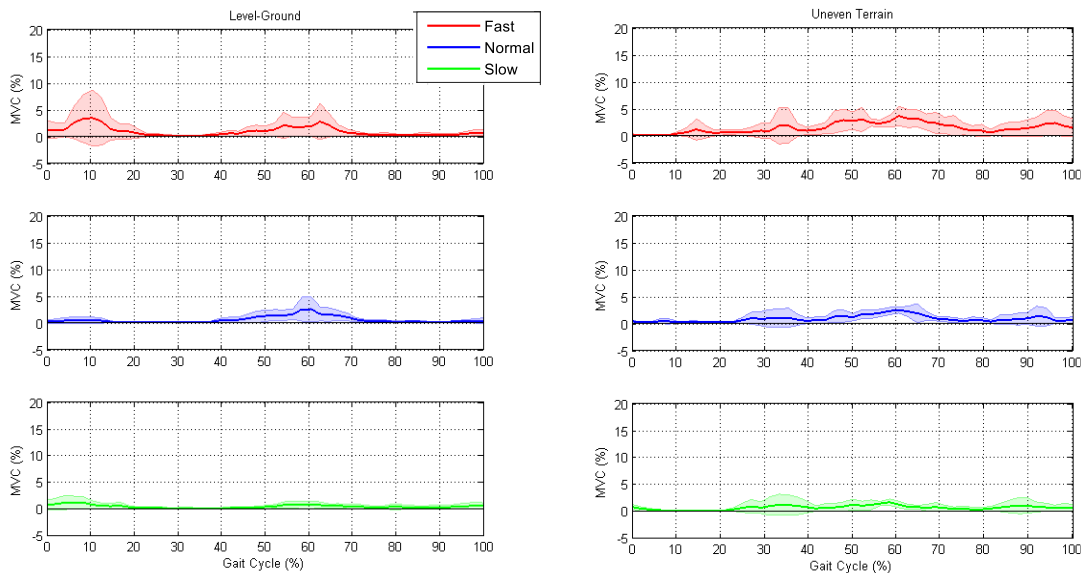
Figure 3.13: Participant group VM EMG data (N = 120 trials for each speed, per terrain)
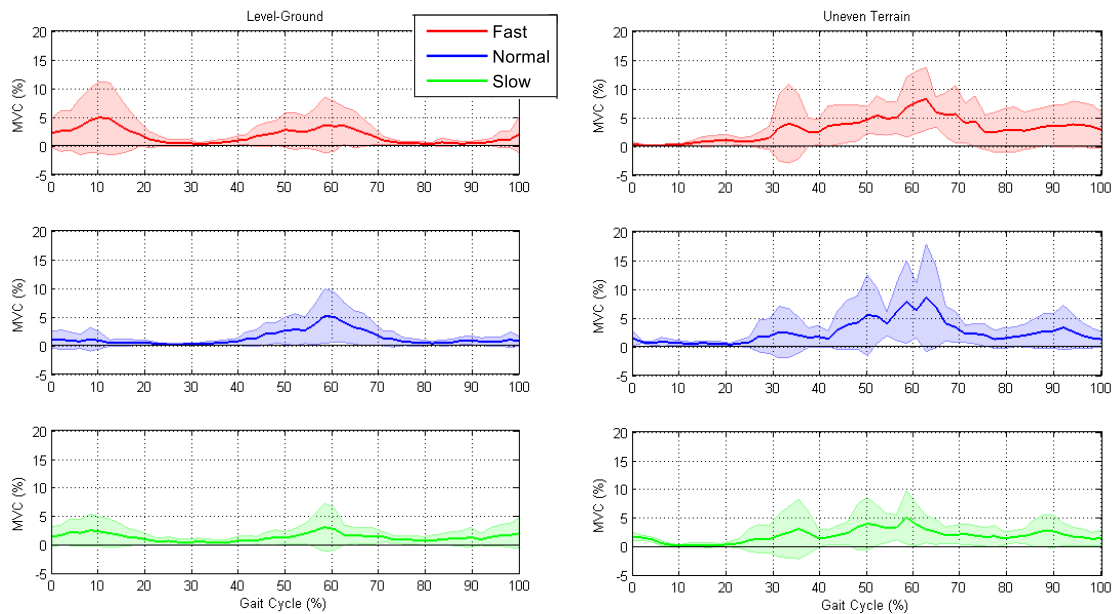
Figure 3.14: Participant group VL EMG data (N = 120 trials for each speed, per terrain)

The hamstring muscles, namely bicep femoris (BF) (fig. 3.15) and semitendinosus (ST) (fig. 3.16), were the least active of all the muscles investigated. Level-ground BF and ST activation during fast and slow walking was similar to that reported in other studies [96, 106, 107]. Peak activations occurred during terminal stance (<±80% gait cycle) for both muscles. There was also increased activation just after initial contact (< 10% gait cycle). The activations during the latter part of push-off were similar to those reported by den Otter et al [107].

The normal walking EMG activations were dissimilar to those reported in other similar gait studies [96, 106, 107]. Muscle activation just after heel-strike was again smaller than expected, similar to the quadriceps muscles. The difference in the EMG patterns during normal walking, compared to other studies, suggested that the participants within this study adapted their muscle activation. This adaptation was such that the thigh muscles were predominantly used to stabilise the knee joint during push-off. This was while the lower leg muscles facilitated forward propulsion. The hamstrings' peak activation remained largely similar even with changes to walking speed, particularly for ST.

Hamstring EMG activation during the uneven terrain trials was also largely the same across all walking speeds. Peak activation was around foot flat (±10% gait cycle) for both muscles and was attributed to knee joint and overall limb stabilisation. This muscle group is responsible for knee extension during healthy

able-bodied gait. The EMG data indicated that participants strived to ensure adequate foot contact before loading the lead foot. This notion was supported by the delayed activation of TA during the uneven terrain trials. A second activation peak was present for BF during push-off (±40-60% gait cycle). This was owing to the need for knee joint stabilisation when pushing off to ensure sufficient foot clearance to mount the succeeding sloped step.
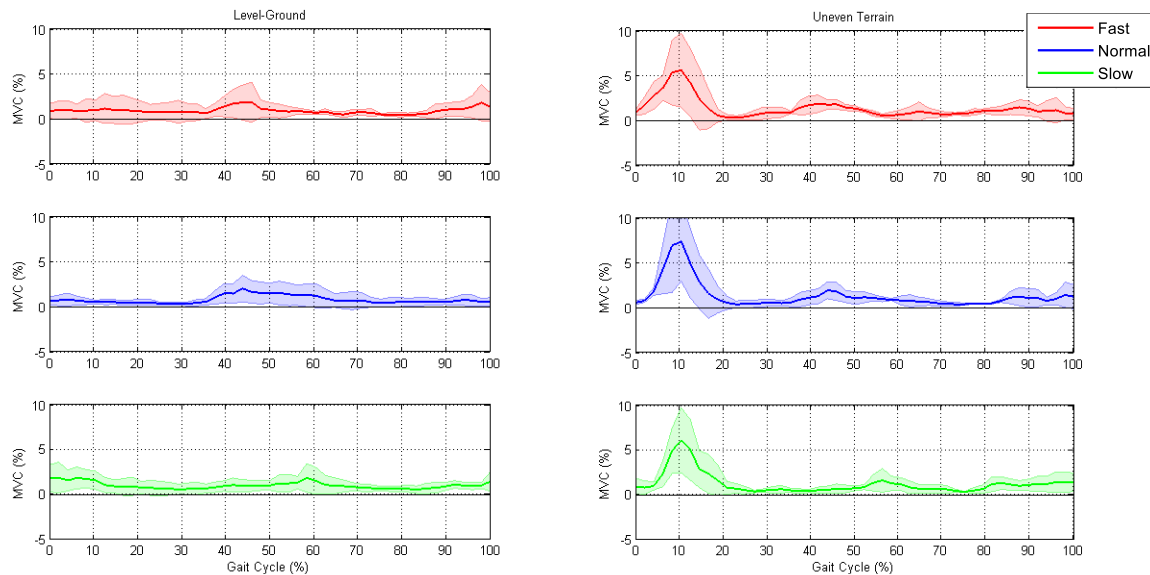
Figure 3.15: Participant group BF EMG data (N = 120 trials for each speed, per terrain)
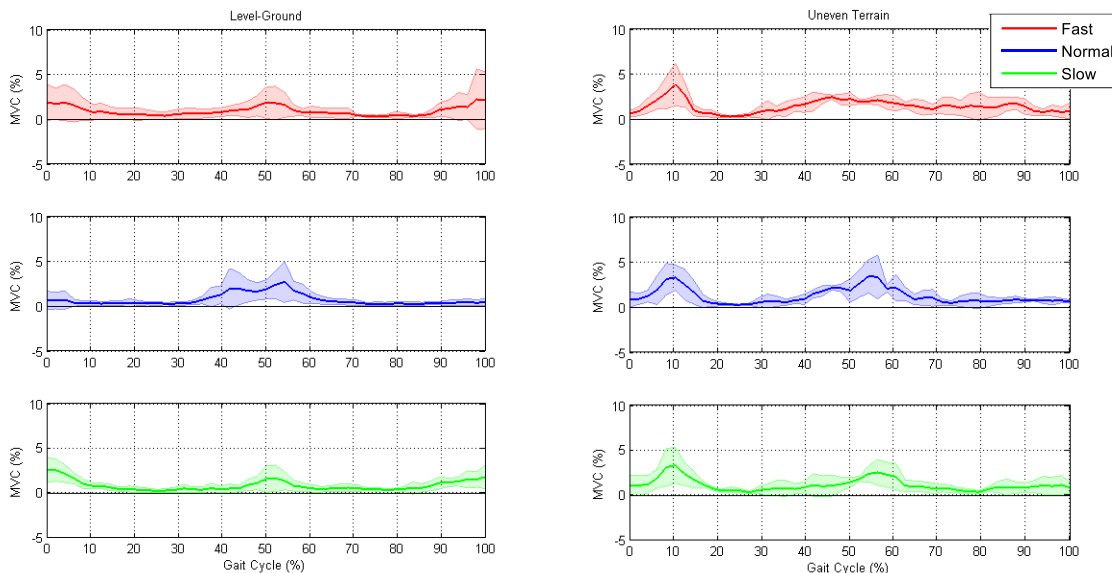
Figure 3.16: Participant group ST EMG data (N = 120 trials for each speed, per terrain)

3.4 Discussion

3.4.1 Influence of walking speed

The GRF data was similar to that reported in other literature. The magnitude of the reaction forces increased in response to walking speed. However, walking speed had not significant effect on the resulting GRFs ($p = 0.995$).

The complimentary muscle contractions of the antagonist muscle pairs are evident in the presented participant group EMG data. The general patterns of the participant group EMG data were comparable to that reported in other literature [4, 50, 96, 106, 107]. The noticeable difference in the participant group's muscle activations with respect to walking speed were in activation timings [4]. An example of this was push-off occurring slightly later ($\pm 5\%$) during fast walking, compared to slow walking. Similar to the GRF data, walking speed had no significant effect on the EMG data ($p = 0.12$).

3.4.2 Influence of terrain

The GRFs were similar between both terrains, i.e. level-ground and the uneven terrain. Though there were more fluctuations in the uneven terrain anterior-posterior and medial-lateral GRFs, particularly following heel-strike. The type of terrain had a significant influence on the vertical GRFs ($p = 0.01$). However, it did not have a significant effect on the anterior-posterior ($p = 0.06$) and medial-lateral ($p = 0.32$) GRFs.

The noticeable difference in the participant group's muscle activations with respect to terrain type was the degree of activation [4].The largest muscle activation occurred in the lower limb muscles, namely TA, MGas and LGas. This was due to the need for increased stability along the medial-lateral plane when performing foot inversion [105].

The terrain type had a significant effect on the EMG data ($p = 0.01$). Overall, greater activation was observed for all muscles, and for all three walking speeds, during the uneven terrain trials [105, 109]. This was with the exception of the ST muscle which remained relatively unchanged. This was owing to the increased need for CoM and joint stabilisation when traversing the uneven terrain.

3.4.3 Implications of GRF and EMG results

Muscle co-contraction was observed for TA and MGas during the uneven terrain trials. This TA/MGas co-contraction, as opposed to TA/LGas or TA/combined gastrocnemii activation, was due to the presented EMG data being that of participants performing foot inversion. This muscle co-contraction coupled with the force variation observed in the medial-lateral GRFs highlighted the stabilisation strategy used by the participants when traversing the uneven terrain. This was most prominent at walking speeds other than normal walking.

The uneven terrain muscle co-contraction also suggested that the participants favoured overall stability over minimising the energetic costs associated with ambulation [110]. This highlighted the importance of the second degree of freedom (DoF) present in the biological ankle joint. The second DoF enables the foot to better conform to terrains of different orientations and slopes, thus allowing for more stable traversal of said terrains. Naturally, the movement of the foot along its second DoF is facilitated primarily by the lower limb muscles, namely TA, MGas and LGas.

3.5 Conclusion

The uneven terrain GRF results gave an indication of the importance of the ankle joint having a second degree of freedom (DoF). In healthy able-bodied walking, GRFs along the medial-lateral plane are the smallest, though also the most variable. Movement or adjustments along said plane have a significant influence on the overall gait. This is most evident in the field of orthoses where insoles are used to augment and improve people's gait. Conversely, a lack of necessary movement along this plane has a negative influence on resultant gait, particularly when traversing uneven terrain.

The activation patterns and magnitudes of the lower leg antagonist muscle pair were more varied and pronounced during the uneven terrain trials. This was compared to those of the upper leg antagonist muscle pair. This indicated that most of the compensatory work done to maintain stability over the uneven terrain was carried out by the lower leg muscles. The variation of GRF along the medial-lateral plane, coupled with co-activation of the lower leg muscles, demonstrated the importance of the second DoF in the human ankle-foot system. These findings informed the design of the transtibial powered prosthesis prototype presented in the succeeding chapter.

Chapter 4
Prototype Development

Bearing in mind the overarching research objective, which was the development of an EMG driven control strategy to control a multiaxial a transtibial powered prosthesis. With the control strategy being developed to enable users to walk over varied, fixed terrains. A prototype physically capable of facilitating the desired motion was required. Therefore, the objective was to create a device that could move in a manner similar to a healthy human ankle-foot system.

4.1 The Design Evolution of Transtibial Prostheses

Some of the initial documented attempts to replace amputated lower limbs date back centuries. These include devices such as peg legs [8] which though functional, with regards to restoring some level of mobility, did not allow for prolonged use due to their construction.

Lower limb prostheses, called conventional feet were the next evolutionary step for transtibial prostheses. These prostheses were passive in nature and were built to be more aesthetically similar to the biological limbs they replaced. Due to increased focus on rehabilitation, these prostheses had sockets which increased user comfort and allowed for prolonged use. This reduced injuries such as pressure sores [111].

Passive energy-storage-and-return (ESR) transtibial prostheses succeeded conventional feet. These prostheses were developed to store energy during early to mid-stance of the gait cycle, largely by employing mechanical springs. These prostheses then supplied the stored energy to the user during push-off. When compared to able-bodied gait, the supply of stored energy resulted in decreased gait deviation demonstrated by prosthetic users. Previous gait deviation included increased knee and hip flexion. This occurred when users over flexed the knee or hip joints on the affected side to ensure that their prosthetic foot cleared the ground during swing phase [26].

ESR prostheses were usually enveloped within artificial feet, making them aesthetically similar to biological feet. ESR prostheses have been in existence since the 1980's. However, their passive nature resulted in users having to expand more energy when walking at speeds similar to that of their able-bodied counterparts [14, 112].

This was due to these prostheses not generating additional positive work (output energy) to assist users to propel themselves forward, unlike biological limbs. These devices only return the passive energy they store during stance phase. Examples of ESR prostheses are shown in figure 4.1.

a) VA Seattle foot [113]

b) Flex-foot (Össur, Reykjavik, Iceland)

c) Talux foot (Össur, Reykjavik, Iceland)

Figure 4.1: Examples of commercial ESR prostheses

Transtibial powered prostheses succeeded ESR prostheses and further improved user gait. They accomplished this by suppling energy during push-off [16, 57, 114]. This was achievable due to both the physical structure of the prostheses and the way actuation was performed. These factors enabled improved push-off and increased foot traction during push-off. The physical structure of transtibial powered prostheses is usually made up of both active and passive elements. Active elements, such as geared motors and ball or lead screws, supply energy to the system. Passive elements, such as springs and other elastic elements, absorb and later release stored energy.

A few research groups have continued to undertake the challenge of designing improved transtibial powered prostheses [16, 37, 40, 114-116]. The prostheses prototypes from these groups have allowed participants to achieve gait that is similar to that of able-bodied individuals. These devices were all tested either on a treadmill [40], level-ground [115, 116], a ramp [37] or a combination thereof. Therefore, it is uncertain how they would fare when tested on uneven terrain.

However, many of these devices only have a single degree of freedom (DoF) ankle joints. As such, it is within reason to venture that they would be unable to easily facilitate gait that was similar to that of able-bodied individuals when traversing uneven terrain. As noted from the gait experiment results presented in chapter 3, traversing uneven terrain requires foot movement along the medial-lateral plane, two DoFs.

Research has been conducted with regards to developing transtibial prostheses with more than a single DOF. Rice, J.J. and Schimmels, J.M. [117] developed a 2DoF passive transtibial prosthesis prototype. The functionality of their prototype is illustrated in figure 4.2. The first DoF was along the sagittal plane with the foot performing dorsiflexion and plantarflexion. However, the second DoF was along the z-axis. This was translational (up and down) movement of the linkage system which led to movement along the sagittal plane. The frontal plane movement was not supported.
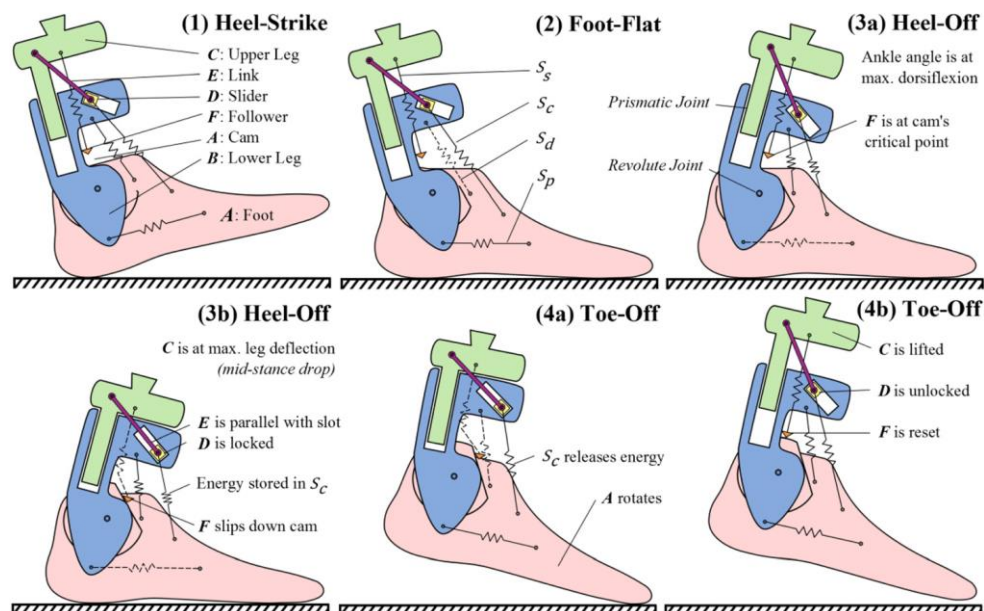
Figure 4.2: CamWalk at key stance positions. Springs in dashed lines provide no force at the instant shown [117]

Bellman et al [118] designed a 2DoF transtibial prostheses called Sparky 3. Their design was a further development based on their 1DoF Sparky 2 prototype. Their Sparky 1 reached dorsiflexion and plantarflexion angles of 9° and 23°, respectively [39]. Sparky 3 was designed to be actuated using two brushless DC motors, two helical springs, a 1mm-lead roller screw transmission and a robotic tendon. However, details regarding the development and testing of this prototype design have not been published.

Ficanha et al [119] developed a cable-driven 2DoF ankle–foot prosthesis. An image of their prototype is included as figure 4.3. Their prototype was controlled using a microcontroller executing impedance control. Two brushless DC motors with gearboxes made up the actuation system and a universal joint was used as the artificial ankle joint. Torque was transferred to the foot by means of four Bowden cables attached to a carbon fibre plate spring on the foot. Their prototype achieved a biologically similar range of motion (ROM). This was accomplished by tracking an input reference ankle joint trajectory. They tested their device during level-ground walking and when performing turning steps [120]. Structurally, their device has the capability of facilitating gait over uneven terrain. However, it is uncertain how it would perform over said terrain as a reference ankle joint trajectory would not be available for it to track. Walking on uneven terrain follows non-cyclic behaviour which would be challenging to impossible to accurately anticipate beforehand.
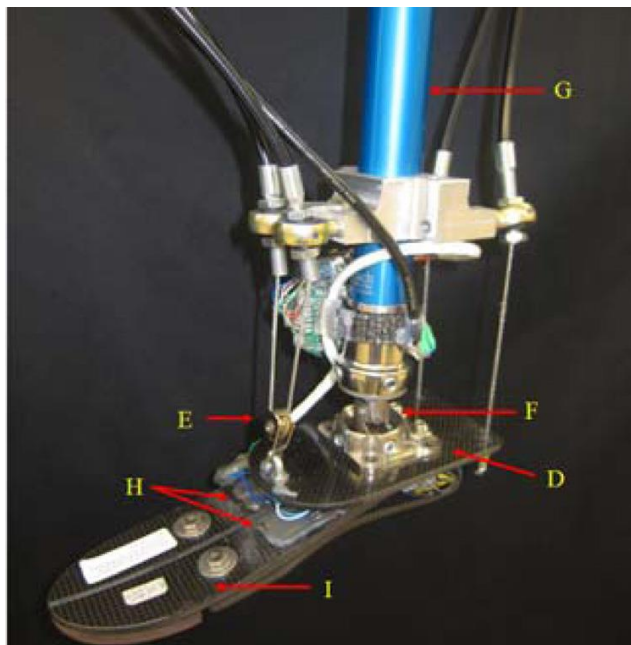
Figure 4.3: A 2DOF cable-driven ankle–foot prosthesis by Ficanha et al. [119]

Each evolutionary prosthesis iteration has led to improvements in the overall functionality of these devices and minimising some of their shortfalls. However, each new device comes with its own deficits to be overcome by the next evolutionary iteration. A comparison summary of the different types of transtibial prostheses is presented in table 4.1. The devices discussed in table 4.1 all have 1DoF, except for the research based 2DoF devices.

Table 4.1: Comparison of the different types of transtibial prostheses

Prosthesis Type	Actuation Type	Disadvantages	Advantages
Conventional feet	Passive	• Limited functionality • User gait deviations • No energy return	• Aesthetically similar to biological foot • Do not require power
Energy-storage-and-return (ESR)	Passive	• Higher energy expenditure by users, compared to able-bodied individuals • Different types of devices required for different activities	• Stored energy supplied at push-off • Reduced gait deviations • Do not require power
Commercial powered prostheses	Powered	• Heavier than ESR • Require power • Usually only fitted to highly active users	• Users achieve a more biologically similar gait • Reduces user energy expenditure
Research based 2DoF prostheses [118, 119, 120]	Powered	• Heavier than ESR • Require power • Control 'outside' of user – relies on input reference ankle trajectory [119, 120]	• Movement along the frontal plane – such as healthy human ankle-foot system • Users achieve a more biologically similar gait

4.2 Mechanical Structure

The basis for the prototype design was the results acquired from the gait experiment and data regarding known movements of the human ankle-foot system during able-bodied walking [29, 121]. The findings from the gait experiment supported the concept of developing a true multi-axial transtibial powered prosthesis prototype.

The prototype was designed using SolidWorks 2014 and had a two DoF ankle joint to enable both dorsiflexion/plantarflexion and eversion/inversion movements. The design criteria are presented in table 4.1. This criterion was also used in ascertaining the performance of the prototype design during FEA testing.

Table 4.2: Prototype Design Criteria and FEA Implications

Design Criteria	Implications to FEA
Stable base of support and compact in size (similar to human foot)	No failure or permanent deformation of the foot sections
Biologically similar ROM	2 degree of freedom (DoF) movement
Store and release passive energy during stance phase	Incorporate an elastic element
Active actuation	Powered by DC voltage
Robust enough to perform validation testing	No failure at loads of <15kg
Prototype mass <5kg	N/A

Several design iterations led to the annotated, prototype design presented in figure 4.4. The shape of the prosthetic foot was designed to mimic that of the human foot. The arch in the foot was incorporated to enable the prototype to storage of passive energy during weight bearing activities. This would be as a user transitioned through stance phase. The foot was designed to be made from a material with some elasticity, such as tough resin (when 3D printed) or carbon fibre. Such a material would allow it to bend slightly as it took on weight and to subsequently return said energy during push-off. This action would be similar to the work done by the plantar fascia ligament and the anterior and posterior tibialis, flexor digitorum longus, flexor hallucis and fibularis longus muscles during healthy able-bodied gait.

Prosthetic foot shapes similar to that of the developed prototype exist in commercially available prosthetic feet. These include Össur's Pro-Flex [122], Freedom Innovation's Pacifica [123] and Fillauer's Ibex [124]. These feet have been shown to be more energy efficient than flat foot designs or to the traditional SACH foot [125, 126]. The roll over shape was not considered in the design of this prototype due to two reasons.

The first being that it was desired to have the prototype foot be similar in shape and aesthetics to that of the biological human foot. The second was that this initial prototype was to be used primarily to test the real-time performance of the developed control system. As such, functionality of the control system was to be established prior to testing the entire system with loads. The view was that the prototype would be improved in preparation for future weight bearing testing.
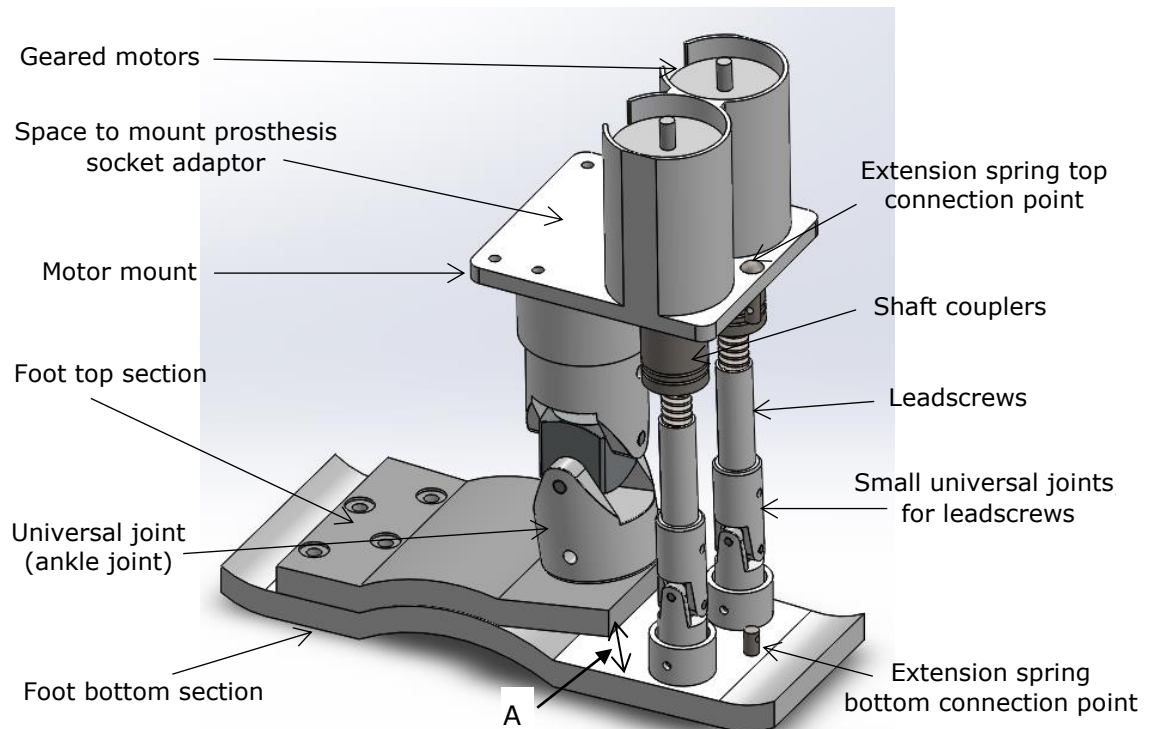
Figure 4.4: Transtibial powered prosthesis prototype design

Other groups within this area of research have used commercially available prosthetic feet for their work. However, for this research, it was decided to design and 3D print a foot. This was done to avoid any issues that could have arose from retro-fitting another device to fit the purpose of this work. The prosthetic foot was originally designed to be 24cm in length, equivalent to a women's UK size 6. Though due to manufacturing constraints, the foot length was reduced to 20cm which was equivalent to a women's UK size 4.

The foot was composed of two sections, a top and bottom section. Each section was 3D printed from ABSplus P430 [127] using a Stratasys dimension 1200 3D printer. The 3D parts were then post cured for at least 30 minutes to maximise mechanical properties. The mechanical properties of the material from which the prototype was 3D printed are presented in table 4.2.

The top section of the foot supported a universal joint which was analogous to the human ankle and enabled the desired 2DoF movement. Two smaller universal joints were also part of the actuation system. They ensured that the actuators (lead screws) did not impede the multi-axial movement of the prototype foot. All the universal joints were fabricated from alloy steel.

Table 4.3: Material properties for P430 ABSplus™ [127]

Yield strength	Ultimate tensile strength	Tensile (elastic) modulus	Tensile elongation at break	IZOD Impact, notched
31 MPa	33 MPa	2,200 MPa	6%	106 J/m

The distance from the ground to the prototype ankle's axis of rotation, with the foot flat on the ground, was 80mm, similar to a human leg. A 3D printed motor mount was used to keep the motors and the actuation system in place. It also connected the actuation system to the prototype foot, via the top section of the main universal joint (prototype ankle). The motor mount was designed in such a way that a prosthetic socket adaptor could be attached on top. This would subsequently enable a user with a transtibial amputation to don the prototype for testing.

The gap between the back portion of the top foot section and the bottom foot section, indicated with an 'A' in figure 4.4, was designed in anticipation for weight bearing prototype testing. The gap was incorporated to allow the top foot section to deform slightly during heel strike, rather than it snapping off from absorbing the full shock. In the case of weight bearing testing, the bottom foot section would absorb shock at heel-strike primarily through the arch and through an incorporated extension spring.

The arch at the bottom foot section had a radius of 70°. This angle was about half of the medial-longitudinal human arch, which ranges between 132°-160° [128]. The radius of the prototype arch was limited by the size of the foot, which was imposed by manufacturing restrictions.

It was envisioned that the slight deformation of the top foot section would translate to less energy being transferred to a prospective user, particularly at the residual limb-prosthesis socket interface. The prototype engineering drawings are included in Appendix D.

4.3 Actuation System

Actuation of the prototype was achieved using brushed DC motors and a leadscrew transmission system. Two 12.8W brushed DC geared motors, each rated at 12 V/4930 rpm, were used. The rotational motion from the motor-gear systems was converted to linear motion using two 10mm diameter leadscrews. The actuation system ensured that positive energy would be supplied to the prototype during gait.

Further to absorbing some of the shock at initial foot contact for future weight bearing tests, an extension spring was incorporated to store and release energy during gait. The spring was incorporated to assist the actuation system in supplying power during gait, which one of the design criteria. It would also ensure that the prototype could still be used if the active elements went 'offline' during weight bearing use. According to Winter [41], a person weighing 75kg walking at a normal cadence on level-ground produces a peak ankle joint torque of 120Nm and generates 250W of power at push off. This power requirement was taken into consideration when choosing the specification for the extension spring.

The first criterion was for a spring to deliver ±100W of power at push off. The second criterion was the spring length, only a spring with a free length of ±70mm could be implemented. This was due to the dimensional limitations, and maximum range of ankle motion along the sagittal plane, imposed by the prototype design. Taking normal adult walking speed to be 1.4m/s (±two steps per second on average), the push-off phase for a single stride would take approximately 0.14s. The walking speed of 1.4m/s was based on the normal walking speed observed during the level-ground trials, presented in chapter 3 and on [129].

Thus, the ideal spring stiffness was calculated to be 5N/mm. This was with consideration to a participant weighing ±75kg using the prototype. An extension spring with a stiffness of 1.26N/mm was ultimately chosen. This was based on spring availability and with the view of not over stiffening the system. The spring would have to be substituted for another with an appropriate stiffness for users whose body weight was more than 10kg higher or lower than 75kg.

The spring would only be implemented during weight bearing tests. This was due to its incorporation being grounded on user weight being present to elongate it, predominately during stance phase.

4.4 Overall Prototype Functionality

As part of the design criteria, the prototype was designed to achieve a range of motion (ROM) similar to the human ankle-foot system. The prototype ankle (the universal joint) could move through ±120° along the two desired planes of motion. However, the prototype's ROM targets were set as indicated in table 4.3. These were synonymous to the ROM capabilities of the human ankle-foot system [130, 131].
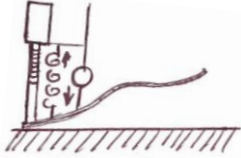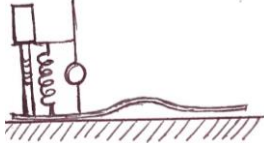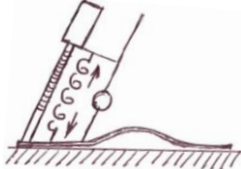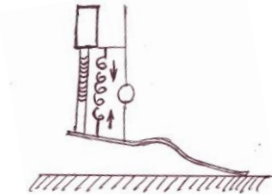
Table 4.4: Prototype ankle ROM

Type of movement	ROM	Plane of movement
Dorsiflexion	30°	Sagittal
Eversion	20°	Medial
Inversion	30°	
Plantarflexion	40°	Sagittal

The weight of a prosthesis is an important factor as it has an effect on the performance of the device [132-134]. The weight of the final prototype was a factor considered during design. As such, measures were taken to ensure that the developed prototype would have a weight comparable to that of a similar sized human ankle-foot system. However, this was not a priority concern as the prototype was a proof of concept device which would be improved following further design iterations. The weight of the assembled prototype, excluding a power supply, was 4kg. This was comparably to the weight of a lower leg for a 70kg man [135].

A priority when developing the prototype was to minimise the amount of active power required by the system whilst not compromising its output behaviour. This meant that the plantarflexion torque could be similar to that observed during healthy human walking. The actuation system essentially resulted in a linear actuator in parallel with an elastic element. The configuration of the actuation system and the spring meant that the combination would work in unison to actuate the prototype. This would occur under weight bearing conditions, as is illustrated in table 4.4. During weight bearing conditions, the back drivable leadscrew system would work to minimise energy expenditure from the actuation system.

Table 4.5: Actuation system and spring work during gait

Gait Phase	Work Done by Each Part	Type of Work
Powered Dorsiflexion Terminal swing (< ±80%) – Initial contact (±0%)	o Motor at work o Spring extension due to actuator; energy storage	Opposing work
Neutral Position Initial contact (±0%) – Foot flat (±10%)	o No motor work, leadscrews back driving o Spring returning stored energy o Actuator and spring return to 'rest' position	No opposing work
Passive Dorsiflexion Foot flat (±10%) – Pre-Heel off (±40%)	o No motor work; leadscrews rotating under user body weight o Extension of spring due to user body weight, CoM transition over the foot; energy storage	No opposing work
Powered Plantarflexion Pre-Heel off (±40%) – Push off/Toe off (±60%)	o Motor supplying positive work o Spring returning stored energy	Complementary work
Foot clearance Toe off (±60%) – Mid-swing (±80%)	o No motor work, leadscrews back driving o Spring returning stored energy o Actuator and spring return to 'rest' position	No opposing work

4.5 FEA testing

FEA (finite element analysis) was carried out to ensure that the developed prototype was strong enough to be used for testing, both with and without bearing weight. The analysis was done using SolidWorks 2014. Three foot position scenarios were simulated. These are presented in table 4.5 along with the points of fixation and the angle of the applied force for each scenario. The fixation points were set to be under the bottom foot section. The load was applied at the top of the motor mount for each position scenario. The angle of the applied force was with respect to the horizontal axis, which constituted 0°. This is illustrated in figure 4.5.

These specific scenarios were chosen because they encompassed the movement of an ankle-foot system during healthy human walking. These were similar to the prosthesis foot testing approach done by other researchers [136, 137]. Foot eversion and inversion were also encompassed within the three position scenarios. This was due the ankle-foot system conforming to the slanted/uneven walking surface during uneven terrain traversal, resulting in a foot flat position.

Table 4.6: FEA foot position scenarios and fixation points

Position scenario	Fixation point	Angle of applied force
Dorsiflexion	Heel section of foot	30° CCW
Foot flat	Entire foot sole	90°
Plantarflexion	Toe section of foot	40° CW

* CCW and CW refer to the counter-clockwise and clockwise directions, respectively, from the horizontal axis.

a) Foot flat   b) Dorsiflexion   c) Plantarflexion
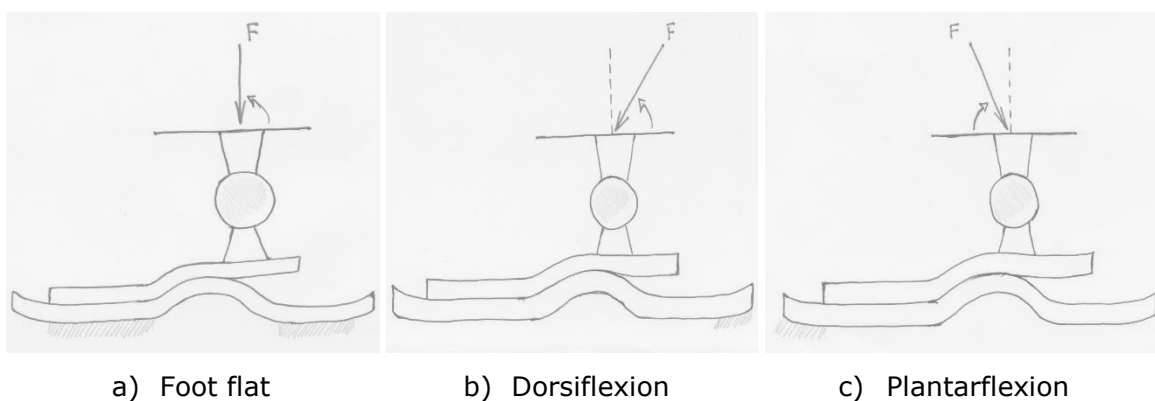
Figure 4.5: FE model loading scenarios

The FEA results for each position scenario are presented below. The main failure criterion was a maximum von Mises stress above the foot material's yield strength of 31MPa. This was the point where the material would deform past its elastic state of 'bouncing back' and into its plastic state of permanent deformation. The 'h-adaptive' method was selected with a loop count of 3 and a 95% target accuracy. This meant that the FEA was performed three times until a confidence level of 95% was obtained for the acquired results. This ensured the accuracy of the FEA results with regards to real-world conditions. The 'large displacement' option was also selected for the analysis to encompass a greater range of possible outcomes. The details of the FE model for each foot flat scenario are presented in table 4.6. The actuation system and the extension spring were excluded from the analysis for the reason of simplifying the model to allow for solution convergence.

Table 4.7: FE model details for foot flat scenario

Description	Foot flat scenario		
	75kg	40kg	25kg
Material	ABS P430		
Mesh elements	3D tetrahedral solid elements, 2D triangular shell elements and 1D beam elements		
Mesh type	Mixed		
Maximum element size	6.20107 mm		
Total number of nodes	36520	36549	36364
Total number of elements	22797	22807	22657

4.5.1 Foot Flat Scenario

The prototype was first simulated in the foot flat position. A load of 75kg (735.8N) was initially simulated. The stress and strain concentrations were around the front bend of the top foot section, marked as 'A' in figure 4.6. These results indicated the mostly likely failure point for the prototype under the specified loading and fixation conditions. The stress and strain peaked at 104MPa and 0.03ESTRN (equivalent strain), respectively. These would result in prototype failure (permanent deformation) of the prototype foot.
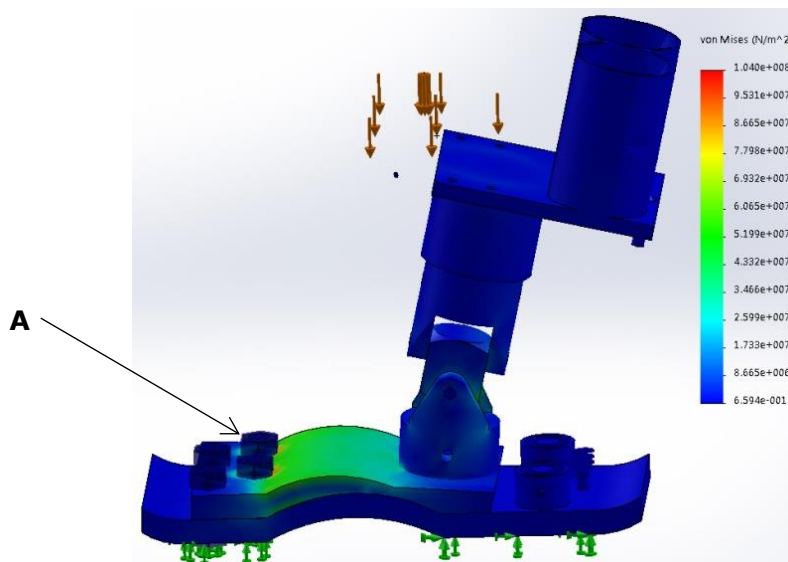
Figure 4.6: Stress response to 75kg foot flat loading

The largest displacement was that of the motor mount which peaked at 50mm. This displacement was deemed unacceptable and indicated that the current, 3D printed prototype would be unsuitable for weight bearing testing with a load of 75kg. However, it is worth noting that the inclusion of the actuation system would add some rigidity to the prototype.

The prototype was then simulated with a load of 40kg (392.4N) again in the foot flat position scenario. The stress and strain concentrations were again at the front bend of the top foot section, evident in figure 4.7, respectively. However, the peak magnitudes were almost halved at 39.84MPa and 0.013ESTRN, respectively, compared to those of the 75kg loading condition. The largest resulting displacement was 20mm and was that of the motor mount. This was still unacceptable as the maximum von Mises stress was higher than the foot materials' yield strength.

A loading condition of 25kg (245.3N) was then simulated for the foot flat scenario. The maximum displacement was reduced to 14.5mm and was again mainly the displacement of the motor mount. The stress and strain peaks were reduced to 26MPa and 0.01ESTRN, respectively. This was acceptable at the foot would not permanently deform under this load.
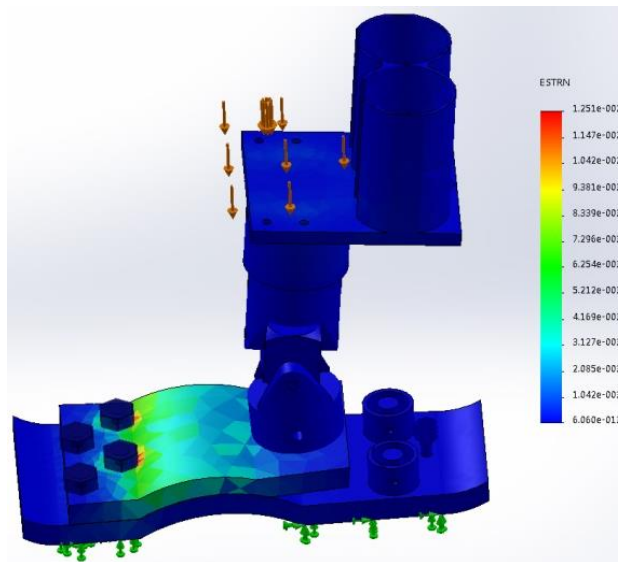
Figure 4.7: Strain response to 40kg foot flat loading

4.5.2 Dorsiflexion Scenario

The remaining foot position scenarios were then simulated using a load of 25kg (245.3N). This load was applied as functions of its Fx and Fy components, as described in table 4.5. The Fx and Fy components were calculated as a factor of the applied load angle. Details of the FE model details for these scenarios are presented in table 4.7. The main failure criterion was a resulting maximum von Mises stress above the foot materials yield strength of 31Mpa. The 'h-adaptive' method was again selected with a loop count of 3 and a 95% target accuracy.

Table 4.8: FE model details for foot flat scenario

Description	Dorsiflexion scenario	Plantarflexion scenario
Material	ABS P430	
Mesh elements	3D tetrahedral solid elements, 2D triangular shell elements and 1D beam elements	
Mesh type	Mixed	
Maximum element size	6.20107 mm	
Total number of nodes	36520	36549
Total number of elements	22797	22807

The stress and strain concentrations were near the fixture point. This is shown in figure 4.8. The foot did slide forward by 6.58mm. This was not of concern given the direction of motion and the small magnitude. During motion, the foot would displace towards a foot flat position. The peak stress and strain were 30.14MPa and 0.012ESTRN, respectively, presented in figure 4.8. These peak values would not result in permanent damage of the prototype as they were still within the materials' range of elastic deformation. As such, the performance of the prototype under the dorsiflexion scenario was acceptable.
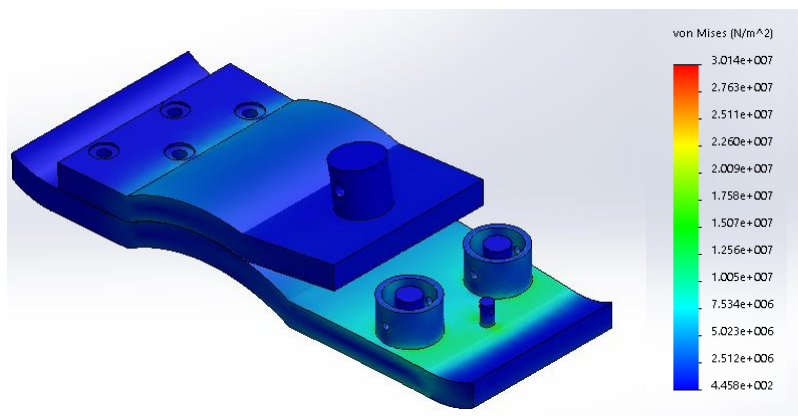
Figure 4.8: Stress response to 25kg dorsiflexion loading

4.5.3 Plantarflexion Scenario

The peak stress and strain with a 25kg load were 34.45MPa and 0.014ESTRN, respectively. The results were unacceptable as the maximum von Mises stress was above the materials yield stress of 31MPa. As such, the model was simulated again using a load of 22kg. This resulted in a peak stress and strain of 30.45MPa and 0.012ESTRN, respectively. These results were acceptable, as shown in figure 4.9. The maximum displacement was 4.65mm backward (20 mm with the motor mount moving downwards towards the bottom foot section). The direction of displacement was synonymous to the natural displacement of a human foot during forward propulsion (walking).
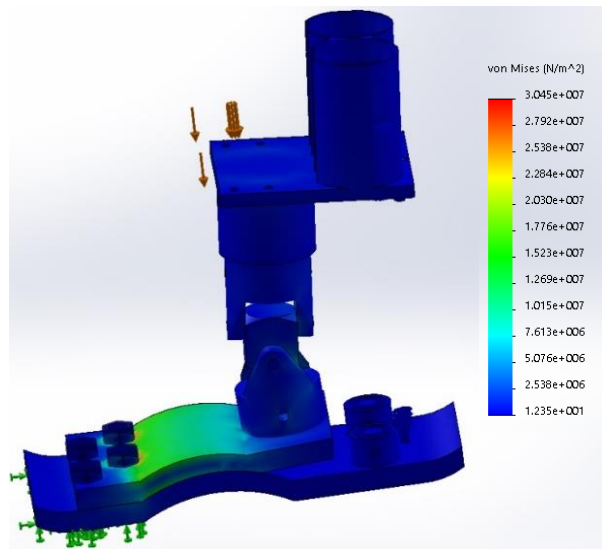
Figure 4.9: Stress response to 22kg plantarflexion loading

4.5.4 Carbon fibre simulations

The effect of changing the material of the foot section to a more rigid material was also explored. Carbon fibre was the material chosen due to it being incorporated in most state-of-the-art lower limb prostheses [122, 138]. The two foot sections that made up the prototype foot were changed to carbon fibre and the FEA was performed again. The mechanical properties of the carbon fibre material are presented in table 4.8. The FE model was simulated according the three foot scenarios specified in table 4.5. The results of these simulations are presented in table 4.9. The 'h-adaptive' method was selected with a loop count of 3 and a 95% target accuracy.

Table 4.9: Material properties used for carbon fibre [139]

Yield strength	Ultimate tensile strength	Tensile (elastic) modulus	Compressive strength	Poisson's ratio
350 MPa	600 MPa	70 GPa	570 MPa	0.1

Table 4.10: Results summary for carbon fibre foot

Scenario	Max. von Mises (MPa)	Max. Strain (ESTRN)	Max. Displacement (mm)
Foot flat	87.05	0.033	12.7
Dorsiflexion	90.2	0.035	21.4
Plantarflexion	99.1	0.038	14.05

4.5.5 Inclusion of an elastic element

The elastic spring originally designed to be incorporated into the final prototype was omitted during the FEA simulations. This was done to simplify the model, particularly as a nonlinear FEA would have been required for the elastic element alone. As such, the implications of incorporating the extension spring were investigated by means of simulating the spring. Plain carbon steel was specified for the spring; the mechanical properties are included in table 4.10. The failure criterion for the spring was it being displaced further than 70mm, which was its maximum free length.

Table 4.11: Material properties used for plain carbon steel (SolidWorks 2014)

Yield strength	Ultimate tensile strength	Tensile (elastic) modulus	Shear modulus	Poisson's ratio
220 MPa	400 MPa	210 GPa	79 GPa	0.28

The spring was fixed on one end, at the loop, and a pulling force was applied on the other end, at the loop. Dissimilar to the standard mesher used in the other simulations, a curvature based mesher was used for the spring simulation. The minimum and maximum element sizes were 1.16mm and 3.47mm, respectively. The total number of nodes and elements were 77504 and 41210, respectively.

The FEA results indicated that the spring could withstand a pulling force of up to 58.86N. This led to a final displacement of 53.1mm, as presented in figure 4.10. In doing so, the spring would be able to elongate and store energy during gait. It would also attenuate vibrations gait and shock during heel-strike.
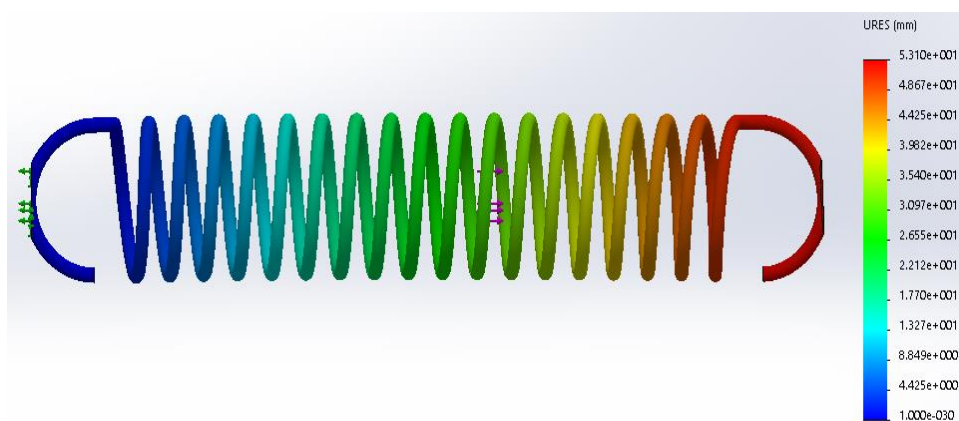
Figure 4.10: FEA results – spring displacement

4.6 Discussion

The FEA simulations highlighted the structural capabilities and rigidity of the designed prototype. The results from the foot flat scenario FEA indicated that the current prototype design would be able to support a load or user weight of up to 25kg. A 20% factor of safety was incorporated with the 25kg load. However, simulation with the plantarflexion scenario indicated a load of 25kg would lead to permanent deformation of the prototype foot. This highlighted the benefit of simulating the prototype design under different scenarios.

Based on the simulation results, the prototype would be able to withstand a weight of up to 22kg without failing. This weight would be acceptable for all three scenarios simulated; namely foot flat, dorsiflexion and plantarflexion. This would be 22kg with a ±20% load factor of safety. This is with the prototype being fabricated by 3D printing it from ABS P430.

The simulations demonstrated that plantarflexion movement would be the most demanding for the prototype. The results indicated that the prototype would be able to handle dynamic movement without failure. This was based on the simulation response under the different foot scenarios and with loading at different angles for dorsiflexion and plantarflexion.

Simulating the extension spring indicated that it could be displaced up to 53.1mm, while withstanding stresses of up to its yield strength. This indicated that the elastic element would perform some damping when loaded as part of the prototype. This would be most prevalent during initial foot contact (heel-strike). Incorporating the spring would add functionality to the prototype that was more comparable to the human ankle-foot system. The elastic element would be synonymous to the passive elastic element (PEE) detailed in the Hill-based muscle model (section 2.1.1). The implications of the spring FEA results were that incorporating such an elastic element could:

1. reduce vibrations as a result of the actuation system,
2. provide damping during weight bearing testing, particularly at heel strike, and
3. store and release passive energy during the stance phase of weight bearing testing.

Changing the foot material to carbon fibre during the simulations indicated that the system would be able to support a weight of up to 75kg. When simulated, the carbon fibre foot could comfortably actually support of weight of up to 150kg in all three foot scenarios. This meant that the weight specifications for the carbon fibre foot would have been similar to commercially available transtibial prostheses [138, 140]. Such a change would have made performing weight bearing tests possible. However, due to time and budgetary restraints, the foot material was not changed. This was also because a proof of concept experiment was to be carried out at this stage of this research project.

4.7 Conclusion

The best performing position scenario was foot flat. This was due to it having a larger fixation point (the entire sole of the foot) through which the applied load could be distributed. The highest von Mises stresses, within the materials yield strength specification, occurred during the plantarflexion scenario. This was attributed to the applied load being at its maximum, out of line position from the ankle joint. It was also attributed to the smaller fixture point, in comparison to that of the foot flat scenario.

The FEA results indicated that weight bearing testing would only be possible if the prototype was redesigned or fabricated from a more rigid material, such as carbon fibre. The results also supported the notion that incorporating an elastic element would provide system damping and a means to store and release passive energy. This would be the case during weight bearing testing.

In comparing the designed prototype to commercially available transtibial powered prostheses, the prototype would not be as rigid when 3D printed from ABS P430. However, the FEA results suggest that the prototype would perform similar to its commercially available counterparts were it to be fabricated from carbon fibre and incorporate an elastic element. Thus, the prototype could enable users to achieve a biologically comparable gait as a function of its physical design. This would even be possible if it were used without being powered, as a passive device. Though in such a case, the returned energy would be limited to that only stored by the elastic element. The prototype being a multi-axial (2DoF) device would allow its users to manoeuvre over more varied terrain. This would be as opposed to current commercially available transtibial prostheses which do not have fully realised multiple axes of movement.

The central focus of developing the prototype was to test and ascertain the real-life functionality of the developed control strategy. This was as opposed to testing the design and functionality of the prototype itself. As such, the prototype was used as is for validation testing. Due to budgetary and time limitations, it would not have been possible to fabricate a carbon fibre prototype in-house (within the university's workshop). Nonetheless, the designed and 3D printed prototype was rigid enough to perform the validation experiment.

Chapter 5
User Intent Prediction Strategy

The developed control strategy was essentially the brain of the prototype and formed the most significant aspect of this research project. It was composed of two key parts, the first being to measure user muscle activation (EMG) signals and to determine the movement solicited. The second part being to facilitate the desired movement on the prototype, ensuring that it is carried out in a manner that is similar to that of able bodied individuals. The first part of the overall developed control strategy is presented in this chapter. It is referred to as the high-level controller. The second part is presented in chapter 6 and is referred to as the output level controller.

Hierarchical control strategies have been successfully implemented to control powered prostheses as reported by other researchers [37, 54, 80, 141, 142]. The hierarchical control approach used in this research allowed each control part to be developed independently. This meant that any failures were localised and could be traced back to a specific controller, which was useful with regards to troubleshooting.

The premise of this research was to enable volitional control of a transtibial powered prototype and, in so doing, allow prospective users to traverse terrains of varying orientation and type with greater ease. The approach taken was to enable control based solely on data and input from a participant. As such, no extrinsic (prosthesis mounted) sensors were implemented in determining the output motion to be carried out by the prototype.

The approach implemented was to use intrinsic sensors. This was as opposed to using extrinsic sensors to read the movement of the prototype (or participant) in response to the walking terrain and then facilitating movement. This could include enabling plantarflexion once the foot transitions through mid-stance. This meant 'listening' to a participant's movement or intended movement in the case of an individual with transtibial amputation and enabling the beckoned motion. In so doing, the prototype would not 'drive' a user but rather, it would respond to the user's movement requests. The envisioned control approach was to develop a strategy that would allow a user to control the prototype in a manner similar to their now amputated biological leg.

The EMG data acquired from the gait experiment was used to develop the backbone/skeletal architecture of the high-level controller. The data used was from the tibialis anterior (TA), medial (MGas) and lateral (LGas) gastrocnemius muscles. These muscles were chosen for two reasons. The first being that these were the most dominant muscles during both the level-ground and uneven terrain walking trials, as presented in chapter 3. Secondly, the aim was to make the system as minimally invasive as possible. This meant making use of the least number of sensors to successfully facilitate the desired control strategy.

The first step in developing the high-level controller was deriving a way of using raw EMG data to decipher participant motion and to specify prototype output movement. EMG data is variable in its nature. As such, features have to be calculated in order to ascertain meaningful information from the data. For the gait experiment, the objective was to determine the muscle activation patterns and magnitudes. This was done to study the gait strategies implemented in response to walking at different speeds and on different terrains. However, for the purpose of controlling the powered prosthesis prototype, the objective of calculating EMG features was to: 1) enable the differentiation between unique gait-related movements and 2) determine to what accuracy this could be done.

5.1 Feature Selection

A number of features could have been chosen for the purpose of controlling the prototype. Therefore, features that could easily be implemented in real-time were given first preference. This resulted in the selection of mostly time domain features because they do not require any signal transformation and are less 'computationally draining', compared to frequency domain features, whilst still yielding good classification accuracy [55, 62, 73].

The first step was determining which features, or which combination thereof, yielded the highest classification accuracy. Six features were explored, namely variance (VAR), wavelength (WL), integrated EMG (IEMG), autoregressive (AR), root mean square (RMS) and moving average (MAV). Autoregressive features were the only frequency domain features explored. They were included due to their ease of calculation and their reported classification accuracy [56, 143].

The mathematical definitions of these features are presented in Appendix E. These features were calculated from the EMG data for each of the three muscles of interest, namely TA, MGas and LGas.

Machine learning algorithms go hand in hand with EMG features. This is because they enable the determination of patterns and the differentiation of data, with respect to unique groupings/classes. Based on other research in this field, detailed in chapter 2, Linear Discriminant Analysis (LDA) was the first classification algorithm chosen to predict user motion. LDA was chosen due to its ease of implementation and being 'computationally light'. Whilst still resulting in comparable or even better classification of EMG data, compared to more complex classification algorithms [55, 62, 144].

An incremental analysis window approach was taken to processing and classifying EMG data. This took the form of using a window size of 150ms with no window overlap. The basis of this was taken from previously reported research presented in section 2.4.3, in chapter 2. When implemented in real-time, the analysis window was the data from which user intent was predicted.

A data set was created from the EMG data acquired during the gait experiment. The data set was used to train and to test different features and combinations thereof. The data set was split such that 70% of it was used for training and 30% was used for testing the predictor's accuracy in response to new data. A single entry of the data set was made up of five EMG data samples, one for each movement type. Each data sample was equivalent to a window size of 150ms, as per the chosen analysis window size. A single entry was taken from one valid gait trial of one participant. Three data entries, comprising of all five movement types, were taken from each participant. Thus, the complete data set was made up of 18 unique data entries. The valid trials from which the data entries were taken were chosen at random. The data set was segmented using Matlab R2014a, using a custom written code.

Two kinds of participant EMG data were initially used to test classification accuracy based on three features. The first was raw EMG data as read by the electrodes; this was case A. The second was raw, amplitude normalised EMG data. The normalisation was done using participants' MVCs (maximum voluntary contractions) recorded as part of the gait experiment. This was case B. Raw EMG data was

ultimately chosen for implementation as it yielded overall better classification accuracy and did not require prior processing before feature calculation and classification, unlike MVC data. The comparison of classification accuracy when using raw and MVC amplitude normalised EMG data is presented in Appendix F.

The five movement classes that made up the complete data set were dorsiflexion, foot flat, plantarflexion, eversion and inversion. The swing phase was omitted on the premise that the foot could be actuated to a dorsiflexed position to clear the ground during swing. Dorsiflexion, foot flat and plantarflexion EMG data was extracted from the level-ground walking trials. Inversion data was extracted from the uneven terrain walking trials during which participants performed inversion with their right feet.

As part of the gait experiment, participants were asked to perform foot eversion while in a seated position with their heel contacting the ground. This procedure was similar to the protocol used for MVC capture. The eversion data was recorded after MVC capture but before the walking trials were started. For each participant, three eversion movements were captured for each foot. This formed the eversion data included in the set of movement classes.

LDA was used to test the performance of the individual features and their combinations. Details of the LDA algorithm used are presented in Appendix G. Two variations of LDA were used. These were the standard linear approach and either the 'diagquadratic' (naive Bayes) or the Mahalanobis distance. Two variants were tested to give a better indication of the performance of the features. The classification accuracy of the individual features and basic combinations thereof are presented in table 5.1 and 5.2, respectively.

Table 5.1: Classification accuracies of individual features

Feature	Classification Accuracy (%)		Feature	Classification Accuracy (%)	
	Linear	Mahalanobis		Linear	Mahalanobis
VAR	40	37	AR	43	57
WL	57	53	RMS	40	47
IEMG	70	50	MAV	40	43

Table 5.2: Classification accuracies of basic feature combinations

Feature	Classification Accuracy (%)		Feature	Classification Accuracy (%)	
	Linear	Mahalanobis		Linear	Mahalanobis
VAR+WL	70	67	AR+RMS	53	67
VAR+IEMG	70	77	AR+MAV	60	67
WL+IEMG	67	73	RMS+MAV	43	63
VAR+WL+ IEMG	73	70	AR+RMS +MAV	63	67

The goal of feature selection was to ascertain which combination of well performing features resulted in the best classification accuracy. Based on the accuracies of certain basic combinations, other feature combinations were tested. Their classification performance is presented in table 5.3.

Two combinations resulted in the highest classification accuracies. These were VAR+IEMG+MAV (80%) and using all six features (93%). The classification (prediction) accuracy was calculated as shown by equation 5.1. The features chosen for real-time implementation were all six features. There were no computational delays when implementing any of the feature combinations.

$$Accuracy\ (\%) = \frac{T_c}{n} \times 100 \qquad \dots \text{(eq. 5.1)}$$

where;

    T_c is the total number of correctly classified samples

    n is the total number of samples classified

The prediction accuracies obtained in this research were comparable to those presented in other research. Huang et al [55] reported classification errors of between 13-18% when using data from the lower leg (shank). This was as able-bodied participants performed seven locomotion tasks, including level-ground walking. These results were obtained using EMG data from six muscles. In their study, the lowest classification errors occurred when using EMG data from 16 muscles in both the upper and lower leg.

Table 5.3: Classification accuracies of extended feature combinations

Feature	Classification Accuracy (%)		Feature	Classification Accuracy (%)	
	Linear	Mahalanobis/ diagquadratic		Linear	Mahalanobis/ diagquadratic
VAR+IEMG & AR	77	80	WL+IEMG & AR	67	80
VAR+IEMG & RMS	70	73	WL+IEMG & RMS	70	70
VAR+IEMG & MAV	80	77	WL+IEMG & MAV	70	77
VAR+IEMG & AR+RMS	77	67	WL+IEMG & AR+RMS	63	67
VAR+IEMG & AR+ MAV	80	67	WL+IEMG & AR+MAV	63	67
VAR+IEMG & RMS+MAV	70	63	WL+IEMG & RMS+MAV	57	63
VAR+IEMG & AR+RMS+MAV	77	67	WL+IEMG & AR+RMS+MAV	70	67
VAR+WL+IEMG + AR+RMS+MAV (All six features combined)				93	63

5.2 Development of the Prediction Algorithm
5.2.1 Classification Algorithms
5.2.1.1 Machine learning classifiers

A decision tree was also explored as an alternative machine learning based classification algorithm. Details of the classification tree that was used are presented in Appendix G. Machine learning algorithms were explored because of their ability to segregate and class data, especially in cases where data from the different classes tends to be very similar.

The structure of decision trees is similar to that of biological trees with regards to how they are trained and how they classify new data. The training set is presented at the root/trunk level and each separation of data, based on thresholds or feature differences, results in a new branch being created. This leads to a fully formed tree where new data starts at the 'trunk level'. New data is then is directed to the appropriate branch (group/class) based on whether it is higher or lower than a threshold limit at each branching point [145, 146].

The decision tree was included due to its ease of training and implementation. A graphical representation of the tree is presented in figure 5.1. It illustrates how incoming data was classified with the top being the starting point and each split being a data separating threshold. The similarities of the five motions of interest are evident from figure 5.1. This highlights the challenge of accurately grouping such data.

The original data set which was initially split 70/30 for LDA training and testing was recombined to create a larger data set from which the decision tree could be trained. The LDA classifier was also retrained using this larger data set. This larger feature set had a total of 90 data entries. Each entry was composed of all six features and again encompassed the five motions. These were dorsiflexion, foot flat, plantarflexion, eversion and inversion.
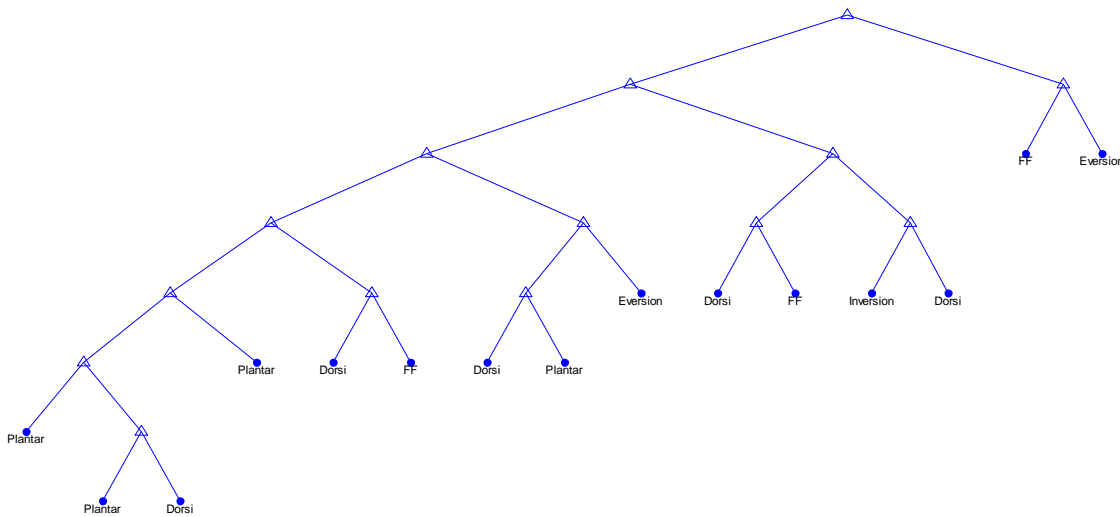
Figure 5.1: Decision tree classification branch-offs

5.2.1.2 Non-machine learning classifiers

Based on the classification accuracies observed during the determination of the best feature set combination, a classifier that was not reliant on machine learning was developed. This was called the deterministic classifier; details of which are presented in Appendix G. This classifier was based on known/fundamental biomechanics knowledge of healthy human walking EMG patterns [41, 96].

This meant the expectation of certain muscle activation amplitudes and patterns during the five specified types of motion, illustrated in table 5.4. As such, no prior training was required. In addition to the LDA and tree, the deterministic classifier became the third classification algorithm tested.

Table 5.4: Deterministic control logic

Movement type	Muscle activation		
	Tibialis Anterior	Medial Gastrocnemius	Lateral Gastrocnemius
Dorsiflexion	Maximum	Minimum	
Foot flat	Maximum	Medium	
Plantarflexion	Minimum	Maximum	
Eversion	Maximum	Minimum	Medium
Inversion	Maximum	Medium	Minimum

Classification algorithms have their strengths and weaknesses. It is common for an algorithm to fare well for specific data and for it to be outperformed by another algorithm when classifying a different type of data set. An example of this could be classifying level-ground versus uneven terrain data. Therefore, a voting scheme classification approach was also incorporated for testing. Details of the voting scheme are presented in Appendix G.

Implementing the voting scheme involved each of the three aforementioned classifiers independently predicting participant motion. Their individual outputs were then used to determine a final prediction output based on the classification agreement of at least two of the classifiers. Failing which, the classification output was set to default to that of the deterministic classifier. This was due to it not being reliant on prior learning. This is further explained in table 5.5. A visual representation of the classifiers tested and their relation to one another is presented in figure 5.2.

Table 5.5: Examples of final classification outcome based on the voting scheme

Actual motions from incoming data	Classification outcome			
	LDA	Decision tree	Deterministic	Voting Scheme
Dorsiflexion	Foot flat	Dorsiflexion	Dorsiflexion	Dorsiflexion
Foot flat	Dorsiflexion	Inversion	Eversion	Eversion
Plantarflexion	Plantarflexion	Plantarflexion	Foot flat	Plantarflexion
Eversion	Plantarflexion	Eversion	Foot flat	Foot flat
Inversion	Foot flat	Dorsiflexion	Inversion	Inversion
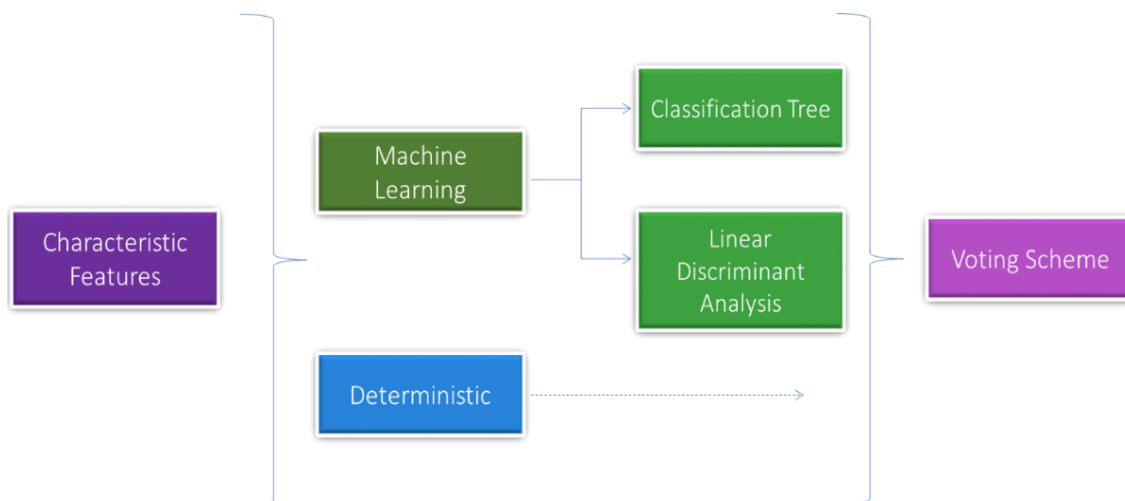
Figure 5.2: Visual representation of classification procedure

5.2.2 Prediction Approaches

Testing a classification algorithm on a partitioned portion of a larger data set used to train it often results in higher classification accuracy. This is when compared to testing said algorithm on entirely new data. This is also often the case for offline classification versus online/real-time classification. As such, different prediction approaches were explored to ascertain which yielded the best accuracy with regards to 1) the data type (i.e. combined or separated level-ground and uneven terrain data) and 2) the classification algorithm implemented. This was done to determine the best pairing of prediction approach and classification algorithm for real-time prototype testing.

5.2.2.1 Generic approach

The first prediction approach tested was based on implementing classifiers trained on the complete feature set. As the feature set used was made up of data from all six gait experiment participants. This approach was named the generic approach. It had the advantage of retaining a broader spectrum of what constituted healthy, able-bodied gait. Thus, it had a larger data pool from which the machine learning based classification algorithms could be trained.

5.2.2.2 Controller specificity: Walking style approach

The generic approach was developed further to explore whether more user centric prediction approaches would result in higher prediction accuracies. The goal was to develop prediction approaches that would be specific to each new participant without the need for extensive prior training or the need to create entirely new classifiers. The idea was to maximise the EMG data acquired from the gait experiment and use it to implement a prediction approach that required minimal time to conform to new users.

The overarching method involved first determining a participant's walking pattern. Six walking patterns were identified and defined within this research. These were hyper TA, hyper MGas, hyper LGas, moderate MGas, moderate LGas and an optimum walking style. A muscle was defined as being 'hyper' when it was the highest activated muscle during a gait phase wherein it should have been minimally active. Moderate MGas or LGas occurred when either muscle had higher activation, when transitioning into foot flat, than TA. Foot flat was defined as the point at the beginning of single leg support. This was when TA activation was still higher than MGas or LGas but decreasing in magnitude as the foot transitioned through foot flat, to mid-stance and into heel off.

Hyper activation was a higher walking style priority than moderate activation. This meant that if a participant's walking style could be classed as either hyper MGas or moderate LGas, the walking style would be defined as hyper MG. This was done to avoid inappropriate prototype output behaviour, particularly during dorsiflexion or plantarflexion. This is because such prototype behaviour could lead to user injury during future weight bearing tests.

The walking style definitions are further explained in table 5.6. The numbers indicate how many times, with regards to the calculation outcomes, a muscle was activated higher than the muscle(s) that should have been the most active during that gait phase. During plantarflexion, the highest activation was expected from either one of the gastrocnemii heads, medial or lateral gastrocnemius.

Table 5.6: Walking style definitions

Foot motion	TA	MGas	LGas	Foot motion	TA	MGas	LGas
Dorsiflexion	0	0	0	**Dorsiflexion**	0	0	4
Foot flat	0	3	1	**Foot flat**	0	2	2
Plantarflexion	0	0	0	**Plantarflexion**	0	0	0
Walking style	Moderate MGas			**Walking style**	Hyper LGas		

EMG data from twelve gait trials was used to determine the walking style of each gait experiment participant (chapter 3). This included the first six valid level-ground walking trials and another six trials at intervals of 2-4, e.g. trial 7, 9, 11, 13, 15 and 17. The walking styles identified from the group data were two hyper TA, two moderate LGas, one moderate MGas and one optimum walking style.

In fully exploring the notion of individuals having different walking styles, EMG features that were walking pattern specific were recalculated. As such, different feature sets composed of the six types of features were calculated for each walking pattern identified from the gait experiment data. Data from a further six walking trials were taken from the moderate MG and optimum walking style participants. This was done to ensure there was sufficient data from which the classifiers could be trained. The resulting feature sets had a total of 43 data samples for the hyper TA, 44 for the moderate LGas, 48 for the moderate MGas and 47 for the optimum walking style.

This approach was aptly named the walking style approach. Its implementation involved creating machine learning classifiers that were trained using the walking style specific EMG features. This meant it could possibly be a good fit for most new participants without the need for classifier augmentation. However, this approach relied on first determining a participant's walking pattern and then choosing the appropriate machine learning classifier.

The clustering and 3D locations of the calculated gait experiment participant group EMG features are presented in figure 5.3. The clusters are as a function of walking style, for each of the three muscles of interest. Once again, the challenge of accurately classifying user motion based solely from EMG data is illustrated by the feature clustering (fig. 5.3).

A) Features for TA muscle

B) Features for MGas muscle

C) Features for LGas muscle
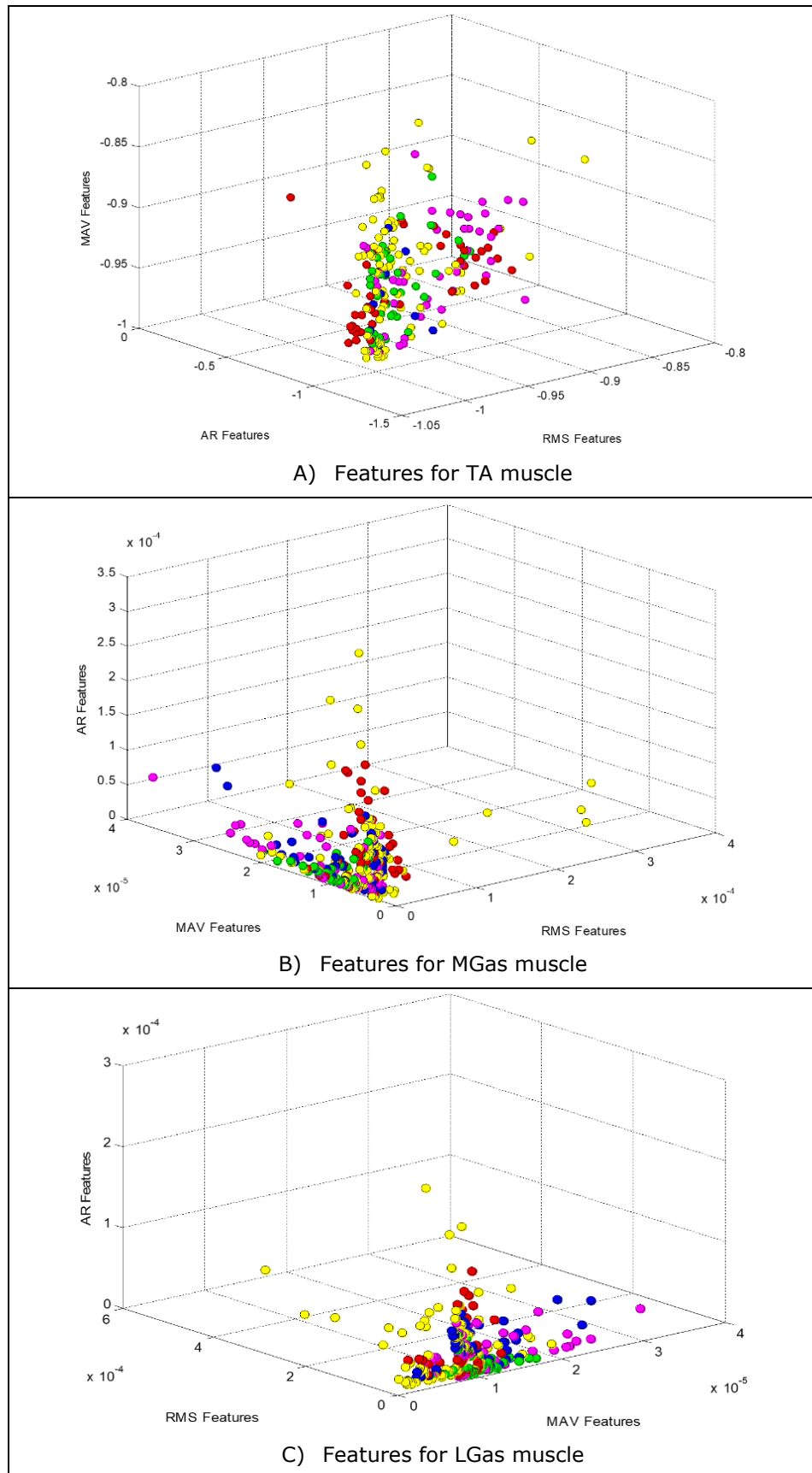
Figure 5.3: Walking style features for each muscle

5.2.2.3 Biased Generic Approach

Once participants' walking styles were determined, the percentage by which they deviated from the defined optimum walking style was calculated. This percentage was then applied to the incoming EMG data for each muscle channel such that the data was biased to reflect that of optimum walking. This approach meant that the same EMG features that were calculated for the generic approach could be used. As such, this approach was called the biased generic approach.

The definition of the optimum walking pattern was based on documented healthy human walking EMG patterns [96, 121]. This meant having an expectation of certain muscle(s) being activated during specific gait phases. This also included an expectation of how those muscles' activation levels would change from one gait phase to another. This is further explained in table 5.7.

Table 5.7: Optimum walking style definition

Movement type	Muscle activation		
	Tibialis Anterior	**Medial Gastrocnemius**	**Lateral Gastrocnemius**
Dorsiflexion	High	Low	
Foot flat	High -> Medium	Low -> Medium	
Plantarflexion	Low	High	
Eversion	High -> Medium	Low	Medium
Inversion	High -> Medium	Medium	Low

5.2.2.4 Deterministic classifier specificity

An improvement of the deterministic classifier's accuracy was also sought. As such, an approach taking into consideration participants' quiet standing EMG data was tested. EMG data was read from the three muscles of interest as participants remained stationary in a relaxed, standing position for three intervals. Each interval was three seconds long. The three samples of quiet standing data were averaged and subtracted from incoming EMG data before the data was classified using the deterministic classifier. This augmentation of EMG data was implemented when the walking style approach was used for the machine learning based algorithms.

5.2.3 Participant Demographics and Experiment Setup

Three individuals participated in testing the accuracy of the classifiers and developed prediction approaches. The participants were two males and a female, all of which were able-bodied and healthy. They were within the age range of 18-55 years, as delineated for the gait experiment (chapter 3) and had no musculoskeletal limitations. Their average height and weight was 1.74m (±0.06) and 72.7kg (±0.09), respectively.

These participants were different to those that took part in the initial gait experiment. Thus, the EMG data used to test the classifiers and prediction approaches was entirely new. The data used to test the prediction strategy was acquired from level-ground and uneven terrain walking trials. The protocol used for the gait experiment was also used for this experiment. However, MVC (maximum voluntary contraction) data was not recorded. Surface EMG electrodes were placed on top of the participants' TA, MGas and LGas muscles. The muscles were located by palpation with the participants in a standing position.

The participants performed eight walking trials at their normal, self-selected speed over level-ground and the fixed uneven terrain, respectively. One participant also performed an additional 10 walking trials at a fast and slow walking speed, respectively. These were done over both level-ground and the uneven terrain. The walking trials were conducted in the same gait lab as that used for the gait experiment. The participants started each trial from the same side of the gait lab.

Participants sequentially contacted two 3D force plates during each valid walking trial. The force plate contact was used to segment the participant's EMG data into gait phases that made up the five motions of interest. This segmentation and data processing was done in Matlab using a custom written program. The participants' EMG data was read into Matlab where features were calculated and used to predict their motion.

The walking patterns of the participants who took part in testing the various control strategies were calculated solely from level-ground walking trials. Uneven terrain trials were not used in determining walking style. They were omitted to ensure that the defined walking patterns were true to the participants' everyday walking patterns and not due to any gait strategies employed for uneven terrain traversal.

The participants' walking styles were calculated from eight valid gait trials and were determined to be moderate MG. The appropriate walking style classifiers were implemented when testing the various prediction approaches.

5.2.4 Data Sets and Types

The effect of the type of EMG data used for classification was also of interest. The first change investigated was that of EMG quality. As such, an electrode shift (ES) condition was tested for comparison against an optimal condition. Even though an ES condition was explored in this research, the resulting change in signal pattern and quality could be due to various other reasons. Such reasons could include muscle fatigue or the presence of sweat, which introduces signal noise.

The optimal condition was one wherein the electrodes were accurately positioned above the muscles of interest. The ES condition involved two electrodes being accurately placed, and the third electrode being slightly misplaced above a specific muscle. The choice of which muscle would have the misplaced electrode was based on the participants' walking styles. As such, the EMG electrode was misplaced above the MGas muscle.

The midpoint of the misplaced electrode was shifted approximately 2cm above to the optimum position. This meant the electrode was placed 2cm further up from the foot than in the case of the optimum position. Data from two participants made up the optimal condition data type and that from the remaining participant made up the ES condition data type.

The objective of the overall developed control strategy was to enable traversal over uneven terrain. As such, the first kind of data set to be classified was a combination of both level-ground (LG) and uneven terrain (UT) EMG data. The motion to be predicted for the optimal and ES conditions was from EMG data for both LG and UT walking trials. This was named the combined data set. The inclusion of swing phase data was also tested to determine its effect on overall prediction accuracy.

Another data set explored was one based on using only LG or UT data to predict motion. This was investigated to further determine the best pairing of prediction approach to classification algorithm.

It was to also investigate whether a 'decoupled' data approach would yield better accuracy in the pursuit of enabling the traversal of a larger variety of terrain. This was named the decoupled data set.

5.2.5 Statistical Analysis

Two-tailed paired t-tests were performed to investigate the influence of:

1) EMG quality – optimum condition versus the electrode shift condition.

2) Including unknown data – the inclusion of swing data for which the classifiers were not trained.

3) The data set – combined data versus separated LG and UT data.

A one-way ANOVA was also performed to investigate whether the different walking speeds had a significant effect on the prediction accuracy. A confidence level of 95% was used for all the analyses ($\alpha = 0.05$).

5.3 Prediction Results and Accuracies

5.3.1 Combined Data Set

5.3.1.1 Generic approach

The confusion matrices illustrating the classification accuracy of each classifier using the generic approach are presented in figures 5.4 A and B, respectively. This is for both the optimal and ES conditions. The highest prediction accuracy was obtained with the optimal condition, as was expected. The voting scheme yielded the highest accuracy for the optimal condition, followed by the LDA (fig. 5.4 A).

The decision tree was also outperformed by the deterministic classifier whose misclassifications were mostly other motions being misclassified as foot flat. The misclassifications of eversion as foot flat could be attributed to the similar nature of EMG data from these two motions, which meant the deterministic classifier was unable to differentiate between the two motions. The decision tree had similar misclassifications, with foot flat motions being mostly misclassified as either eversion or dorsiflexion. The eversion misclassifications could be as a result of how the eversion data was acquired.

The majority of LDA misclassifications for the optimal condition were also foot flat data being misclassified as eversion, followed by foot flat data being misclassified as inversion. This again highlighted the similarity of foot flat, eversion and inversion EMG data.

The LDA performed best for the electrode shift condition, followed by the decision tree (fig. 5.4 B). For the ES condition, LDA misclassifications were other motions mostly being classified as inversion. This was due to the misplaced electrode along the MG muscle. The misclassification of other data as dorsiflexion for the decision tree suggested that it could have had a bias to the dorsiflexion group. Such a bias would lead to gait issues, particularly during uneven terrain transversal, and would affect the delivery of the required torque during push-off (plantarflexion).

The poor performance of the voting scheme was due to the performance of the other classifiers. Similar to its performance with the optimal condition, eversion and inversion data was misclassified as foot flat by the deterministic classifier with the ES condition.

The classification accuracies obtained for the optimal condition were lower than those reported in other research [56, 59, 60]. This was attributed to factors such as using only three lower leg (shank) muscles for prediction. This was as opposed to using more muscles [60] or incorporating mechanical sensor data [56]. Another factor could have been that continuous EMG data was used, as opposed to making predictions at specific phases within the gait cycle. An example of this was a study by Miller et al [59] wherein they reported accuracies of 96.9% (±2.42). This was when using four muscles, two of which were thigh muscles.

5.3.1.2 Biased generic approach

The optimal condition followed the same trend as it did for the generic approach. The best classification accuracy was again that of the voting scheme, followed by the LDA (fig. 5.4 C). The overall performance of this approach was similar to that of the generic approach with only a 1% reduction in accuracy for the LDA and decision tree, respectively. The misclassifications for each classifier were also similar to those observed for the generic approach, indicating that the biased generic approach had no positive effect on the prediction accuracy.

For the ES condition, there was an increase of 8% and 7% in the prediction accuracies of the decision tree and LDA, respectively (fig. 5.4 D). Nonetheless, the misclassifications for the decision tree were other motions still being classified as dorsiflexion. Other motions were being misclassified as inversion for the LDA. The misclassifications for the deterministic classifier and the voting scheme were again similar to what they were for the generic approach.

5.3.1.3 Walking style approach

Overall, the walking style approach did not fare as well for the optimal condition compared to the generic approach (fig. 5.4 E). There was a 10% increase in accuracy for the decision tree, outperforming the LDA across all prediction approaches. However, the 35% decrease in LDA prediction accuracy contributed to the 7% decrease in voting scheme accuracy. This was in comparison to the voting scheme's prediction accuracy when implementing the generic approach. The majority of LDA misclassifications were foot flat being classified as plantarflexion, followed by other motions being misclassified as inversion.

The decrease in voting scheme accuracy was also as a result of its outcome prediction defaulting to that of the deterministic classifier in the event of no majority vote. The misclassifications for the deterministic classifier remained as they were for the generic approach, which was expected due to the classifier being independent of EMG features and focusing solely on the raw EMG data.

For the decision tree, the misclassifications of foot flat data as dorsiflexion were corrected using the walking style approach. This was in comparison to using the generic and biased approaches, respectively. The foot flat misclassification as eversion remained unchanged.

A small increase in prediction accuracy of 1% and 2% was achieved using the decision tree and the voting scheme, respectively, for the ES condition (fig. 5.4 F). This was in comparison to using the generic approach. However, the LDA had a 13% decrease in its accuracy.

Overall, the walking style approach did not perform better than the biased generic approach for the ES condition. Unlike for the two other approaches, misclassifications for the decision tree when using the walking style approach were mainly inversion and dorsiflexion data being classified as foot flat.

It was a similar case for the LDA, which mostly had dorsiflexion and inversion data being misclassified as plantarflexion. With regards to gait, the misclassifications for the decision tree would be less detrimental than those of the LDA for the ES condition. Nonetheless, both scenarios would greatly affect user gait.
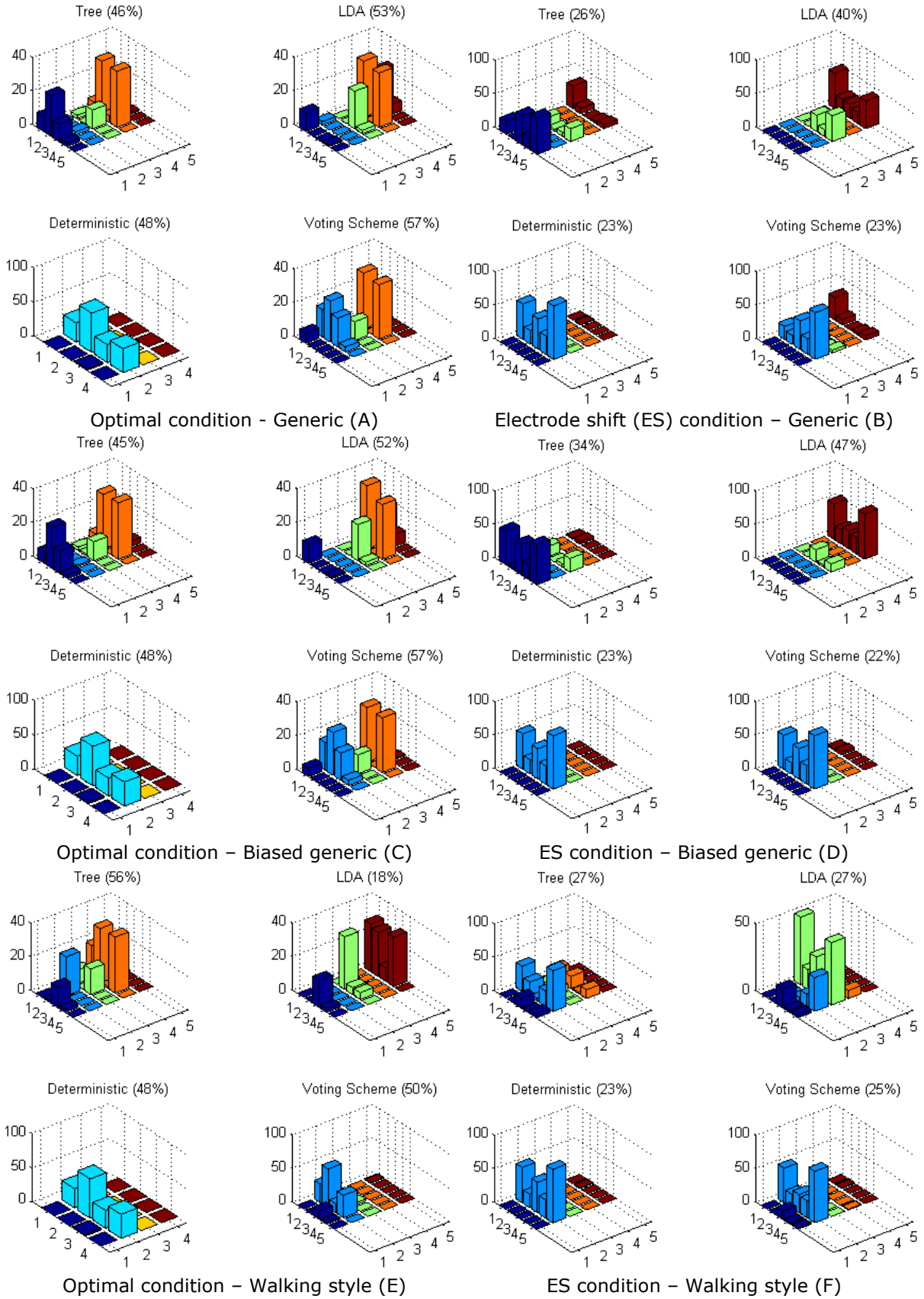
Figure 5.4: Combined data set prediction accuracy

5.3.2 Inclusion of Swing Data

Swing phase data was also incorporated to test how the classifiers would perform in the presence of entirely unknown data. The inclusion of unknown data, which was not part of the data groupings (classes), led to a reduction in prediction accuracy, as was expected. The results of which are presented in figure 5.5. There was an average reduction in accuracy of 16.5% and 9.5% for the optimal and ES conditions, respectively. This was when using their best performing prediction approaches.

The voting scheme yielded the highest accuracy for the optimal condition, followed by the LDA (fig. 5.5 A). The majority of swing data misclassifications were eversion data being classified as swing. This was for both the decision tree and LDA. The incorporation of swing data was not registered by the deterministic classifier as it was not designed to incorporate such data. This affected the accuracy of the voting scheme due to its defaulting algorithm.

There was only a 9.5% reduction in accuracy for the ES condition. Most of the misclassifications were eversion data being classified as swing for the LDA (fig. 5.5 B). Misclassifications for the decision tree and deterministic classifier followed a similar trend to that of their no swing data results. Swing data was mostly misclassified as foot flat for the tree and deterministic classifier, respectively.

The effect of training a controller using data it is expected to classify was also demonstrated in a study by Young et al [142]. This is particularly the case when using machine learning based controllers. In their study, they found that the classification error when classifying transitional data reduced from ±90% to ±18% when including transitional data in the training data set. This was as opposed to only using steady state data in the training data set.

5.3.3 Decoupled Data Set

5.3.3.1 Optimal condition

Separating the EMG data to be classified gave an indication of the degree to which each classifier contributed to the prediction accuracy for the combined data set. LG and UT data were classified independently of each other. The confusion matrices and prediction accuracies for the optimal condition, when using each of the three prediction approaches, are presented in figure 5.6.
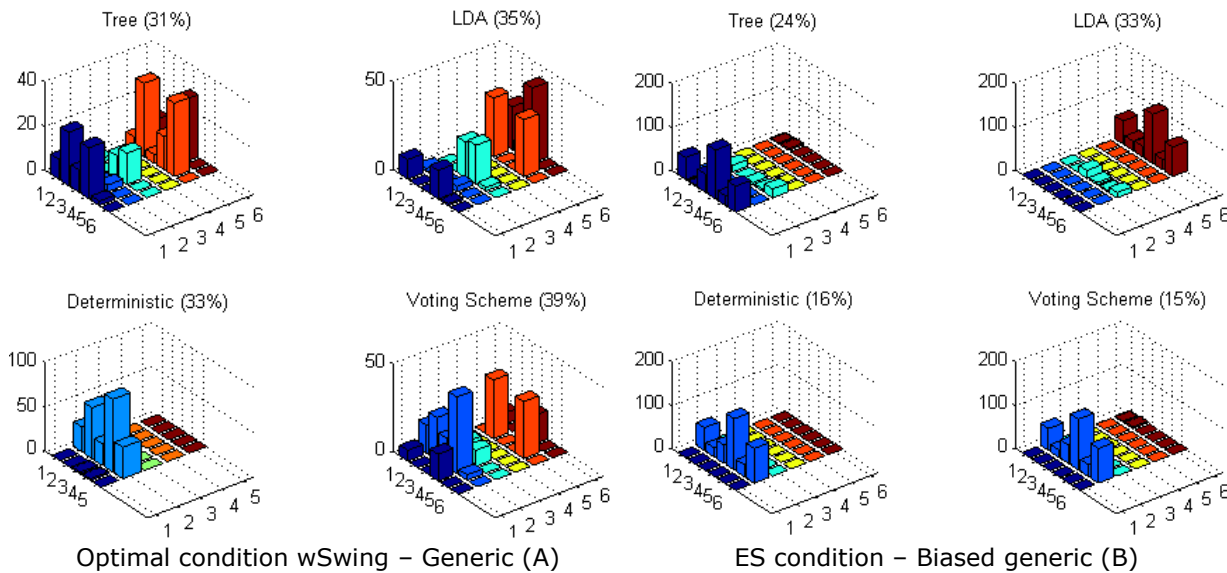
Figure 5.5: Swing data inclusion – Combined data set prediction accuracy

The deterministic classifier performed well across all three prediction approaches for the optimal condition LG data (fig. 5.6 A, C and E). The voting scheme performed the best with its highest accuracy of 71% being achieved when implementing the walking style approach (fig. 5.6 E). The increase in prediction accuracy was due to the ±23% increase in accuracy for the decision tree when using the walking style approach. This was in comparison to the decision tree's accuracy when using the other two approaches.

The accuracy of the LDA classifier was its lowest using the walking style approach for both LG and UT data. This suggested that such participant specific controller adaptation limited its robustness. Across all three approaches, foot flat motion was mostly misclassified as eversion. Such misclassification would negatively affect the achievable gait, particularly for varied terrain traversal. However, it would not be detrimental to overall prototype functionality and user mobility. On the other hand, the misclassification of foot flat as dorsiflexion would cause problems for the user (fig. 5.6 A and C). This is in regard to either the generic or biased generic approaches implementing the tree.

The deterministic classifier had poor performance for the UT data because of the similar nature of foot flat, eversion and inversion data. The highest accuracy was achieved by the LDA using the generic approach (fig. 5.6 B), with misclassifications being dorsiflexion being classified as eversion.

The tree experienced similar misclassifications with its dorsiflexion data. It was likely that these misclassifications were as a result of how the eversion data was acquired, as mentioned in section 5.1. The decision tree also experienced plantarflexion motion being misclassified as dorsiflexion. This would be unacceptable if the control strategy were implemented on a physical lower limb prosthesis. The prediction accuracies obtained when decoupling the data set were similar to those reported from other studies.

Optimal condition – Generic LG (A)

Optimal condition – Generic UT (B)

Optimal condition – Biased generic LG (C)

Optimal condition – Biased generic UT (D)

Optimal condition – Walking style LG (E)   Optimal condition – Walking style UT (F)
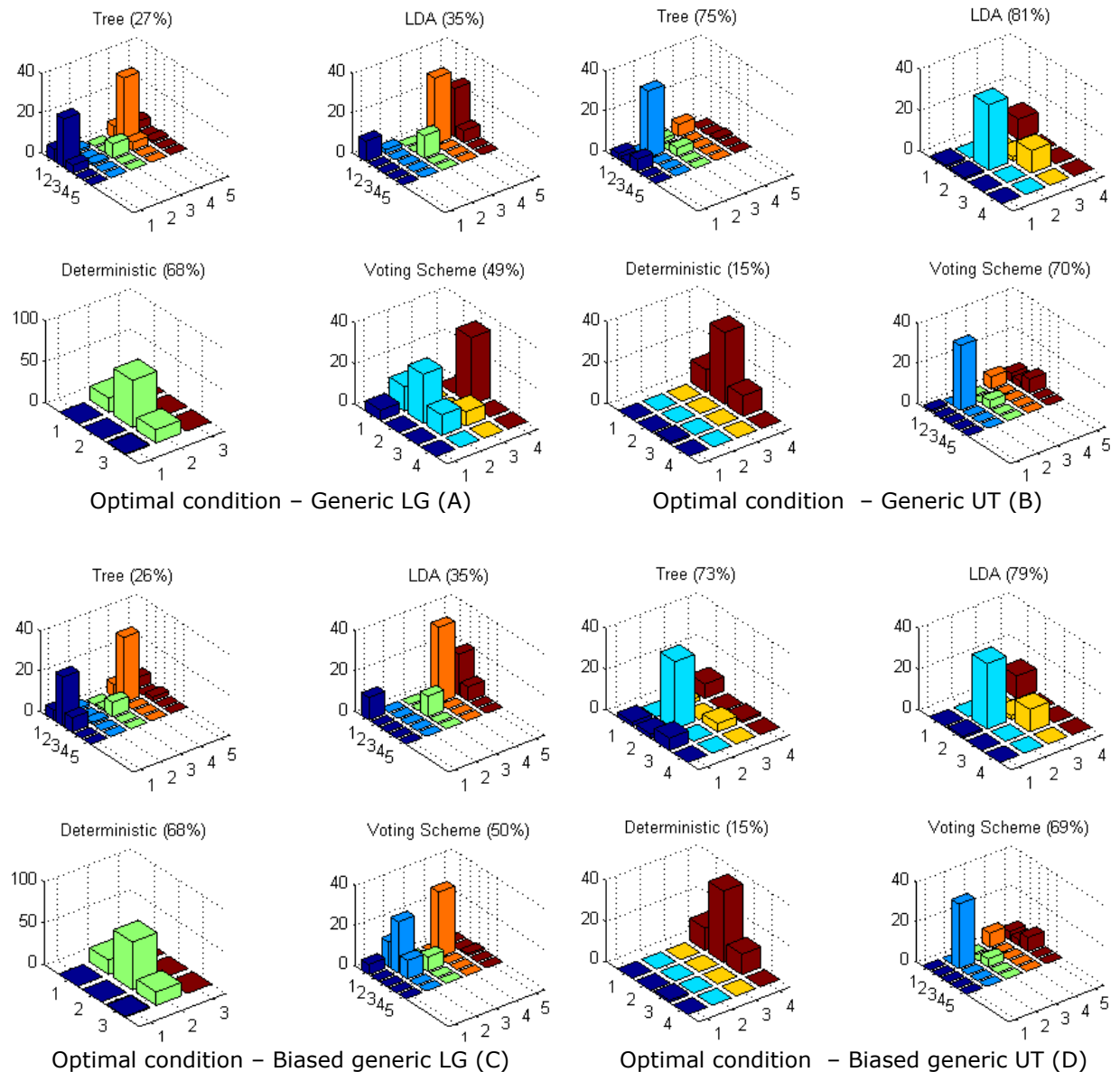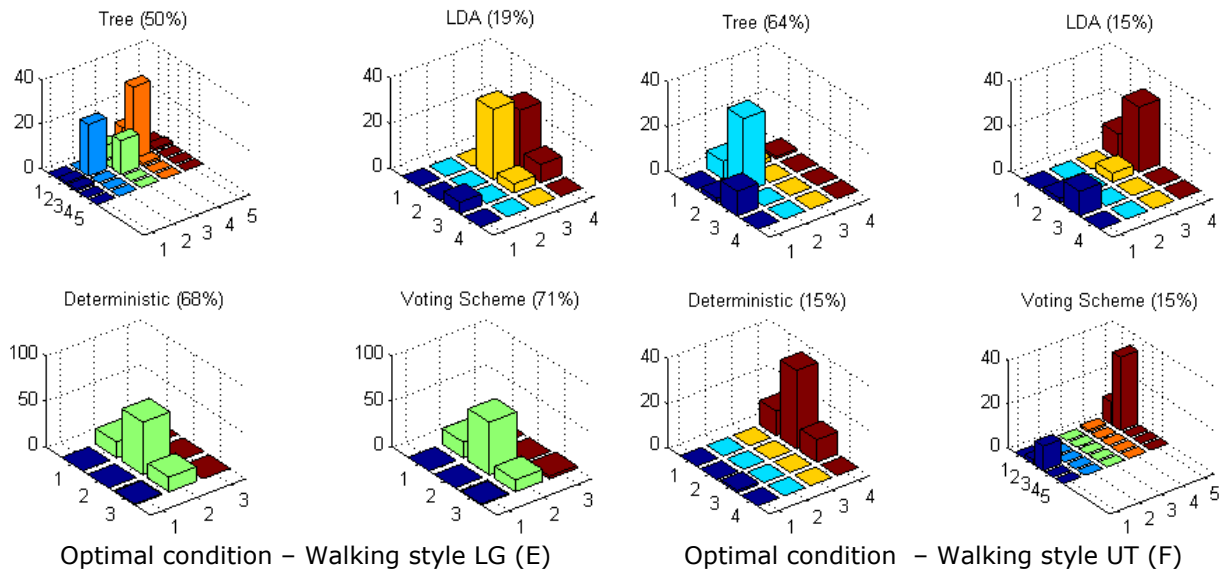
Figure 5.6: Optimal condition – Decoupled data set prediction accuracy

5.3.3.2 Electrode shift condition

The confusion matrices and prediction accuracies for the ES condition, using the decoupled data set, are presented in figure 5.7 for the three prediction approaches. The walking style approach performed the best for the LG data (fig. 5.7 A). The poor performance of all four classifiers indicated the effect of an altered EMG signal being used for intent prediction, corroborating the findings of other researches [59].

Most of the misclassifications were other motions being classified as foot flat for both the decision tree and the deterministic classifier. Other motions were mostly misclassified as plantarflexion for the LDA. Either scenario of misclassifications would negatively affect the achievable gait.

For the UT data, the performance of the decision tree remained unchanged for the best performing approach, which was the biased generic approach (fig. 5.7 B). The performance of the LDA demonstrated the classifiers ability to deal with altered EMG data, particularly when some adaptation has been implemented with respect to the overall approach. In this case, it was using a more participant specific control strategy that leveraged the broad spectrum of possible input data, on which the generic approach was based. UT data misclassifications were mostly other motions being classified as dorsiflexion for the decision tree. Other motions were being misclassified as eversion for the deterministic classifier. This also

affected the performance of the voting scheme due to its defaulting algorithm mentioned in section 5.2.1.2.

ES condition – Walking style LG (A)   ES condition – Biased generic UT (B)
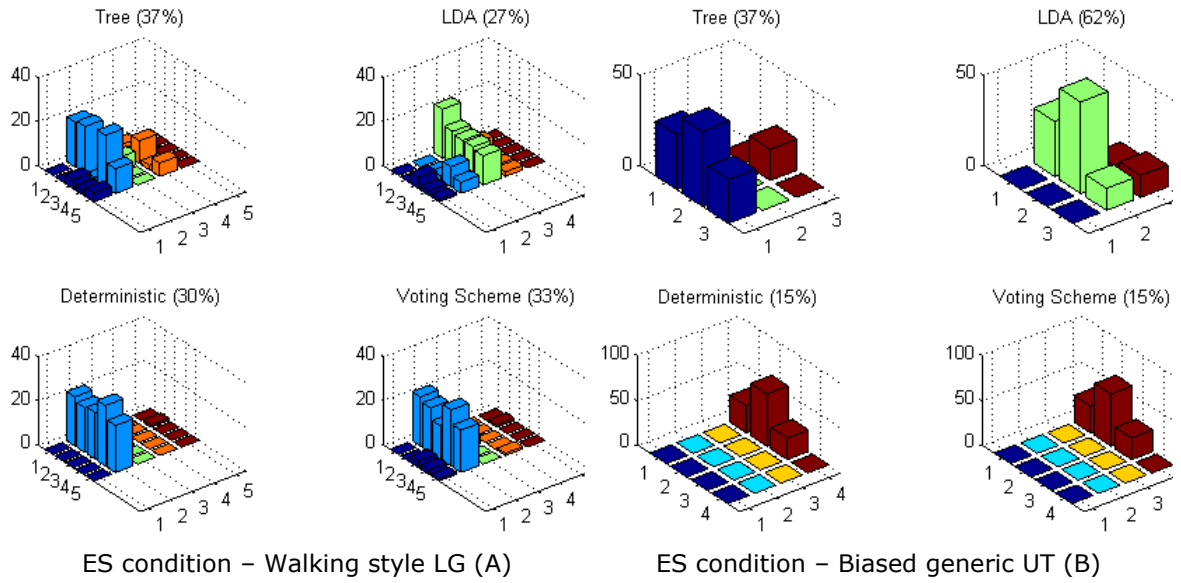
Figure 5.7: Electrode shift condition – Decoupled data set prediction accuracy

5.3.4 Effect of Walking Speed: Decoupled Data Set

The prediction accuracies acquired when classifying data from fast and slow walking are presented in figure 5.8. The walking style approach performed best with the different walking speeds (fig. 5.8 A and C). There was little to no change in prediction accuracy when using the generic or biased generic approaches. The prediction accuracies dropped from 40% to 38% for the decision tree but remained the same at 42% and 46% for the LDA and deterministic classifiers, respectively. Confusion matrices for the other prediction approaches are presented in Appendix H.

The deterministic classifier again performed the best for the LG data of both walking speeds. Its performance was only bested by the accuracy achieved by the voting scheme for slow walking. Most of the misclassifications for the machine learning based classifiers, for both walking speeds, were foot flat motion being classified as eversion. This indicated that the change in walking speed had little to no effect on prediction accuracy. This was more evident when comparing these misclassifications to those observed for the optimal condition decoupled data.

The prediction accuracies for slow walking were also the same for the generic and biased generic approaches. Prediction accuracies of 29%, 32%, 66% and 31% were achieved for the decision tree, LDA, deterministic classifier and the voting scheme, respectively.

However, most of the misclassifications were foot flat motion being classified as inversion. Such misclassifications would have a negative effect on the achievable gait, but would not be detrimental to overall user mobility, particularly during level-ground traversal.

The generic approach performed the best for both walking speeds' UT data (fig. 5.8 B and D). The highest accuracies were achieved by the LDA for each walking speed, followed by the decision tree. Most misclassifications for the LDA were dorsiflexion being classified as eversion. This was also the case for the fast walking data when implementing the decision tree (fig. 5.8 B). However, for the decision tree, foot flat motion was also misclassified as plantarflexion and plantarflexion motion was misclassified as dorsiflexion for slow walking (fig. 5.8 D).

There was a large difference in prediction accuracy for fast walking data when using approaches either than the generic approach for UT data. LDA accuracy decreased from 83% to 15% when using the walking style approach instead of the generic or biased generic approaches. A similar decrease was observed for the decision tree and voting scheme classifiers. Their accuracies fell from 77% to 60% and 72% to 15%, respectively, when using the walking style approach instead of the generic approach. The accuracy of the deterministic classifier remained unchanged at 15%. The confusion matrices are included in Appendix H.

There was a similar decrease in accuracy for slow walking data when using the walking style approach. The accuracies of the decision tree, LDA and voting scheme classifiers decreased from 63% to 52%, 77% to 17% and 56% to 17%, respectively, using the walking style approach. This was compared to using the generic approach. The accuracy of the deterministic classifier again remained unchanged across the different prediction approaches used. The confusion matrices are included in Appendix H.
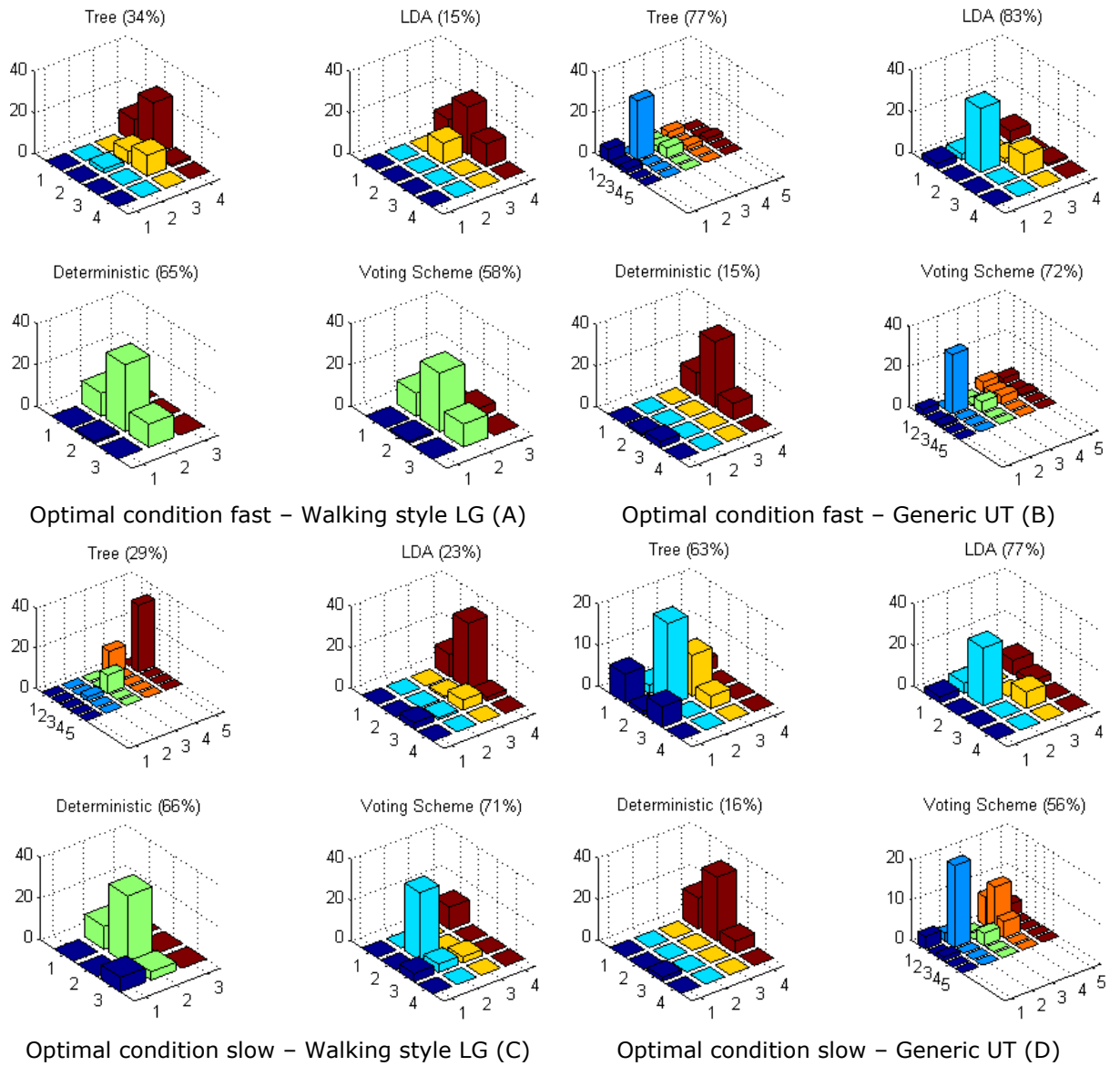
Figure 5.8: Effect of walking speed on prediction accuracy

5.4 Discussion
5.4.1 EMG quality versus Prediction Approach Specificity

The placement of the EMG electrode, and thus the EMG quality, had a significant effect on the prediction accuracy ($p = 0.0002$). Overall prediction accuracies for the optimum condition were higher than those of the ES condition.

There was a slight increase in prediction accuracy when implementing more participant specific prediction approaches for the ES condition. This demonstrated that such prediction approaches were beneficial in the presence of varying EMG quality. This suggested that an adaptive control approach could be beneficial for lower limb powered prostheses, and those particularly driven by EMG data.

130

Such an approach could take the form of using a specific control approach when "optimal" signals can be measured. Another approach would then be used when the quality of the EMG signals begins to vary outside pre-set threshold boundaries.

The overall poor performance of the walking style approach could have also been attributed to the small data set from which the machine learning based classifiers were trained [147, 148].

The generic approach performed the best for UT data. Its performance was attributed to the wider scope of possible input EMG data on which the approach was developed. This proved to be useful because of how similar in nature foot flat, eversion and inversion EMG data was, particularly in their raw form. This was similar to the ability of machine learning based classifiers to more accurately predict data using a small training sample has been used [142].

5.4.2 Influence of Unknown Data and Walking Speed

There was minimal reduction in prediction accuracy when including swing data, particularly for the ES condition. This indicated that compromising the quality of the EMG data had a greater effect on overall accuracy. Such a compromise meant a change in the quality and fundamental patterns of the EMG signal. As such, including entirely unknown data (i.e. swing data) had less influence on prediction accuracy compared to the quality of the EMG data used. However, the inclusion of unknown data did have a significant effect on prediction accuracy ($p = 0$). This was when comparing the prediction accuracies of the optimum and ES conditions with and without swing phase data.

Walking speed was also found to have no significant effect on the prediction accuracy ($p = 0.897$). This meant that the prediction approaches and algorithms maintained their accuracy even when the walking speed, and the resulting EMG data, was altered. The results obtained when predicting data from the different walking speeds was similar to that of Miller et al [59]. They reported a classification accuracy of 84.9% (±2.42) when classifying level-ground walking data at different speeds.

The consistency of the prediction accuracies obtained in this research even at the different walking speeds had positive implications. These were that the developed control strategy could be implemented for other activities of varying gait speeds. The walking speed statistical analysis was done using results from a decoupled data set.

5.4.3 Data Set versus Classification Algorithm

Statistical analysis indicated that decoupled the data set had no significant effect on the prediction overall prediction accuracy (p = 0.98). However, the improved prediction accuracy when using a decoupled data set highlighted the similarity in EMG data for the foot flat, eversion and inversion motions. These motion similarities led to numerous misclassifications, particularly for the combined data set. The decoupled data set was able to minimise such misclassifications by having foot flat data separate from the similar eversion and inversion data. It was anticipated that if the machine learning based classifiers were retrained to classify solely LG or UT data, higher prediction accuracies could be achieved.

The prediction accuracies obtained when decoupling the data set were more comparable to those reported from other studies [56, 59, 60], as opposed to using a combined data set. In their study, Young et al [60] reported classification errors of ±28% and ±6% for transitional and steady-state data, respectively. This was when using EMG data from nine muscles, as opposed to three muscles used in this research.

The poor performance of the machine learning algorithms when classifying LG data suggested that these classifiers had some generalisation issues. These classifiers were bested by the deterministic classifier which performed well for LG data. Its performance suggested that it could be developed further to better encompass UT data with the possibility of it yielding improved prediction accuracy for such data.

The implementation and overall performance of the voting scheme indicated the benefits of leveraging the strengths of individual classification algorithms, whilst minimising the effects of their weaknesses. There were no computational delays when implementing the voting scheme. However, there is a potential for such delays if more complex classification algorithms are included in the "decision pool".

Another cause of such as a delay could be implementing the overall control strategy on a less powerful processor, such as a microcontroller. It would then become a trade-off between prediction accuracy and system performance/reaction time.

5.4.4 Generalisation and Robustness of Classification Algorithms

There was a stark contrast in the prediction accuracy achieved during feature set selection and when using new data to explore the best performing prediction algorithms. This suggested that the machine learning based classifiers, particularly the LDA, had issues with robustness.

The performance of the machine learning based classifiers highlighted their poor generalisation. This issue of controller generalisation was also highlighted in a study by Young et al [143]. These algorithms often suffer from over-fitting or biasing which limits their accuracy when classifying new data. The task of minimising the probability or extent of over-fitting usually means that a large data set is required for training. It could also mean that more extensive training is required. Both of which can be time consuming, especially when the desire is to develop algorithms that are able to adapt to changing EMG signals.

5.5 Conclusion

The best overall classification accuracies were obtained using the generic approach. This suggested that a smoothing effect was achieved when using walking data from a variety of able-bodied participants. This resulted in a control strategy that could better conform to new participants compared to more participant specific control strategies. The best overall classification algorithm was the decision tree.

The significance of the classification accuracy achieved by the generic approach was the potential of paving a way to enabling the collection of EMG data from able-bodied individuals from around the world. This data could then be used to continuously improve the accuracy of developed control algorithms in the long run. This could lead to an approach such as creating an Internet of Things for transtibial powered prostheses control algorithms. Thus, possibly resulting in reduced controller training times when users acquire new transtibial powered prostheses.

The best performing pairings of prediction approach and classification algorithm, with respect to the different data sets and types explored, are presented in tables 5.8 and 5.9:

Table 5.8: Best performing pairings - combined data set

Optimal condition:	Generic approach + voting scheme (followed by the decision tree)
ES condition:	Biased generic approach + LDA

Table 5.9: Best performing pairings - decoupled data set

Optimal condition – LG:	Walking style approach + voting scheme (followed by the deterministic classifier)	
	UT:	Generic approach + LDA
ES condition – LG:	Walking style approach + decision tree	
	UT:	Biased generic approach + LDA

Based on the overall prediction accuracies, the generic approach-decision tree pairing was the best pairing to be implemented for real-time prototype testing. This was because to the data to be classified would be a combined data set, composed of both LG and UT data. This pairing was taken forward and tested by implementing it on the transtibial powered prosthesis prototype. The results of this further testing are presented and discussed in the succeeding chapter.

Further prototype testing could entail implementing a decoupled data set. This could take the form of the walking style approach-deterministic classifier pairing being used for LG data and the generic approach-LDA classifier pairing being used for UT data. However, the downside of such a decoupled data set approach would be the need to include a means of communicating a change in terrain type to the prototype control strategy.

Nonetheless, this could be explored in future iterations of the prototype and the advancement of this research. However, at the point of presenting this research, the objective was facilitating a control strategy that was as volitional as possible. This meant having a control strategy being as close in its execution to the way able-bodied individuals control their biological lower limbs.

Chapter 6
Prototype Control Strategy and Implementation

The developed control strategy was made up of two distinct parts. The first was responsible for reading user EMG signals, deciphering the intended motion and specifying the prototype output parameters to achieve said movement. This was the high-level controller. The second part was responsible for setting the parameters and ensuring that the requested motion was appropriately carried out by the prototype, within its physical limits. This was the output-level controller.

The implementation of the high-level controller was done using custom written Matlab [149] code and was presented in the preceding chapter. The output parameters and prototype actuation were then carried out by the output-level controller using a PIC microcontroller running custom written C code. The output-level controller and the implementation of the complete control strategy will be presented in this chapter, along with the validation experiment performed to determine the performance of the control strategy when implemented on the developed multiaxial transtibial powered prototype, which was presented in chapter 4.

6.1 Control Link: High-Level to Output-Level

Once a participant's motion was determined (predicted) by the high-level controller, prototype movement was carried out by the output-level controller. Each movement type had a pre-defined specific output parameter to be communicated to and executed by the output-level controller. The parameter set to be communicated included which motor should be active and in which direction it should operate. The amount of torque to be produced by each motor was also communicated. This torque specification ensured that positive energy would be supplied at each phase of the gait cycle, especially during plantarflexion, and when traversing uneven terrain.

A finite set of parameters were communicated to the output-level controller based on the predicted participant motion. An example of these is presented in table 6.1. As such, a finite state machine (FSM) approach was implemented to ensure that specific parameter sets were communicated to the output-level controller based on certain motion predictions.

These finite set of parameters were sufficient to facilitate both level-ground walking and the traversal of uneven terrain. A model of the implemented FSM is presented in figure 6.1. The state transition conditions were the classification outputs from the high-level controller.

Table 6.1: Output parameters based on determined predicted participant motion

Deciphered motion	On/Off status		Commutation direction	
	Motor 1	Motor 2	Motor 1	Motor 2
Dorsiflexion	On	On	CW (clockwise)	
Foot flat	On	On	CW or CCW (counter clockwise) *	
Plantarflexion	On	On	CCW	
Eversion	Off	On	-	CCW
Inversion	On	Off	CCW	-

* Foot flat motor commutation direction was dependent on the spatial position of the prototype foot
  with respect to the foot flat position
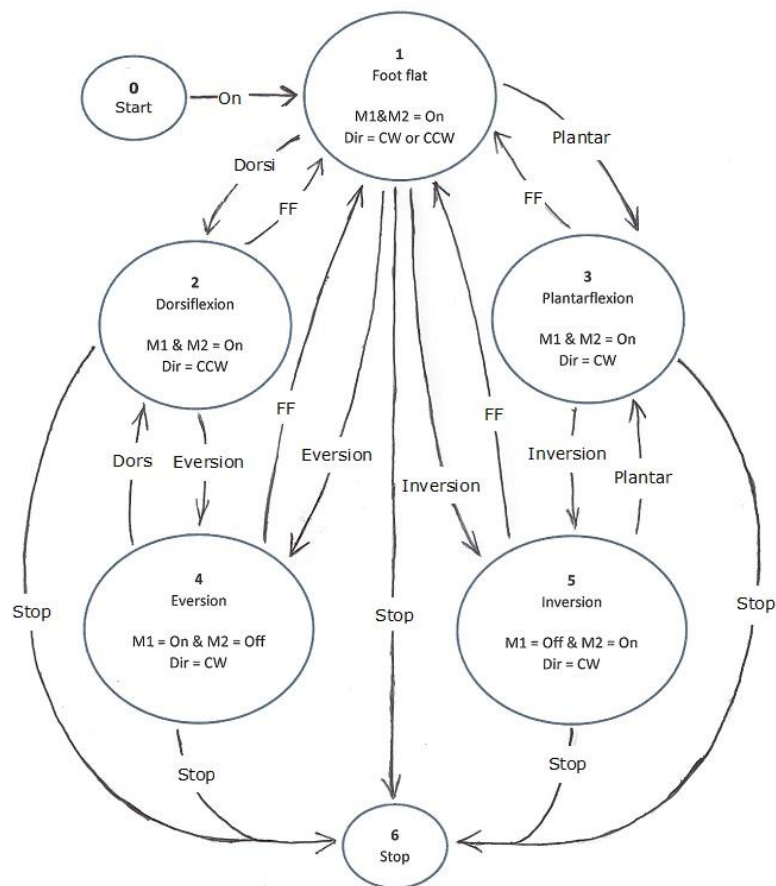
Figure 6.1: Finite state machine (FSM) model of output controller

6.2 Output-Level Controller

A microcontroller [150] was used to control the prototype's output behaviour. The output parameters were communicated over Wi-Fi from the high-level controller, running on a PC, to the output-level controller on the PIC. Motor actuation and control was implemented using PWM (pulse width modulation).

The value of the PWM duty cycle was dependent on the prediction output from the high-level controller. The required pulse width was calculated by the PIC using equations 6.1-6.3 [150]. Motor control using PWM meant that torque control could be performed as the load remained quasi static within the specific gait phases. The schematic of the output-level controller circuit is presented in Appendix I. A dual channel 10A DC motor driver circuit from Cytron Technologies (Malaysia) was used to control the two brushed DC motors of the prototype [151].

$$T_{PWM} = [(PR2 + 1) \times 4 \times T_{OSC} \times (TMR2\, Prescale\, Value)] \qquad \text{... (eq. 6.1)}$$

$$DC = 100\% \times \frac{T_{PWM}}{T_{OSC}} \qquad \text{... (eq. 6.2)}$$

$$V_{out} = DC \times V_{in} \qquad \text{... (eq. 6.3)}$$

where;

T_{PWM} is the PWM time period

$PR2$ is the period register for the PIC's timer 2 function register

T_{OSC} is the period of the PIC, based on its oscillation frequency

$TMR2$ is the PIC's function register that controls the PWM period and duty cycle

DC is the calculated duty cycle

V_{in} is the input voltage from the power supply

V_{out} Is the output voltage to the motors

Figure 6.2 illustrates the flow of data from the wireless EMG electrodes (A), to the high-level controller (B) and then to the output-level controller (C). XBees [152] were used to wirelessly communicate the output parameters from the high-level controller to the output-level controller. Preliminary tests were done to ascertain the viability of this communication method during real-time application.

137

The data used for feature set selection was used to test the viability of implementing wireless communication for the prototype control strategy. During the preliminary tests, there were no observable delays between the classification of EMG data, communicating the output parameters and executing the outputs. The motors were actuated during this preliminary testing but were not attached to the prototype. They were allowed to actuate freely.

A)
EMG
electrodes

B)
High-level controller
(executed on a laptop)

C)
Output-level controller
(on the prototype circuitry)
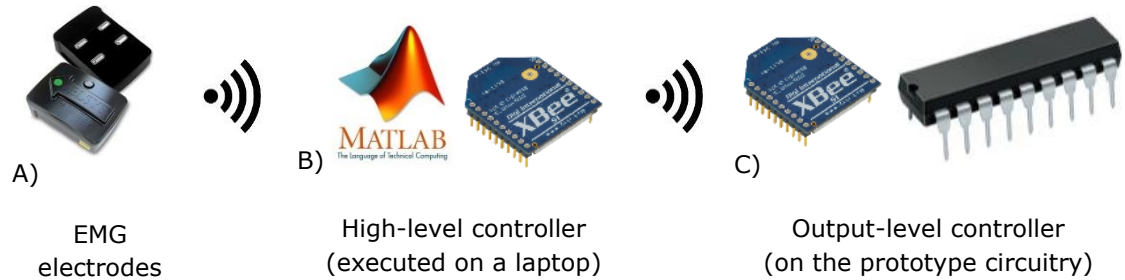
Figure 6.2: Data flow from high-level to output-level controller

A means of tracking the real-time 3D position of the prototype foot, with respect to its physical range of motion (ROM) limits, was implemented. This was done to ensure that the prototype was not inadvertently damaged by it being actuated beyond said ROM limits. A 3-axis digital accelerometer was used to track the position of the prototype foot. Motor actuation was stopped when the foot reached its ROM limit along either of its two degrees of freedom (DoF). Actuation was not reinitiated if the prototype was still near its physical ROM limit.

The motion tracking was used as a fail-safe system for the prototype. On the high-level controller, a "quit" command could be prompted at any point. This command was included to ensure that prototype functionality could be stopped at any time, should it be necessary. Motion tracking accomplished using a custom written C code which was executed by another PIC to which the accelerometer was connected. This motion tracking circuit was placed under the prototype foot, at the front end. The motion tracking circuit schematic is also presented in Appendix I. A summary of the prototype design specifications is detailed in table 6.2. These were comparable to those of some commercially available prostheses, detailed in Appendix A.

Table 6.2: Summary of prototype specifications

Design aspect	Details
Control	Microcontroller
Actuation	Powered – brushed DC motors with lead screw transmission
Degrees of Freedom	Two – active (powered)
Sensors	Accelerometer – spatial motion tracking, no bearing on high-level control
Range of Motion	Biologically inspired – 2DoF
Weight specifications	~4kg (of device)
Weight withstood	Sufficient for suspended testing, >20kg
Dimensions	20cm length x 8cm wide (at widest point)

6.3 Methodology: Validation Experiment

The purpose of the validation experiment was to test the developed control strategy within real-life application. This meant implementing it to drive and control the developed transtibial powered prosthesis prototype. Testing was conducted to ascertain the following:

1. the ability of the control strategy, both high and output levels, to accurately decipher and execute the required motion and

2. the functionality of the prototype in response to real-time movement of an able-bodied participant.

This experiment served as a proof of concept, validating the research conducted. It also served to investigate the real-life capability of the control strategy when implemented on a prototype that could be a viable transtibial powered prostheses.

6.3.1 Equipment Used

The following equipment was used for the validation experiment to determine the behaviour of the control strategy and the prototype.

i.   Wireless Delsys Trigno surface EMG electrodes – measuring participant EMG signals for input to the high-level controller.

ii. An Acer laptop – facilitating high level control.

iii. Vicon motion capture system – tracking the 3D movement of the prototype.

iv. A test rig – suspending the prototype and allowing it enough space for free movement.

v. A power supply – providing the required power to the prototype and its circuitry.

6.3.2 Test Rig

A rig was designed, and custom made, to safely support both the weight and dynamic movement of the prototype. The rigidity of the rig and its capability to support a weight of up to 10kg was verified using FEA. The simulations were done in SolidWorks 2014. All the parts of the rig, excluding the base, were fabricated from mild steel. The base was fabricated from wood.

The test rig was assembled and secured together by means of grub bolts (screws), washers and nuts. This resulted in a steady rig that did not collapse or move during the experiment. An illustration of the assembled rig is presented in figure 6.3. Brackets positioned between the side plates and top plate of the rig, indicated with an 'A' in figure 6.3, allowed the rig to better support and distribute the load and movement of the prototype during the experiment.
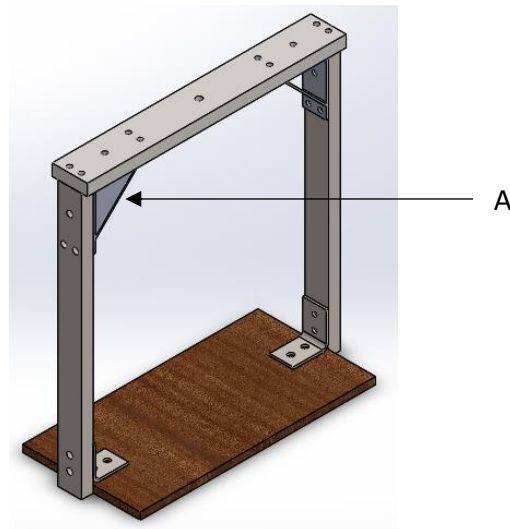
Figure 6.3: Rig for suspended testing

6.3.3 Participant Details and Preparation

Two able-bodied individuals, with no musculoskeletal limitation or disease, took part in the validation experiment. The participants were within the age range of 18-55, as delineated for the gait experiment able-bodied participant group (chapter 3). The participants' height and weight were 1.69m and 65kg and 1.8m and 83kg, respectively.

EMG electrodes were used to measure the activity of the tibialis anterior (TA), medial gastrocnemius (MGas) and lateral gastrocnemius (LGas) muscles, respectively. The muscles were located using palpation whilst the participants were in a standing position. Prior to placement of the electrodes, the participants' skin was prepared using the SENIAM recommendations [94].

The EMG electrode placement procedure used for the gait experiment, detailed in section 3.1.4, was also used for the validation experiment. The EMG data quality was verified in real-time using the Delsys EMGWorks Acquisition propriety software. This was done prior to beginning the validation experiment. Figure 6.4 illustrates EMG electrode placement on one of the participants.

The participants performed 10 walking trials for each of three walking speeds, namely normal (self-selected), fast and slow. As such, 30 walking trials were conducted on level-ground (LG). Another 30 trials were conducted over the same fixed uneven terrain (UT) described in chapter 3 for the gait experiment. Each trial was started at the same position within the gait lab. This enabled repeatability of the experiment with the different participants. Data was collected in one session, on the same day, for each participant. As such, the entire validation experiment was completed over two days. The position of the prototype and the video camera was not moved between the experiment days. The position of both devices remained the same for each of the two participants.

Figure 6.4: EMG electrode placement on a participant

The participants wore shorts that were no longer than knee length. This meant no item of clothing contacted the EMG electrodes, avoiding the introduction of signal noise.

The participants also wore a t-shirt, as access to the upper body was not required for this experiment. Participants walked bare footed and sequentially made contact with two AMTI 3D force plates that were flush with the laboratory floor.

6.3.4 Experiment Set Up

The experiment took place in a gait laboratory at the University of Manchester. This was the same room used for the gait experiment with the able-bodied participant group (chapter 3). The prototype was secured to the top plate of the test rig by means of four bolts. It hung in place and could move unrestricted when powered and controlled.

The prototype and test rig were placed on top of a wooden table and were positioned within the motion capture volume. This ensured that the motion capture cameras had full view of the prototype. The circuitry used to control the prototype was placed next to the test rig and did not interfere with the movement of the prototype. The rig and prototype setup are presented in figure 6.5. The position of the rig and prototype did not interfere with participant walking.
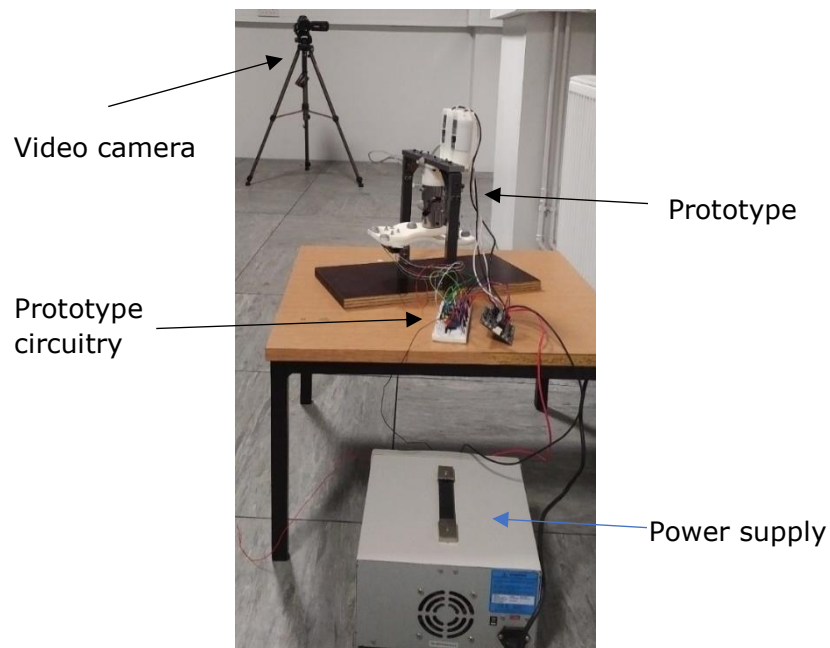
Figure 6.5: Rig and prototype setup

A two-channel power supply was used for the experiment. Each channel had a maximum voltage and current rating of 24V and 2A, respectively. The power supply provided 5V to the prototype circuitry. It also powered the two brushed DC motors with a baseline voltage of 8.6V each.

The motors could also draw the full available current of 2A. Even though a baseline voltage was supplied to the motors, the actual voltage they drew varied with respect to the specified duty cycle. Reflective markers were placed on the prototype so that its ROM could be measured using the motion capture system. The reflective markers were placed on the prototype as described in table 6.3 and shown in figure 6.6. The laptop was placed outside the capture volume.

Table 6.3: Prototype reflective marker descriptions

Landmark	Location Description	Anatomical Equivalent
AMM	Front side of motor mount	Anterior, middle section of shin the tibia
IUJ	Interface of large universal joint (mid-point)	Above the talus/talar dome
BSM	Bridge foot section (midpoint of top foot section)	Medial/lateral cuneiform bone
CAR	Back/heel section of bottom foot section	Upper ridge of the calcaneus
FMR	Front/'inner' side of bottom foot section	Dorsal aspect of the first metatarsal head (right foot)
VMR	Front/'outer' side of bottom foot section	Dorsal aspect of the fifth metatarsal head (right foot)
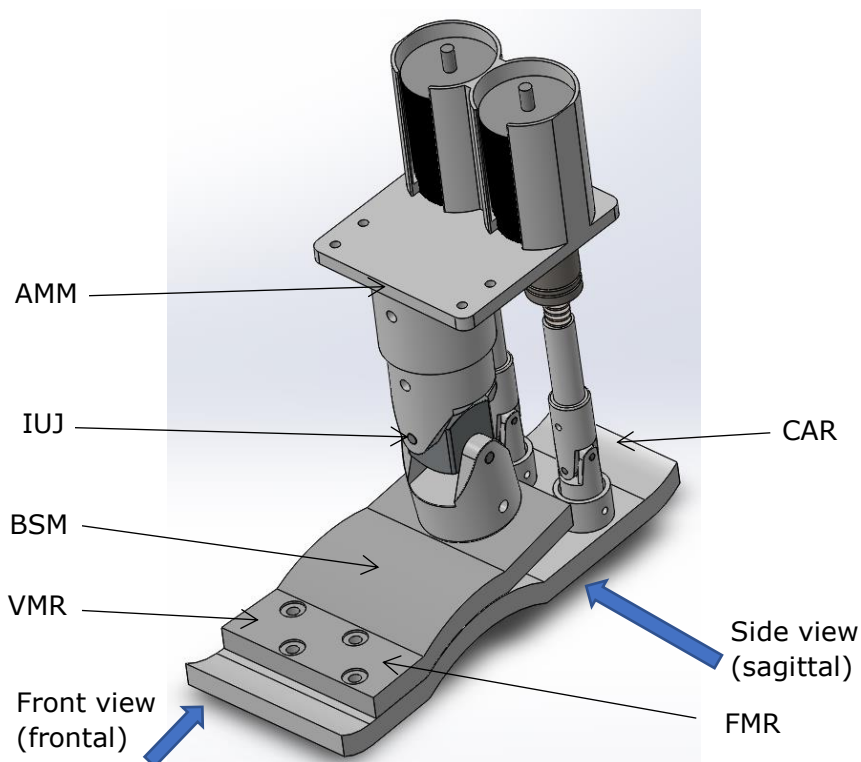
Figure 6.6: Position of reflective markers on the prototype

Participants were cued to walk before each trial. This ensured that both the high-level controller and the motion capture system were active with each trial. The systems were started independent of one another. Synchronisation between the two systems was not required. This was because the acquired EMG data was independent of the Vicon system. The EMG data was only fed into the high-level controller. The aim of the validation experiment was to ascertain the performance of the developed control strategy implemented on the prototype, not conducting a biomechanics gait experiment.

The motion capture system was calibrated using its proprietary software and a calibration wand with four reflective markers. This was done to ensure accurate and robust motion capturing. The system calibration procedure is detailed in the Vicon online documentation, under the section *Calibrate a Vicon system* [93]. Motion data was captured at 200Hz and EMG data was captured at 1926Hz. The specifications of the EMG system are presented in Appendix C. The high-level controller was initiated first, followed by the motion capture system being started.

Prototype motion during the experiment was also captured using a video camera. The video camera was placed at the same side of the laboratory from which the participants began each walking trial. It was not in the motion capture volume and did not interfere with participant walking.

The real-time EMG data was fed into the high-level controller. Motion was then predicted based on six computed features, as discussed in chapter 5. These features were variance (VAR), wavelength (WL), integrated EMG (IEMG), autoregressive (AR), root mean square (RMS) and moving average (MAV). The EMG data was processed in batches of 1763 bytes at a time. This resulted in real-time processing of the data as it was read from the sensors.

6.3.5 Data Processing

The motion capture data was used to determine the prototype ankle's level-ground and uneven terrain ROM, in comparison to that of the human ankle-foot system. The data was taken from the 4th step for each of the 10 walking trials, per walking speed, for each participant. One walking trial was made up of six steps (three strides). This was done for both the level-ground and uneven terrain data, for each participant.

The ROM along the sagittal and frontal planes was calculated based on the FMR, VMR and CAR reflective marker coordinate data. The angle measurement is illustrated in figure 6.7. The ROM was calculated with reference to the markers' static capture positions which were captured prior to beginning the validation experiment with each participant.

a) Side view – Sagittal plane ROM   b) Front view – Frontal plane ROM
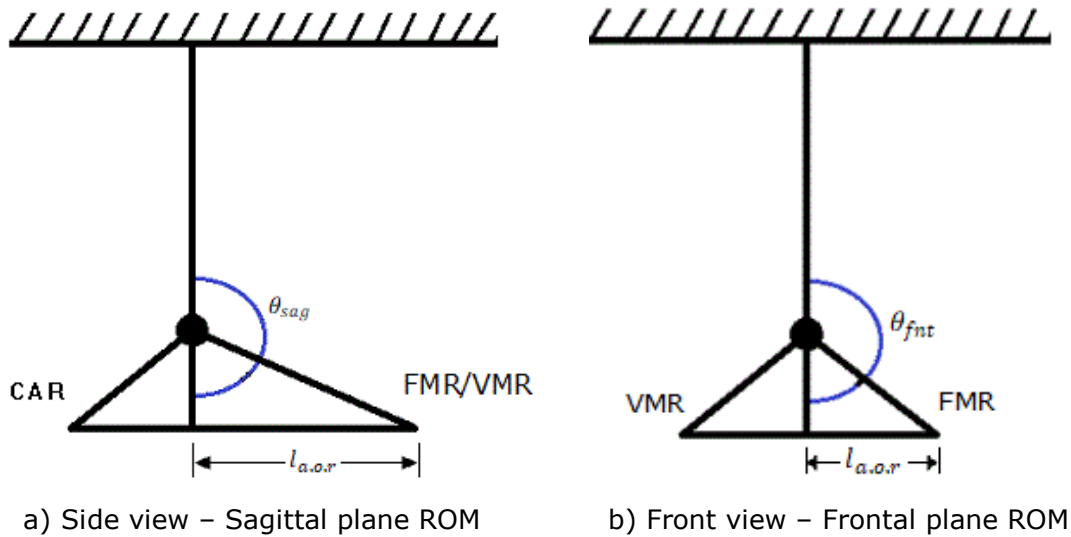
Figure 6.7: Graphic representation of ROM measurement

ROM was calculated for each participant. This was done for both their level-ground and uneven terrain trials. The data was interpolated to 300 points. This was done to ensure that the ROM data was the same length for both participants and across the different walking speeds. This interpolation served as a time normalisation procedure. It also enabled the data from the different participants to be plotted on the same graph. The choice of interpolating the data to 300 points was due to it being the next round number closest to the longest data length, which was from slow walking. This ensured that the data was not distorted.

Each participant's ROM profile was computed by averaging their ROM data from all 10 trials, per walking speed. This resulted in the creation of intra-participant ROM profiles for each walking speed and terrain type. The participants' intra-participant data was then averaged such that a representative inter-participant ROM profile was created for each walking speed and terrain type. The standard deviation for the participant group's ROM data was computed from the inter-participant data. Positive angle values represented the ankle joint in dorsiflexion for the sagittal plane and eversion for the frontal plane, respectively.

Equations 6.4-6.6 present the general approach developed to calculate ROM from the marker coordinate data. This method was used to calculate ROM along the sagittal and frontal planes, respectively. The ROM calculation presented in equations 6.4 and 6.5 uses the FMR marker data. The same approach was used with the VMR marker data. The CAR marker data was incorporated to supplement the marker data when calculating the sagittal plane ROM. This was only for cases where there was missing FMR or VMR marker data. Such cases did not occur.

The calculated FMR and VMR angles were subtracted from each other in equation 6.6 because these markers moved in different directions along the frontal plane. However, they were displaced the same distance with respect to the foot flat (rest) position.

$$\theta_{FMR_i} = \frac{\tan^{-1}\left(FMR_{motion} - FMR_{ref}\right)}{l_{a.o.r}} \quad \text{... (eq. 6.4)}$$

$$\theta_{sag} = \frac{1}{n}\sum_{i=1}^{n} \frac{\theta_{FMR_i} + \theta_{VMR_i}}{2} \quad \text{... (eq. 6.5)}$$

$$\theta_{fnt} = \frac{1}{n}\sum_{i=1}^{n} \frac{\theta_{FMR_i} - \theta_{VMR_i}}{2} \quad \text{... (eq. 6.6)}$$

where;

θ_{FMR}	is the ROM angle, in degrees, calculated using the FMR maker data
FMR_{motion} FMR_{ref}	are the motion capture data for the FMR marker during the walking trials (when in motion) and from a static capture calibration trial, similar to that done for the motion capture data during the gait experiment (chapter 3).
$l_{a.o.r}$	is the perpendicular length from the reflective marker to the axis of rotation (a.o.r) of the movement plane of interest
θ_{sag} θ_{fnt}	is the computed ROM angle along the sagittal and frontal planes, respectively
i	is the experiment trial number from which the group ROM angle was calculated
n	is the total number of trials from which the marker data was used to calculate the ROM angle for the movement plane of interest

The torque output of the prototype was calculated as a function of the voltage and current drawn by the motors. This was recorded using the video camera. The torque data was taken from the fifth walking trial for the level-ground and uneven terrain, respectively, for each participant. This was done for each of the three walking speeds. The voltage and current readings were taken at nine points of the gait cycle as observed from the video camera footage. These were the start (0% gait cycle), heel-strike, early stance (dorsiflexion), foot loading (foot flat), mid-stance, heel-off, push-off (plantarflexion), initial-to-mid-swing and terminal swing. The torque from each participant's data was calculated using equations 6.7 and 6.8. These equations are standard in electrical engineering, calculating power and torque.

The torque output based on each participant's data was averaged, resulting in torque outputs based on both participant's data (N=2 trials). This inter-participant data was then smoothed by interpolating it to 1000 points. This was done for each walking speed. All the data processing was done offline using custom written Matlab programs. A list of the custom written Matlab programmes used in this research is detailed and provided in Appendix J.

$$P_{OUT} = \tau \times \omega \qquad \dots \text{(eq. 6.7)}$$

$$\tau = \frac{P_{in} \times \varepsilon \times 60}{rpm \times 2\pi} \qquad \dots \text{(eq. 6.8)}$$

where:

P_{OUT} is the power output

τ is torque from the motors, the prototype output torque

ω is the angular velocity of the motors

P_{in} is the input power, $I \times V$ from the power supply

ε is the efficiency of the DC motors, which was 70%

rpm is the motor rated speed in revolutions per minute, which was 6000

6.3.6 Statistical Analysis

Single standard deviations were computed from the inter-participant data and are included in the results. Statistical analysis was performed on the inter-participant data. A two-tailed paired t-test was performed to investigate whether the prototype's ROM was similar to that of biological ROM. Another t-test was performed to investigate whether there was a significant difference in the two participant's ROM data. A one-way ANOVA was also conducted to investigate the influence of walking speed on the ROM. This was done both for LG and UT trials. A confidence level of 95% ($\alpha = 0.05$) was used for all analyses.

6.4 Results

Overall, the prototype functioned well in response to participant motion. However, there were some actuation delays when initially activating the high-level controller. These were communication delays mainly due to data being wirelessly transmitted from the EMG electrodes to the high-level controller for execution. The prototype movement sequence is presented in figure 6.8 for a full gait cycle of normal level-ground (LG) walking. The uneven terrain motion is not included as a second video camera was not available to capture the frontal plane movement of the prototype.

The prototype transitioned through the entire gait cycle (fig. 6.8). However, its swing phase motion was not similar to that of able-bodied individuals. This was due to swing motion not being part of the movement classes the control strategy was trained to recognise, classify and execute. As such, the prototype's transition through swing phase was not as smooth as that of able-bodied individuals, such as the experiment participants. During swing phase, the prototype lingered around foot flat before transitioning into a dorsiflexion position for the next step. This was synonymous to the decision trees' misclassifications of swing data, presented in section 5.3.2 of chapter 5. The lingering of the prototype around foot flat was due to the swing data being misclassified as eversion and foot flat.

Weight bearing prototype testing would have to be conducted to ascertain the extent to which such 'irregular' swing motion affects gait. Nonetheless, any adverse effects could be remedied by incorporating contact switches to reset the foot to a specific position when not in contact with the ground. However, this could limit the volitional control capacity of the system.

1) Start position	2) Step initiation	3) Heel strike (dorsiflexion)
4) Loading leading leg	5) Mid-stance (foot flat)	6) Heel-off
7) Push-off (plantarflexion)	8) Initial to mid-swing	9) Terminal swing
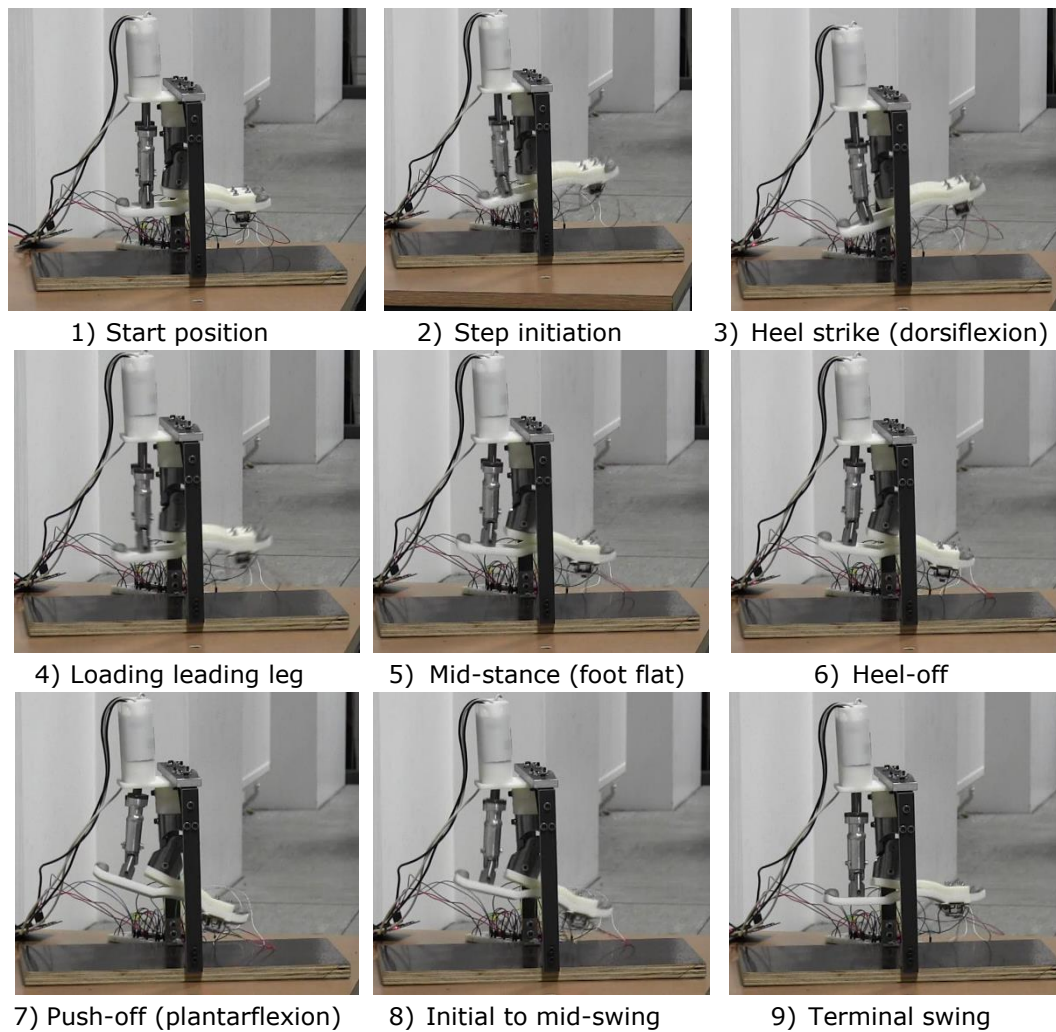
Figure 6.8: Prototype gait sequence for LG normal walking

6.4.1 Range of Motion: Primary Axis

The ROM was computed for each of the two DoF along which the prototype could move. The primary axis was defined as the plane along which the predominant motion was carried out with regards to the walking terrain. As such, the primary axis for the level-ground (LG) trials was along the sagittal plane. The primary axis for the uneven terrain (UT) trials was along the frontal plane.

The prototype's ROM is presented in figures 6.9 and 6.10 for the primary axis of the LG and UT trials, respectively. The results shown are for the inter-participant (group) data for each walking speed. A single standard deviation is also shown as the shaded portion in each figure.

6.4.1.1 Level ground

The overall prototype ROM for the LG trials was similar to reported ankle ROM for able-bodied individuals both in magnitude and pattern [41, 153]. The prototype moved along dorsiflexion (heel strike), foot flat (mid-stance), plantarflexion (push off) and swing phases of human walking. The prototype's ROM was also similar to that of other one DoF transtibial powered prostheses [53, 120, 153]. However, its push-off occurred at around 75% of the gait cycle. This meant that push-off from the prototype was ±15% later than that observed during able-bodied walking.

The delayed push-off was primarily due to data transmission delays from the high-level controller to the output-level controller. Nonetheless, the prototype's ROM results indicated that it was capable of mimicking able-bodied gait. This indicated the prototype was capable of mimicking able-bodied gait.

The largest ROM deviations occurred during fast walking swing phase. This was due to the controller misclassifications during this phase of the gait cycle. The swing phase was not accounted for when developing the control strategy. This led to prediction misclassifications, as discussed in section 5.3.2. The absence of a damping medium on the prototype could have also attributed to the deviations observed in the ROM data.
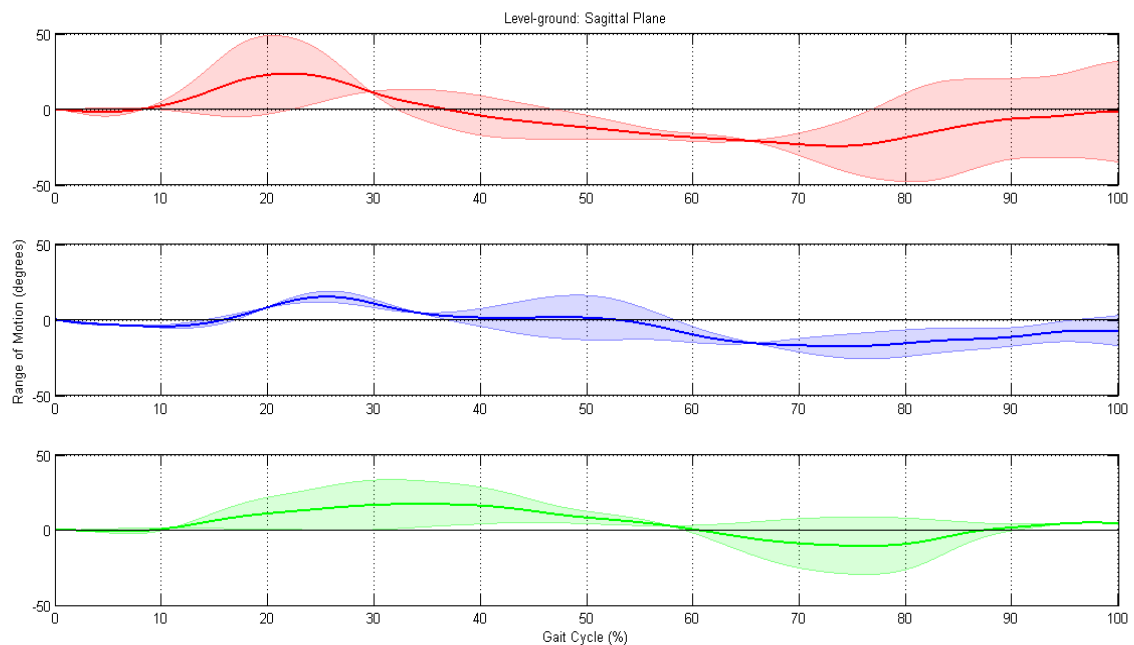
Figure 6.9: Prototype LG ROM along primary axis (N=20 trials for each speed)

6.4.1.2 Uneven terrain

Unlike for the LG trials, comparison against able-bodied data was not possible for the UT ROM as the walking trials were performed on a custom made uneven terrain. Nonetheless, movement along the frontal plane was expected. Prototype ROM along the frontal plane was smaller in magnitude than was anticipated. However, the ROM patterns indicated that the prototype performed foot inversion in response to the participants performing inversion with their right feet (fig. 6.10).

This demonstrated that the control strategy and prototype were responsive to the participants' motion along this second DoF. The small magnitudes of inversion angles could have been due to numerous factors such as participants stepping higher up on the sloped terrain, to them opting to maintain stability by adjusting their knee and hip joints to a larger degree then their ankle joints.

The prototype remained in foot inversion for the duration of the observed gait cycle. This was due to the participants' feet being displaced along the frontal plane, with respect to their foot flat position when on level-ground, when stepping on the sloped terrain.

The reduction in walking speed led to higher ROM variation, with regards to the different walking trials. This was most evident for the slow walking speed which had a greater standard deviation band. This highlighted the reaction of the prototype in response to the fluctuations of the incoming participant's EMG data. These fluctuations were due to the participants traversing the uneven terrain at slower walking speeds. This was also evident in the medial/lateral GRF and lower leg EMG data of the participant group during the gait experiment (presented in chapter 3). The resulting prototype ROM indicated the sensitivity of the control system and its ability to facilitate biologically similar gait.
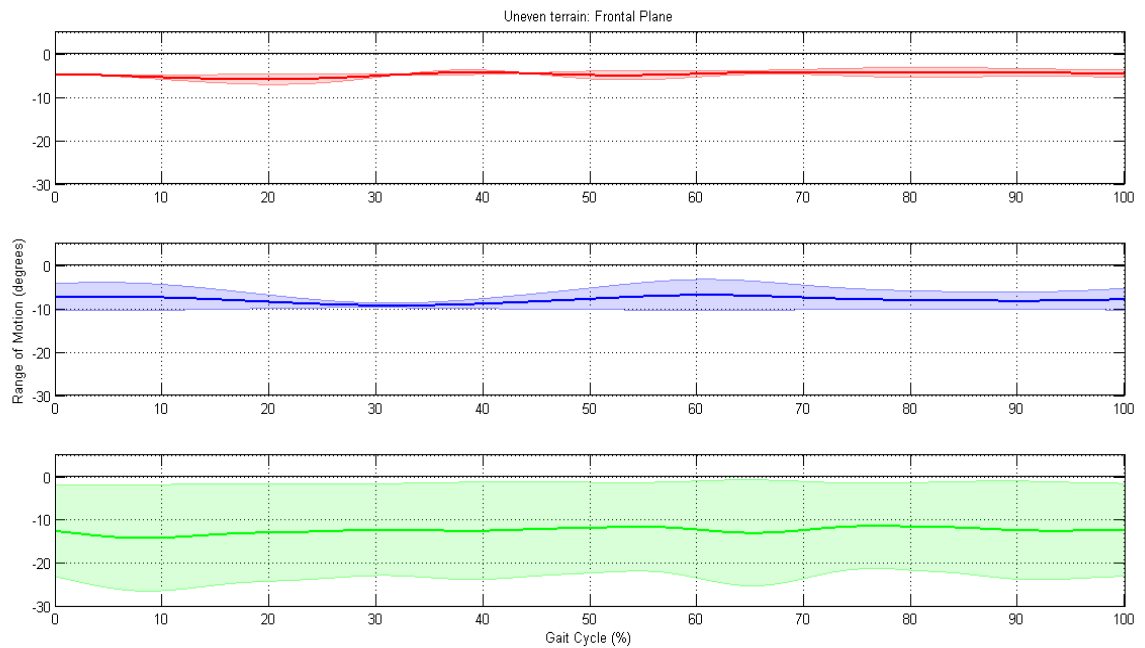
Figure 6.10: Prototype UT ROM along primary axis (N=20 trials for each speed)

6.4.2 Range of Motion: Participant Specific

The prototype's ROM as a result of each participant's data during the LG trials is presented in figure 6.11 (A-C). The ROM for the UT trials is presented in figure 6.11 (D-F). These results are the ROM along the primary axis. The prototype UT ROM motion was as a result of the participants performing right foot inversion. The data presented was for a single gait phase, from heel strike through to the end of swing phase for the same leg.

The secondary axis was defined as movement along the frontal plane during LG trials and movement along the sagittal plane during the UT trials. The prototype motion along the secondary axis was of interest as it gave a broader indication of the prototype's functionality. The prototype ROM results for motion along the secondary axes are presented in figure 6.12 for both LG and UT trials.

6.4.2.1 Primary Axis: Level ground

Prototype ROM with regards to the individual participants demonstrated the unique walking pattern of each participant. For participant A, the prototype's largest motion was dorsiflexion, particularly during slow walking (fig. 6.11 C). Decreasing ROM was observed in response to decreasing walking speed, which was expected due to less push-off force being required at slower walking speeds.

152

This indicated proper functionality of both the control strategy and the prototype. Prototype ROM that was most similar to reported able-bodied ankle ROM was observed during normal walking for participant A. The similarities included the peak angles for dorsiflexion and plantarflexion, with regards to the gait cycle [41, 153].

For participant B, the overall prototype ROM was a better representation of able-bodied ankle ROM. On average, the dorsiflexion and plantarflexion angles peaked around 17° and 29°, respectively. The increased plantarflexion angle during fast walking (fig. 6.11 A) was attributed to the need for greater push-off force to facilitate the increased walking speed. The large prototype plantarflexion angles observed for participant B data could be attributed to the participant's higher foot arches which resulted in higher supination [154]. Increasing prototype ROM in response to increasing walking speed, also observed for participant A, demonstrated that the prototype could facilitate biologically similar gait.

6.4.2.2 Primary Axis: Uneven terrain

Increasing prototype inversion in response to decreasing walking speed was observed for participant A. This was due to the increased duration of stance phase which imposed the need for centre of mass (COM) stabilisation. The muscle co-activation required to maintain dynamic stability when walking over uneven terrain was also evident in the prototype's ROM data, particularly for participant A (fig. 6.11 D and F). This manifested as oscillations in the ROM data as the lower leg muscles worked to maintain centre of mass (COM) stability. This suggested that the prototype could also facilitate a biologically similar gait during uneven terrain traversal.

Prototype ROM patterns for participant B remained similar across all three walking speeds. The inversion angle increased from fast to normal walking, as anticipated due to the increased time spent in stance phase. The reduced inversion angle during slow walking was attributed to the manner with which the participant traversed the uneven terrain. The participant stepped higher up on the sloped step, minimising their foot's degree of movement along the frontal plane. This adaptation was likely done to ensure better COM control and thus, facilitate a more stable gait over the uneven terrain when walking at the reduced speed.
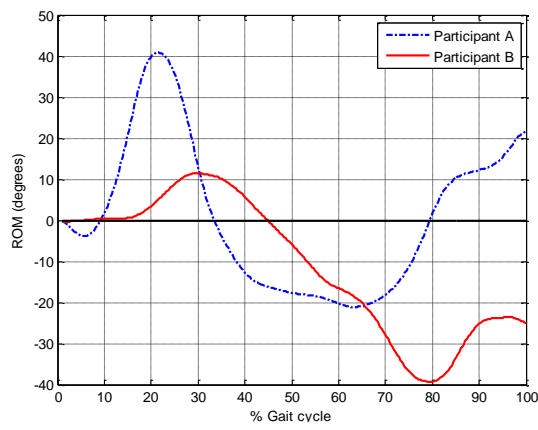
Fast walking – LG (A)
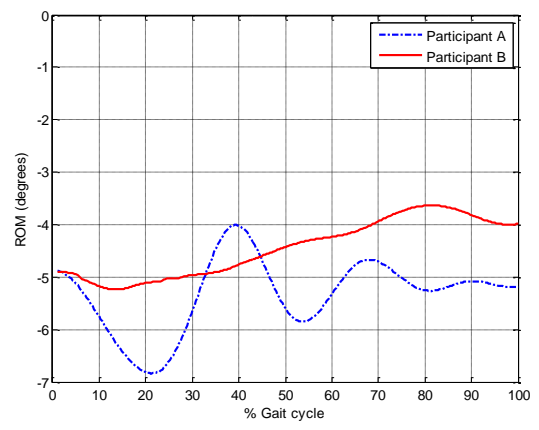
Fast walking – UT (D)
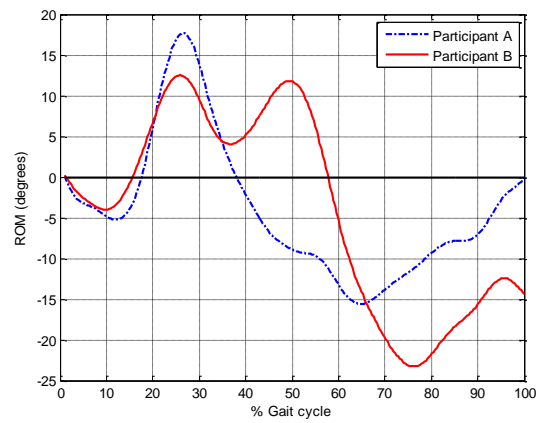
Normal walking – LG (B)
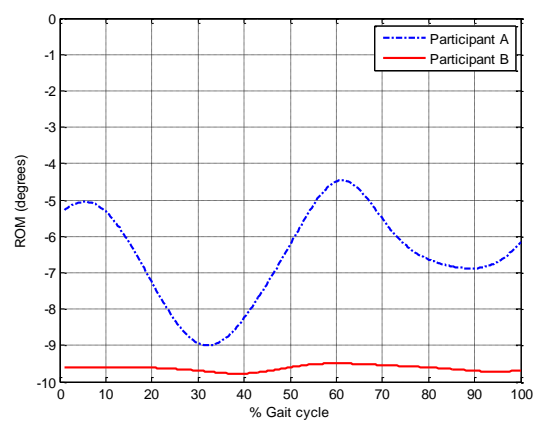
Normal walking – UT (E)
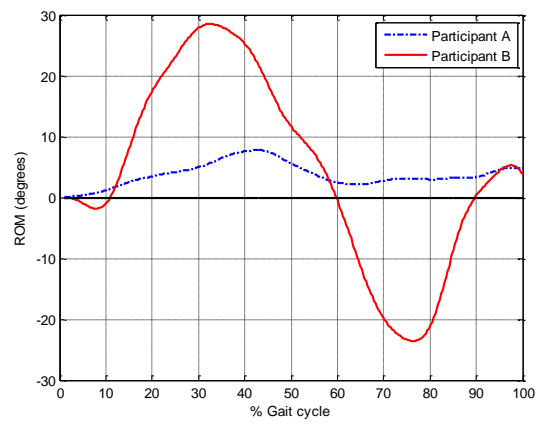
Slow walking – LG (C)
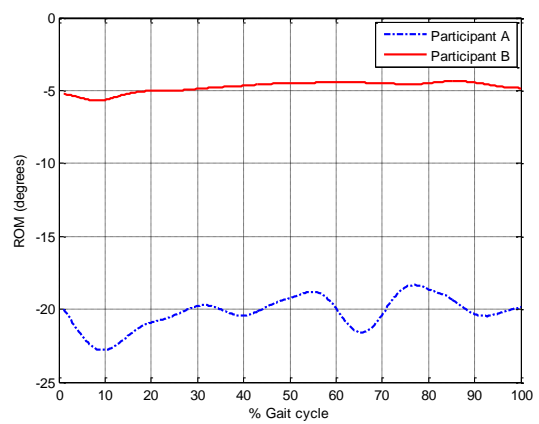
Slow walking – UT (F)

Figure 6.11: Prototype ROM along the primary axis of movement (N=10 trials for each speed, per participant)

6.4.2.3 Secondary Axis: Level ground

The minimal frontal plane movement during the LG trials was similar to ROM reported for healthy able-bodied individuals [29, 41, 105]. This supported the observation that the prototype could facilitate biologically similar gait. The increasing eversion angle in response to increasing walking speed further supported this observation. For participant A, the increasing eversion angle was a result of increasing pronation (foot roll angle during gait) as the foot transitioned through stance phase faster [154, 155]. The increased prototype ROM along the frontal plane for participant B was attributed to the participant's higher foot arches which affect pronation [156]. This was most evident for the two speeds that were not the participant's 'comfortable' walking speed.

6.4.2.4 Secondary Axis: Uneven terrain

It is worth noting that sagittal plane movement was expected during the UT trials as participants had to propel themselves forward, over the uneven terrain. As such, dorsiflexion was required to ensure foot clearance and to facilitate heel-strike, and plantarflexion was required to facilitate push-off and forward motion.

The prototype exhibited a ROM that was similar to its primary axis ROM for participant A. The early and increasing plantarflexion angle, in response to decreasing walking speed, was as a result of the increased need for CoM stabilisation. The increased prototype dorsiflexion during fast and slow walking for participant B was due to the participant's high foot arches and also to the priority being on ensuring adequate foot clearance in preparation for the next sloped step, particularly when walking at speeds either than the 'comfortable', normal speed.
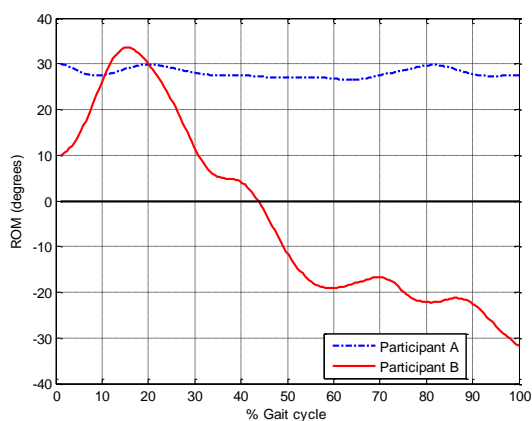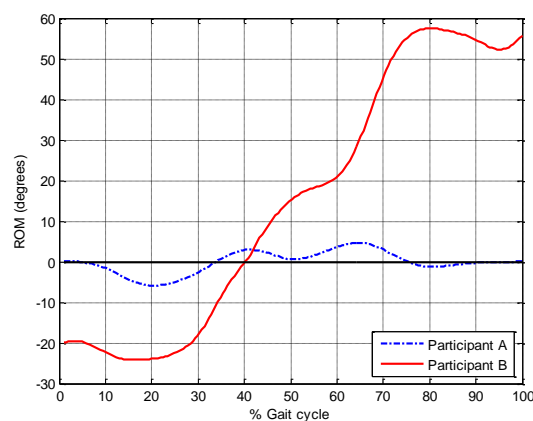
Fast walking – LG (A)   Fast walking – UT (D)
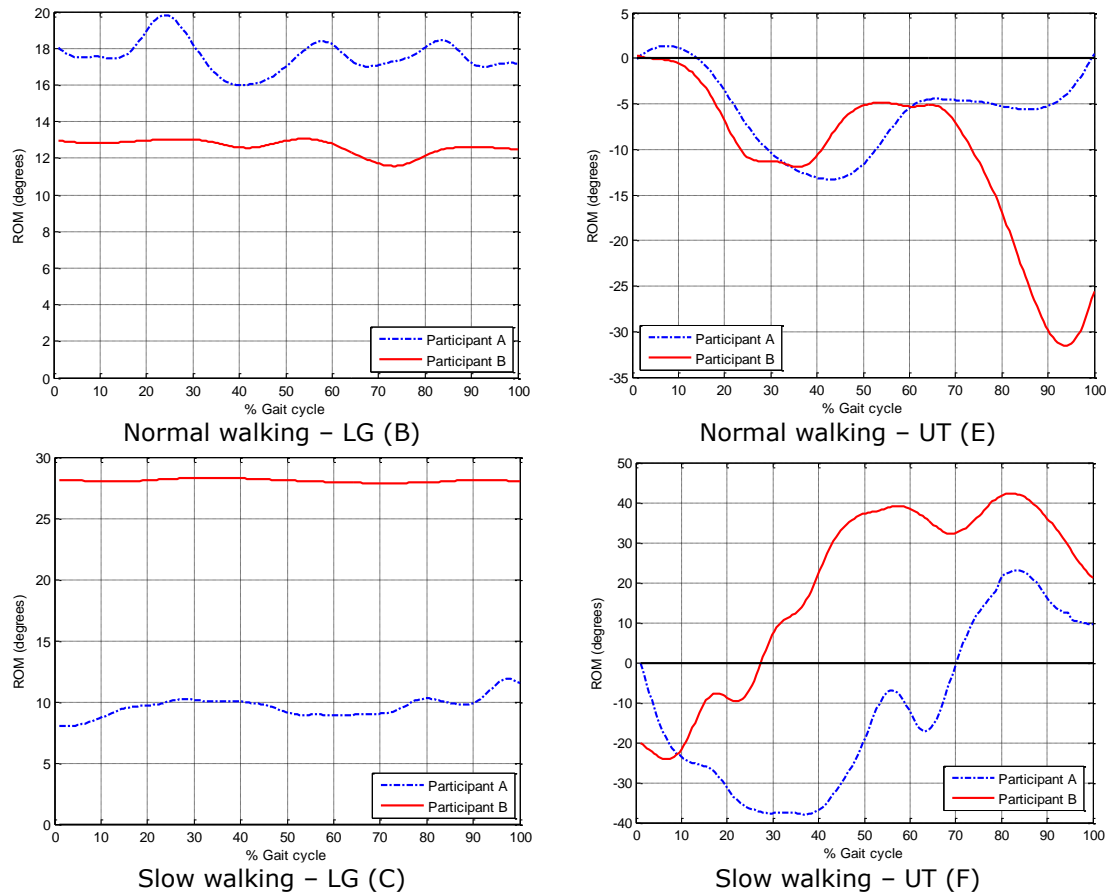
Figure 6.12: Prototype ROM along the secondary axis of movement (N=10 trials for each speed, per participant)

6.4.3 Torque (Moment)

Safe and efficient walking also relies on the ability of the human ankle-foot system to absorb and dissipate energy throughout the gait cycle. It also relies on its ability to produce additional torque at key stages of the gait cycle. As such, the prototype's torque output was of interest.

The prototype output torque is presented in figure 6.13 for all three walking speeds. The torque output was synonymous to the moments generated by the human ankle during gait [41]. The calculated torque gave an indication of the prototype's capability. However, it was not a true reflection of its torque potential due to two reasons. Firstly, because suspended testing was done, the prototype was not required to produce the necessary torque required to compensate for user weight and to facilitate gait. Secondly, the motors did not have access to the full 10A for which they were rated.
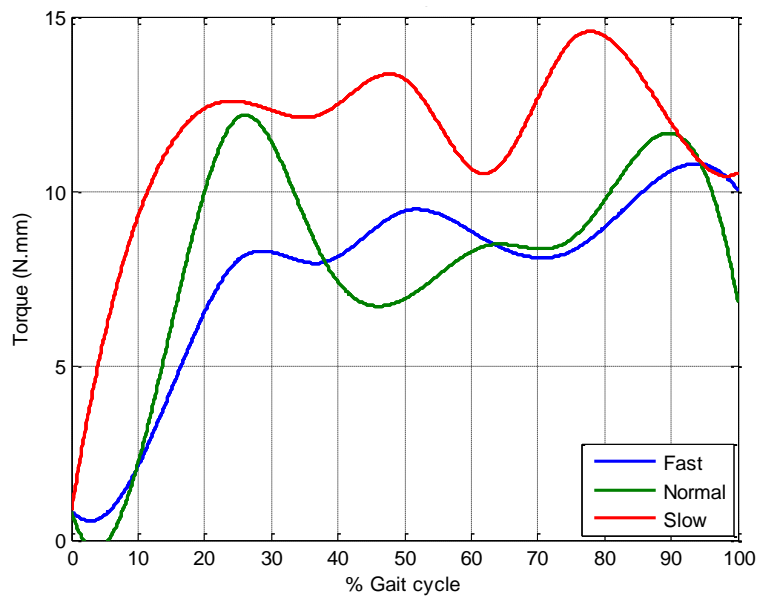
A) LG walking
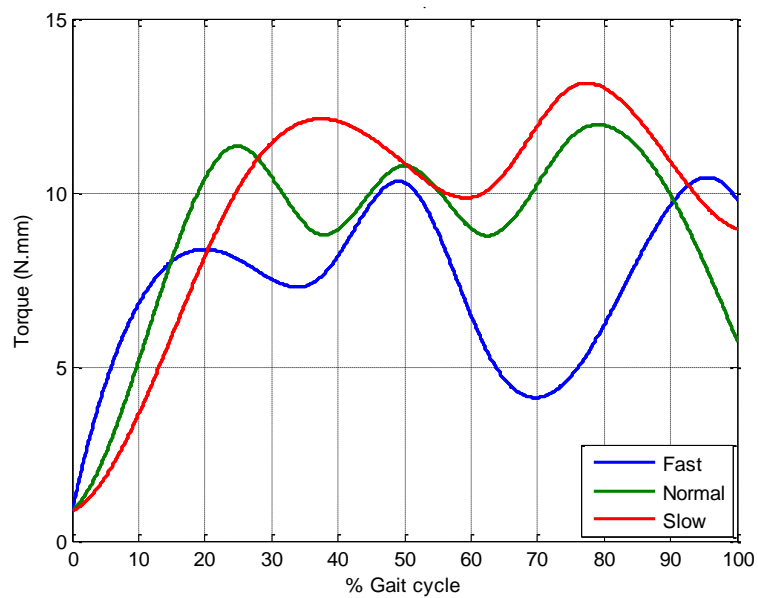
B) UT walking

Figure 6.13: Prototype torque output (N=2 for each speed, per terrain)

The prototype torque was considerably smaller in magnitude compared to that of able-bodied individuals during LG gait [41]. This was attributed to the motors used, the limited current available to said motors and because passive energy could not be stored during the experiment, suspended testing was carried out. The addition of passive energy, from an incorporated tension spring, would have supplemented the output torque delivered by the system, bringing it closer to that achieved by able-bodied individuals.

Nonetheless, the torque trajectory was comparable to that observed for healthy human walking [41, 153]. The prototype output torque varied along the gait cycle, in response to gait phase progression. The largest torque occurred around heel-off to push-off (plantarflexion) for fast and slow walking, for both LG and UT trials. This made it synonymous to able-bodied torque output during walking. This was with the exception of the peak torque output during normal walking which occurred around early mid-stance. The increase in torque around early-mid swing phase was due to the prototype actuating back to a dorsiflexion position in preparation for the next step. This dorsiflexion movement meant a rapid change in the direction of rotation for the leadscrews, which required the motors to draw more power to facilitate the change.

Unlike human ankle moments, the prototype torque output did not reduce to near zero during swing phase [41, 153]. This was because the prototype needed to be actuated through swing phase. Incorporating the tension spring and allowing the actuation system to back drive during certain gait phases would result in a torque output trajectory that is similar to that of able-bodied individuals during swing phase, when conducting weight bearing testing. Another factor that influenced the torque output during swing phase were the misclassifications of swing data as other motion due to it not being part of the five motions the high-level controller was trained to recognise. This was presented in section 5.3.2 of chapter 5.

The observed prototype torque was as a result of the manner in which the motors were commutated. The need for fast system response with respect to the cyclic, though transitional, nature of human walking meant that the motors were continuously transitioning from one gait phase to the next. This resulted in a reduced time window wherein motor torque could be built up and supplied.

6.5 Discussion

6.5.1 Terrain Type vs. Prototype Performance

Prototype performance remained consistent across the different terrains and walking speeds. This supported the finding that the prototype could facilitate biologically similar motion. Deviations in prototype ROM, in comparison to able-bodied ROM, were observed when looking at ROM data due to the individual participant data. However, ROM that was better indicative of able-bodied gait would be attained if testing were done with a larger participant group. As such, there was a significant difference between biological ROM and the prototype's LG ROM.

Though this was marginal (p=0.042). The able-bodied data was interpolated from the results presented by Rábago et al [153].

The differences in frontal plane ROM reported in literature, and that presented in this research, suggests that some standardisation is required for measuring human ankle ROM along the frontal plane [157]. Overall, the results demonstrated that the implemented control strategy achieved repeatable performance and could facilitate gait that was similar to able-bodied individuals.

There were significant differences in the participant's individual ROM results. This was for both the LG (p = 0.049) and UT (p = 0) trials. This was congruent with the observation that the prototype facilitated behaviour that was in response to each participant's *unique* EMG data. However, the resulting prototype ROM data was still similar to that of able-bodied individuals.

6.5.2 Walking Speed vs. Prototype Performance

Overall, increased prototype ROM was observed in response to increased walking speed. This was for both LG and UT trials. Walking speed did have a significant effect on the prototype's ROM for both the LG (p = 0) and UT (p = 0) trials. This corroborated the visual results of the prototype's ROM responded accordingly with respect to walking speed, similar to that of able-bodied participants. This was evident when comparing the trend of the fast and slow walking ROM to that of the normal walking ROM.

The torque output decreasing in response to decreasing walking speed was attributed to the reduced time span in which the system could draw and deliver the required output energy. This highlighted one of the challenges in developing transtibial powered prostheses. Currently, available actuation solutions are incapable of matching the power output and response times of biological limbs. This is made more challenging by the desire to have these systems be the same size as the biological limb they are replacing.

In relation to the prototype's response time, there was no observable difference with changing walking speed. There was also no discernible overall motion trend with regards to the physical motion of the prototype during the experiments. For participant A, the physical motion of the prototype improved with increasing walking speed, which translated to having less movement fluctuations (jerking).

However, for participant B, the prototype motion had more fluctuations during fast walking. The best motion was achieved during normal walking.

6.5.3 Proportional Control vs Feedback Control

During the UT trials, it was also observed that continued participant motion within the same gait phase resulted in continued prototype motion as well. This was due to the system programming which allowed such motion, it demonstrated that a means of proportional control was being facilitated by the prototype. The prototype being able to remain in a particular position (gait phase) as held by a participant, suggested that the prototype could enable participants to perform non-cyclic motions such as going up onto their toes or remaining in dorsiflexion when balanced on their heels.

To the author's knowledge, this movement potential is something current commercially available prostheses are unable to facilitate. Further development of such a feature could enable other non-cyclic behaviour, which would be a realisation of a true volitionally controlled lower limb prosthesis. This would allow transtibial powered prosthesis to become better replacements of the amputated lower limbs.

A PID controller could be implemented to ensure that the output behaviour of the prototype agrees with what was communicated by the high-level controller. The physical system could be modelled to develop a PID controller that would be representative of the prototype. As the prototype was essentially an actuation system in series with a prosthetic foot, modelling the entire system would be equivalent to modelling only the actuation system.

Given that torque output was the reference quantity to be tracked and controlled, implementing such feedback control could result in more efficient prototype performance without completely negating the semi-proportional control method currently implemented. The implication of incorporating PID control on the output-level controller would be the necessity to integrate additional prototype mounted sensors to better monitor the output behaviour of the system.

6.5.4 Other Factors

Increasing the system baseline voltage did not increase the prototype's reaction time or lead to any improvements. Conversely, the prototype motion had more fluctuations when the system baseline voltage was increased to 12V, compared to its original setting of 8.6V. The fabrication and assembly of the prototype also had a bearing on its performance. Another factor that affected the performance of the prototype was the motors sometimes pushing up and out of their mount. This led to a shortening of the leadscrew on the side the motor had pushed up on, which affected the prototype's ROM and overall movement.

Using a power supply with a rated maximum current of 2A meant that a limited output torque could be delivered by the actuation system. This was not an issue during this research as suspended testing was done. However, an untethered power source capable of supplying higher current would be required for weight bearing testing to ensure that sufficient torque can be delivered by the prototype during gait.

6.5.5 Experiment Limitations

The original prototype design was such that an elastic element could be incorporated, an extension spring. The spring would have absorbed energy during early to mid-stance phase of the gait cycle and release said energy during push-off. Conducting suspended testing resulted in the spring being omitted. This was because including the spring would have been energy inefficient. The motors would have been required to perform more work to elongate the spring, along with facilitating actuation. As such, the vibrations (foot fluctuations) experienced by the foot with each motor actuation were carried through the entire system. This led to gait transitions being jerky (not smooth). The vibrations experienced by the prototype did not affect the high-level controller. However, they did affect the output-level controller, particularly the motion tracking circuit.

The extension spring originally selected for inclusion into the prototype would have been capable of delivering ±50W of power at push-off. The extent to which incorporating the extension spring would influence the performance of the system would have to be investigated during a weight bearing test. Another limitation of the current validation approach was not being to investigate the prototype output torque under load.

As such, at this point, it is uncertain how the physical prototype would perform when loaded. However, this was not detrimental to this research as the main aim was the development of a control strategy to facilitate level-ground and uneven terrain traversal.

The shock loading influence on EMG data, particularly during initial contact (heel-strike), was introduced into the system though the EMG data from the able-bodied participants. Therefore, the high-level controller was functional even under these circumstances. As such, it stands to reason that shock loading during weight bearing testing would not negatively affect the performance of the control strategy.

6.6 Conclusion

The results from the validation experiment indicated that the developed control strategy could facilitate able-bodied human gait on the transtibial powered prosthesis prototype. The prototype ROM indicated the importance of frontal plane movement for varied terrain traversal and demonstrated that the prototype would be able to conform to a greater variety of terrain compared to single DoF prostheses. The prototype torque output had a similar trajectory to that of ankle moments during gait. This indicated that the actuation system was supplying energy to the prototype foot in a manner that was synonymous to lower leg muscles actuating the human foot.

It also demonstrated that even though the functionality of the prototype was not yet 100% accurate, real-time user acquired EMG data could be used to facilitate volitional control. Particularly to control a transtibial powered prosthesis for uneven terrain traversal; thus, proving the concept. It stands to reason that the incorporation of other data would improve the accuracy and performance of the prototype. This has been evidenced in findings from other researchers as discussed in chapter 2.

Even though upper limb powered prostheses driven by EMG signals are commercially available, there remains a lag in the application of this technology for the lower limbs. The significance of the observed prototype ROM was demonstrating that such a device could function as an actual prosthesis following further development. The observed ROM also suggested that such a prototype could assist a user achieve an able-bodied walking gait, particularly when traversing fixed, uneven terrain.

Chapter 7
Conclusion

The overarching aim of this research was to develop a control strategy that, when implemented on a multi-axial transtibial powered prostheses prototype, could facilitate traversal over fixed, uneven terrain. In pursuit of this endeavour, several sub-objectives were met. Most of these sub-objectives had some foundation on previous research conducted in the field of lower limb powered prostheses, which was presented in chapter 2.

The research presented in this thesis was a proof of concept with regards to using of limited EMG data to facilitate a 2DoF powered control over a transtibial powered prosthesis prototype. The core objectives of this research (presented in chapter 1) have been achieved, as evidenced by the results presented in chapters 5 (User Intent Prediction Strategy) and 6 (Prototype Control Strategy and Implementation).

The key contributions of this research and the novelties thereof included:

1. Demonstrating that a generic approach, coupled with a classification tree algorithm, yielded the best prediction accuracy when using a combined data set. Also, that a generic approach adapted better to new users, resulting in higher prediction accuracy, than more user centric approaches.
2. Facilitating powered control of a 2DoF powered prototype solely using real-time EMG data from lower leg muscles. Thus, allowing the prototype to exhibit ROM comparable to that of able-bodied individuals during level-ground and uneven terrain traversal.
3. Facilitating user centric, responsive (volitional) control on a transtibial powered prosthesis prototype using limited EMG data. This was data from only the tibialis anterior, medial gastrocnemius and lateral gastrocnemius muscles.

7.1 Activities Undertaken and Their Contribution to This Research Area

The gait experiment with able-bodied participants walking over level-ground and the fixed, uneven terrain highlighted the importance of the human ankle being able to move along more than a single plane. This was presented in chapter 3. The participants' feet being able to conform to the variable terrain demonstrated an

important feature when ambulating over irregular terrain and substantiated the inclusion of additional DoF for transtibial prostheses.

Studying the results from the gait experiment revealed the cyclic nature of lower limb muscle activation. This was observed for both level-ground and uneven terrain trials. The larger muscle co-activation of the antagonist muscle pair of the lower leg, coupled with greater ground reaction force (GRF) fluctuations along the medial-lateral plane, gave an indication of how the able-bodied participants maintained their stability when walking over the varied terrain. The data highlighted how the ankle movement and muscle activation worked in unison to stabilise the participants' centre of mass (CoM), allowing them to maintain their forward walking trajectory, while also minimising energy expenditure. These findings influenced the design of the multi-axial transtibial powered prostheses prototype presented in chapter 4.

The inspiration behind the prototype design, and what formed the design criteria, was the range of motion (ROM) capabilities of the human ankle-foot system and its ability to not only support an individual's body weight, but also its capability of absorbing and distributing the force and moments introduced during everyday ambulation. As with most engineering designs, cost, manufacturing and time constraints also had a bearing on the final design and the choice of material when developing the prototype. The prototype foot was 3D printed in-house, at the University of Manchester. This approach was taken due to the speed and cost effectiveness with which prototype iterations could be developed. FEA simulation of the prototype design was done using various foot position scenarios. These scenarios were congruent with positions a human ankle-foot system transitions through during normal level-ground walking. The FEA results indicated weight limitations for the foot, though also indicated that physical, dynamic testing of the prototype would be possible.

In an effort to mimic the control behaviour that made up the gait adaptation strategies that were observed for the gait experiment, a control strategy was developed using the EMG data acquired from said experiment. A hierarchical approach was taken for the developed control strategy. It consisted of a high-level, decision making controller and an output-level, execution controller. In developing the high-level controller, various prediction algorithms were tested in pursuit of the most optimal with respect to facilitating volitional control.

This was presented in chapter 5. Optimal EMG features were selected based off EMG data from only the tibialis anterior (TA), medial gastrocnemius (MGas) and lateral gastrocnemius (LGas) muscles. Time domain features were of preference as they were best suited to facilitate real-time system implementation. Prediction approaches that were generic and user specific were explored, along with classification algorithms that were machine learning and non-machine learning based. The best overall pairing of prediction approach and classification algorithm, particularly for use during both level-ground and uneven terrain traversal, was found to be a generic prediction approach coupled with a decision tree classification algorithm.

The overall performance of the different prediction strategies was not as good as that reported in other user intent prediction research. This was due to limited EMG data being used in this research and also because no mechanical sensors were included in predicting user motion. As such, it is within reason to expect that the classification accuracy would improve with the inclusion of other sensors. The significance of the performance of the prediction strategies explored in this research, was the indication that such user driven control strategies could be viable for implementation in daily use lower limb powered prosthesis.

Suspended testing was conducted using the developed prototype to ascertain how well the control strategy faired in reproducing able-bodied human walking. This was presented in chapter 6, along with a description of the output-level controller. The prototype's ROM was similar to that of able-bodied individuals, as reported in other research. This demonstrated that the prototype could not only move along two degrees of freedom (DoF) but also that it could do so in a manner comparable to able-bodied individuals – which meant it could facilitate walking over fixed, uneven terrain.

The next area of interest was the prototype's torque output. The prototype fell short of the torques achieved by the human ankle-foot system, though its overall torque trajectories were similar. The prototype's torque shortfall was attributed to the manner with which actuation was facilitated. The time required for the actuation system to draw power from the supply and deliver it to the prototype foot was shortened with increasing walking speed. This resulted in torque output decreasing with increasing walking speed. Nonetheless, the trend indicated how energy was supplied to the prototype foot during the validation experiment.

It suggested that the prototype could assist an individual with a transtibial amputation attain a gait that was similar to able-bodied individuals. However, an actuation system with a higher torque rating would have to be used. This would enable further system testing, particularly under weight-bearing conditions.

The results presented in this thesis have answered the research questions posed in chapter 1, section 1.4:

1. Real-time EMG data was used as the sole control signal to drive a transtibial powered prosthesis. This was demonstrated by the prototype functionality and ROM from the validation experiment (chapter 6).

2. The developed control strategy allowed the prototype to respond appropriately as the able-bodied participants walked over level-ground and traversed the uneven terrain during the validation experiment (chapter 6).

3. Even though there was a reduction in the control strategy's prediction accuracy, it adapted to new users (new data) reasonably well, particularly when using a decoupled data set (chapter 5).

4. As demonstrated by the ROM results presented in chapter 6, the physical structure of the prosthesis being able to move along 2DoF (the design of which was presented in chapter 4) meant that the prototype could realise motion that was similar to that of the able-died participants as they walked over the uneven terrain during the validation experiment.

7.2 Research Limitations and Areas of Improvement

Due to the weight restrictions of the system, only suspended testing was conducted. Changing the material from which the prototype was manufactured would allow for weight bearing testing. As an alternative to manufacturing another prototype foot, a commercial prosthetic foot could be retrofitted and used to enable weight bearing tests. A prosthetic foot such as the Flexfoot by Össur (Reykjavik, Iceland) could serve the purpose. However, new ethical approval would have to be sought before such an experiment was conducted. The torque produced by the prototype during weight bearing testing would be reliant on the power supply used. The addition of user weight would mean that passive energy could be stored through the incorporated extension spring during stance phase. The addition of user weight could also lead to an increase in the prototype's ROM.

The weight of the system was slightly above that of a similarly sized human ankle-foot system. A redesign of the system, using components made from lighter material, such as for the universal joints, could reduce the system weight. The sore point for this research, and for the entire powered prostheses research field, remains the supply of power to prostheses. A benchtop power supply being used during the validation test meant that no additional system weight was introduced. Conducting weight bearing testing would necessitate the use of either extension wires from a benchtop power supply to the prototype, or a battery with sufficient capacity either mounted on the prototype or secured to the user. Even though this was outside the scope of this research, optimisation of the prototype's power requirements would be a key area of improvement and would also be useful for other lower limb powered prostheses. This would make it easier to commercialise these devices.

The use of in-vivo EMG electrodes would also increase the quality of data used to control the prototype and could lead to an improvement in classification accuracy. Going a step further and using EMG data from muscles that have undergone targeted muscle reinnervation (TMR) could ensure accurate and known muscle activation for individuals with transtibial amputations, which could also improve system performance. However, either of these approaches would be counter intuitive to the stance taken in this research, which was to be as minimally invasive as possible.

7.3 Future Work

The next step for this work is to conduct weight bearing tests, first with an able-bodied participant and then with an individual with a transtibial amputation. This would allow for improvement of the current control strategy and prototype. This would be succeeded by further system testing with a larger participant group made up of individuals with transtibial amputations.

The influence of shock loading and the vibrations that propagate through the prototype would be investigated during the weight bearing experiments. It is expected that the incorporation of the extension spring (detailed in sections 4.3 and 4.5.5) would lead to reduced system fluctuations. It is also expected that the system torque output would increase due to the addition of passive energy stored and released by the extension spring during gait.

The purpose of the future tests would be to further explore the performance of the control strategy during real-life application. Another key area of investigation would be the influence of the residual limb-prosthesis socket interface, particularly with regards to the classification (prediction) accuracy of the high-level controller. The shock loading at initial contact (heel-strike) is not expected to negatively affect the performance of the high-level controller. This is because the influence of the shock loading on the EMG data was already fed into the system during the validation experiment. This was from the EMG data of the able-bodied participants as they performed the gait trials.

Conducting further system testing, for weight bearing conditions, would follow the same protocol detailed in chapter 3 and 6. Participants would walk over level-ground and the same uneven terrain detailed in this thesis. The uneven terrain could also be extended to include walking over other uneven terrain such as loose gravel. This would lead to more robust testing of the developed control strategy and prototype.

In the quest to develop lower limb powered prostheses that are true functional replacements of their biological counterparts, somatosensory feedback naturally present in the human body would also have to be established between the artificial limb (the prosthesis) and a user's nervous system. This would help transition the artificial limb from being just an "add-on" to an extension of both the skeletal and nervous system of the user.

With regards to future work within the wider field of lower limb powered prostheses research, the focus will have to be on 1) developing actuation solutions that better mimic the power and dexterity of the human limb replaced, 2) establishing a somatosensory link between the artificial limb and the nervous system and 3) implementing adaptive control strategies capable of mimicking the muscle memory humans possess as a result of years of repetitive task training. It is upon this muscle memory that humans rely to unconsciously carry out a plethora of locomotion tasks, which vary from reaching for an object on a high surface whilst being solely supported on the balls of the feet to traversing various uneven terrain without sustaining injuries.

7.4 Possible application areas of this research

The key finding and contribution of this research was demonstrating the possibility of developing a volitionally controlled transtibial powered prostheses. This was controlling a prototype prostheses using real-time user EMG data from only three lower leg muscles. It was also facilitating ambulation over more varied terrain. The implication of these findings is the potential of enabling prosthetic users to undertake a larger variety of locomotive activities using a single device.

The findings of this research could also be used in the development of upper limb powered prostheses wherein EMG control continues to be improved on. Exoskeleton research could also apply some of the findings presented in this thesis, particularly research that is focused on rehabilitation. This could include using EMG data to better correct or supplement user movement at appropriate instances.

The ongoing objective is to continue research within this field and to further develop this multi-axial powered prosthesis prototype into a commercially viable device. The control strategy presented in this thesis served as a proof of concept with regards to the volitional control of a transtibial powered prosthesis. The next iteration of the controller will incorporate more prototype acquired feedback, such as foot contact, ground reaction force (GRF) and/or foot centre of pressure, to allow weight bearing walking trials to be conducted.

7.5 Publications Resulting from This Research

The following research outputs have resulted from the work presented in this thesis:

1. Gregory, U. and Lei, R., *The effects of walking speed and terrain on muscle activation and joint kinetics*. MACE PGR Conference 2016. The University of Manchester, UK. March 2016.

2. Gregory, U. and Lei, R., *User intent prediction for a multi-axial transtibial prosthesis*. IEEE Transactions on Biomedical Engineering, 2018 – (To be submitted).

3. Gregory, U. and Lei, R., *Preliminary development of an EMG driven multi-axis transtibial prosthesis*. Journal of NeuroEngineering and Rehabilitation, 2018 – (To be submitted).

References

1. Choi, J.T. and A.J. Bastian, *Adaptation reveals independent control networks for human walking.* Nature Neuroscience, 2007. **10**: p. 1055 - 1062.
2. Lam, T., M. Anderschitz, and V. Dietz, *Contribution of Feedback and Feedforward Strategies to Locomotor Adaptations.* Journal of Neurophysiology, 2006. **95**(2): p. 766–773.
3. MacLellan, M.J. and A.E. Patla, *Adaptations of walking pattern on a compliant surface to regulate dynamic stability.* Experimental Brain Research, 2006. **173**(3): p. 521-530.
4. Voloshina, A.S., Kuo, A. D., Daley, M. A. & Ferris, D. P., *Biomechanics and energetics of walking on uneven terrain.* Journal of Experimental Biology, 2013. **216**(21): p. 3963-3970.
5. Gates, D.H., et al., *Gait characteristics of individuals with transtibial amputations walking on a destabilizing rock surface.* Gait & Posture, 2012. **36**(1): p. 33-39.
6. Poulter, D. *£11 million funding boost to improve NHS care for war veterans*. Armed forces and Ministry of Defence reform, 2013.
7. Geil, M. *Military-funded prosthetic technologies benefit more than just veterans*. Science and Technology, 2017.
8. Gutfleisch, O., *Peg legs and bionic limbs: the development of lower extremity prosthetics.* Interdisciplinary Science Reviews, 2003. **28**(2): p. 139-148.
9. Comprehensive Prosthetics and Orthotics. *Prosthetics: Lower extremity*. [Website] 2017 [cited 2017; Levels of lower extremity amputations:]. Available from: http://www.cpousa.com/prosthetics/lower-extremity/.
10. Demet, K., et al., *Health related quality of life and related factors in 539 persons with amputation of upper and lower limb.* Disability and Rehabilitation, 2003. **25**(9): p. 480-486.
11. Ziegler-Graham, K., et al., *Estimating the Prevalence of Limb Loss in the United States: 2005 to 2050.* Archives of Physical Medicine and Rehabilitation, 2008. **89**(3): p. 422-429.
12. Flowers, W.C., *A man-interactive simulator system for above-knee prosthetics studies*, in *Department of Mechanical Engineering*1973, Massachusetts Institute of Technology: Cambridge, MA, USA.
13. Mann, R.W., *Cybernetic limb prosthesis: The ALZA distinguished lecture.* Annals of Biomedical Engineering, 1981. **9**(1): p. 1-43.
14. Gailey, R.S., Wenger, M. A., Raya, M., Kirk, N., Erbs, K., Spyropoulos, P. & Nash, M. S., *Energy expenditure of trans-tibial amputees during ambulation at self-selected pace* Prosthetics and Orthotics International, 1994. **18**(2): p. 84-91.
15. Agrawal, V., Gailey, R. S., Gaunaurd, I., O'Toole, C. & Finnieston, A. A., *Comparison between microprocessor-controlled ankle/foot and conventional prosthetic feet during stair negotiation in people with unilateral transtibial amputation* Journal of Rehabilitation Research and Development, 2013. **50**(7): p. 941-950.
16. Herr, H.M. and A.M. Grabowski, *Bionic ankle – foot prosthesis normalizes walking gait for persons with leg amputation* Proceedings of the Royal Society B-Biological Sciences, 2012. **279**(1728): p. 457-464.
17. Morgenroth, D.C., et al., *The effect of prosthetic foot push-off on mechanical loading associated with knee osteoarthritis in lower extremity amputees.* Gait & Posture, 2011. **34**(4): p. 502-507.
18. Grabowski, A.M. and S. D'Andrea, *Effects of a powered ankle-foot prosthesis on kinetic loading of the unaffected leg during level-ground walking.* Journal of NeuroEngineering and Rehabilitation, 2013. **10**.

19.	Dawley, J.A., K.B. Fite, and G.D. Fulk. *EMG Control of a Bionic Knee Prosthesis: Exploiting Muscle Co-Contractions for Improved Locomotor Function*. in *International Conference on Rehabilitation Robotics*. 2013. Seattle, Washington, USA.

20.	Seyedali, M., Czerniecki, J. M., Morgenroth, D. C. & Hahn, M. E., *Co-contraction patterns of trans-tibial amputee ankle and knee musculature during gait.* Journal of NeuroEngineering and Rehabilitation, 2012. **9**(29).

21.	Cavanagh, P.R. and P.V. Komi, *Electromechanical delay in human skeletal muscle under concentric and eccentric contractions.* European Journal of Applied Physiology and Occupational Physiology, 1979. **42**(3): p. 159-163.

22.	Begovic, H., Zhou, G., Li, T., Wang, Y. & Zheng, Y. (2014). *Detection of the electromechanical delay and its components during voluntary isometric contraction of the quadriceps femoris muscle.* Frontiers in Physiology, 2014. **5**: p. 494.

23.	Sutherland, D.H., *An Electromyographic Study of the Plantar Flexors of the Ankle in Normal Walking on the Level.* JBJS, 1966. **48**(1).

24.	Perry, J., *Clinical gait analyzer.* Bulletin of prosthetics research, 1974: p. 188-192.

25.	Sutherland, D.H., *The evolution of clinical gait analysis part l: kinesiological EMG.* Gait and Posture, 2001. **14**: p. 61-70.

26.	Novacheck, T.F., *The biomechanics of running.* Gait & Posture, 1998. **7**(1): p. 77-95.

27.	Kluwer, W., *Acland's Video Atlas of Human Anatomy*, in *Volume 2: The Lower Extremity; The Leg and Ankle* 2013.

28.	Oberg, T., A. Karszina, and K. Oberg, *Basic gait parameters: Reference data for normal subjects, 10-79 years of age.* Journal of Rehabilitation Research and Development, 1993. **30**(2): p. 210-223.

29.	Richards, J., *Biomechanics in clinic and research: An interactive teaching and learning course*. 2008: Churchill Livingstone Elsevier.

30.	Brockett, C.L. and G.J. Chapman, *Biomechanics of the ankle.* Orthopaedics and Trauma, 2016. **30**(3): p. 232-238.

31.	Oberg, T., Karsznia, A. and Oberg, K., *Basic gait parameters: Reference data for normal subjects, 10-79 years of age.* Journal of Rehabilitation Research and Development, 1993. **30**(2): p. 210-223.

32.	Whittle, M.W., *Clinical gait analysis: A review.* Human Movement Science, 1996. **15**(3): p. 369-387.

33.	Hill, A.V., *The heat of shortening and the dynamic constants of muscle.* Proceedings of the Royal Society of London. Series B - Biological Sciences, 1938. **126**(843): p. 136.

34.	Huxley, A.F., *Muscle structure and theories of contraction.* Prog. Biophys. Biophys. Chem, 1957. **7**: p. 255-318.

35.	Winters, J.M., *Hill-Based Muscle Models: A Systems Engineering Perspective*, in *Multiple Muscle Systems: Biomechanics and Movement Organization*, J.M. Winters and S.L.Y. Woo, Editors. 1990, Springer New York: New York, NY. p. 69-93.

36.	van den Bogert, A.J., K.G.M. Gerritsen, and G.K. Cole, *Human muscle modelling from a user's perspective.* Journal of Electromyography and Kinesiology, 1998. **8**(2): p. 119-124.

37.	Eilenberg, M.F., H. Geyer, and H. Herr, *Control of a powered ankle–foot prosthesis based on a neuromuscular model*, in *IEEE Transactions on neural systems and rehabilitation engineering*2010. p. 164-173.

38.	Au, S.K. and H.M. Herr, *Powered ankle-foot prosthesis—The importance of series and parallel motor elasticity.* IEEE Robotics and Automation Magazine, 2008. **15**(2): p. 52-59.

39.	Holgate, M.A., Hitt, J. K., Bellman, R. D., Sugar, T. G. & Hollander, K. W., *The SPARKy (Spring Ankle with Regenerative Kinetics) Project: Choosing a*

DC Motor Based Actuation Method. in *2nd Biennial IEEE/RAS-EMBS International Conference on Biomedical Robotics and Biomechatronics*. 2008. Scottsdale, AZ, USA.

40.   Cherelle, P., Grosu, V., Matthys, A., Vanderborght, B. & Lefeber, D., *Design and Validation of the Ankle Mimicking Prosthetic (AMP-) Foot 2.0.* IEEE Transactions on Neural Systems and Rehabilitation Engineering, 2014. **22**(1): p. 138-148.

41.   Winter, D.A., *The biomechanics and motor control of human gait: Normal, elderly and pathological*. Vol. 2. 1991, Waterloo, Canada: University of Waterloo Press.

42.   Wang, J., O.A. Kannape, and H.M. Herr. *Proportional EMG Control of Ankle Plantar Flexion in a Powered Transtibial Prosthesis*. in *IEEE International Conference on Rehabilitation Robotics*. 2013. Seattle, Washington USA.

43.   Horn, G.W., *Electro-Control: an EMG-Controlled A/K Prosthesis* Medical and Biological Engineering, 1972. **10**(1): p. 61–73.

44.   Darling, D.T., *Automatic damping profile optimization for computer controlled above-knee prostheses*, in *Department of Mechanical Engineering*1978, Massachusetts Institute of Technology: Cambridge, MA, USA.

45.   Grimes, D.L., *An active multi-mode above-knee prosthesis controller*, in *Department of Mechanical Engineering*1979, Massachusetts Institute of Technology: Cambridge, MA, USA.

46.   Dyck, W.R., Onyshko, S., Hobson, D. A., Winter, D. A. & Quanbury, A. O., *A voluntarily controlled electrohydraulic above-knee prosthesis.* Bulletin of prosthetics research, 1975: p. 169-186.

47.   Szmidt-Salkowska, E., K. Rowinska-Marcinska, and R.E. Lovelace, *EMG dynamics in polymyositis and dermatomyositis in adults.* Electroencephalography and Clinical Neurophysiology, 1985. **61**(3): p. S76.

48.   Misra, U.K., J. Kalita, and P.P. Nair, *Diagnostic approach to peripheral neuropathy.* Annals of Indian Academy of Neurology, 2008. **11**(2): p. 89-97.

49.   Ivanenko, Y.P., R.E. Poppele, and F. Lacquaniti, *Five basic muscle activation patterns account for muscle activity during human locomotion.* The Journal of Physiology, 2004. **556**(1): p. 267-282.

50.   Hof, A.L., Elzinga, H., Grimmius, W. & Halbertsma, J. P. K., *Speed dependence of averaged EMG profiles in walking.* Gait & Posture, 2002. **16**(1): p. 78-86.

51.   Childress, D.S., *Historical Aspects of Powered Limb Prostheses* Clinical Prosthetics and Orthotics, 1985. **9**(1): p. 02-13.

52.   Saxena, S.C. and P. Mukhopadhyay, *EMG operated electronic artificial-leg controller.* Medical and Biological Engineering and Computing, 1977. **15**(5): p. 553–557.

53.   Huang, S., J.P. Wensman, and D.P. Ferris, *An Experimental Powered Lower Limb Prosthesis Using Proportional Myoelectric Control.* Journal of Medical Devices, 2014. **8**(2).

54.   Hargrove, L.J., Simon, A.M., Young, A.J., Lipschutz, R.D., Finucane, S.B., Smith, D.G. and Kuiken, T.A., *Robotic Leg Control with EMG Decoding in an Amputee with Nerve Transfers* The New England Journal of Medicine, 2014. **369**(13): p. 1237-1242.

55.   Huang, H., T.A. Kuiken, and R.D. Lipschutz, *A strategy for identifying locomotion modes using surface electromyography.* IEEE Transactions on Biomedical Engineering, 2009. **56**(1): p. 65-73.

56.   Huang, H., Zhang, F., Hargrove, L. J., Dou, Z., Rogers, D. R. and Englehart, K. B., *Continuous locomotion-mode identification for prosthetic legs based on neuromuscular–mechanical fusion.* IEEE Transactions on Biomedical Engineering, 2011. **58**(10): p. 2867-2875.

57.   Au, S., M. Berniker, and H. Herr, *Powered ankle-foot prosthesis to assist level-ground and stair-descent gaits.* Journal of Neural Networks, 2008. **21**: p. 654-666.

58.   Au, S.K., P. Bonato, and H. Herr. *An EMG-position controlled system for an active ankle-foot prosthesis: An initial experimental study*. in *IEEE 9th International Conference on Rehabilitation Robotics*. 2005. Chicago, IL, USA.

59.   Miller, J., M.S. Beazer, and M.E. Hahn, *Myoelectric Walking Mode Classification for Transtibial Amputees.* IEEE Transactions on Biomedical Engineering, 2013. **60**(10): p. 2745-2750.

60.   Young, A.J., Kuiken, T.A., and Hargrove, L.J., *Analysis of using EMG and mechanical sensors to enhance intent recognition in powered lower limb prostheses* Journal of Neural Engineering, 2014. **11**(5).

61.   Ajiboye, A.B. and R.F. Weir, *A heuristic fuzzy logic approach to EMG pattern recognition for multifunctional prosthesis control* IEEE Transactions on Neural Systems and Rehabilitation Engineering, 2005. **13**(3): p. 280-291.

62.   Varol, H.A., F. Sup, and M. Goldfarb, *Multiclass Real-Time Intent Recognition of a Powered Lower Limb Prosthesis* IEEE Transactions on Biomedical Engineering, 2010. **57**(3): p. 542-551.

63.   Markowitz, J., et al., *Speed adaptation in a powered transtibial prosthesis controlled with a neuromuscular model.* Philosophical Transactions of The Royal Society B-Biological Sciences, 2011. **366**(1570): p. 1621-1631.

64.   Hargrove, L.J., K. Englehart, and B. Bernard Hudgins, *A Comparison of Surface and Intramuscular Myoelectric Signal Classification* IEEE Transactions on Biomedical Engineering, 2007. **54**(5): p. 847-853.

65.   Tello, R.M.G., Bastos-Filho, T., Costa, R. M., Frizera-Neto, A., Arjunan, S. & Kumar, D. (2013). *Towards sEMG Classification Based on Bayesian and k-NN to Control a Prosthetic Hand*. in *4th ISSNIP IEEE Conference on Biosignals and Biorobotics*. 2013. Rio de Janeiro, Brazil.

66.   Johnson, L.A. and A.J. Fuglevand, *Evaluation of probabilistic methods to predict muscle activity: implications for neuroprosthetics.* Journal of Neural Engineering, 2009. **6**(5).

67.   Pistohl, T., Cipriani, C., Jackson, A. & Nazarpour, K. (2013). *Abstract and Proportional Myoelectric Control for Multi-Fingered Hand Prostheses* Annals of Biomedical Engineering, 2013. **41**(12): p. 2687-2698.

68.   Tang, Y., Wodlinger, B. and Durand, D.M., *Bayesian spatial filters for source signal extraction: a study in the peripheral nerve* IEEE Transactions on Neural Systems and Rehabilitation Engineering, 2014. **22**(2): p. 302-311.

69.   Parker, P.A. and R.N. Scott, *Myoelectric control of prostheses.* Critical Reviews in Biomedical Engineering, 1986. **13**(4): p. 283-310.

70.   Zecca, M., Micera, S., Carrozza, M. C. & Dario, P. (2002) *Control of multifunctional prosthetic hands by processing the electromyographic signal.* Critical Reviews in Biomedical Engineering, 2002. **30**(4-6): p. 459–485.

71.   Rechy-Ramirez, E.J. and H. Huosheng, *Stages for Developing Control Systems using EMG and EEG signals: A survey*, 2011, School of Computer Science and Electronic Engineering, University of Essex. p. 1-33.

72.   Go, S.A., K. Coleman-Wood, and K.R. Kaufman, *Frequency analysis of lower extremity electromyography signals for the quantitative diagnosis of dystonia.* Journal of Electromyography and Kinesiology, 2014. **24**(1): p. 31-36.

73.   Hargrove, L.J., Simon, A.M., Lipschutz, R., Finucane, S.B. and Kuiken, T.A., *Non-weight-bearing neural control of a powered transfemoral prosthesis* Journal of NeuroEngineering and Rehabilitation, 2013. **10**(62): p. 1-11.

74.   Chen, B., et al., *Locomotion mode classification using a wearable capacitive sensing system* IEEE Transactions on Neural Systems and Rehabilitation Engineering, 2013. **21**(5): p. 744-755

75.   Taylor, D.R. and F.R. Finley. *Myoelectric signal processing for control of prosthetic devices*. in *Proceedings of the 1974 Annual ACM Conference*. 1974.

76.   Zhang, F. and H. Huang, *Source selection for real-time locomotion mode recognition* IEEE Journal of Biomedical and Health Informatics, 2013. **17**(5): p. 907–914.

77.   Endo, K., E. Swart, and H. Herr. *An Artificial Gastrocnemius for a Transtibial Prosthesis*. in *31st Annual International Conference of the IEEE EMBS* 2009. Minneapolis, Minnesota, USA.

78.   Sup, F., Varol, H.A. and Goldfarb, M., *Upslope Walking With a Powered Knee and Ankle Prosthesis: Initial Results with an Amputee Subject.* IEEE Transactions on Neural Systems and Rehabilitation Engineering, 2011. **19**(1): p. 71-78.

79.   Fite, K., J. Mitchell, and F. Sup. *Design and Control of an Electrically Powered Knee Prosthesis*. in *10th IEEE International Conference on Rehabilitation Robotics*. 2007. Noordwijk, Netherlands.

80.   Lawson, B.E., Varol, H.A., Huff, A., Erdemir, E. and Goldfarb, M., *Control of stair ascent and descent with a powered transfemoral prosthesis* IEEE Transactions on Neural Systems and Rehabilitation Engineering, 2013. **21**(3): p. 466-473.

81.   Landreneau, L.L., et al., *Lower limb muscle activity during forefoot and rearfoot strike running techniques.* International Journal of Sports Physical Therapy, 2014. **9**(7): p. 888-897.

82.   Landreneau, L.L., et al., *Corrigendum.* International Journal of Sports Physical Therapy, 2016. **11**(4): p. 497-497.

83.   Silver-Thorn, B., T. Thomas Current, and B. Kuhse, *Preliminary investigation of residual limb plantarflexion and dorsiflexion muscle activity during treadmill walking for trans-tibial amputees.* Prosthetics and Orthotics International, 2012. **36**(4): p. 435–442.

84.   Geethanjali, P., *Myoelectric control of prosthetic hands: state-of-the-art review.* Medical Devices (Auckland, N.Z.), 2016. **9**: p. 247-255.

85.   Huang, S. and D.P. Ferris, *Muscle activation patterns during walking from transtibial amputees recorded within the residual limb-prosthetic interface.* Journal of NeuroEngineering and Rehabilitation, 2012. **9**(55).

86.   Lawson, B.E., et al. *Stumble detection and classification for an intelligent transfemoral prosthesis* in *32nd Annual International Conference of the IEEE Engineering Medicine and Biology Society (EMBS)*. 2010. Buenos Aires, Argentina.

87.   Zhang, F., et al., *Towards Design of a Stumble Detection System for Artificial Legs* IEEE Transactions on Neural Systems and Rehabilitation Engineering, 2011. **19**(5): p. 567-577.

88.   Hoover, C.D., G.D. Fulk, and K.B. Fite, *Stair Ascent With a Powered Transfemoral Prosthesis Under Direct Myoelectric Control* IEEE/ASME Transactions on Mechatronics, 2013. **18**(3): p. 1191 – 1200.

89.   Whittle, M.W., *Three-dimensional motion of the center of gravity of the body during walking.* Human Movement Science, 1997. **16**: p. 347-355.

90.   McIntosh, A.S., et al., *Gait dynamics on an inclined walkway.* Journal of Biomechanics, 2006. **39**(13): p. 2491-2502.

91.   Lieberman, D.E., et al., *Foot strike patterns and collision forces in habitually barefoot versus shod runners.* Nature, 2010. **463**(7280): p. 531-535.

92.   Yan, A.F., et al., *Impact attenuation during weight bearing activities in barefoot vs. shod conditions: A systematic review.* Gait and Posture, 2013. **38**(2): p. 175-186.

93.   Vicon. *Vicon Documentation: Calibrate a Vicon system*. 2018 [cited 2018 05 April]; Available from: https://docs.vicon.com/display/Nexus25/Calibrate+a+Vicon+system.

94. Hermens, H.J., Freriks, B., Disselhorst-Klug, C. & Rau, G., *Development of recommendations for SEMG sensors and sensor placement procedures.* Journal of Electromyography and Kinesiology, 2000. **10**(5): p. 361-374.

95. Rainoldi, A., G. Melchiorri, and I. Caruso, *A method for positioning electrodes during surface EMG recordings in lower limb muscles.* Journal of Neuroscience Methods, 2004. **134**(1): p. 37-43.

96. Winter, D.A. and H.J. Yack, *EMG profiles during normal human walking: Stride-to-stride and inter-subject variability.* Electroencephalography and Clinical Neurophysiology, 1987. **67**(5): p. 402-411.

97. Delsys. *EMGworks® software* 2018 [cited 2018 05 April]; Information regading the Delsys EMGworks® software]. Available from: https://www.delsys.com/products/software/emgworks/.

98. Hsu, W.L., V. Krishnamoorthy, and J.P. Scholz, *An alternative test of electromyographic normalization in patients.* Muscle & Nerve, 2006. **33**(2): p. 232-241.

99. Yang, J.F. and D.A. Winter, *Electromyographic amplitude normalization methods: Improving their sensitivity as diagnostic tools in gait analysis.* Archives of Physical Medicine and Rehabilitation, 1984. **65**(9): p. 517-521.

100. Cappozzo, A., et al., *Position and orientation in space of bones during movement: anatomical frame definition and determination.* Clinical Biomechanics, 1995. **10**(4): p. 171-178.

101. Ren, L., R.K. Jones, and D. Howard, *Whole body inverse dynamics over a complete gait cycle based only on measured kinematics.* Journal of Biomechanics, 2008. **41**(12): p. 2750-2759.

102. De Lisa, J.A., *Gait Analysis in the Science of Rehabilitation*, D.o.V. Affairs, Editor 1998: Baltimore Rehabilitation: US. p. 112.

103. Halaki, M. and K. Ginn, *Normalization of EMG Signals: To Normalize or Not to Normalize and What to Normalize to?*, in *Computational Intelligence in Electromyography Analysis: A Perspective on Current Applications and Future Challenges*, G.R. Naik, Editor. 2012, InTech. p. 175-194.

104. De Luca, C.J., *The Use of Surface Electromyography in Biomechanics.* Journal of Applied Biomechanics, 1997. **13**(2): p. 135-163.

105. John, C.T., et al., *Contributions of muscles to mediolateral ground reaction force over a range of walking speeds.* Journal of Biomechanics, 2012. **45**(14): p. 2438-2443.

106. van Hedel, H.J.A., L. Tomatis, and R. Müller, *Modulation of leg muscle activity and gait kinematics by walking speed and bodyweight unloading.* Gait and Posture, 2006 **24**: p. 35–45.

107. den Otter, A.R., et al., *Speed related changes in muscle activity from normal to very slow walking speeds.* Gait & Posture, 2004. **19**(3): p. 270-278.

108. Gordon, K.E., C.R. Kinnaird, and D.P. Ferris, *Locomotor adaptation to a soleus EMG-controlled antagonistic exoskeleton.* Journal of Neurophysiology 2013. **109**: p. 1804–1814.

109. Kuo, A.D. and J.M. Donelan, *Dynamic principles of gait and their clinical implications.* Physical Therapy, 2010. **90**(2): p. 157-174.

110. Hunter, L.C., E.C. Hendrix, and J.C. Dean, *The cost of walking downhill: Is the preferred gait energetically optimal?* Journal of Biomechanics, 2010. **43**(10): p. 1910-1915.

111. Klette, R. and G. Tee, *Understanding human motion: A historic review*. Human Motion: Understanding, Modelling, Capture, and Animation, ed. B. Rosenhahn, Klette, R. and Metaxas, D. Vol. 36. 2008. 1-22.

112. Genin, J.J., et al., *Effect of speed on the energy cost of walking in unilateral traumatic lower limb amputees* European Journal of Applied Physiology, 2008. **103**(6): p. 655-663.

113. Burgess, E.M., Poggi, D.L., Hittenberger, D.A., Zettl, J.H., Moeller, D.E., Carpenter, K.L. and Forsgren, S.M. , *Development and preliminary*

evaluation of the VA Seattle foot. Journal of Rehabilitation Research and Development, 1985. **22**(3): p. 75-84.

114. Hitt, J., Sugar, T., Holgate, M., Bellman, R. & Hollander, K. (2009). *Robotic transtibial prosthesis with biomechanical energy regeneration.* Industrial Robot: An International Journal 2009. **36**(5): p. 441-447.

115. Wang, Q.N., Yuan, K. B., Zhu, J. Y. & Wang, L., *Finite-state control of a robotic transtibial prosthesis with motor-driven nonlinear damping behaviors for level ground walking*, in *IEEE 13th International Workshop on Advanced Motion Control*2014, IEEE: Keio University, Hiyoshi Campus, Yokohama, Japan. p. 155-160.

116. Zhu, J., Q. Wang, and L. Wang, *On the design of a powered transtibial prosthesis with stiffness adaptable ankle and toe joints*, in *IEEE Transactions on industrial electronics*2014. p. 4797-4807.

117. Rice, J.J. and J.M. Schimmels, *Evaluation of a Two Degree of Freedom Passive Ankle Prosthesis With Powered Push-Off.* Journal of Medical Devices, 2015. **9**(3): p. 030915-030915-2.

118. Bellman, R.D., M.A. Holgate, and T.G. Sugar. *SPARKy 3: Design of an active robotic ankle prosthesis with two actuated degrees of freedom using regenerative kinetics*. in *2008 2nd IEEE RAS & EMBS International Conference on Biomedical Robotics and Biomechatronics*. 2008.

119. Ficanha, E., M. Rastgaar Aagaah, and K.R. Kaufman, *Cable-Driven Two Degrees-of-Freedom Ankle–Foot Prosthesis.* Journal of Medical Devices, 2016. **10**(3): p. 030902-030902-2.

120. Ficanha, E. and M. Rastgaar, *Preliminary design and evaluation of a multi-axis ankle-foot prosthesis*, in *5th IEEE RAS & EMBS International Conference on Biomedical Robotics and Biomechatronics*2014, IEEE: Sao Paulo, Brazil. p. 1033-1038.

121. Winter, D.A., *Biomechanical Motor Patterns in Normal Walking.* Journal of Motor Behavior, 1983. **15**(4): p. 302-330.

122. Össur. *Pro-Flex foot*. 2017 [cited 2017 23 October]; Available from: https://www.ossur.com/proflex.

123. Innovation, F. *Pacifica foot*. 2015 [cited 2017 23 October]; Available from: http://www.freedom-innovations.com/pacifica/.

124. Fillauer. *Ibex foot system*. 2017 [cited 2017 23 October]; Available from: http://fillauer.com/Prosthetics/Ibex.html.

125. Paradisi, F., et al., *The Conventional Non-Articulated SACH or a Multiaxial Prosthetic Foot for Hypomobile Transtibial Amputees? A Clinical Comparison on Mobility, Balance, and Quality of Life.* The Scientific World Journal, 2015. **2015**: p. 10.

126. Wagner, J., et al., *Motion Analysis of SACH vs. Flex-Foot in Moderately Active Below-Knee Amputees.* Clinical Prosthetics and Orthotics, 1987. **11**(1): p. 55-62.

127. Stratasys. *ABSplus-P430: Production-grade thermoplastic for design series 3D printers*. 2015 [cited 2018 19 April]; Available from: http://usglobalimages.stratasys.com/Main/Files/Material_Spec_Sheets/MSS_FDM_ABSplusP430.pdf.

128. Balsdon, M.E.R., et al., *Medial Longitudinal Arch Angle Presents Significant Differences Between Foot Types: A Biplane Fluoroscopy Study.* Journal of Biomechanical Engineering, 2016. **138**(10): p. 101007-101007-6.

129. Browning, R.C., et al., *Effects of obesity and sex on the energetic cost and preferred speed of walking.* Journal of Applied Physiology, 2006. **100**(2): p. 390-398.

130. Washington State: Department of Social and Health Services. *Range of Joint Motion Evaluation Chart*. 2014 28 September 2016; March 2014 [1-2]. Available from: https://www.dshs.wa.gov/sites/default/files/FSA/forms/pdf/13-585a.pdf.

131. American Academy of Orthopaedic Surgeons. *Average ranges of motion*. 2011 [cited 2016 28 September 2016]; Available from: https://www.fgc.edu/wp-content/uploads/2011/12/averages-of-rom.pdf.

132. Gailey, R.S., et al., *Energy expenditure of trans-tibial amputees during ambulation at self-selected pace.* Prosthetics and Orthotics International, 1994. **18**(2): p. 84-91.

133. Mattes, S.J., P.E. Martin, and T.D. Royer, *Walking symmetry and energy cost in persons with unilateral transtibial amputations: Matching prosthetic and intact limb inertial properties.* Archives of Physical Medicine and Rehabilitation, 2000. **81**(5): p. 561-568.

134. Mattes, S.J. *Is lighter better? Thoughts on the relationship between device weight and function*. The O&P Edge, 2014.

135. Dempster, W.T., *Space requirements of the seated operator*, 1955, Armed services technical information agency: Document service center, Knott building, Dayton, 2, Ohio.

136. Saunders, M.M., Schwentker, E. P., Kay, D. B., Bennett, G., Jacobs, C. R., Verstraete, M. C. & Njus, G. O. (2003). *Finite Element Analysis as a Tool for Parametric Prosthetic Foot Design and Evaluation. Technique Development in the Solid Ankle Cushioned Heel (SACH) Foot.* Computer Methods in Biomechanics and Biomedical Engineering, 2003. **6**(1): p. 75-87.

137. South, B.J., Fey, N. P., Bosker, G. & Neptune, R. R. (2009). *Manufacture of Energy Storage and Return Prosthetic Feet Using Selective Laser Sintering.* Journal of Biomechanical Engineering, 2009. **132**(1): p. 015001-015001-6.

138. Ottobock. *Meridium*. [cited 2018 02 April]; Available from: https://professionals.ottobockus.com/Prosthetics/Lower-Limb-Prosthetics/Feet--Microprocessor/Meridium/p/1B1.

139. Composites, A. *Mechanical Properties of Carbon Fibre Composite Materials, Fibre/Epoxy resin (120°C Cure)*. 2014 [cited 2018 05 May]; Available from: http://www.acpsales.com/upload/Mechanical-Properties-of-Carbon-Fiber-Composite-Materials.pdf.

140. Ottobock. *Empower foot*. [cited 2018 02 April]; Available from: https://professionals.ottobockus.com/Prosthetics/Lower-Limb-Prosthetics/Feet--Microprocessor/1A1-1-Empower/p/1A1-1.

141. Yuan, K., et al. *Motion control of a robotic transtibial prosthesis during transitions between level ground and stairs*. in *2014 European Control Conference (ECC)*. 2014.

142. Young, A.J., A.M. Simon, and L.J. Hargrove, *A Training Method for Locomotion Mode Prediction Using Powered Lower Limb Prostheses.* IEEE Transactions on Neural Systems and Rehabilitation Engineering, 2014. **22**(3): p. 671-677.

143. Young, A.J., et al. *Classifying the intent of novel users during human locomotion using powered lower limb prostheses*. in *2013 6th International IEEE/EMBS Conference on Neural Engineering (NER)*. 2013.

144. Ha, K.H., H.A. Varol, and M. Goldfarb, *Volitional Control of a Prosthetic Knee Using Surface Electromyography* IEEE Transactions on Biomedical Engineering, 2011. **58**(1): p. 144-151.

145. Breiman, L., et al., *Classification and Regression Trees*. 1984, Monterey, CA: Wadsworth & Brooks/Cole Advanced Books & Software.

146. Breiman, L., *Random Forests.* Machine Learning, 2001. **45**(1): p. 5-32.

147. Kavzoglu, T. and I. Colkesen. *The effects of training set size for performance of support vector machines and decision trees*. in *10th International Symposium on Spatial Accuracy Assessment in Natural Resources and Environmental Sciences*. 2012. Florianopolis-SC, Brazil.

148. Zhu, X., et al., *Do We Need More Training Data?* International Journal of Computer Vision, 2016. **119**(1): p. 76-92.

149. Mathworks. *Matlab*. 2017 [cited 2018; Available from: https://uk.mathworks.com/.
150. Microchip. *PIC16F917 data sheet* 2007 [cited 2018 27 January]; Available from: http://ww1.microchip.com/downloads/en/DeviceDoc/41250F.pdf.
151. Cytron. *Cytron Dual Channel 10A DC Motor Driver*. 2017 [cited 2018 08 January]; Available from: https://www.cytron.io/p-mdd10a.
152. Digi. *Digi XBee 802.15.4*. 2017 [cited 2017 24 October]; Available from: https://www.digi.com/products/xbee-rf-solutions/2-4-ghz-modules/xbee-802-15-4.
153. Rábago, C.A., J.A. Whitehead, and J.M. Wilken, *Evaluation of a Powered Ankle-Foot Prosthesis during Slope Ascent Gait.* PLOS ONE, 2016. **11**(12): p. e0166815.
154. Harrast, M.A. and J.T. Finnoff, *Sports Medicine: Study Guide and Review for Boards*. 2012: Demos Medical Publishing.
155. Bytomski, J. and C. Moorman, *Oxford American Handbook of Sports Medicine*. 2010, Oxford University Press.
156. FootSmart. *Supination*. Health resource center 2018 [cited 2018 January]; Available from: https://www.footsmart.com/health-resource-center/foot/supination.
157. Moriguchi, C.S., T.O. Sato, and H.J.C. Gil Coury, *Ankle movements during normal gait evaluated by flexible electrogoniometer.* Brazilian Journal of Physical Therapy, 2007. **11**: p. 205-211.

Appendix A: Summary of state-of-the-art commercially available transtibial prostheses

Some state-of-the-art commercially available transtibial prostheses are detailed in this appendix. Reminiscent of the devices available, the prostheses detailed in this summary only have one active degree of freedom. Powered motion is facilitated along the sagittal plane, allowing for dorsiflexion and plantarflexion control. The basic specifications for each device are presented in table A.1. Additional details are presented in table A.2.

Table A.1: Basic prostheses specifications

Dorsiflexion angle	Plantarflexion angle	Device weight	Max. User weight	Dimensions
Meridium (Ottobock) [1, 2]				
14.5°	22°	1,25 – 1,55kg	100kg	166 –178 mm
EchelonVT (Blatchford) [3, 4]				
15° (with e-carbon springs)	9° PF (with e-carbon springs)	0,855kg	125kg	168 – 178 mm
emPOWER foot (Ottobock previously BioM) [5-8]				
±12°	±18° (or ±9°)	1,93kg	130kg	168 – 178 mm

Table A.2: Additional prostheses details

Control	Actuation	Sensors	Additional comments
Meridium (Ottobock) [1, 2]			
Microcontroller System adjusts foot position and behaviour based on the ground conditions and the user's walking speed.	Powered – hydraulic Passive – carbon fibre springs at the ankle and another at the frame and heel.	Inertial measurement (gyroscopes and accelerometers). Angle Moment, measuring ground contact forces.	Relief function – the foot is lowered to the floor when a load is applied at the heel for a prolonged period of time. The foot automatically adjusts itself for heel heights of up to 5 cm and has a movable toe plate.

EchelonVT (Blatchford) [3, 4]			
None – structural. Shock absorption and the addition of energy at push-off is facilitated by the hydraulic unit and springs.	Powered – hydraulic. Passive – 1-4 axial springs based on user weight, two e-carbon springs at heel and toe and internal titanium spring.	None.	The foot is dorsiflexed during swing phase. Split toe design to facilitate passive limited frontal plane flexion.
BioM emPOWER ankle (Ottobock) [5-8]			
Microcontroller	Powered – brushless DC motor with ball screw actuation Passive – carbon-composite leaf spring in series with the actuation system and a unidirectional leaf spring.	Encoders for motor shaft and measuring ankle joint. A 6DoF inertial measurement (3 gyroscopes and 3 accelerometers).	The torque generated by the foot's actuation system increases in response to a user increasing their walking speed. This is measured from the ankle joint torque. The torque increase is carried out during mid- to late stance phase.

References

1. Ottobock. *Meridium*. [cited 2018 07 April]; Available from: https://professionals.ottobockus.com/Prosthetics/Lower-Limb-Prosthetics/Feet--Microprocessor/Meridium/p/1B1
2. Ottobock. *Meridium brochure*. [cited 2018 07 April]; Available from:https://www.ottobock.co.uk/media/local-media/brochures/prosthetics/meridium/meridium-cpo-brochure.pdf
3. Blatchford. *EchelonVT*. [cited 2018 07 April]; Available from: http://www.blatchford.co.uk/endolite/echelonvt/
4. Endolite. *EchelonVT*. (2012) [cited 2018 07 April]; Available from: http://www.endolite.com/catalogue/feet/echelonvt/flyer/en_US/echelonVTUS%20WEB.pdf
5. Ottobock. *Empower foot.* [cited 2018 07 April]; Available from: https://professionals.ottobockus.com/Prosthetics/Lower-Limb-Prosthetics/Feet--Microprocessor/1A1-1-Empower/p/1A1-1
6. Herr H. & Grabowski A., *Bionic ankle-foot prosthesis normalizes walking gait for persons with leg amputation.* Proc Biol Sci. 2012. **279**(1728): pp. 457–464.

7. Gates D., Aldridge J., Wilken J., *Kinematic comparison of walking on uneven ground using powered and unpowered prostheses*. Clinical Biomechanics 2013. **28**: pp. 467–472.
8. Esposito E., Whitehead A.J.M. & Wilken J.M., *Step-to-step transition work during level and inclined walking using passive and powered ankle-foot prostheses*, Prosthetics and Orthotics International 2015. **40**(3): pp. 311-319

Appendix B: UREC Ethical Approval Letter

![The University of Manchester logo]

Secretary to Research Ethics Committee 1
Email: katy.boyle@manchester.ac.uk
Phone: +44(0)161 275 1360

Ref: ethics/16086

Miss Unéné Gregory, Dr Ren Lei
MACE
School of Mechanical, Aerospace and Civil Engineering
University of Manchester
M13 9PL

unene.gregory@postgrad.manchester.ac.uk / lei.ren@manchester.ac.uk

15 April 2016

Dear Miss Gregory, Dr Lei,

Study title: Designing a control strategy for a powered ankle-foot prosthesis using EMG signals **(ref 16086)**

Research Ethics Committee 1

Thank you for attending the University Research Ethics Committee meeting held on 24th March 2016 to discuss the above study. I am pleased to confirm a favourable ethical opinion for the above research on the basis described in the application form and supporting documentation, as submitted to and approved by the Committee.

This approval is effective for a period of five years. If the project continues beyond that period an application for amendment must be submitted for review. Likewise, any proposed changes to the way the research is conducted must be approved via the amendment process (see below). Failure to do so could invalidate the insurance and constitute research misconduct.

You are reminded that, in accordance with University policy, any data carrying personal identifiers must be encrypted when not held on a secure university computer or kept securely as a hard copy in a location which is accessible only to those involved with the research.

Reporting Requirements:

You are required to report to us the following:

1   Amendments
2   Breaches and adverse events
3   Notification of Progress/End of the Study

Feedback

It is our aim to provide a timely and efficient service that ensures transparent, professional and proportionate ethical review of research with consistent outcomes, which is supported by clear, accessible guidance and training for applicants and committees. In order to assist us with our aim, we would be grateful if you would give your view of the service that you have received from us by completing a feedback sheet https://survey.manchester.ac.uk/pssweb/index.php/197138/lang-en.

We hope the research goes well.

Yours sincerely,

Katy Boyle
Secretary to University Research Ethics Committee 1

Appendix C: Delsys Trigno Wireless System Specifications

The specifications of the Delsys Trigno Wireless system are presented below. This was the EMG system and surface electrodes used throughout this research. The complete Trigno wireless system users guide from which these specifications were extracted is available from [164]; specifically on pages 35-38.

- o Trigno Wireless EMG System (Natick, MA, USA)
- o 1cm interelectrode distance
- o 20-450 Hz bandpass filter
- o Butterworth filter design
- o 1926 Hz sampling rate
- o Gain of 300
- o Signals displayed as 11mV r.t.i. (referred to input) – (when collected digitally)
- o 168 nV/bit EMG resolution

References

1. Delsys. *Trigno Wireless System User's Guide*. [cited 2018 26 March]; Available from: http://delsys.com/Attachments_pdf/manual/MAN-012-2-7.pdf

Appendix D: Prototype Part Details and Drawings

Table D1 presents details of the prosthesis prototype parts that were commercially sourced. The CAD drawings of the other parts that were designed and fabricated are also presented in this appendix. The in-house fabricated parts include the bottom and top foot sections, the motor mount and the shaft coupler.

Table D.1: Details of commercial parts

Part	Manufacturer	Material	Key Dimension(s)	Qty	Ref.
Brushed DC motors	RS components	N/A	212g weight	2	[1]
Universal joint – 'ankle'	ABSSAC	Stainless steel (AISI 304)	350g weight 86mm length	1	[2]
Universal joint – small, lead screws			80g weight 52mm length	2	
Lead screws	Automotion components	Stainless steel	10mm diameter 60mm length	2	[3]
Custom nut		Acetal resin	70mm length (catchment)	2	
Extension spring	Airedale springs	BS 5216 drawn	69.91mm free length estimated	2	[4]

References

1. RS Components. [cited 2018 05 May]; Available at: https://uk.rs-online.com/web/p/dc-geared-motors/8347679/
2. ABSSAC. [cited 2018 05 May]; Available at: https://www.abssac.co.uk/p/Universal+Joints/37/#.Wu4Y5Yjt7IU
3. Automotion Components. [cited 2018 05 May]; Available at: https://www.automotioncomponents.co.uk/en/catalog/linear/lead-screws-and-nuts/precision-lead-screws/l1348
4. Airedale Springs Ltd. [cited 2018 05 May]; Available at: https://www.airedalesprings.co.uk/springs/extension-springs/

Foot sections
Bottom and top

A4

Ø30
Ø5
12,40
12,40
63
20
40
120
30
80
15
16 16 16 15
Ø5
6
6
Ø5
15

Ø22
Ø3
8,50
14
200
10
10
R70
R70
Ø5

18
33,76
TRUE R9,70

MATERIAL: AISI 430

DATE
15 April 2018
20 April 2018

Views and dimensions:

90
100
6

R12.50
R21
Ø5
3
Ø4
Ø4
7
16
7.50
80

16
2.07
40
18
10
Ø5
Ø19
40

PART | DATE
DRWN | Unirek Gregory | 11 April 2016
APP'D | Dr Tai Ran | 20 April 2016

MATERIAL: ABS P430

REVISION 01
TITLE: Motor mount

SCALE:1:1 SHT 1 OF 1

F

E

R1.50

Ø22

R.90

11

30

Appendix E: Mathematical Definitions of EMG Features

Frequency domain

Auto-Regressive coefficients (AR) represent each EMG signal segment as a linear combination of previous segments, along with a white noise error term e_k; a_i is AR coefficient and N is the order of the AR model which determines the number of coefficients calculated [2].

$$x_k = -\sum_{i=1}^{N} a_i x_{k-i} + e_k$$

Time domain

Mean Absolute Value (MAV) is an estimation of the mean absolute value of the EMG signal MAV_k; it is calculated as presented below, by adding all the absolute values for a given signal segment k and dividing by the length of the segment N [3].

$$MAV_k = \frac{1}{N} \sum_{i=1}^{N} |x_i|$$

Root Mean Square (RMS) is the square root of mean squares of an EMG signal segment and gives an indication of the strength of the EMG signal segment [1, 2].

$$RMS_k = \sqrt{\frac{1}{N} \sum_{i=1}^{N} x_i{}^2}$$

Integrated EMG (IEMG) is a summation of the absolute values of the EMG signals, calculated as given below [4]:

$$IEMG_k = \sum_{i=1}^{N} |x_i|$$

Variance (VAR) is a calculation of the variance present in the EMG signal, given by the equation below, where $\bar{x}$ is the mean value of the signal segment k [5]:

$$VAR_k = \frac{1}{N} \sum_{i=1}^{N} (x_i - \bar{x})^2$$

Waveform Length (WL) is the cumulative length of the EMG signal (the waveform) which gives a measure of the signal's amplitude, duration and frequency presented as a single parameter [3].

$$WL_k = \sum_{i=1}^{N-1} |x_{i+1} - x_i|$$

References

1. Rechy-Ramirez, E.J. & Hu, H. *CES-513 Stages for Developing Control Systems using EMG and EEG Signals: A survey*. UNSPECIFIED. CES-513, 2011. University of Essex, Colchester. Available from: (http://repository.essex.ac.uk/14259/1/CES-513.pdf)

2. Phinyomark, A., Limsakul, C. & Phukpattaranont, P., *A novel feature extraction for robust EMG pattern recognition*. Journal of Computing, 2009 **1**(1): pp. 71–80.

3. Englehart, K. & Hudgins, B., *A robust, real-time control scheme for multifunction myoelectric control*. IEEE Transactions on Biomedical Engineering, 2003. **50**(7): pp. 848–854.

4. [39] Huang, H.P. & Chen, C.Y., *Development of a myoelectric discrimination system for a multi-degree prosthetic hand*, in 1999 IEEE International Conference on Robotics and Automation, 1999. **3**: pp. 2392–2397.

5. Oskoei, M.A. & Hu, H., *GA-based feature subset selection for myoelectric classification*, in IEEE International Conference on Robotics and Biomimetics, 2006. pp. 1465–1470.

Appendix F: Raw vs MVC EMG Data Classification Accuracy

Different LDA (linear discriminant analysis) variants were used in testing and comparing the classification accuracy of the two kinds of input EMG data. These were the 'linear', 'diaglinear' (Naïve Bayes) and 'mahalanobis', all available in Matlab's built-in 'classify' function. No prior probabilities were specified for either the training or testing data sets.

Five types of movement initially made up the complete data set. These were dorsiflexion, foot flat, plantarflexion, inversion and swing. The classification accuracies for each variant type and each data set case are presented in table C1.

Table F.1: Classification accuracies of LDA variants using five movements

Feature Combinations	Classification Accuracy (%)					
	Raw EMG Data (Case A)			MVC Normalised Raw EMG Data (Case B)		
	linear	diag linear	mahalanobis	linear	diag linear	mahalanobis
AR	34	32	36	34	32	36
RMS	36	37	37	36	30	39
MAV	33	33	39	28	29	34
AR & RMS	57	40	64	50	33	59
AR & MAV	49	43	67	48	41	54
RMS & MAV	44	36	61	44	31	50
AR, RMS & MAV	50	42	78	49	43	78

It was later found that omitting the swing phase data resulted in higher classification accuracy. The classification accuracies for the new data set consisting of four movement types, with the swing phase excluded, are presented in table C2. The data set used to train and test the LDA variants was the same.

Table F.2: Classification accuracies of LDA variants using four movements, excluding swing phase

Feature Combinations	Classification Accuracy (%)					
	Raw EMG Data (Case A)			MVC Normalised Raw EMG Data (Case B)		
	linear	diag linear	mahalanobis	linear	diag linear	mahalanobis
AR	43	31	46	43	31	46
RMS	38	39	47	35	28	43
MAV	43	40	42	32	36	40
AR & RMS	57	43	71	56	40	63
AR & MAV	61	46	74	58	42	57
RMS & MAV	43	40	68	46	32	53
AR, RMS & MAV	58	44	82	58	47	79

Appendix G: Classification Algorithm Details and Settings

Linear Discriminant Analysis (LDA)

The general steps involved in conducting a linear discriminant analysis are as follows:

1. Computing the mean vectors for each data set and also of the entire data set.

$$\mu_{all} = \frac{1}{n}\sum_{c=1}^{n} p_i \times \mu_c$$

where $c = 1, 2, 3, 4, 5$ are the five classes to which data is to be classified; thus n = 5.

p is the probability of data belonging to a specific class; it was set to 0.2. This meant that data was equally probable to belong to each of the five classes.

2. Computing the scatter matrices, both in-between-class and within-class. These were used to create the data separability criteria, with respect to the different classes. This was done by computing the class-covariance matrices.

Within class scatter

$$S_w = (n-1)\sum_{c=1}^{n} S_c$$

and

$$S_c = \frac{1}{N-1}\sum_{c=1}^{N}(x - \mu_c)(x - \mu_c)^T$$

where;
N are the number of samples for each data set $c = 1, 2, 3, 4, 5$ are the five classes to which data is to be classified; thus n=5
S_c is the scatter matrix for each target class

Between class scatter

$$S_B = \sum_{c=1}^{n} N(\mu_c - \mu_{all})(\mu_c - \mu_{all})^T$$

where:
N are the number of samples for each data set.
μ_{all} and μ_c are the group and individual class means, respectively.

3. Computing the eigenvectors (e) and corresponding eigenvalues (λ) for the scatter matrices.

$$[e \quad \lambda] = S_W{}^{-1}S_B$$

4. Sorting the eigen-pairs, the eigenvectors and corresponding eigenvalues, from highest to lowest order. The eigenvectors with the lowest eigenvalues have the least information pertaining to the distribution of the dataset. The top five eigenvectors were kept, corresponding to the five movement classes.

5. Choosing k eigenvectors with the largest eigenvalues, therefore reducing the dimensionality. Such that W was a matrix with the top (5x4) eigen-pairs.

$$W = e(5 \times 4)$$

6. Using the eigen-pairs matrix W to transform the dataset (samples) onto a new subspace.

$T = X \times W$ where X is the dataset (samples) and T is the matrix with the samples transformed to a new sub-space

7. Classifying new data. This is done by transforming the new data to the new subspace and using the Euclidean distance of the new data vectors. The smallest of the n Euclidean distances, $n = 5$ corresponding to the five movement classes, classifies the new data as class n.

$E_d = \sqrt{\sum_{i=1}^{n} |x_i - y_i|^2}$ where x_i and y_i are the spatial coordinates of the new data transformed to the new subspace

i is the number of dimensions.

LDA assumes the data to be normal distributed for the features to be statistically independent and the covariance matrices for each class to be identical. This is particularly for classification using LDA. However, LDA has been found to perform well even when this is not the case [1]. The settings of the Matlab LDA function used in this research are presented in table G.1.

Table G.1: Matlab LDA settings

Property Name	Setting
Type – 'DiscrimType'	Linear
Prior probabilities – 'Prior'	Uniform
All other settings	Default

Decision tree

The Matlab classregtree function used in this research uses the CART algorithm [2]. The algorithm recursively partitions the training data set until it obtains subsets that best represent the target classes to which the data belongs. Each node of the decision tree tests the incoming data and splits it, either left or right, according to a criterion. This can be visualised as;

$$T_l = \{t \in T : t(F) \leq x\}$$

$$\text{and}$$

$$T_r = \{t \in T : t(F) > x\}$$

where F is an attribute or feature, x is a criterion constant and T is a branch leading to a particular class.

As such, T_l is a left branch split and T_r is a right branch split.

The algorithm explores and evaluates all possible splits of the data. It selects a split that best decreases the impurity of the parent node, such that error is minimised. The Gini index is most commonly used as an impurity measure. It is presented below.

$$Gini\,(E) = 1 - \sum_{i=1}^{n} d_i^{\,2}$$

$$c_i = \frac{|\{t \in D : t[C] = c_i\}|}{|D|}$$

where n is the number of classes, d_i is a portion of the data set in D the target class c_i.

The settings of the Matlab decision tree function used in this research are presented in table G.2.

Table G.2: Matlab tree settings

Property Name	Setting
Type	Classification – compact tree
Predictor Selection	'all splits' – Standard CART (Default)
Prior probabilities – 'Prior'	'empirical'
Prune Criterion	'error'
Prune	Not performed
All other settings	Default

Deterministic classifier

The deterministic classifier was developed to classify incoming data into one of the five motion classes based on the equation below.

$$C_{det} \rightarrow \begin{cases} 1, & (p \wedge q) \\ 3, & (\sim p \wedge \sim q) \\ 4, & (p \wedge \sim r) \wedge \sim q \\ 5, & (q \wedge r) \wedge \sim p \\ 2, & otherwise \end{cases}$$

where $p \rightarrow TA > MGas$, $q \rightarrow TA > LGas$ and $r \rightarrow MGas > LGas$.

Such that;

$$TA = max(\textstyle\sum_{i=1}^{n} TA(i))$$

$$MGas = max(\textstyle\sum_{i=1}^{n} MGas(i))$$

$$LGas = max(\textstyle\sum_{i=1}^{n} LGas(i))$$

Voting scheme

The voting scheme used the prediction outcomes of the three classifiers to specify a motion prediction. These were the predictions from the LDA, decision tree and the deterministic classifier. This was defined based on the equation below.

$$C_{VS}(t) = \begin{cases} C_{LDA}(t), & C_{LDA}(t) = C_{Tree}(t \\ C_{Tree}(t), & C_{Tree}(t) = C_{det}(t) \\ C_{det}(t), & C_{det}(t) = C_{LDA}(t) \\ C_{det}(t), & Otherwise \end{cases}$$

where;

t is the current prediction outcome.

C_{LDA}, C_{Tree} and C_{det} are the prediction outcomes for the LDA, classification tree and deterministic classifiers, respectively.

References

1. Li, T., Zhu, S. & Ogihara, M., *Using discriminant analysis for multi-classification: An experimental investigation*. Knowledge and Information Systems 2006. **10**(4): pp. 453–472.
2. Breiman, L., Friedman, J., Olshen, R., and Stone, C., *Classification and Regression Trees*. 1984, Monterey, CA: Wadsworth & Brooks/Cole Advanced Books & Software.
3. Coppersmith, D., Hong, S.J. & Hosking, J.R.M., *Partitioning nominal attributes in decision trees*. Data Mining and Knowledge Discovery 1999. **3**: pp. 197–217.

Appendix H: Confusion Matrices for Different Walking Speeds

The decoupled data set was used to investigate the effect a change in walking speed had on prediction accuracy when using different prediction approaches and classification algorithms.

Optimal condition fast – Generic LG

Optimal condition fast – Biased generic UT

Optimal condition fast – Biased generic LG

Optimal condition fast – Walking style UT

Optimal condition slow – Generic LG

Optimal condition slow – Biased generic UT

Optimal condition slow – Biased generic LG

Optimal condition slow – Walking style UT
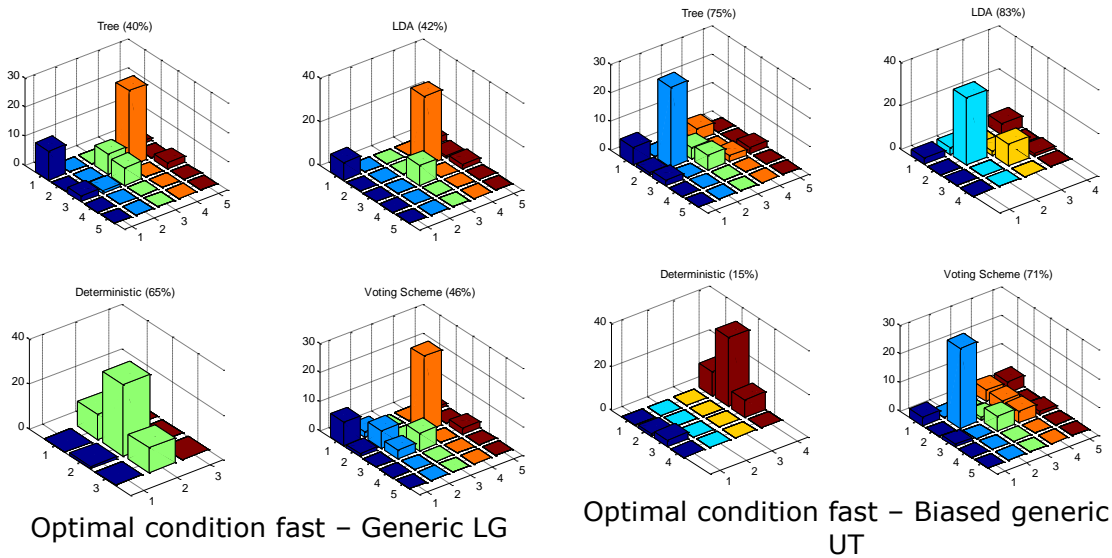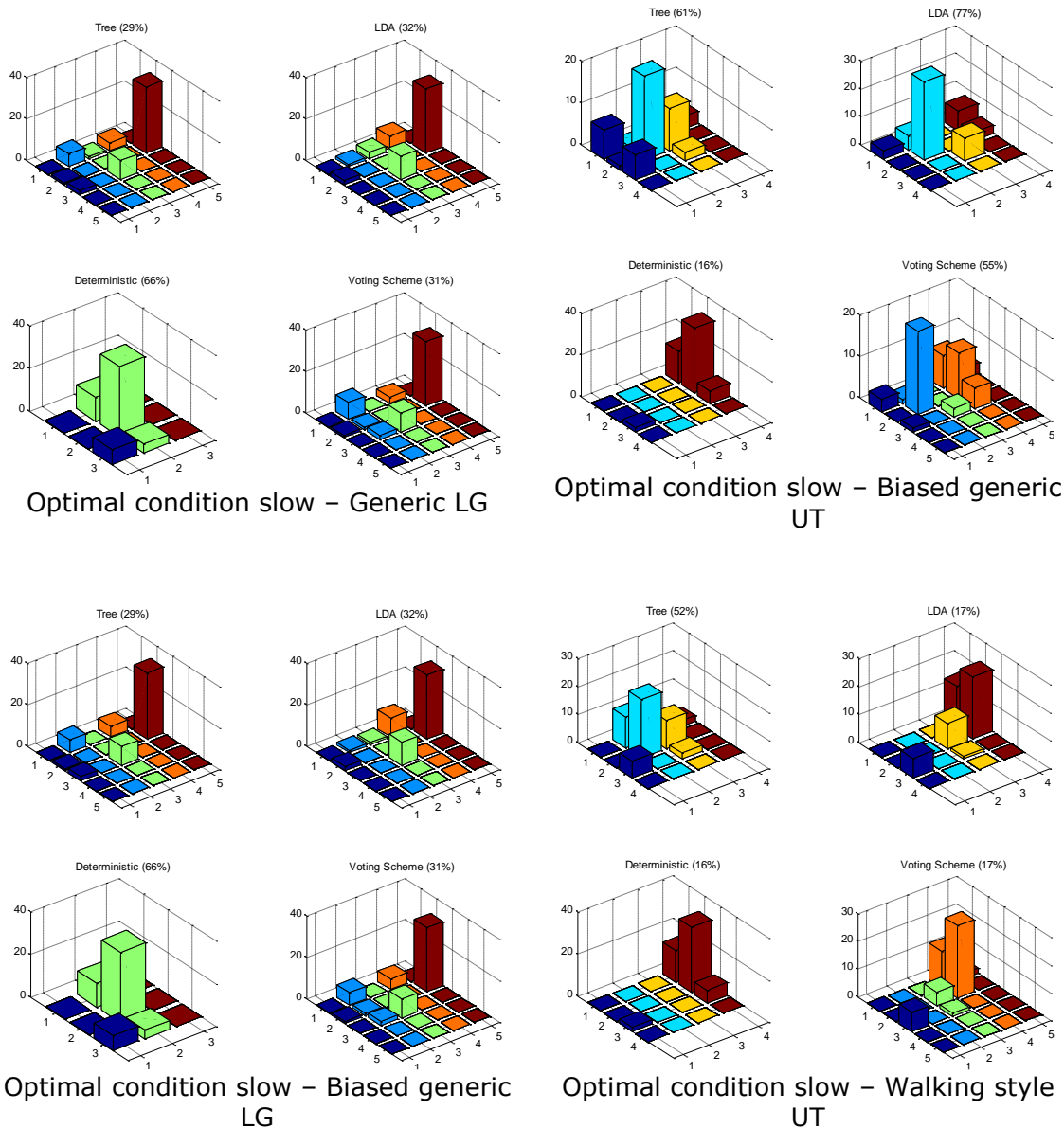
Figure H.1: The effect of walking speed on prediction accuracy – additional results

Appendix I: Circuit Schematics

Presented below are the schematic diagrams for the circuits developed and used for implementing the developed control strategy. These circuits were responsible for actuating the prosthesis prototype for the validation experiment presented in chapter 6. The output-level controller circuit (fig. I.1) was responsible for executing the prototype output motion by setting the pulse-width modulation (PWM) duty cycle. This was used to drive the brushed DC motors. The circuit also ensured that actuation was halted when the prototype range of motion (ROM) limits were reached. The PWM signal from the output-level controller circuit was sent to the motor driver circuit, along with the on/off specification for each motor. The motion tracking circuit (fig. I.2) was used to monitor the 3D position of the foot with respect to its rest position and its physical ROM limits. It helped ensure that the prototype was not damaged due to over-actuation beyond it limits.

Figure I.1: Output-level controller circuit

Figure I.2: Motion tracking circuit

Appendix J: Matlab Code Used in This Research

The Matlab and C codes developed to execute and realise the work presented in this thesis are included in the accompanying CD. Below is a list and description of the codes as included on the CD.

Name	Description
Chapter 3: Gait Experiment	
Automating_Data_ Extraction_LG	Automating gait experiment data extraction, segmentation and normalisation for the level-ground data files
Automating_Data_ Extraction_UT	Automating gait experiment data extraction, segmentation and normalisation for the uneven terrain data files
DataSegmentation	Function to automatically segment gait experiment data based on the activation of the 3D force plates
Automated_Ave_N orm_Data	Grouping the segmented participant group data for further processing - for all three walking speeds
EMG_MVC_ Computation	Processing the EMG MVC data to perform amplitude normalisation
EMG_Amplitude_N orm	Amplitude normalisation of the raw EMG data based on MVC
ANormaliseEMG	Function called into EMG_Amplitude_Norm
Group_Data_ Averaging	Amplitude normalisation of each participant's GRF data, with respect to their body weight. Also calculating the mean and standard deviation - for all three walking speeds
LG_UT_GRF_Plot	Plotting the normalised GRF data for the participant groups' LG and UT trials
LG_UT_EMG_Plot	Plotting the normalised EMG data for the participant groups' LG and UT trials
Chapter 5: User Intent Prediction Strategy	
EMG_FeatureSet_E xtraction	Extracting EMG data, from the valid gait files, for feature set computation to create the inputs and targets/labels for LDA classification
Eversion_ Features_Comp	Extracting and computing EMG eversion data, both left and right leg, for inclusion in the five motion types for user intent prediction
MVC_Norm_ Classification	MVC normalisation of raw participant EMG data for optimal feature selection
Original_Feature_A ccuracy	Comparing prediction accuracy of three individual EMG features, namely AR, RMS and MAV
New_Feature_ Accuracy	Comparing prediction accuracy of another three different features, namely VAR, IEMG and WL
Combined_Feature _Accuracy	Determining the best performing feature set combinations from the six features, namely VAR, IEMG, WL, AR, RMS and MAV.

Feature_ Computation	Feature computation, combining the individual features to create inputs and targets to train the LDA classifier
Prediction_LDA	LDA classification function
Create_Full_Tree	Creating a decision tree from EMG features for the five motions of interest
Prediction_Tree	Function predict EMG data using the classification tree
Deterministic_prediction	Classification algorithm for the deterministic classifier
Data_Segment_Gait_Style	Segmenting participant EMG data to determine their walking style
Walking_style_ localMax	Determining the participants' walking style from segmented EMG data
FeatureSet_ Plotting	Plotting the walking style specific feature set clusters
Controller_ Validation	Determining the classification performance of the different prediction approaches and classification algorithms trialled
Prediction_ Plotting	Plotting the prediction outcome, the accuracy and confusion matrices, from testing the different prediction strategies
Chapter 6: Prototype Control Strategy Implementation	
Real_Time_Prediction	The programme used during the validation experiment. Reading in the wireless EMG data, performs motion prediction and specifies the output parameters. Data is wirelessly communicated to the prototype circuit via the XBees
Segmenting_VE_Data_ROM_ Analysis	Extracting and segmenting the prototype motion capture data from the validation experiment
VE_ROM_ Analysis_Pt1_2	Data preparation for ROM computation. Data extraction, segmenting and zeroing, with respect to the reference stationary marker data. Computing the prototype ROM from the motion capture data and plotting the results
ROM_Mean_StdDev_Plot	Reading in the mean and standard deviation ROM data and plotting the results
Torque_Data_ Analysis_Plot	Ankle torque calculation from the validation experiment and plotting the results
Prototype Output_Actuation Control	C code implemented on the output level control circuit to actuate the prototype.
Motion_Tracking_Limiting	C code implemented on the motion tracking circuit to measure the 3D position of the foot and flag when ROM limits are reached
Adafruit license	License of the C header files used in the motion tracking limiting code

Appendix K: Complete Ethical Approval Application

Application form for ethical approval of a research project by a University Research Ethics Committee

The University Research Ethics Committees meet on a weekly basis between September and July each year. All applications must be submitted to our office by the end of June or it will not be considered until September. We would therefore recommend sending your form to your designated Signatory no later than the middle of June. Please see here for the calendar of UREC meetings. The normal expectation is that your application will be reviewed in the third week after submission by the School/Institute Signatory. Please note that the School/Institute signatory process aims to take an average of 10 working days.

Guidance on completing the form

This form should be completed by the Principal Investigator(s). For student research, the Supervisor must provide guidance to the student on the application and sign off the form.

Guidance can be found by clicking on the links provided with some sections. Additionally, guidance can be found here.

The form must be completed **succinctly** and in **plain, jargon-free English** so that committee members, who may not be familiar with your academic discipline, are able to understand it.

Applicants are asked to forward all supporting papers in **one document**, preferably in a PDF format. Experience indicates that it is easy for separate documents to get misplaced as they are transferred from one office to another during the review process.

Submitting the form

Your form must be submitted to the UREC via your assigned School/Institute Signatory. Please see here for a list of current Signatories

Checklist of documentation to include

Please DO NOT include CVs

- ☒ **Participant Information Sheet**
- ☒ **Consent form**
- ☐ **Letters to gatekeepers (i.e. those from whom permission is required such as employer or data custodian) if applicable**
- ☐ **Questionnaire (if using)**
- ☐ **Interview/focus group schedule (if using)**
- ☐ **Any advertisements/flyers/posters to be used**
- ☒ **Research Protocol (if applicable) ***

Please note:** A research protocol is **NOT** a substitute for information provided on the UREC form and should only be submitted for clinical trials. In addition, **please do not attach grant proposals.

Insurance Questions

Please answer all of the following questions. If in doubt, err on the side of caution and answer yes. If you answer yes to any of the questions below (apart from the first question) then your application, Participant

Information Sheet and Consent form will be forwarded to the Insurance Office by the Research Governance, Ethics and Integrity team. For additional guidance for completing the Insurance Questions, <u>please see here</u>.

Title of Research: Designing a control strategy for a powered ankle-foot prosthesis using EMG signals

Principal investigator: Miss Unéné Gregory and Dr Lei Ren

School/Institute: Mechanical, Aerospace and Civil Engineering (MACE)

Question	Yes/No
Is any part of the research, or use of the protocol, to be carried out outside the UK (including internet-based research that could include respondents from abroad)?	No
If yes, does the research also involve medical content?	N/A
Does the research involve "first into man" use of a medicinal product?	No
Do the research subjects deliberately include: • pregnant women?	No
• children aged five or under?	No
• adults who lack the capacity to give informed consent?	No
Does the research include medical intervention involving: • investigating a medical device?	No
• contraception?	No
Is the research to be carried out by other organisations where the University is required by contract to provide insurance cover for the research if it proceeds?**	No

Signed (PI):   *Unéné Gregory*   Date: 01 February 2016

**If you are unclear of the responsibilities please provide any contract conditions/agreements for review.

Insurance Office approval (not required if all answers above are 'No')

Signed: Date:

203

SECTION A – Administrative information

** Do you also need to obtain NHS R&D approval?
☐ **Yes** ☒ **No**
**If yes, have you already contacted your <u>University sponsor</u> regarding NHS R&D approval? N/A
☐ **Yes** ☐ **No**

<u>IMPORTANT: You MUST contact your University sponsor regarding NHS R&D approval PRIOR to submitting a UREC application. Any UREC applications submitted prior to contacting your University sponsor will be returned.</u>

1. Title of the research:
Designing a control strategy for a powered ankle-foot prosthesis using EMG signals

2. Investigator(s) *(nb. In the case of postgraduate student applications the supervisor is always the joint investigator):*

	Student	Supervisor/Staff
Title	Miss	Dr
Surname	Gregory	Ren
First name	Unéné	Lei
Post		Senior Lecturer in Biomechanics
Qualifications	MSc Electronic Engineering MTech Electrical Engineering	PhD
School/Unit/Institute	MACE	MACE
Contact Address	School of Mechanical, Aerospace and Civil Engineering University of Manchester Manchester, M13 9PL D floor Pariser Building, desk N4	School of Mechanical, Aerospace and Civil Engineering University of Manchester Manchester, M13 9PL Office: C13 Pariser Building
Email address	unene.gregory@postgrad.manchester.ac.uk	lei.ren@manchester.ac.uk
Telephone	+44 (0) 74 3713 8885	+44 (0) 161 306 4251

3. School contact (if applicable): The School/Institute Signatory will receive a copy of the outcome of the ethical review, *If the School wishes anyone else to receive a copy, the relevant details should be entered here.*
   Name:
   Post:
   Email address:
4. Is this study, or any part of this study a student project? <u>**Yes**</u>/No
   If Yes what degree is it for?
A doctorate degree (PhD) in mechanical engineering.
5. Please provide the names and email addresses of any academic staff or students involved, other than those named at 2 above:
None.

SECTION B – Details of Project

6. When will the data collection take place? (*If your research will be conducted outside the UK borders, please specify the duration for each country*)
Start date: 14 March 2016
End date: 15 July 2016

7. What is the principal research question?
How do muscle activation and limb kinetics of the legs differ when able-bodied humans walk on different types of terrain and at different speeds?

8. What is the academic justification for the research?
Gaining an understanding of the gait strategies employed by able-bodied individuals as they walk over firm, uneven terrain, such as those encountered within an urban environment, as compared to level-ground; and using said understanding to develop a transtibial powered prosthesis capable of replicating said gait.

9. Give a brief summary of the design and methodology of the planned research. It should be clear exactly what will happen to the research participant, how many times and in what order. Describe any involvement of research participants, participant groups or communities in the design of the research.

The gait experiments will take place in an indoor gait laboratory in Pariser building which has internal heating. Participants will walk barefoot at three self-selected speeds over level-ground and a firm uneven terrain. The uneven terrain will consist of six sloped steps inclined at 12°, each 60cm long x 40cm wide in size, arranged along the sagittal and frontal planes. The sloped steps will be fabricated from sheet metal, their edges will be filleted and they will be covered with a thin layer of rubber to provide a non-slip walking surface.

Kinetic data will be captured using two 3D force plates. Reflective markers will be placed on participants using double sided tape so that their motion can be captured using a motion capture system. Participants will wear only shorts to ensure that all the reflective markers secured to them, including on their torso, can be 'seen' by the motion capture system. Surface electromyography (EMG) electrodes will also be placed on participants; this will be done to capture the muscle activations of eight muscles in each leg. The electrodes will be secured to participants using special, easily removable double sided tape from Delsys. 20 valid trials for each walking speed will be captured for both the level-ground and uneven terrain experiments; this will result in a total of 120 valid gait trials per participant.

*(This section must be completed in simple language and should be no longer than half a page. A research protocol is **NOT** a substitute for information provided on the UREC form and should only be submitted for clinical trials. In addition, **please do not attach grant proposals**).*

10. How has the scientific quality of the research been assessed? *(Tick all that apply)*

☒ Internal review (e.g. involving colleagues, academic supervisor)
☐ Review within a multi−centre research group
☐ Independent external review
☐ Review within a commercial company
☐ None external to the investigator
☐ Other, e.g. in relation to methodological guidelines *(give details below)*

If relevant, describe the review process and outcome. If the review has been undertaken but not seen by the researcher, give details of the body which has undertaken the review:

11.1 Does the research involve the administration of any physically invasive procedures, physical testing or psychological intervention (apart from the administration of standard psychological tests)?
☐ **Yes** ☒ **No**

If No, proceed to 11.2   If Yes, please ensure you complete Section F

11.2 Does the research involve human blood or tissue samples? If you are unsure, please see <u>here for guidance relating to HTA.</u>
☐ **Yes** ☒ **No**

If No, proceed to 11.3

11.3 Does the research involve interviewing participants or focus groups?
☐ **Yes** ☒ **No**

If No, proceed to 11.4

If Yes, please describe briefly how they will be conducted

11.4 Does the research involve the administration of questionnaires?
☐ **Yes** ☒ **No**

If No, proceed to 11.5

If Yes, please describe the process of delivery and collection

11.5   Is statistical sampling relevant to this research?
☐ **Yes** ☒ **No**

If No, proceed to 11.6

If Yes, please answer the following questions:

11.5.1   Has the protocol submitted with this application been the subject of review by a statistician independent of the research team? Select one of the following:

☐ Yes – copy of review enclosed

☐ Yes -
details of review available from the following individual or organisation (give contact details)

☐ No – justify below

11.5.2   If relevant, specify the statistical experimental design and why it was chosen.

11.6 If you are not using statistical sampling how was the number of participants decided upon?

The number of participants was chosen based on the trend observed in literature from other similar biomechanics research.

11.7   Describe the methods of analysis (statistical or other appropriate methods, e.g. for qualitative research) by which the data will be evaluated to meet the study objectives.

GMAS software, a developed Matlab toolbox, will be used to process the motion capture data in order to compute the joint forces, moments and the mechanical power from the walking trials. EMGWorks Analysis, Delsys propriety software, will be used to process and analyse the muscle activation data. The EMG data will be high pass filtered with a cut-off frequency of 20Hz to remove motion artefact. The RMS (root mean square) will be computed for each EMG signal to attain a rectified representation of the participants' muscle activation. Each participant's EMG data will be amplitude normalised using their maximum voluntary contraction (MVC) for each muscle in order to facilitate intra- and inter-subject data comparison,. The EMG data will also be time-normalized to percentage of the gait cycle, thus aligning it with the motion capture data.

12.1 What do you consider to be the main ethical issues which may arise with the proposed study?

Placing reflective markers and EMG electrodes on human participants and having them perform the gait experiment.

12.2 What steps will be taken to address the issues raised in question 12.1?

Ensuring that the participants understand what will be asked of them during the gait experiments and that their participation is voluntary.

12.3 What qualifications/experience do the researchers have relevant to the conducting of this research? (*For details about requirements for specific types of research* <u>click here</u>)

The supervisor is experienced in conducting biomechanics experiments similar to the gait experiment being proposed. The student is experienced with using Matlab and EMGWorks, software which is required to adequately process the acquired data.

13. Has this or a similar application been previously considered by a Research Ethics Committee in the UK, the European Union or the European Economic Area?

○ Yes

● <u>No</u>

If Yes give details of each application considered, including:

Name of Research Ethics Committee or regulatory authority:

Decision and date taken:

Research ethics committee reference number:

SECTION C – Details of participants

14.   How many participants will be recruited? (*If there is more than one group, state how many participants will be recruited in each group. For international studies, say how many participants will be recruited in __each country__ and in total. Please ensure you clearly state the total number of participants*)

Seven able-bodied male participants, all within Manchester, will be recruited for the gait experiment.

15.   Age range of participants (*Please note that an upper age limit is not required and should only be stated if a proper justification can be provided for doing so. In addition, it is standard to stipulate that participants must be at least 16 to participate in research projects. If you will be using participants who are younger you will need to justify their inclusion*)

Participants must be at least 18 years old to participate in the gait experiment.

16.   What are the principal inclusion criteria for participants? (*Please justify*)

Able-bodied male participants with no musculoskeletal disease or limitations that would lead to their gait at self-selected speeds deviating from that reported of healthy able-bodied gait.

17.   What are the principal exclusion criteria for participants? (*Please justify*)

Participants will be excluded if they have any musculoskeletal disease or limitations as this could lead to their gait at self-selected speeds deviating from that reported of healthy able-bodied gait. Only male participants will be included in the experiment as participants will be required to only wear shorts so that the reflective markers placed on their legs and torso can be 'seen' by the motion capture system and that said markers remain secured onto the participants.

18.1 Will the participants be from any of the following groups? *(Tick all that apply)*

- ☒ Adult healthy volunteers (i.e. not under medical care for a condition which is directly relevant to the application)
- ☐ Children under 16
- ☐ Adults with learning difficulties
- ☐ Adults who have a terminal illness
- ☐ Adults with mental illness (particularly if detained under mental health legislation)
- ☐ Adults with dementia
- ☐ Adults in care homes
- ☐ Adults or children in emergency situations
- ☐ Prisoners
- ☐ Young offenders
- ☐ Those who could be considered to have a particularly dependent relationship with the researcher, e.g. students taught or examined by the researcher.
- ☐ Other vulnerable groups

Please note: If an adult participant is not able to give informed consent (eg through mental capacity or is unconscious) or if a prisoner or young offender is involved in health related research ethical review should be undertaken by an appropriate NHS Research Ethics Committee.

18.2 If you will be using participants other than healthy volunteers please justify their inclusion:

N/A.

19. How will the potential participants be identified, approached and recruited? *(Where research participants will be recruited via advertisement, please append a copy to this application)*

Male members within our research group will be approached and recruited as they are able-bodied individuals and have an understanding of the research area.

20. Will individual research participants receive *reimbursement of expenses* or any other *incentives* or *benefits* for taking part in this research?

☐ Yes ☒ No

(If yes, indicate how much and on what basis this has been decided)

21. What is the expected total duration of participation in the study for each participant? *For ethnographic research focussing on one or more groups rather than individual participants, indicate the approximate period of time over which research will focus on particular groups*

The duration of the gait experiment for a single participant will be approximately 5 hours (± 1 hour).

22. What is the potential benefit to research participants?

None.

23. Will any benefit or assistance, which the participant would normally have access to, be withheld as part of the research?

☐ Yes ☒ No

(If yes, give details and justification)

SECTION D – Consent

24.1 Will informed consent be obtained from the research participants?

☒ Yes ☐ No

If Yes, give details of how consent will be obtained. Give details of your experience in taking consent and of any particular steps to provide information to participants before the study takes place eg information sheet, videos, interactive material.

If participants are recruited from any of the potentially vulnerable groups listed in Question 19.1, give details of extra steps taken to assure their protection. Describe any arrangements to be made for obtaining consent from a legal representative.

If consent is not to be obtained, please explain why not.

Participants will be given a participant information sheet (PIS) to read through and a consent form to complete prior to them participating in the gait experiment. Participants will also be encouraged to ask questions about the experiment and about what would be expected of them. One of the principal investigators, the supervisor, has experience in conducting similar biomechanics research, including receiving signed consent to participate in such studies.

24.2 Will a signed record of consent be obtained?

☒ Yes ☐ No

If not, please explain why not. Please append any <u>consent forms</u> to this application.

25. How long will the participant have to decide whether to take part in the research? (*If less than 24 hours please justify***)**

Participants will be given a week from the time they are recruited to decide whether they want to participant in the gait experiments.

26. What arrangements have been made for participants who might not adequately understand verbal explanations or written information given in English, or who have special communication needs? *(e.g. translation, use of interpreters etc.)*

Potential participants who have been identified from the research group all understand verbal explanations and written English, as such no arrangements are required in this regard.

SECTION E – RISKS AND SAFEGUARDS

27.   Activities to be undertaken (*This should be in the form of a brief list, such as answering a questionnaire, being interviewed***)**

o   Reflective markers and surface electromyography (EMG) electrodes will be placed on participants, taking approximately 1.5 hours.

o   Participants will perform maximum voluntary contractions (MVC) of all the muscle groups under investigation, taking approximately 45 minutes.

o   Static and dynamic calibration capturing the reflection marker positions when stationary and to compute the hip joint centres from dynamic movement will be performed. This will take approximately 45 minutes.

o   Participants will walk at three self-selected walking speeds from one side of the gait laboratory to the other. Participants will walk over level-ground and firm, uneven terrain within the gait lab. This will take approximately 2 hours, with a

rest period between terrain types and also between different walking speeds if required.

28. Where will the research/data collection take place?
The experiment will take place in a gait laboratory located in Pariser building at the university, room A4.

29.1 What are the potential adverse effects, risks or hazards for <u>research participants</u>, including potential for pain, discomfort, distress, inconvenience or changes to lifestyle for research participants? Are they any greater than those that would arise from normal social interaction?
The only effects participants could face is slight discomfort when removing the double sided tape used to secure the reflective markers and the EMG electrodes, particularly if participants are hairy.

29.2 Could individual or group interviews/questionnaires raise any topics or issues that might be sensitive, embarrassing or upsetting, or is it possible that criminal or other disclosures requiring action could take place during the study (e.g. in the application of screening tests for drugs)?
☐ Yes ☒ No
If yes, provide your distress policy/give details of procedures in place to deal with these issues:

29.3 What precautions have been taken to minimise or mitigate the risks identified above? *(Please note that researchers must provide a specific time point at which participants can no longer withdraw their data e.g. at the time of publication or at the point of anonymising transcriptions)*
Any hair at the locations where the double sided tape is to be secured would be trimmed down to minimise discomfort when removing the double sided tape once the experiment is complete and to also ensure that the reflective markers and the EMG electrodes remain fixed onto the participant.

30.1 What is the potential for adverse effects, risks or hazards, pain, discomfort, distress, or inconvenience to the <u>researchers</u> themselves? *(If any)*
None.

30.2 What precautions have been taken to minimise or mitigate the risks identified above? (*If the research means working alone in a location which is not public, semi-public or otherwise risk-free, please describe your lone worker policy or append a copy*)
N/A.

31. ☒ I confirm that any adverse event requiring a radical change of method or design, or even abandonment of the research, will be reported to the Committee.

SECTION F – MEDICAL INTERVENTION
<u>This section need only be completed by applicants whose project involves any form of medical or other therapeutic intervention or any physically invasive procedures, physical testing or psychological intervention (apart from the administration of standard psychological tests) (i.e. you answered 'Yes' to question 12.1)</u>

32. Drugs and other substances to be administered (if applicable)

Indicate status, eg full product licence, CTC, CTX. Attach: evidence of status of any unlicensed product; and Martindales Phamacopoeia details for licensed products

DRUG   STATUS   DOSAGE/FREQUENCY/ROUTE

33. Procedures to be undertaken

Details of any invasive procedures, and any samples or measurements to be taken. and/or any psychological tests etc. What is the experience of those administering the procedures?

34. Will any procedures which are normally undertaken be withheld?

35.1   Will the research participants' General Practitioner be informed that they are taking part in the study?
☐ Yes ☐ No
If No, explain why not

35.2   If you answered yes to question 35.1, will permission be sought from the research participants to inform their GP before this is done?
☐ Yes ☐ No
If No, explain why not

36.   What are the criteria for electively stopping research prematurely?

SECTION G – Data protection and confidentiality

37.1. Will the research involve any of the following activities at any stage (including identification of potential research participants)? *(Tick all that apply)*

Storage of personal data on any of the following:

☐ Storage of personal data on manual files
☐ Storage of personal data on laptops or other personal computers
☒ Storage of personal data on University computers
☐ Storage of personal data on NHS computers
☐ Storage of personal data on private company computers
☒ Use of audio/visual recording devices
☐ Use of personal addresses, postcodes, faxes, e-mails or telephone numbers
☐ Electronic transfer by magnetic or optical media, e-mail or computer networks
☐ Examination of medical records by those outside the NHS, or within the NHS by those who would not normally have access
☐ Sharing of data with other organisations
☐ Export of data outside the European Union
☐ Publication of direct quotations from respondents
☐ Publication of data that might allow identification of individuals

37.2 Please provide details of how you plan to store and protect the study data as stated in 37.1 above.

All the gait and EMG data acquired during the gait experiments will be stored on secure university computers that are password protected. The data will only be accessible to the principal investigators.

38. What measures have been put in place to ensure confidentiality of personal data? Give details of what encryption or other anonymisation procedures will be used and at what stage? *Note: the <u>University requires</u> all personal data stored electronically to be held on wholly managed University servers or to be encrypted.*

Only participant initials will be used to identify participants and their data. All the acquired data will be stored on secure, wholly managed university computers that are password protected.

39.
  Where will the analysis of the data from the study take place and by wh om will it be undertaken?

Data from the experiment will be analysed on secure, university computers that have been allocated to the principal investigators and will be analysed by the principal investigators.

40.1 Who will control and act as the custodian for the data? *Note: for a student project this must be a supervisor or a permanent member of staff*

The supervisor will act as the custodian of the acquired data.

40.2   Who will have access to the data and where are they based?

Only the principal investigators, the student and the supervisor, will have access to the data and they will be based in Pariser building at the university.

40.3   Will the data be stored for use in future studies? If yes, has this been addressed in the consent process?

Yes, the acquired data may be used in future studies; this issue has been addressed in the participant information sheet.

41. For how long will the data from the study be stored?
  For a minimum of five   Years
  Note: the University requires non-medical data to be held for a minimum of 5 years and medical data to be held for a minimum of 10 years after the completion of the research. Some funding bodies require storage for longer periods.

42. What arrangements are in place to ensure participants receive any information that becomes available during the course of the research that may be relevant to their continued participation?

The participants will be from our research group so contacting with them would not be problematic.

43. What arrangements are in place for monitoring the conduct of the research by parties other than the researcher?

None.
  Will a data monitoring committee be convened?
  ☐ Yes
  ☒ Not relevant

SECTION H – Conflict of Interest

44.1 Will individual *researchers* receive any personal payment over and above normal salary and reimbursement of expenses for undertaking this research?
  ☐ Yes ☒ No
  If Yes, indicate how much and on what basis this has been decided:

44.2 Does the principal researcher or any other investigator/collaborator have any direct personal involvement (e.g. financial, share-holding, personal relationship etc.) in the organisation sponsoring or funding the research that may give rise to a possible conflict of interest?

☐ Yes ☒ No
If Yes, give details:

45. Will the host organisation or the researcher's department(s) or institution(s) receive any payment of benefits in excess of the costs of undertaking the research?
☐ Yes ☒ No
If Yes, give details:

SECTION I - Reporting Arrangements

46. How is it intended the results of the study will be reported and dissemi nated? *(Tick as appropriate)*

☒   Peer reviewed academic journals
☐   Book or contribution to a book
☐   Other   published   outlets e.g.   ESR or Cochrane Review,
☒   Thesis/dissertation
☒   Conference presentation
☐   Internal report
☐   Other e.g. deposition in University Library

47. How will the results of research be made available to research participants and communities from which they are drawn?

☒   Presentation to participants or relevant community group
☐   Written feedback to research participants
☐   Other e.g. videos, interactive website

48.1 Will dissemination allow identification of individual participants?
☐ Yes ☒ No
If No, proceed to 49
If Yes, indicate how these individuals' consent will be obtained:

48.2 Will dissemination involve publication of extended direct quotations from identified participants and/or distribution of audiovisual media in which identified participants play leading roles?
☐Yes ☒ No
If No, proceed to 49
If Yes, indicate how the participants' possible Intellectual Property or Performance Rights in these outputs will be negotiated. Where relevant, attach a model of the release form that will be used.

48.3 Are special arrangements needed to provide indemnity and/or compensation in the event of a claim by, or on behalf of, participants on grounds such as libel, breach of confidence and infringement of Intellectual Property or Performance Rights?
No.

SECTION J – Funding

49.   Has external funding for the research been secured?

☐ Yes ☒ No

If Yes, give details of funding organisation(s) and amount secured and duration:

Organisation:

UK contact:

Amount (£):

Duration: Months

SECTION K – Confirmation of Application

Note: Student applications must also be signed by their supervisor

Signature(s) of applicant(s):

Unéné Gregory   01/02/2016

_____   _____

SIGNATURE (Name in italics is sufficient)   DATE

Unéné Gregory, Doctoral candidate (MACE)

NAME AND POST OF APPLICANT (PLEASE PRINT)

Signature of supervisor (if applicable):

Lei Ren   01/02/2016

_____   _____

SIGNATURE (Electronic signature is required)   DATE

Dr Lei Ren, Senior Lecturer in Biomechanics

NAME AND POST OF SUPERVISOR (PLEASE PRINT)

Please note: Once complete, please submit this application form and ALL supporting documentation to your <u>signatory</u> for review. Please <u>DO NOT</u> send directly to <u>Research.Ethics@manchester.ac.uk</u> or your application will be returned to you.

Experiment Protocol – Gait Trials

1. Purpose

The primary purpose of a prosthesis is to replicate the functionality of the amputated limb, including its capability to maintain stability when traversing uneven terrain. If one is to develop a true functional replacement of a biological limb, the mechanisms that govern and drive the biological limb have to be understood and replicable by a controller implemented on a powered prosthesis.

As such, the objective of the gait trials will be to ascertain the gait strategies and muscle activation patterns employed by able-bodied individuals when walking over uneven terrain, such as those encountered within an urban environment. The main focus will be on the lower limbs and partially on the upper body, from which postural stability can be deduced.

The database acquired from the gait experiments will be used to develop a control strategy for a powered lower limb prosthesis that would be capable of enabling a user to traverse uneven terrain such as those encountered within urban environments.

2. Methods
2.1. Participants

2.1.1. Seven able-bodied individuals will participate in the gait trials.

2.1.2. Participants will have no musculoskeletal disease or limitations that would lead to their gait at self-selected speeds deviating from that of healthy able-bodied gait.

2.1.3. Participants will walk barefoot when performing the gait trials in order to minimise differences in gait that could be introduced by participants wearing different kinds of shoes [1, 2].

2.2. Experiment Composition

2.2.1. The gait trials will take place in an indoor gait laboratory which has two triaxial force plates that are placed flush with the ground such that they are level with the floor.

2.2.2. Participants will perform level-ground walking over even terrain, which will serve as the control motion, and walk over constructed, uneven terrain.

2.2.3. Participants will walk at three self-selected speeds; these will be normal, slow and fast.

2.2.4. The experiment was divided into two sessions, both of which consisted of level-ground walking and walking over the uneven terrain.

2.2.5. The first session was a pilot study and involved a single participant; the objective of which was to ensure the fidelity of the recorded data and the thoroughness of the experiment protocol. An average of 20 valid walking trials for each walking speed was captured for both level-ground and uneven terrain experiments.

2.2.6. The second session will involve six participants. 20 valid trials for each walking speed will again be captured for both level-ground and uneven terrain experiments. This will result in a total of 120 valid gait trials per participant.

2.2.7. During the level-ground gait trials, participants will walk a distance of 6m, from one end of the gait laboratory to the other, activating the 3D force plates in succession.

2.2.8. A trial will only be deemed valid if participants step over both force plates in succession during the trial; this will ensure that kinetic and kinematic data for that trial can be computed from the motion capture data.

2.2.9. All sensor data will be recorded and synchronised for all gait trials.

2.3.   Motion Capture System

Motion data will be captured so that variables such as participants' joint moments and angles can be computed using inverse dynamics algorithms, with regards to rigid body dynamics, and the data from the triaxial force plates. The resulting data will be aligned with the EMG data so that the correlation between the participants' motion and their muscle activation during the gait trials can be ascertained.

2.3.1. Prior to any motion data being captured, camera system calibration, force plate calibration and two calibration trials will be performed, a static trial and a dynamic trial. The calibration trials will be based on the CAST (Calibrated Anatomical System Technique) technique [3].

2.3.2. The Vicon system will be calibrated using its proprietary software and a calibration wand with four reflective markers. This procedure will be done to ensure accurate and robust motion capturing.

2.3.3. The static trial will be conducted to record anatomical landmark locations. This will be done to determine the 3D spatial description of the body segments which will later be used to determine the anthropometric data of the body segments in order to perform inverse dynamics calculations.

2.3.4. The dynamic trial will be conducted so that the hip joint centre location can be determined. Participants will continuously perform flexion and extension with their

hips at least three times, thus increasing the likelihood of recording all the marker positions.

2.3.5. The locations of the anatomical landmarks for each major body segment will largely be based on [4] and are given in table 1.

Table 2.3.1: Anatomical Landmarks of Each Major Body Segment

Anatomical Landmark	Description	Property/Type
Trunk		
IJUG	Jugular Notch	bony
PXIP	Xiphoid Process	bony
C7SP	Spinous Process C7	bony
T8SP	Spinous Process T8	bony
Pelvis		
RASIS	Right Anterior Superior Iliac Spine	bony
LASIS	Left Anterior Superior Iliac Spine	bony
RPSIS	Right Posterior Superior Iliac Spine	bony
LPSIS	Left Posterior Superior Iliac Spine	bony
Right Femur		
RLEP	Right Lateral Epicondyle	bony
RMEP	Right Medial Epicondyle	bony
HJCR	Right Hip Joint Centre	Virtual
Left Femur		
LLEP	Left Lateral Epicondyle	bony
LMEP	Left Medial Epicondyle	bony
HJCL	Left Hip Joint Centre	Virtual
Right Shank		
RTTB	Right Tibial Tuberosity	bony
RHFB	Right Apex of Fibula Head	bony
RMML	Right Medial Malleolus	bony
RLML	Right Lateral Malleolus	bony
Left Shank		
LTTB	Left Tibial Tuberosity	bony
LHFB	Left Apex of Fibula Head	bony
LMML	Left Medial Malleolus	bony
LLML	Left Lateral Malleolus	bony
Right Foot		
RCAR	Right Upper Ridge of the Calcaneus	bony
RFMR	Right Dorsal Aspect of the First Metatarsal Head	bony
RSMR	Right Dorsal Aspect of the Second Metatarsal Head	bony
RVMR	Right Dorsal Aspect of the Fifth Metatarsal Head	bony
Left Foot		
LCAR	Left Upper Ridge of the Calcaneus	bony

LFMR	Left Dorsal Aspect of the First Metatarsal Head	bony
LSMR	Left Dorsal Aspect of the Second Metatarsal Head	bony
LVMR	Left Dorsal Aspect of the Fifth Metatarsal Head	bony

2.3.6. Once calibration is complete, the gait trials will be performed. Motion capture data will be collected at 200Hz.

2.3.7. Technical reflective markers will be attached to each major body segment of interest on the participants. These markers will enable the Vicon motion capture cameras to keep track of the participants' 3D motions. The list of the technical markers is given in table 2.

Table 2.3.2: Technical Maker List of Each Major Body Segment of Interest

Landmark	Description	Property/Type
Pelvis		
LASIS	Left Anterior Superior Iliac Spine	Bony
RASIS	Right Anterior Superior Iliac Spine	Bony
L4SP	Spinous Process L4 (Lumbar 4)	Bony
Right Femur/Thigh		
RRFM	Right Rectus Femoris Muscle	Musculature
RBFM	Right Biceps Femoris Muscle	Musculature
ROSM	Right Semitendinosus Muscle	Musculature
Left Femur/Thigh		
LRFM	Left Rectus Femoris Muscle	Musculature
LBFM	Left Biceps Femoris Muscle	Musculature
LOSM	Left Semitendinosus Muscle	Musculature
Right Tibia/Shank		
RTAM	Right Tibialis Anterior Muscle	Musculature
RLGM	Right Lateral Gastrocnemius Muscle	Musculature
RMGM	Right Medial Gastrocnemius Muscle	Musculature
Left Tibia/Shank		
LTAM	Left Tibialis Anterior Muscle	Musculature
LLGM	Left Lateral Gastrocnemius Muscle	Musculature
LMGM	Left Medial Gastrocnemius Muscle	Musculature
Right Foot		
RCAR	Right Upper Ridge of the Calcaneus	Bony
RFMR	Right Dorsal Aspect of the First Metatarsal Head	Bony
RSMR	Right Dorsal Aspect of the Second Metatarsal Head	Bony
RVMR	Right Dorsal Aspect of the Fifth Metatarsal Head	Bony
Left Foot		
LCAR	Left Upper Ridge of the Calcaneus	Bony
LFMR	Left Dorsal Aspect of the First Metatarsal Head	Bony

LSMR	Left Dorsal Aspect of the Second Metatarsal Head	Bony
LVMR	Left Dorsal Aspect of the Fifth Metatarsal Head	Bony

2.3.8. Participants will then perform the gait trials, walking over level-ground and the uneven terrain. During the gait trials, the 3D coordinates of the reflective markers will be recorded by the Vicon motion capture cameras. The recorded raw data will then be processed using GMAS in order to assess the participants' motion. GMAS is a 3D motion analysis Matlab toolbox used to analyse kinematic and kinetic data.

2.3.9. Participants will also step over two 3D force plates in succession during the gait trials. The ground reaction forces and moments will be recorded at 1 KHz.

2.3.10. The global coordinate system for recording the 3D spatial marker coordinates will be defined as shown in figure 1. The directions of the three Cartesian axes are mutually perpendicular.

2.3.11. The y axis is parallel to gravity, though it points upwards. The x axis defines the direction of progression and is along the anterior-posterior plane, pointing in the anterior direction. The z axis points to the right and is perpendicular to both the x and y axes.

2.3.12. The local coordinate system will be defined based on ISB recommendations and on [4] so that the angular orientations of the body segments can be computed.
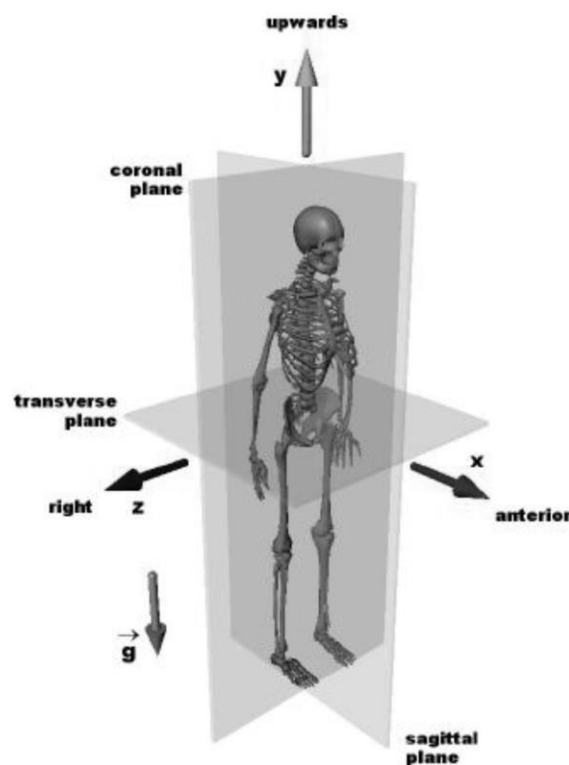

Figure 2.3.1: Global Anatomical Coordinate System and Planes

2.4. EMG System

Muscle activation data will be recorded from participants' lower limbs to study which muscles are activated during the gait trials and to what extent. This will also include studying muscle co-activation from which, in some cases, stability maintenance could be inferred.

2.4.1. Participants will have both their lower limbs instrumented with the EMG surface electrodes. Instrumenting both limbs will allow for muscle activation comparisons to be made.

2.4.2. EMG electrodes will be placed based on the SENIAM recommendations [5], [6] and palpation.

2.4.3. EMG surface electrodes will be placed over the participants' lower limb muscles as shown in figures 2 and 3. These particular muscles were chosen as they are largely responsible for actuating the ankle and knee joints respectively.
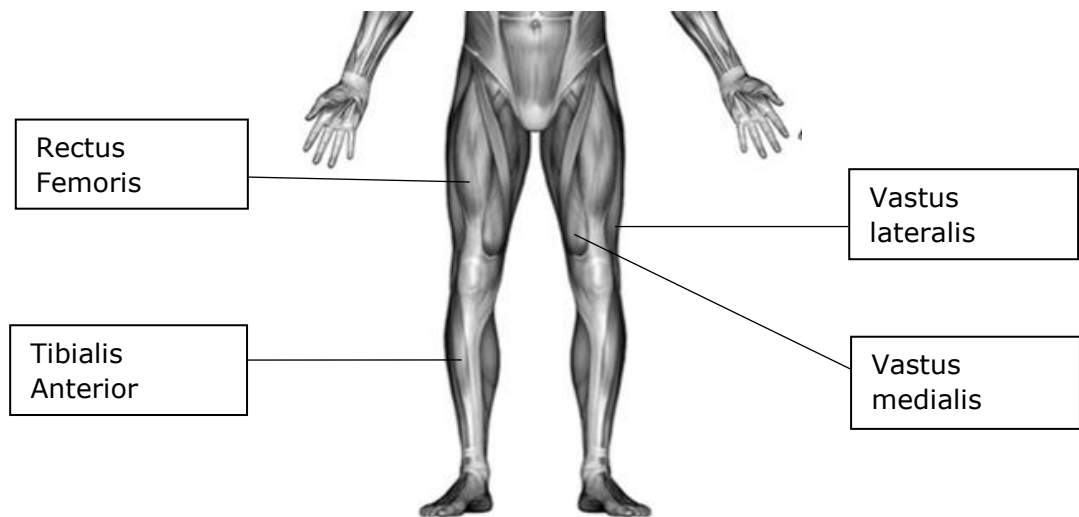

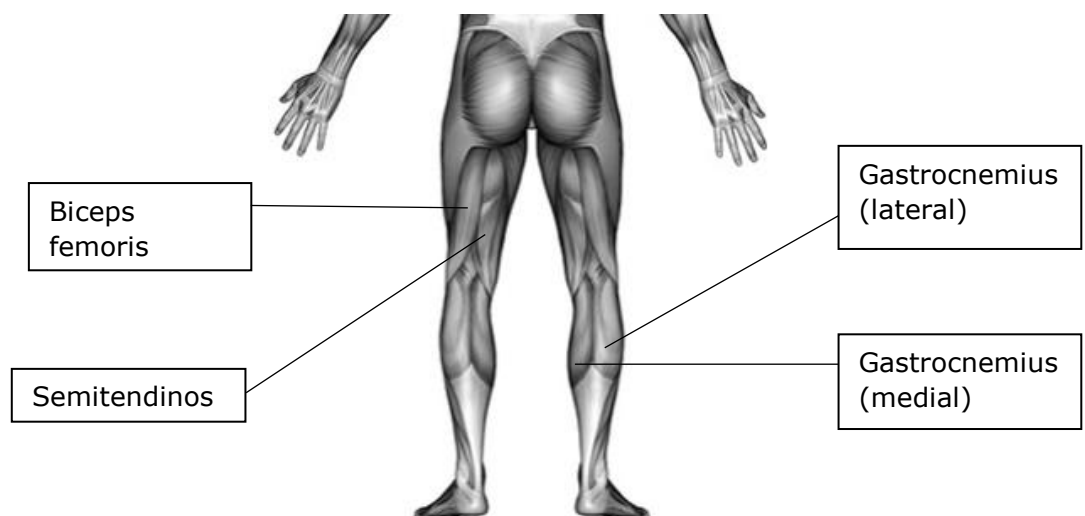Figure 2.4.1: Anterior View of EMG Surface Electrode Placement

Figure 2.4.2: Posterior View of EMG Surface Electrode Placement

2.5.   Uneven Terrain

The uneven terrain to be used for the gait trials was constructed in such a way as to mimic fixed uneven walking surfaces commonly encountered within an urban environment, such as uneven paving. The layout of the uneven terrain will be done in such a way that walking over the terrain will necessitate participants to perform muscle activation and gait manoeuvres in order to maintain dynamic stability and to retain their centre of mass (COM) within their base of support (BOS).

2.5.1.   The uneven terrain will consist of sloped steps fabricated from sheet metal, each 60cm long x 40cm wide in size. The layout of the uneven terrain will be the same for all walking speeds and for all participants which will allow for gait and muscle activation comparisons amongst the participants.

2.5.2.   The uneven terrain slopes were fabricated in such a manner that they will remain rigid as participants walk over them at varying speeds.

2.5.3.   The uneven terrain is modular in design so that it can be taken apart and re-assembled as desired.

2.5.4.   All the edges of the sloped steps were filleted, and the slopes were covered with a thin layer of rubber to provide a safe, non-slip and comfortable walking surface.

2.5.5.   The sloped steps have an incline of 12° along either the sagittal or frontal plane. An inclination of 10° has been shown to be the point where participants' gait begins to emulate that of ramp traversal [7], the point when the COM can be displaced outside the BOS; thus 12° was chosen because it is the lowest inclination higher than but not boarding 10°.

2.5.6.   The uneven terrain will be composed of six sloped steps in total. Once placed on the ground, the sloped steps are secure and do not move or slide.

2.5.7.   Participants will be asked to walk as naturally as possible over the uneven terrain ensuring that both feet come in contact with the terrain.

2.5.8.   The complete length of the uneven terrain will be 6.6m. The uneven terrain will be lengthwise and width wise aligned with the two triaxial force plates. The spacing between each slope will ensure that participants remain unaware of where the force plates are located. An illustration of the uneven terrain is shown in figure 4;
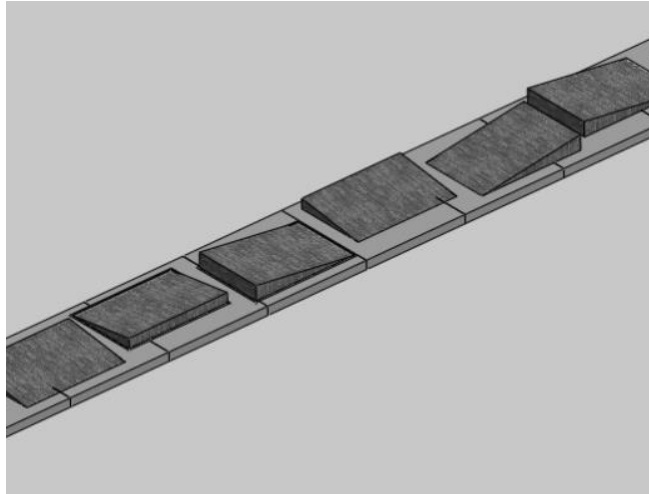
Figure 2.5.1: 3D Representation of the Uneven Terrain

3. Materials and Sensors

3.1. A workspace computer to record the data.

3.2. Delsys surface EMG electrodes.

3.3. Six camera motion capture system (Vicon T-series).

3.4. Two AMTI 3D force plates.

3.5. Delsys EMGworks Analysis software.

3.6. GMAS software (a developed Matlab toolbox).

4. Controls

4.1. Participants will begin each walking trial from the same side of the laboratory, thus ensuring the force plates are activated in the same manner for each trial.

4.2. Participants will contact the first force plate with their right foot.

4.3. The level-ground gait trials (even terrain) will also serve as a control for the uneven terrain gait trials.

5. Data Processing/Interpretation
5.1.   Motion Capture Data

GMAS software [4], a developed Matlab toolbox, will be used to process the motion capture data in order to compute the joint angles, moments and the mechanical power at each joint [8].

5.1.1. The 3D anatomical landmark coordinates and technical marker positions from the calibration trials will be calculated.

5.1.2. The hip joint centre position will be calculated using a functional method [4]. The ankle and knee joint centres will be determined directly from the bony anatomical landmarks.

5.1.3. Any missing marker coordinates will be computed and filled using a physical based method and an interpolation method.

5.1.4. Digital filters will be used to smooth the raw data, such as a low pass, zero lag 4th order Butterworth filter with a cut-off frequency of 6Hz [9].

5.1.5. The local coordinate system for each body segment will be defined and the Euler and Cardan angles for each body segment will be computed.

5.1.6. The angular velocities and accelerations for each body segment will be calculated.

5.1.7. The coordinates of the centre of mass for each body segment will be calculated.

5.1.8. The linear velocities and accelerations of mass centres for each body segment will be calculated.

5.1.9. Forces, moments and mechanical power at each joint will be calculated using Newton-Euler equations, starting from all solvable segments, calculating the forces and moments at their adjacent joints and running iteratively until no solvable segment remains [4].

5.1.10. The data from the motion capture system will also be used to identify gait events, such as heel strike and toe off based on the force plate data.

5.1.11. The variables of interest calculated from the motion capture data and the force plate data will be time-normalized to percentage of the gait cycle.

5.2. EMG Data

The data recorded by the EMG surface electrodes will be used to determine which muscles are active during the gait trials and to what degree [10]. Muscle co-activation at certain points of the gait cycle could also be used to deduce stability maintenance strategies.

5.2.1. EMG data analysis will be performed using Delsys EMGworks Analysis software.

5.2.2. A linear envelop will be created from the raw EMG data. This will involve full-wave rectification of the raw data to ensure that only the positive elements of the EMG signal are retained, followed by low-pass filtering of the data with a cut-off

frequency of 6Hz using a 2nd order Butterworth filter. The linear envelop will ensure that only muscle activity is retained, without any motion artifact [11].

5.2.3. The linear envelop will be computed for each recorded EMG signal, giving a rectified representation of the participants' muscle activation throughout the gait cycle.

5.2.4. The EMG data will be time-normalized to percentage of the gait cycle.

References

1. Lieberman, D.E., Venkadesan, M., Werbel, W.A., Daoud, A.I., D'Andrea, S., Davis, I.S., Mang'Eni, R.O. and Pitsiladis, Y., *Foot strike patterns and collision forces in habitually barefoot versus shod runners.* Nature, 2010. **463**(7280): p. 531-535.

2. Yan, A.F., Sinclair, P.J., Hiller, C., Wegener, C. and Smith, R.M., *Impact attenuation during weight bearing activities in barefoot vs. shod conditions: A systematic review.* Gait and Posture, 2013. **38**(2): p. 175-186.

3. Cappozzo, A., Catani, F., Della Croce, U. and Leardini, A., *Position and orientation in space of bones during movement: anatomical frame definition and determination.* Clinical Biomechanics, 1995. **10**(4): p. 171-178.

4. Ren, L., Jones, R.K. and Howard, D. , *Whole body inverse dynamics over a complete gait cycle based only on measured kinematics.* Journal of Biomechanics, 2008. **41**(12): p. 2750-2759.

5. Hermens, H.J., et al. *SENIAM recommendations for sensor placement*. [website] 1995 [cited 2015 12 October].

6. Rainoldi, A., G. Melchiorri, and I. Caruso, *A method for positioning electrodes during surface EMG recordings in lower limb muscles.* Journal of Neuroscience Methods, 2004. **134**(1): p. 37-43.

7. McIntosh, A.S., Beatty, K.T., Dwan, L.N. and Vickers, D.R., *Gait dynamics on an inclined walkway.* Journal of Biomechanics, 2006. **39**(13): p. 2491-2502.

8. Kadaba, M.P., Ramakrishnan, H.K. and Wootten, M.E., *Measurement of Lower Extremity Kinematics During Level Walking.* Journal of Orthopaedic Research, 1990. **8**(3): p. 383-392.

9. Winter, D.A., Sidwall, H.G. and Hobson, D.A., *Measurement and reduction of noise in kinematics of locomotion.* Journal of Biomechanics, 1974. **7**(2): p. 157-159.

10. De Lisa, J.A., *Gait Analysis in the Science of Rehabilitation*, D.o.V. Affairs, Editor 1998, Baltimore Rehabilitation: US. p. 112.

11. De Luca, C.J., *The Use of Surface Electromyography in Biomechanics.* Journal of Applied Biomechanics 1997. **13**(2): p. 135-163.